UNIVERSITY OF CALIFORNIA, SAN DIEGO

# Transmit Beamforming for Multiple Antenna Systems with Imperfect Feedback

A dissertation submitted in partial satisfaction of the
requirements for the degree Doctor of Philosophy
in
Electrical and Computer Engineering
(Communication Theory and Systems)

by

Yogananda R. Isukapalli

Committee in charge:

Professor Bhaskar D. Rao, Chair
Professor Robert Bitmead
Professor William Hodgkiss
Professor Tara Javidi
Professor Kenneth Kreutz-Delgado

2009

The dissertation of Yogananda R. Isukapalli is approved, and it is acceptable in quality and form for publication on microfilm and electronically:

_____

_____

_____

_____

_____

Chair

University of California, San Diego

2009

TABLE OF CONTENTS

LIST OF FIGURES

LIST OF TABLES

ACKNOWLEDGEMENTS

I would first like to thank my advisor, Prof. Bhaskar D. Rao, for his patience in the beginning, encouragement throughout the duration of my Ph.D. study, and for dedicating a great amount of time and effort on my thesis topic. I am also thankful to him for the uninterrupted financial support. It was a privilege to work with him. I would also like to thank my committee members, Professors Robert Bitmead, William Hodgkiss, Tara Javidi, and Kenneth Kreutz-Delgado for their time and helpful comments.

I owe a lot to my collaborators Prof. Kreutz-Delgado, Jun Zheng, and Ramesh Annavajjala. I would like to thank them for many insightful discussions and critical feedback. I also would like to thank my family, friends, and research group members: Diba Mirza, Aditya Jagannatham, Shankar Shivappa, Chandra Murthy, David Wipf, Cécile Levasseur, Abhijeet Bhorkar, Ethan Duni, Sarath Kasarla, Rathinakumar Appuswamy, Seyhan Karakulak, Nandan Das, Matthew Pugh, Brandon Burdge, Konstantinos P. Liolis, Liwen Yu, Yuzhe Jin, Bharath Sriperumbudur, Zhilin Zhang, Shue-Shue Tan, Hadi Djahanshadi, Wenyi Zhang, Oleg Tanchuk, Sagnik Ghosh, Alireza Masnadi-Shirazi, Anh Nguyen, Yichao Huang, and Eddy Kwon, for their encouragement and helpful discussions.

This work was supported in part by CoRe grant No. 02-10109 sponsored by Ericsson and in part by the U. S. Army Research Office under the Multi-University Research Initiative (MURI) grant No. W911NF-04-1-0224.

The text of Chapter 2, in part, has appeared in Y. Isukapalli, R. Annavajjala, and B. D. Rao, "Performance analysis of transmit beamforming for MISO systems with imperfect feedback," *IEEE Transactions on Communications*, vol. 57, no. 1, pp. 222-231, Jan. 2009 and Y. Isukapalli, R. Annavajjala, and B. D. Rao, "Average SEP and BEP analysis of transmit beamforming for MISO systems with imperfect feedback and M-PSK constellation," *IEEE Symp. on Pers. Indoor and Mobile Radio Comm. (PIMRC)*, Athens, Greece, Sep. 2007.

The text of Chapter 3, in part, has appeared in Y. Isukapalli and B. D. Rao,

"Analyzing the effect of channel estimation errors on the average block error probability of a MISO transmit beamforming system," *IEEE Global Telecom. (Globecom) Conf.*, New Orleans, LA, Dec. 2008, Y. Isukapalli and B. D. Rao, "An analytically tractable approximation for the Gaussian Q-function," *IEEE Communications Letters*, vol. 12, no. 9, pp. 669-671, Sep. 2008, and Y. Isukapalli and B. D. Rao, "Performance analysis of finite rate feedback MISO systems in the presence of estimation errors and delay," *IEEE Asilomar Conf. on Sig. Syst. and Comp.*, CA, Oct. 2007. The text of Chapter 3, in part, is under review in Y. Isukapalli and B. D. Rao,"Packet error probability of a transmit beamforming system with imperfect feedback," *IEEE Transactions on Signal Processing*, submitted, May 2009, revised, Jul. 2009.

The text of Chapter 4, in part, has appeared in Y. Isukapalli, J. Zheng, and B. D. Rao, "Optimum codebook design and average SEP loss analysis of spatially independent and correlated feedback based MISO systems with rectangular QAM constellation," *IEEE Transactions on Signal Processing*, vol. 57, no. 5, pp. 2017-2024, May 2009, Y. Isukapalli and B. D. Rao, "Finite rate feedback for spatially and temporally correlated MISO channels in the presence of estimation errors and feedback delay," *IEEE Global Telecom. (Globecom) Conf.*, Washington D.C., Nov. 2007, and Y. Isukapalli, J. Zheng and B. D. Rao, "Average SEP loss analysis of transmit beamforming for finite rate feedback MISO systems with QAM constellation," *IEEE Intern. Conf. on Acous. Speech and Sig. Proc. (ICASSP)*, Hawaii, vol. 3, pp. 1520-6149, Apr. 2007.

The text of Chapter 5, in part, has appeared in Y. Isukapalli and B. D. Rao, "Ergodicity of wireless channels and temporal prediction," IEEE Asilomar Conf. on Sig. Syst. and Comp., CA, Oct. 2006. The text of Chapter 5, in part, is manuscript under preparation, Y. Isukapalli and B. D. Rao, "Multi-antenna wireless channel modeling: statistical properties and prediction," in preparation, *IEEE Transactions on Signal Processing*.

## VITA

| | |
|---|---|
| 2000 | B.E., Electronics and Communication Engineering<br>University College of Engineering (Autonomous)<br>Osmania University, Hyderabad, India |
| 2004 | M.S., Electrical and Computer Engineering<br>Villanova University, Philadelphia, U.S.A. |
| 2009 | Ph.D., Electrical and Computer Engineering<br>University of California, San Diego, U.S.A. |

## PUBLICATIONS


[J1] Y. Isukapalli, J. Zheng, and B. D. Rao, "Optimum codebook design and average SEP loss analysis of spatially independent and correlated feedback based MISO systems with rectangular QAM constellation," *IEEE Transactions on Signal Processing*, vol. 57, no. 5, pp. 2017-2024, May 2009.

[J2] Y. Isukapalli, R. Annavajjala, and B. D. Rao, "Performance analysis of transmit beamforming for MISO systems with imperfect feedback," *IEEE Transactions on Communications*, vol. 57, no. 1, pp. 222-231, Jan. 2009.

[J3] Y. Isukapalli and B. D. Rao, "An analytically tractable approximation for the Gaussian Q-function," *IEEE Communications Letters*, vol. 12, no. 9, pp. 669-671, Sep. 2008.

[J4] K. K-Delgado and Y. Isukapalli, "Use of the Newton method for blind adaptive equalization based on the constant modulus algorithm," *IEEE Transactions on Signal Processing*, vol. 56, no. 8, part. 2, pp. 3983-3995, Aug. 2008.

[J5] Y. Isukapalli and B. D. Rao, "Packet error probability of a transmit beamforming system with imperfect feedback," submitted, *IEEE Transactions on Signal Processing*, submitted, May 2009, revised, Jul. 2009.

[J6] Y. Isukapalli and B. D. Rao, "Multi-antenna wireless channel modeling: statistical properties and prediction," in preparation, *IEEE Transactions on Signal Processing*.

[C1] Y. Isukapalli and B. D. Rao, "Analyzing the effect of channel estimation errors on the average block error probability of a MISO transmit beamforming system," *IEEE Global Telecom. (Globecom) Conf.*, New Orleans, LA, pp. 1-6, Dec. 2008.

[C2] Y. Isukapalli and B. D. Rao, "Finite rate feedback for spatially and temporally correlated MISO channels in the presence of estimation errors and feedback delay," *IEEE Globecom Conf.*, Washington D.C., pp. 2791-2795, Nov. 2007.

[C3] Y. Isukapalli and B. D. Rao, "Performance analysis of finite rate feedback MISO systems in the presence of estimation errors and delay," *IEEE Asilomar Conf. on Sig. Syst. and Comp.*, CA, pp. 1931-1935, Oct. 2007.

[C4] Y. Isukapalli, R. Annavajjala, and B. D. Rao, "Average SEP and BEP analysis of transmit beamforming for MISO systems with imperfect feedback and M-PSK constellation," *IEEE Symp. on Pers. Indoor and Mobile Radio Comm. (PIMRC)*, Athens, Greece, pp. 1-5, Sep. 2007.

[C5] Y. Isukapalli, J. Zheng and B. D. Rao, "Average SEP loss analysis of transmit beamforming for finite rate feedback MISO systems with QAM constellation," *IEEE Intern. Conf. on Acous. Speech and Sig. Proc. (ICASSP)*, Hawaii, vol. 3, pp. 1520-6149, Apr. 2007.

[C6] Y. Isukapalli and B. D. Rao, "Ergodicity of wireless channels and temporal prediction," *IEEE Asilomar Conf. on Sig. Syst. and Comp.*, CA, pp. 473-477, Oct. 2006.

[C7] Y. Isukapalli and S. S. Rao "Exploiting the nature of extrinsic information in iterative decoding," IEEE Asilomar Conf. on Sig. Syst. and Comp., CA, Oct. 2004.

[C8] Y. Isukapalli and S. S. Rao "A new form of MUSIC algorithm for the instantaneous estimation of DOA and spatial spread," IEEE Elec. Info. Tech. (EIT) conf., Indianapolis, IN, Jun. 2003.

[C9] Y. Isukapalli and S. S. Rao "A heuristic explanation for the improvement in turbo codes performance with number of iterations," IEEE EIT conf., Indianapolis, IN, Jun. 2003.

ABSTRACT OF THE DISSERTATION

Transmit Beamforming for Multiple Antenna Systems with Imperfect Feedback

by

Yogananda R. Isukapalli

Doctor of Philosophy in Electrical and Computer Engineering
(Communication Theory and Systems)

University of California, San Diego, 2009

Professor Bhaskar D. Rao, Chair

Multiple antennas can effectively minimize the negative impact of multiplicative fading in wireless communication systems by providing spatial diversity. In this thesis we consider a spatial diversity scheme with multiple antennas at the base station. In order to achieve the optimum performance gains, i.e., to achieve both the array gain and the diversity gain, the transmitter needs to know channel information. In frequency division duplexing systems the channel information has to be fedback to the transmitter. This feedback requirement leads to various forms of imperfection. A typical practical system has three main sources of feedback imperfection, namely, channel estimation errors, channel quantization, and feedback delay. In this thesis we comprehensively study the impact of feedback imperfections on the performance of multi-antenna systems.

We develop a general framework capturing the three forms of feedback imperfection, i.e., estimation errors, quantization, and delay, for both spatially independent and correlated fading scenarios. In the modeling of imperfect feedback, we show that depending on the beamforming vector construction, the feedback delay error term can be *known* or *unknown* at the receiver. On the other hand, channel estimation error term is always *unknown* at the receiver. In a slow fading

context, i.e., in scenarios where channel remains constant for the entire packet, we highlight the fact that both the estimation error term and the delay error term remain *constant*, with estimation error term *unknown* at the receiver and delay error term *known* at the receiver, for the entire packet while the thermal noise changes from symbol-to-symbol. For spatially independent channels, with the help of general framework, we then analytically quantify the effect of the three forms of feedback imperfection on the symbol and bit error probabilities of both $M$-PSK and $M$-ary rectangular QAM constellations with Gray code mapping. We also derive an analytical expression for the average packet error probability with BPSK signaling.

In addition, with channel estimation errors and feedback delay, for spatially correlated channels, we develop codebook design algorithms specific to the modulation format and ergodic capacity. The new optimum codebooks show an improvement in performance compared to the existing set of codebooks available in the literature. Utilizing high resolution quantization theory and assuming perfect channel estimation at the receiver, we analyze the loss in average symbol error probability for spatially independent and correlated finite-rate feedback transmit beamforming multiple input single output systems with $M_1 \times M_2$-QAM constellation.

We also address the issue of minimizing the negative impact of feedback delay. A natural way to combat the effect of feedback delay is channel prediction. We study the role of ergodicity in wireless channel modeling and provide an insight into when statistical channel models that employ ensemble averaging are appropriate for the purpose of channel prediction. Simulation results complement the extensive set of analytical expressions derived in the thesis.

# 1 Introduction

The random nature of multiplicative fading is at the heart of wireless communications. The wireless channel is typically understood in terms of three broadly defined phenomena. The first is the path-loss or slow fading, i.e., the power of electromagnetic waves, carrying the information, decreases exponentially with distance. Second is the shadow fading, which captures the coarse details of the environment of the mobile receiver. Shadow fading captures the loss in the power of electromagnetic waves as they pass through buildings, foliage and various other objects between the transmitter and the mobile receiver. The third phenomena is known as fast fading. Due to scattering and reflection, a number of electromagnetic waves get added up at the receiver thus giving rise to rapid variations in the phase and magnitude of the resulting channel.

Due to the randomness in the environment between the transmitter and the receiver, combined with the motion of transmitter or receiver or both, it is important to note that slow, shadow, and fast fadings are all random processes. However, the time scales of variation are different. Typically the slow and shadow fadings happen at a much slower pace than the fast fading. The power variations caused by slow and shadow fadings can be adjusted and thus, with proper planning, they do not impact the system performance that severely. The fast fading phenomena can cause a signal power drop of about $30 - 40$ dB and the time scale of variation is of the order of milliseconds and hence this is the most detrimental form of fading. In order to see the effect analytically, we consider the impact of fast fading on the performance of a simple binary phase shift keying (BPSK) wireless

communication system.

## 1.1 Fast Fading

In this thesis from here on fading refers to '*fast fading*' among the three broadly defined forms of fading discussed earlier. Also throughout the thesis we consider a frequency flat scenario, i.e., the coherence bandwidth of the wireless channel is larger than the bandwidth of the signal. For simplicity let us begin with a single transmit antenna and single receive antenna scenario. The complex flat fading process is typically modeled as a sum of complex sinusoids [1]-[6]:

$$h(t) = \sum_{n=1}^{N} \beta_n e^{j(\omega_n t + \phi_n)}, \tag{1.1}$$

where, $\beta_n$ is the amplitude, $\phi_n$ is the phase, and $\omega_n$ is the Doppler frequency of the $n^{th}$ multipath. $\omega_n = \omega_{max} \cos\theta_n$ where $\omega_{max}$ is the maximum Doppler frequency and $\theta_n$ is the angle of arrival of $n^{th}$ multipath. $\omega_{max} = 2\pi v/\lambda$ where $v$ is the velocity of mobile and $\lambda$ is the carrier wavelength.

In order to study the system performance over a wide range of environments and assuming that there is rich scattering, the above process (1.1) can be modeled as a zero mean circular symmetric complex Gaussian (CSCG) process with unit variance, denoted as $h \sim \mathcal{NC}(0,1)$ . This statistical modeling of fading process is universally accepted. For the performance analysis we also follow this statistical channel model, i.e., the fading process is assumed to be distributed as $h \sim \mathcal{NC}(0,1)$.

Let $s$ be the transmitted BPSK symbol and $h$ be the multiplicative fast-fading channel between the transmitter and receiver. The discrete time baseband-equivalent of received signal, after the matched filter operation, is given by

$$y[k] = h[k]\, s[k] + \eta[k] \tag{1.2}$$

where $k$ denotes time index, the channel coefficient $h$ is a zero-mean CSCG random variable with unit variance, and $\eta$ is the thermal noise at the front end of the re-

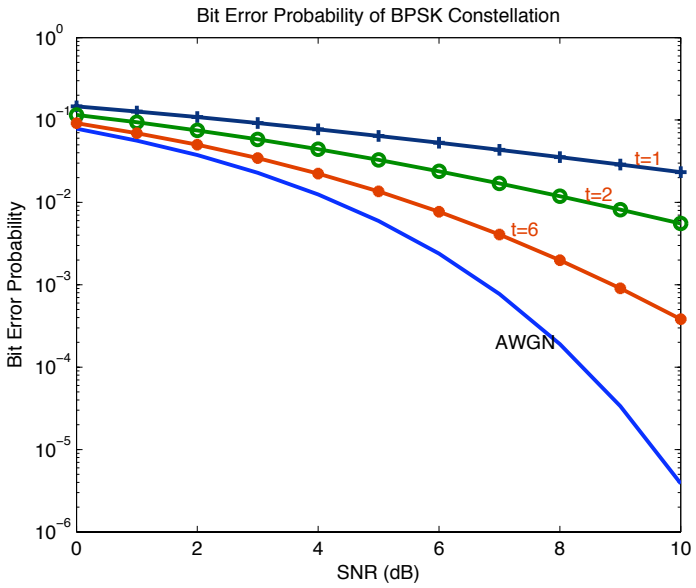


Figure 1.1 Effect of diversity on the bit error probability of BPSK constellation. Degree of diversity $t \in \{1, 2, 6\}$, channel is distributed as $h \sim \mathcal{NC}(0, 1)$. For comparison, the bit error probability in an AWGN channel is also shown.

ceiver. $\eta$ is a zero-mean CSCG random variable with $E[|\eta|^2] = \sigma_n^2$. To understand the impact of fading we now look at the relationship between the bit error probability (BEP), $p_e$, and the signal-to-noise ratio ($SNR$). $p_e$ and $SNR$ are related as [1]

$$p_e \propto \frac{1}{SNR}\,. \tag{1.3}$$

In contrast, in an AWGN channel, with $h = 1$ in (1.2), the relation between BEP and SNR is given by [1]

$$p_e \propto e^{-SNR}\,. \tag{1.4}$$

The performance loss caused by fading can be clearly seen by comparing (1.3) and (1.4). To achieve the same order of performance as an AWGN channel, one has to use an order of magnitude higher power in a fading channel. Note that in both (1.3) and (1.4) the focus is only on how SNR effects the BEP, the exact constants are not relevant to the present discussion.

One of the popular solutions to combat the negative effects of fading is to

provide *diversity*. In a diversity based scheme, multiple copies of the information symbol are transmitted through independently faded channels. These copies are then combined at the receiver. The main idea behind a diversity schemes is that the probability that all the independently faded paths are simultaneously in deep fade is low. To analytically illustrate the effectiveness of diversity, consider a system where $t$ independently faded symbols are available at the receiver. Assuming that the receiver knows all the channel co-efficients perfectly, the $t$ independently faded symbols can be combined coherently. The resulting system's BEP and SNR relation is given by

$$p_e \propto \frac{1}{SNR^t}\,. \tag{1.5}$$

In the above equation $t$ is referred to as the diversity order. As seen in Fig. 1.1, compared to (1.3), the improvement in performance is evident. However, note that to achieve the same performance as an AWGN channel an infinite diversity order is required. There are many ways to provide diversity such as time, frequency, polarization, and spatial diversity.

In wireless communications one of the earlier applications of multiple antennas is in the area of spatial diversity. However, the rapid growth in wireless industry, and the demand for high data rates with high reliability has intensified the research efforts in multiple-input and multiple-output (MIMO) wireless systems in venues other than spatial diversity schemes. It is well-known that the capacity of MIMO systems in a rich scattering environment increases linearly with the minimum number of transmit and receive antennas [7, 8]. It should be noted that the usage of multiple antennas in wireless communications primarily falls into two categories, one is for providing diversity and the other is to provide spatial multiplexing. Generally speaking the diversity schemes provide a reliable link and spatial multiplexing provides parallel data streams and hence higher data rates. This thesis falls under the diversity camp. In recent years, a new point of view has emerged with respect to fading, and the fading is seen as a *friendly phenomena*. If one has no delay constraints and if there is a feedback link, one can

employ opportunistic communication principle and transmit only when the channel is strong. As mentioned earlier, this thesis takes the approach of minimizing the fluctuations in the effective channel between the transmitter and receiver.

## 1.2 Spatial Diversity

In this thesis we consider a spatial transmit diversity scheme in the context of multiple antennas. In this scheme the multiple antennas are placed sufficiently apart so that they experience independent fading. Theoretically speaking one could have multiple antennas at the transmitter, or at the receiver, or at both the transmitter and receiver. However, in a practical system, having multiple antennas at the receiver (mobile) is not an attractive option and hence this thesis considers a system where there are multiple antennas at the transmitter (base station).

In a multiple-input and single-output (MISO) system, if the channel state information (CSI) is available at the transmitter, one can achieve both the diversity and array gains with transmit beamforming via maximal ratio transmission [9], whereas only diversity gain can be realized with space-time coding [10, 11]. Our work studies how the transmitter gets the CSI in a feedback based practical system. In time division duplexing systems using channel reciprocity the transmitter can estimate the channel based on some pilot sequence from receiver. Most of the practical systems are frequency division duplexing (FDD) based and to avoid interference at the transmitter the spacing of uplink and downlink frequencies are selected as far apart as possible. Hence, in FDD systems channel reciprocity does not apply. An important consequence of not having channel reciprocity is that in an FDD system the receiver has the CSI and it has to be conveyed to the transmitter.

In an FDD system, as shown in Fig. 1.2, the transmitter sends a pilot sequence for channel estimation. Using the pilot sequence the receiver estimates

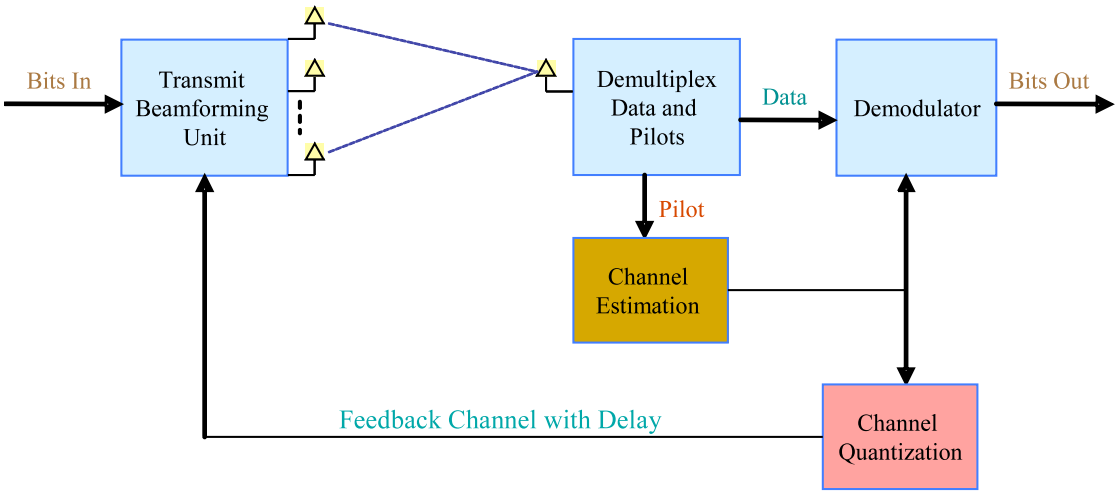


Figure 1.2 Block diagram of a transmit beamforming MISO system with imperfect feedback. Feedback imperfections include, inaccurate channel estimation, channel quantization and feedback delay.

the channel state information. The receiver has to convey the estimated CSI to the transmitter through a feedback link. Due to various practical constraints, generally there is a mismatch between the actual channel and the CSI that is available at the receiver. Some possible sources of mismatch are:

1. The presence of thermal noise at the front end of receiver inevitably creates a mismatch between the actual channel and its estimate. The estimation error can be reduced by having a longer pilot sequence and/or by increasing the power of the pilot sequence. However, it is nearly impossible to have a perfect estimate of channel.

2. In most practical systems the bandwidth of the feedback link is low. Hence the receiver has to convey the estimated CSI, not in its actual form but in a compressed form. An optimum way of doing this is through vector quantization. Based on the channel statistics, a fixed codebook is constructed off-line and it is known at both transmitter and receiver. Based on an optimum criteria, the estimated channel is then used to pick one of the codepoints from the codebook. The index of the selected codepoint is sent to the transmitter

through the low rate feedback link. Assuming that there are no errors (with the help of strong channel coding) in the feedback link, the transmitter then picks the codepoint and uses it to beamform the data.

Since a vector quantized version of channel estimate is sent to the transmitter, there is a further mismatch between the actual channel and the selected codepoint.

3. The third form of imperfection, or source of mismatch, is the delay involved in the feedback process. The receiver has to estimate the channel, quantize it, and feed the index back to the transmitter. By the time the transmitter uses the codepoint to transmit data, the actual channel might have changed. Depending on the channel variations the mismatch due to delay can be severe.

In any practical system the above mentioned three forms of feedback imperfection namely *estimation errors, feedback delay, and channel quantization* are present. The main theme of this thesis is to develop suitable modeling of these three forms of feedback imperfection and the analytical quantification of their effect on some of the commonly accepted performance metrics such as symbol, bit, and packet error probabilities. The thesis is also concerned with optimum codebook design and with the study of some statistical properties of channel models that are important in channel prediction. A brief summary of related work is provided in the next section.

## 1.3 Related Work

In communication systems, in general, it is a common practice to first study the performance of a system under ideal assumptions. In real systems, because of the mismatch between assumed behavior and actual behavior in various system parameters, the performance is worse than what is predicted with ideal system parameters. However, the performance analysis studies carried out under ideal assumptions are important as they provide insight into the system behavior as

well as they can always be used as upper (or lower) bounds on system performance. In the present context of feedback for multi-antenna systems, most of the existing literature dealt with either perfect feedback scenario or with one form of feedback imperfection. As explained earlier, in order to understand the performance under realistic assumptions, in this thesis, we study the various implications of imperfect feedback in transmit beamforming multiple input single output systems. Now, we briefly summarize some of the relevant literature.

Under ideal channel estimate assumption, extensive analytical results quantifying the impact of fading on average symbol and bit error probability (SEP/BEP) are available for various modulation schemes [12]. In [13] authors consider efficient use of channel state information for transmit beamforming. An information theoretic approach to transmit beamforming with imperfect feedback is presented in [14, 15]. With maximum ratio transmission and BPSK modulation, the effect of feedback delay with perfect channel estimation at the receiver is investigated in [16], whereas [17] studies the effect of imperfect channel estimation without feedback delay. In [18], the authors extend the analysis of [16] accounting for the effects of channel estimation errors. The effect of feedback delay and feedback errors on the receiver SNR performance is investigated in [19] for phase-only feedback, whereas [20] analyzes the bit error probability degradation with BPSK due to feedback errors with selection and co-phasing feedback schemes. The effects of finite-rate channel quantization and feedback delay are considered for BPSK in [21].

Approaches for the design and analysis of transmit beamforming schemes under finite-rate constraints are presented in [22]-[27]. While the aforementioned works considered either BPSK (or quadrature PSK, QPSK) with channel estimation errors and perfect quantization [16]- [21], or ideal channel estimation with finite-rate quantization for general modulations [22]- [26], combined effects of various channel imperfections for general modulations is not available in the literature. One of the contributions of this thesis is targeted to fill in this important void.

Channel coding and interleaving can offer some protection from the negative effects of fading. However, in some wireless systems data has to be organized into small packets, which are confined to fixed time slots, with or without interleaving. One popular example of such a system is the slotted multiple access scheme. It is important for the system designers to know the impact of fading on the performance. An important metric for studying the performance of a non-interleaved wireless packet data transmission is the average packet error probability.

Assuming perfect channel estimation, analytical quantification of average packet error probability (PEP), mostly for non-coherent FSK modulation, is studied in [38]-[53]. The non-coherent FSK's SEP, conditioned on the channel, is an exponential function and taking expectation of the higher powers of conditional SEP w.r.t. the fading random variable is analytically tractable. However, closed-form expressions are not available for coherent BPSK and other constellations. Conditional PEP (conditioned on a function of the wireless channel) for a scheme such as coherent BPSK results in integer powers of the Gaussian-$Q$ function. This makes the analysis challenging because in order to derive the average PEP expression, one has to integrate the integer powers of the Gaussian-Q function w.r.t. the random variable that captures the fading environment, an analytically difficult exercise. In this thesis we consider the problem of deriving analytical expressions for PEP of a multiple input single output system with various forms of practical imperfections. We later show that this problem captures various commonly interested performance analysis of wireless systems as special cases.

Much of the past work on feedback delay [16, 18, 62], [64]-[70] effectively make the delay related error term part of receiver noise. Also it is important to note that the work in [64]-[78] treats estimation errors and feedback delay in a similar manner, i.e., either both the error terms are assumed to be known or unknown to the receiver. In this thesis we make an important distinction between channel estimation errors and feedback delay. [92] discussed the importance of using right metric for codebook design. In this thesis we consider the design of an

optimum codebook that minimizes the average SEP of a modulation scheme. We now outline the important contributions and the organization of the thesis.

## 1.4 Contributions and Outline of the Thesis

In the second chapter, we analyze the performance of transmit beamforming on spatially independent multiple-antenna Rayleigh fading channels with imperfect channel feedback. As mentioned in Section 1.2 we characterize the feedback imperfections in terms of noisy channel estimation, feedback delay, and finite rate channel quantization. We develop a general framework, valid for any arbitrary two-dimensional linear modulation, that captures the aforementioned imperfections, and derive the symbol and bit error probability expressions for both $M$-PSK and $M$-ary rectangular QAM constellations with Gray code mapping.

We show that the proposed analytical formulation is valid for frequency-domain duplexing system with/without finite rate channel quantization and time-domain duplexing system. We validate the accuracy of the analysis through simulations, and assess the relative effects of channel estimation inaccuracy, feedback delay, and finite-rate quantization on the symbol and bit error performances for various constellations. Finally, we present a selected set of numerical results showing the impact of various feedback imperfections on the performance of higher order constellations.

Developing a distinction between the delay related error term and estimation related error term, and analyzing its consequences on average packet error probability (PEP) is the main theme of Chapter 3. PEP is an important error statistic for slowly fading wireless communication system designers. In Chapter 3, we address the problem of analytically quantifying the effect of channel estimation errors, feedback delay, and channel vector quantization on the PEP of transmit beamforming multiple input single output systems in a spatially independent fading wireless channel environment. We develop an accurate characterization of

estimation errors as well as errors due to feedback delay and tools relevant for deriving analytical expressions for the PEP.

The modeling presented in Chapter 3 highlights the distinction between errors that arise due to channel estimation from those that arise due to feedback delay and represents an important departure from past work. Analytical expressions are derived for the PEP for BPSK signaling. The derived approximated closed-form analytical expression is complemented by simulations. We also develop some analytical tools in Chapter 3 that help in a simpler evaluation of complicated communication performance metrics.

In Chapter 4, we turn our attention to the spatially correlated channels. In both chapters 2 and 3 the modeling of imperfect feedback and performance analysis was carried out for spatially independent channels. In Chapter 4 we present an optimum codebook design algorithm that minimizes the loss in average symbol error probability (SEP) of a spatially correlated multiple input single output system with finite-rate feedback under both perfect and imperfect channel estimate assumptions. Towards the goal of designing an optimum codebook that minimizes average SEP (ASEP) loss due to finite-rate channel quantization, we derive the distortion function as a first order approximation of the instantaneous SEP loss.

Utilizing high resolution quantization theory and assuming perfect channel estimation at the receiver, we analyze the loss in ASEP for spatially independent and correlated finite-rate feedback transmit beamforming MISO systems with $M_1 \times M_2$-QAM constellation. We then consider the high-SNR regime and show that the loss associated with quantizing the spatially independent channels is related to the loss associated with quantizing the spatially correlated channels by a scaling constant given by the determinant of the channel correlation matrix. We also present simulation results that illustrate the effectiveness of the new codebook design and validate the derived analytical expressions for loss in average symbol error probability.

Also, in Chapter 4, a novel codebook design algorithm that minimizes the

loss in ergodic capacity is proposed. Simulation results show that the new codebook designed under the consideration of estimation errors and feedback delay clearly outperforms the codebook designed under ideal conditions. Analysis for the loss in ergodic capacity for spatially i.i.d channels with channel estimation errors and delay is presented and validated through simulations.

In Chapter 5, we turn our attention to the issue of minimizing the negative impact of feedback delay. One can increase the pilot power and improve the channel estimate quality thus minimizing the mismatch due to channel estimation errors. By increasing the feedback budget (i.e., number of feedback bits) the mismatch due to quantization can be reduced. The only solution possible for combating the effect of feedback delay is to predict the channel.

In the context of channel prediction, we take a close look at an important statistical concept that plays a critical role in deciding which prediction method is appropriate. In Chapter 5 we study the role of ergodicity in wireless channel prediction. Following the sinusoidal channel model, conditions under which the ergodic assumption is valid are presented. This sheds insight into when statistical channel models that employ ensemble averaging are appropriate. Due to the lack of ergodicity in a typical real world wireless channel, Least Squares prediction, an approach based on time averages is motivated as opposed to linear minimum mean squared error channel prediction, an approach based on ensemble averaging. We then study methods such as Forward-Backward and rank reduction for high quality channel prediction. We conclude the thesis in Chapter 6.

Notation: Small and upper case bold letters indicate vector and matrix respectively. $E(.)$, $(.)^T$, $(.)^H$, $|.|$, $(\bar{.})$, and $\|.\|$ denote expectation, transpose, Hermitian, absolute value, complex conjugate, and 2-norm respectively. $x \sim p(x)$ indicates that the random variable $x$ is distributed as $p(x)$. $\mathbf{x} \sim \mathcal{NC}(\boldsymbol{\mu}, \boldsymbol{\Sigma})$ indicates a circularly symmetric complex Gaussian (CSCG) random variable $\mathbf{x}$ with mean $\boldsymbol{\mu}$ and covariance $\boldsymbol{\Sigma}$.

# 2 Modeling of Imperfect Feedback and Error Probability Analysis

In this chapter we first develop a general framework that captures the feedback imperfections, namely, noisy channel estimation, feedback delay, and finite-rate channel quantization. The modeling approach assumes that the receiver does not know the error terms due to both channel estimation and feedback delay. The general framework is shown to be valid for any arbitrary two-dimensional linear modulation schemes.

We show that the proposed analytical formulation is valid for a frequency domain duplexing system with/without finite-rate channel quantization and a time domain duplexing system. We then analyze the performance of transmit beamforming on spatially independent multiple-antenna Rayleigh fading channels with imperfect channel feedback. The performance criteria considered in this chapter are the symbol and bit error probability expressions of both $M$-PSK and $M$-ary rectangular QAM constellations with Gray code mapping. We validate the accuracy of the analysis through simulations, and assess the relative effects of channel estimation inaccuracy, feedback delay, and finite-rate quantization on the symbol and bit error performances. We begin with a brief overview of related work in this area.

## 2.1 Introduction

In a multiple input and single output (MISO) system, if the channel state information (CSI) is available at the transmitter (i.e., CSIT), one can achieve both the diversity and array gains with transmit beamforming via maximal ratio transmission (MRT) [9], whereas only diversity gain can be realized with space-time coding [10, 11].

Transmit beamforming for MISO systems is an active area of research. In [13], the authors consider efficient use of CSIT for transmit beamforming. An information theoretic approach to transmit beamforming with imperfect feedback is presented in [14, 15]. With MRT and binary phase shift keying (BPSK) modulation, the effect of feedback delay with perfect channel estimation (PCE) at the receiver is investigated in [16], whereas [17] studies the effect of imperfect channel estimation (ICE) without feedback delay. In [18], the authors extend the analysis of [16] accounting for the effects of channel estimation errors. The effect of feedback delay and feedback errors on the receiver signal-to-noise ratio (SNR) performance is investigated in [19] for phase-only feedback, whereas [20] analyzes the bit error probability (BEP) degradation with BPSK due to feedback errors with selection and co-phasing feedback schemes. The effects of finite-rate channel quantization and feedback delay are considered for BPSK in [21]. Finally, approaches for the design and analysis of transmit beamforming schemes under finite-rate constraints are presented in [22]-[27].

While the aforementioned works considered either BPSK (or quadrature PSK, QPSK) with channel estimation errors and perfect quantization [16]-[21], or ideal channel estimation with finite-rate quantization for general modulations [22]-[26], combined effect of various channel imperfections for general modulations is not yet investigated. The contribution in this chapter is targeted to fill in this important void. In this part of our work, we present a general framework for the performance analysis of transmit beamforming for MISO systems on spatially

independent Rayleigh fading channels with imperfect channel feedback. The feedback imperfections are characterized in terms of noisy channel estimation at the receiver side, quantization of CSI, and feedback delay. This formulation is shown to be applicable for any linear two-dimensional modulation scheme on spatially independent and identically distributed (i.i.d.) Rayleigh fading channels. Our analytical framework encompasses three popular MISO system models, namely, frequency-domain duplexing (FDD), FDD with finite rate quantization of CSI (FDDQ) and time-domain duplexing (TDD).

The modeling of imperfect feedback assumes that the *receiver does not know* both the estimation related error term and the delay related error term. We analyze average symbol error probability (SEP) and bit error probability (BEP) performances of $M$-PSK and $M$-ary rectangular QAM constellations with Gray code mapping. Our numerical and simulation results show that channel estimation inaccuracy and feedback delay are more harmful to the system performance compared to the effects of channel quantization.

The rest of this chapter is organized as follows. In Section 2.2 we introduce our system model. In Section 2.3 we present a model for imperfect channel feedback, and show that it captures the essential features of FDD system with/without feedback and TDD system. The decision variable (DV) at the receiver with imperfect feedback is also derived in Section 2.3. The average SEP and BEP expressions for $M$-PSK and $M$-QAM modulations are derived in Section 2.4. Numerical and simulation results are presented in Section 2.5. We conclude this chapter in Section 2.6.

Important variables: $t$- number of transmit antennas, $\rho_e$- estimation related correlation co-efficient, $\rho_d$- delay related correlation co-efficient, $\rho$- combined (delay and estimation) correlation coefficient, $\Omega$- variance of the actual channel, $\Lambda$- variance of the estimated channel, $B$- number of feedback bits, and $C$- size of the codebook.

## 2.2 System Model

We consider a MISO system with $t$ antennas at the base station (BS) and one antenna at the mobile station (MS) as shown in Fig. 1.2. The channel between the BS and the MS is modeled as a frequency-flat Rayleigh fading channel. Specifically, let us denote by $h_i[k]$ the complex channel gain at time $k$ between the $i$th antenna at the BS and the MS. We assume that $h_i[k]$ is a zero-mean, circularly symmetric complex Gaussian (CSCG) random variable with variance $E[|h_i[k]|^2] = \Omega$. We also assume that for any $i$ and $j$ $(i \neq j)$, and for any $k_1$ and $k_2$, $h_i[k_1]$ and $h_j[k_2]$ are uncorrelated, which can be justified for sufficient spacing between antenna elements. The vector valued channel at time $k$ is denoted by $\mathbf{h}[k] = [h_1[k], h_2[k], \ldots, h_t[k]]^{\mathsf{T}}$. The transmitted two-dimensional modulation symbol at time $k$ is denoted by $s_m[k]$ which belongs to the constellation $\mathcal{S}$. The average energy of $s_m[k]$ is $E[|s_m[k]|^2] = E_s$. Let us denote by $\mathbf{w}[k] = [w_1[k], w_2[k], \ldots, w_t[k]]^{\mathsf{T}}$, the unit norm (i.e., $\|\mathbf{w}\|^2 = 1$) beamforming vector (BV) at the base station at time $k$. Then, the received signal at the MS at time $k$ is

$$y[k] = \mathbf{h}^H[k]\mathbf{w}[k]s_m[k] + \eta[k] \tag{2.1}$$

where $\eta[k]$ is a zero-mean CSCG random variable with $E[|\eta[k]|^2] = \sigma_n^2$.

## 2.3 A General Framework for Feedback Imperfections

The specific structure of the beamforming vector $\mathbf{w}[k]$ at the base station (or transmitter) depends on various design considerations and system imperfections. However, for both FDD and TDD systems on Rayleigh fading channels, the BV $\mathbf{w}[k]$ is derived from the estimated channel vector which is assumed to be jointly Gaussian with the actual channel $\mathbf{h}[k]$. Note that this assumption is well justified [28] for many practical estimation techniques such as additive channel estimation, minimum mean square error (MMSE) channel estimation, and channel estimation derived from pilot-symbol assisted modulation [29].

We now dwell in detail on three popular channel feedback approaches for which we present a general framework for modeling nonideal feedback for MISO systems, and derive the decision variable at the input of the demodulator. These systems are: *i*) FDD with channel estimation errors and delayed feedback, *ii*) FDD with channel estimation errors, finite-rate quantization, and delayed feedback, and *iii*) TDD with channel estimation errors and channel decorrelation.

### 2.3.1 FDD System

Let us denote by $\widehat{\mathbf{h}}[k] = \left[\widehat{h}_1[k], \widehat{h}_2[k], \ldots, \widehat{h}_t[k]\right]^{\mathsf{T}}$ the channel estimate at the mobile station at time $k$. We assume that the estimate $\widehat{h}_i[k]$ on the path from the MS antenna and the $i$th antenna of the base station is a zero-mean, CSCG random variable with variance $E[|\widehat{h}_i[k]|^2] = \Lambda$. Similar to $\mathbf{h}[k]$, $\widehat{h}_i[k_1]$ and $\widehat{h}_j[k_2]$, for $i \neq j$, are also uncorrelated with each other. The MS simply feeds back the estimate $\widehat{\mathbf{h}}[k]$ to the BS. Assuming a feedback delay of $D$, the channel observed at the BS is $\widehat{\mathbf{h}}[k-D]$. The normalized delayed estimate forms the beamforming vector at the transmitter

$$\mathbf{w}[k] = \frac{\widehat{\mathbf{h}}[k-D]}{\|\widehat{\mathbf{h}}[k-D]\|}\,. \tag{2.2}$$

Let $\rho$ be the complex correlation coefficient between $h_i[k]$ and $\widehat{h}_i[k-D]$. That is,

$$\begin{aligned} \rho &= \frac{E\left[h_i[k]\widehat{h}_i^*[k-D]\right]}{\sqrt{E\left[|h_i[k]|^2\right] \times E\left[|\widehat{h}_i[k-D]|^2\right]}} \\ &= \frac{E\left[h_i[k]\widehat{h}_i^*[k-D]\right]}{\sqrt{\Omega\Lambda}}. \end{aligned} \tag{2.3}$$

As $h_i[k]$ and $\widehat{h}_i[k-D]$ are assumed to be jointly Gaussian, we can write [30]

$$h_i[k] = \rho\sqrt{\frac{\Omega}{\Lambda}}\,\widehat{h}_i[k-D] + \sqrt{(1-|\rho|^2)\Omega}\,\varepsilon_i[k-D], \quad i = 1, \ldots, t \tag{2.4}$$

where $\varepsilon_i[k]$ is zero-mean, CSCG random variable with variance $E[|\varepsilon_i[k]|^2] = 1$ and is uncorrelated with $\widehat{h}_i[k]$. In [28], it is shown that additive channel estimation

errors, MMSE channel estimation, and pilot-symbol assisted modulation-based channel estimation schemes [29] can be modeled by (2.4). Upon stacking the elements $\{h_i[k]\}$ in a column, (2.4) reads as

$$\mathbf{h}[k] = \rho\sqrt{\frac{\Omega}{\Lambda}}\,\widehat{\mathbf{h}}[k-D] + \sqrt{(1-|\rho|^2)\Omega}\,\boldsymbol{\varepsilon}[k-D] \tag{2.5}$$

where $\boldsymbol{\varepsilon}[k] = [\varepsilon_1[k], \varepsilon_2[k], \ldots, \varepsilon_t[k]]^{\mathsf{T}}$. Then, using (2.5), the equivalent received signal of (2.1) can be written as

$$\begin{aligned} y[k] &= \mathbf{h}^H[k]\mathbf{w}[k]s_m[k] + \eta[k] \\ &= \left(\rho\sqrt{\frac{\Omega}{\Lambda}}\,\widehat{\mathbf{h}}[k-D] + \sqrt{(1-|\rho|^2)\Omega}\,\boldsymbol{\varepsilon}[k-D]\right)^H \frac{\widehat{\mathbf{h}}[k-D]}{\|\widehat{\mathbf{h}}[k-D]\|}s_m[k] + \eta[k] \\ &= \bar{\rho}\sqrt{\frac{\Omega}{\Lambda}}\,\|\widehat{\mathbf{h}}[k-D]\|\,s_m[k] + \zeta[k] \end{aligned} \tag{2.6}$$

where

$$\zeta[k] = \sqrt{(1-|\rho|^2)\Omega}\,\left(\boldsymbol{\varepsilon}^H[k-D]\mathbf{w}[k]\right)\,s_m[k] + \eta[k].$$

$\zeta[k]$ conditioned on $|s_m[k]|$, is a zero-mean, CSCG random variable with variance

$$\Sigma^2_{|s_m[k]|} = \sigma_n^2 + |s_m[k]|^2\Omega(1-|\rho|^2).$$

We need the DV at the receiver for demodulation and for SEP/BEP analysis of a transmitted modulation symbol. The mobile station obtains the DV by dividing $y[k]$ by $\|\widehat{\mathbf{h}}[k-D]\|$, provided that the feedback delay $D$ is known. We remark that for constant amplitude signals (i.e., $M$-PSK) such a normalization is not needed as the decision regions are unchanged due to a positive scale factor. In this thesis, we assume that $D$ is known to the MS, so that the decision variable becomes

$$\begin{aligned} r[k] &= \frac{y[k]}{\|\widehat{\mathbf{h}}[k-D]\|} \\ &= \bar{\rho}\sqrt{\frac{\Omega}{\Lambda}}\,s_m[k] + \tilde{\zeta}[k] \end{aligned} \tag{2.7}$$

where $\tilde{\zeta}[k]$, conditioned on $|s_m[k]|$ and $\|\widehat{\mathbf{h}}[k-D]\|$, is a zero-mean CSCG random variable with variance

$$\sigma^2_{\tilde{\zeta}} = \frac{\Sigma^2_{|s_m[k]|}}{\|\widehat{\mathbf{h}}[k-D]\|^2}.$$

For simplicity, let us define

$$\beta \triangleq \frac{\|\widehat{\mathbf{h}}[k-D]\|^2}{\Lambda}.$$

Clearly, $\beta$ is a sum of $t$ i.i.d. exponential random variables, each with unit mean. That is, $\beta$ is gamma distributed with the probability density function (pdf) [30]

$$f_\beta(x) = \frac{e^{-x}x^{t-1}}{\Gamma(t)}, \quad x \geq 0, \tag{2.8}$$

and the cumulative distribution function (cdf) [30]

$$F_\beta(x) = \text{Prob}(\beta \leq x) = 1 - e^{-x}\sum_{k=0}^{t-1}\frac{x^k}{\Gamma(k+1)}, \quad x \geq 0 \tag{2.9}$$

where

$$\Gamma(n) = \int_0^\infty e^{-u}u^{n-1}du$$

is the standard Gamma function [103]. With this, $\sigma^2_{\tilde{\zeta}}$, conditioned on $|s_m[k]|$ and $\beta$, can be written as

$$\sigma^2_{\tilde{\zeta}} = \frac{\Sigma^2_{|s_m[k]|}}{\beta\Lambda}.$$

From (2.7), we notice that the effect of imperfect channel estimation and feedback delay on the DV at the mobile station is that of scaling the transmitted symbol $s_m[k]$ by *an unknown* complex number $\bar{\rho}\sqrt{\Omega/\Lambda}$ and introducing *symbol dependent non-Gaussian noise* $\tilde{\zeta}[k]$. The aforementioned framework can be directly applied to model non-ideal channel feedback effects in an analog feedback system [31], where feedback is not only delayed but also noisy.

To understand the combined effects of delay and estimation errors, we now describe the structure of the combined correlation coefficient $\rho$ and show how it relates to delay only correlation coefficient, $\rho_d$, and estimation error only correlation coefficient, $\rho_e$. With delay and no estimation errors, we have

$$h_i[k] = \rho_d h_i[k-D] + \sqrt{(1-|\rho_d|^2)\Omega}\,\tilde{\nu}_i[k] \tag{2.10}$$

where

$$\rho_d = \frac{E\left[h_i[k]h_i^*[k-D]\right]}{\Omega}. \tag{2.11}$$

On the other hand, estimation errors and no delay allows us to write

$$h_i[k] = \rho_e \sqrt{\frac{\Omega}{\Lambda}}\, \widehat{h}_i[k] + \sqrt{(1-|\rho_e|^2)\Omega}\, \nu_i[k], \tag{2.12}$$

where $\nu_i[k]$ is a zero-mean, CSCG random variable with variance $E[|\nu_i[k]|^2] = 1$ and is uncorrelated with $\widehat{h}_i[k]$. Here, $\rho_e$ is given by

$$\rho_e = \frac{E\left[h_i[k]\widehat{h}_i^*[k]\right]}{\sqrt{\Omega\Lambda}}.$$

Using (2.10) and (2.12) in the definition of $\rho$, given in (2.3), we arrive at

$$\rho = \frac{E\left[\left(\rho_e \sqrt{\frac{\Omega}{\Lambda}}\, \widehat{h}_i[k] + \sqrt{(1-|\rho_e|^2)\Omega}\, \nu_i[k]\right) \widehat{h}_i^*[k-D]\right]}{\sqrt{\Omega\Lambda}}. \tag{2.13}$$

Since $\nu_i[k]$ is uncorrelated with $\widehat{h}_i[k-D]$, (2.13) simplifies to

$$\rho = \rho_e \frac{E\left[\widehat{h}_i[k]\widehat{h}_i^*[k-D]\right]}{\Lambda} = \rho_e \rho_d. \tag{2.14}$$

That is, the combined correlation coefficient $\rho$ is the product of delay only correlation coefficient $\rho_d$ and estimation error only correlation coefficient $\rho_e$. Note that in the derivation of this result no particular structure is assumed for the time-variations of the channel.

### 2.3.2 FDD with Finite Rate Feedback (FDDQ) System

In this subsection we consider the effects of finite rate quantization along with imperfect channel estimation and delay. As illustrated in Fig. 1.2, in FDDQ, the mobile station estimates the channel, and quantizes it into one of $C = 2^B$ code words. The index, which is represented by $B$ bits, of the code word corresponding to the channel estimate is fed back to the base station. In this section, we assume that the feedback channel is error free, which can be justified by employing powerful error correction codes for protecting the index of the code word [22]-[27]. However, in addition to the delay in the feedback channel, channel coding introduces non negligible delay in decoding the code word index. For simplicity, let

$$\widehat{\mathbf{v}}[k-D] = \frac{\widehat{\mathbf{h}}[k-D]}{\|\widehat{\mathbf{h}}[k-D]\|},$$

and $\tilde{\mathbf{v}}[k-D] = \mathbf{w}[k]$. Then,

$$\tilde{\mathbf{v}}[k-D] = \mathcal{Q}\left[\widehat{\mathbf{v}}[k-D]\right], \tag{2.15}$$

where $\mathcal{Q}$ is the vector quantization function. Now, the received signal with (2.15) is given by

$$y[k] = \mathbf{h}^H[k]\tilde{\mathbf{v}}[k-D]\, s_m[k] + \eta[k]. \tag{2.16}$$

After substituting (2.5) for $\mathbf{h}[k]$, the received signal (2.16) can be written as

$$y[k] = \bar{\rho}\sqrt{\frac{\Omega}{\Lambda}}\,\widehat{\mathbf{h}}^H[k-D]\tilde{\mathbf{v}}[k-D]s_m[k] + \upsilon[k]. \tag{2.17}$$

Here, conditioned on $|s_m[k]|$ and $\tilde{\mathbf{v}}[k-D]$, $\upsilon[k]$ is a zero-mean, CSCG random variable with variance

$$\sigma_n^2 + |s_m[k]|^2(1-|\rho|^2)\Omega.$$

Let us define the following to simplify (2.17)

$$\vartheta \triangleq \langle \widehat{\mathbf{v}}[k-D], \tilde{\mathbf{v}}[k-D]\rangle,$$

where $\langle \mathbf{x}, \mathbf{y}\rangle = \mathbf{x}^H\mathbf{y}$. This allows us to write $y[k]$ as

$$y[k] = \bar{\rho}\sqrt{\frac{\Omega}{\Lambda}}\,\|\widehat{\mathbf{h}}[k-D]\|\vartheta s_m[k] + \upsilon[k].$$

Since the delay $D$ is assumed to be known to the receiver (i.e., the mobile station knows $\|\widehat{\mathbf{h}}[k-D]\|$ and $\vartheta$), we form the decision variable as

$$\begin{aligned} r[k] &= \frac{y[k]}{\|\widehat{\mathbf{h}}[k-D]\|\vartheta} \\ &= \bar{\rho}\sqrt{\frac{\Omega}{\Lambda}}\, s_m[k] + \frac{\upsilon[k]}{\|\widehat{\mathbf{h}}[k-D]\|\vartheta} \\ &= \bar{\rho}\sqrt{\frac{\Omega}{\Lambda}}\, s_m[k] + \tilde{\upsilon}[k], \end{aligned} \tag{2.18}$$

where, conditioned on $|s_m[k]|$, $\beta$ and $\tilde{\Delta}$, $\tilde{\upsilon}[k]$ is a zero-mean CSCG random variable with variance

$$\frac{\sigma_n^2 + |s_m[k]|^2(1-|\rho|^2)\Omega}{\beta\tilde{\Delta}\Lambda}.$$

Here, $\tilde{\Delta} \triangleq |\vartheta|^2$. Since finding the exact pdf of $\tilde{\Delta}$ is rather difficult, [25] upper bounded $\tilde{\Delta}$ (i.e., lower bounded the average error performance) by a random variable $\Delta$, whose pdf is given by

$$f_{\Delta}(x) = 2^B(t-1)(1-x)^{t-2}, \quad 1-\psi < x < 1, \tag{2.19}$$

where $\psi = 2^{-B/(t-1)}$. Independently, in [26] the authors showed that (2.19) is a very accurate approximation to the true pdf of $\tilde{\Delta}$. Note that when $B \to \infty$, we have $\psi \to 0$ and (2.19) reduces to $f_{\Delta}(x) = \delta(x-1)$ [22, 25, 26], where, $\delta$ is the dirac delta function. In what follows, we use $\Delta$ in place of $\tilde{\Delta}$.

### 2.3.3 TDD System

In this subsection we briefly describe how the framework developed in the previous Section 2.3.1, with some modifications, is applicable to a time division duplexing system. In a TDD system, assuming channel reciprocity, the mobile station sounds the channel with known symbols to facilitate the base station estimate of the channel. Assuming a single pilot symbol $x_0$, which is known to the base station, the received signal on the $l^{th}$ antenna at the BS is given by

$$p_l[k] = h_l[k]x_0 + \mu_l[k], \quad l = 1, 2, \ldots, t, \tag{2.20}$$

where $\mu_l[k]$ is a zero-mean, CSCG random variable with variance $E[|\mu_l[k]|^2] = \sigma_n^2$, $x_0$ is deterministic with power $|x_0|^2 = \sigma_x^2$, and $h_l[k]$ is the channel between the $l^{th}$ antenna at the base station and mobile station. For simplicity, assuming minimum mean-square error (MMSE) channel estimation, the estimate $\widehat{h}_l[k]$ of the $l$th channel is given by

$$\widehat{h}_l[k] = \left(\frac{\sigma_x \Omega}{\sigma_x^2 \Omega + \sigma_n^2}\right) p_l[k]\,, \quad l = 1, 2, \ldots, t. \tag{2.21}$$

Therefore,

$$\Lambda = E[|\widehat{h}_l[k]|^2] = \frac{\Omega \gamma_{p,\mathsf{T}}}{1 + \gamma_{p,\mathsf{T}}}$$

and

$$\rho_e^2 = \frac{\gamma_{p,\mathsf{T}}}{1+\gamma_{p,\mathsf{T}}}$$

where

$$\gamma_{p,\mathsf{T}} = \frac{\Omega\sigma_x^2}{\sigma_n^2}$$

is the average received SNR for the pilot. For FDD systems, a simple approach to channel estimation is the use of orthogonal pilot transmissions. That is, single a pilot symbol-based channel estimation requires $t$ time units. One approach for fair comparison between TDD and FDD systems is to set the total average received pilot SNR the same. Then, the aforementioned $\Lambda$ and $\rho_e^2$ can be used with

$$\gamma_{p,\mathsf{F}} = \frac{\gamma_{p,\mathsf{T}}}{t}\,.$$

We note that the above formulation can easily be generalized to multiple pilot symbols, time varying channel conditions, and for various practical channel estimation schemes. We also account for a delay $D$ between the time of channel estimation, and the time of its actual use. Note that this delay might not be as severe as that of the delay in FDD schemes. Then, the transmit BV is given by (2.2) and the received signal $y[k]$ is exactly the same as (2.6) of the previous FDD approach, which is reproduced here as

$$y[k] = \bar{\rho}\sqrt{\frac{\Omega}{\Lambda}}\,\|\widehat{\mathbf{h}}[k-D]\|s_m[k] + \zeta[k].$$

For the demodulation of $s_m[k]$, the receiver needs the knowledge of $\|\widehat{\mathbf{h}}[k-D]\|$, which has to come from a feed-forward (as opposed to feedback) channel between the base station and the mobile. This feed-forward requirement in TDD system is counterintuitive to the traditional argument that feedback is not required for TDD systems. Assuming ideal channel knowledge of $\|\widehat{\mathbf{h}}[k-D]\|$ (i.e., in this section we ignore the quantization of $\|\widehat{\mathbf{h}}[k-D]\|$) at the receiver, the decision variable is again given by (2.7), reproduced here as:

$$r[k] \;=\; \bar{\rho}\,\sqrt{\frac{\Omega}{\Lambda}}\,s_m[k] + \tilde{\zeta}[k].$$

## 2.4 Error Probability Analysis

In this section, we analyze the average SEP and BEP performances of $M$-PSK and rectangular $M$-QAM modulation with Gray code symbol mapping. Upon observing (2.7) and (2.18), the decision variable at the demodulation input can be expressed in a parametric form as

$$r[k] = \kappa s_m[k] + \xi[k] = r_I[k] + j r_Q[k], \tag{2.22}$$

where

$$\kappa = \bar{\rho}\sqrt{\Omega/\Lambda} \triangleq \mu_I + j\mu_Q,$$

and $\xi[k]$, conditioned on $|s_m[k]|$, $\beta$ and $\Delta$, is a CSCG random variable with variance

$$\frac{\mathcal{F}(|s_m[k]|)}{\beta\Delta}$$

where

$$\mathcal{F}(|s_m[k]|) = \frac{\sigma_n^2 + (1-|\rho|^2)|s_m[k]|^2\Omega}{\Lambda}.$$

Note that for FDD and TDD schemes, we can set $\Delta = 1$ (i.e., $f_\Delta(x) = \delta(x-1)$). On the other hand, for FDDQ the pdf of $\Delta$ is given by (2.19). It is important to note that, due to the presence of signal dependant noise together with the *unknown constant* $\kappa$, it is not possible to borrow the existing error probability expressions that are available in the literature for PSK and rectangular QAM constellations [12,33], and extend them to the present case of ICE, delay and finite-rate quantization. This motivates us to derive the error probability expressions *ab initio* using the decision variable given by (2.18).

### 2.4.1 $M$-PSK Constellation

Since for $M$-PSK, $|s_m[k]|$ is not a function of the index $m$, we then define

$$\mho \triangleq \mathcal{F}(|s_m[k]|) = \frac{\sigma_n^2 + (1-|\rho|^2)E_s\Omega}{\Lambda}.$$

With $M$-PSK modulation, the DV of interest is the phase angle $\Theta$ of the received signal $r[k]$. Conditioned on $\beta$ and $\Delta$, the cdf of $\Theta$ can be obtained as a special case

of the results presented by Pawula et al. in [36], wherein the authors derived a general expression for the cdf of the phase angle between two vectors corrupted by Gaussian noise. Upon using the results in [36], the conditional cdf of $\Theta$, conditioned on $\beta$ and $\Delta$, when $\theta_m = \frac{2m\pi}{M}$ is the transmitted phase, can be expressed as

$$\begin{aligned} &\text{Prob}(\omega_1 \leq \Theta \leq \omega_2; \lambda|\beta\Delta) \qquad (2.23)\\ &= \begin{cases} F_{\Theta|\beta\Delta}(\omega_2 - \theta_m - \phi_\rho; \lambda) - F_{\Theta|\beta\Delta}(\omega_1 - \theta_m - \phi_\rho; \lambda) + 1 \\ \qquad\qquad\qquad\qquad\qquad\qquad \text{if } \omega_1 < \theta_m + \phi_\rho < \omega_2 \\ F_{\Theta|\beta\Delta}(\omega_2 - \theta_m - \phi_\rho; \lambda) - F_{\Theta|\beta\Delta}(\omega_1 - \theta_m - \phi_\rho; \lambda) \\ \qquad\qquad\qquad\qquad\qquad\qquad \text{if } \omega_1 > \theta_m + \phi_\rho \text{ or } \omega_2 < \theta_m + \phi_\rho, \end{cases} \end{aligned}$$

where $\omega_1 < \omega_2$, $\phi_\rho$ is the phase angle of $\bar{\rho}$, and

$$\begin{aligned} \lambda &= \frac{|\kappa|^2 E_s}{\mho} \\ &= \frac{|\rho|^2\gamma}{1 + (1 - |\rho|^2)\gamma} \end{aligned}$$

where

$$\gamma = \frac{\Omega E_s}{\sigma_n^2}$$

is the average received SNR per symbol with ICE. In (2.23)

$$F_{\Phi|\beta\Delta}(\theta; \lambda) = -\frac{\text{sgn}(\theta)}{2\pi} \int_0^{\pi - |\theta|} \exp\left(-\lambda\beta\Delta \frac{\sin^2\theta}{\sin^2 x}\right) dx, \qquad -\pi < \theta < \pi, \qquad (2.24)$$

which is also referred to as Pawula's $F$ function [12]. In (2.24) $\text{sgn}(x) = 1$ for $x \geq 0$ and is equal to $-1$ otherwise. Due to the discontinuity of $F_{\Phi|\beta\Delta}(\theta; \cdot)$ of (2.24) at $\theta = 0$, for evaluating (2.23) either at $\omega_1 = 0$ or $\omega_2 = 0$ we have to use $F_{\Phi|\beta\Delta}(\omega_1 = 0; \cdot) = -1/2$ and $F_{\Phi|\beta\Delta}(\omega_2 = 0; \cdot) = 1/2$. For more details please refer to [36].

#### 2.4.1.1 Average Symbol Error Probability

In this subsection we derive the expressions for average SEP of $M$-PSK. Upon using the conditional cdf (2.23) of $\Theta$ with $\omega_1 = \theta_m - \pi/M$ and $\omega_2 = \theta_m + \pi/M$

and subtracting the result from unity, we can obtain the average SEP of $M$-PSK modulation, conditioned on $\beta$ and $\Delta$, as

$$P_{s,PSK}(\beta\Delta) = \frac{\mathrm{sgn}(\frac{\pi}{M}-\phi_\rho)}{2\pi}\int_0^{\pi-|\frac{\pi}{M}-\phi_\rho|} e^{-\frac{\lambda\beta\Delta\sin^2(\frac{\pi}{M}-\phi_\rho)}{\sin^2\theta}}d\theta + \frac{\mathrm{sgn}(\frac{\pi}{M}+\phi_\rho)}{2\pi}\int_0^{\pi-|\frac{\pi}{M}+\phi_\rho|} e^{-\frac{\lambda\beta\Delta\sin^2(\frac{\pi}{M}+\phi_\rho)}{\sin^2\theta}}d\theta, \tag{2.25}$$

which is valid for $|\phi_\rho| < \pi/M$[1]. To arrive at the average SEP performance, we need to average (2.25) over $\beta$ and $\Delta$. To reduce the analytical complications, we note that it is important to take the average of (2.25) first over $\beta$ then over $\Delta$. Proceeding further, by averaging (2.25) over the pdf of $\beta$, as given in (2.8), we arrive at

$$\begin{aligned}\tilde{P}_{s,PSK}(\Delta) &= E\left[P_{s,PSK}(\beta\Delta)\right] \\ &= \frac{\mathrm{sgn}(\frac{\pi}{M}-\phi_\rho)}{2\pi}\int_0^{\pi-|\frac{\pi}{M}-\phi_\rho|}\left(\frac{\sin^2\theta}{\sin^2\theta+\lambda\Delta\sin^2(\frac{\pi}{M}-\phi_\rho)}\right)^t d\theta + \\ &\quad \frac{\mathrm{sgn}(\frac{\pi}{M}+\phi_\rho)}{2\pi}\int_0^{\pi-|\frac{\pi}{M}+\phi_\rho|}\left(\frac{\sin^2\theta}{\sin^2\theta+\lambda\Delta\sin^2(\frac{\pi}{M}+\phi_\rho)}\right)^t d\theta. \end{aligned} \tag{2.26}$$

For FDD and TDD schemes, we have $\Delta = 1$. Therefore, the average SEP is given by

$$\overline{P}_{s,PSK,FDD/TDD} = \tilde{P}_{s,PSK}(1). \tag{2.27}$$

With FDDQ, the average SEP can be obtained by averaging (2.26) over the pdf of $\Delta$ which is given (2.19). In Appendix, this averaging is performed in closed-form, and the final expression for the average SEP with FDDQ is

$$\begin{aligned}\overline{P}_{s,PSK,FDDQ} &= \frac{\mathrm{sgn}(\frac{\pi}{M}-\phi_\rho)}{2\pi}\overline{\mathcal{G}}\left(\pi-|\frac{\pi}{M}-\phi_\rho|,\sqrt{\lambda\sin^2(\frac{\pi}{M}-\phi_\rho)},t,B,\psi\right) + \\ &\quad \frac{\mathrm{sgn}(\frac{\pi}{M}+\phi_\rho)}{2\pi}\overline{\mathcal{G}}\left(\pi-|\frac{\pi}{M}+\phi_\rho|,\sqrt{\lambda\sin^2(\frac{\pi}{M}+\phi_\rho)},t,B,\psi\right) \end{aligned} \tag{2.28}$$

where $\overline{\mathcal{G}}(\cdot,\cdot,\cdot,\cdot,\cdot)$ is given by (2.72) in Appendix. With $\rho = 1$ the average SEP, $\overline{P}_{s,PSK,FDDQ}$, simplifies to the results presented in [25].

[1] When $|\phi_\rho| \geq \pi/M$, the result of (2.25) with $|\phi_\rho| < \pi/M$ should be subtracted from unity.

#### 2.4.1.2 Average Bit Error Probability

Since average BEP is also an important performance measure on fading channels, we now derive expressions for the average BEP of $M$-PSK modulation with Gray code labeling. Our approach to average BEP analysis is essentially motivated by [37]. Similar to [37], we define $\mathcal{P}(k;\beta\Delta)$ as the probability of the received signal phase, $\Theta$, falling in a wedge of width $2\pi/M$ centered around the $k$th symbol point $k = 1,\ldots,M-1$, conditioned on $\beta$ and $\Delta$, when $S_0 = \sqrt{E_s}$ is the transmitted signal. With the help of (2.23) and $\theta_m = 0$, $\mathcal{P}(k;\beta\Delta)$ can be expressed as

$$\mathcal{P}(k;\beta\Delta) = \text{Prob}\left(\theta_k - \frac{\pi}{M} \leq \Theta \leq \theta_k + \frac{\pi}{M}; \lambda|\beta\Delta\right). \tag{2.29}$$

To proceed further, let $|\phi_\rho - \theta_k| > \pi/M$. This allows us to simplify (2.29), using (2.23) and (2.24), as

$$\begin{aligned}\mathcal{P}(k;\beta\Delta) &= \frac{\text{sgn}(\theta_k + \frac{\pi}{M} - \phi_\rho)}{2\pi} \int_0^{\pi - |\theta_k + \frac{\pi}{M} - \phi_\rho|} e^{-\frac{\lambda\beta\Delta \sin^2(\theta_k + \frac{\pi}{M} - \phi_\rho)}{\sin^2\theta}} d\theta - \\ &\quad \frac{\text{sgn}(\theta_k - \frac{\pi}{M} - \phi_\rho)}{2\pi} \int_0^{\pi - |\theta_k - \frac{\pi}{M} - \phi_\rho|} e^{-\frac{\lambda\beta\Delta \sin^2(\theta_k - \frac{\pi}{M} - \phi_\rho)}{\sin^2\theta}} d\theta. \end{aligned} \tag{2.30}$$

Note that when $|\phi_\rho - \theta_k| \leq \pi/M$, expressions analogous to (2.30) can be derived in a similar manner. Following the steps of (2.26), $\tilde{\mathcal{P}}(k;\Delta) = E[\mathcal{P}(k,\beta\Delta)]$ (i.e., averaging $\mathcal{P}(k;\beta\Delta)$ over $\beta$) is

$$\begin{aligned}\tilde{\mathcal{P}}(k;\Delta) &= E[\mathcal{P}(k,\beta\Delta)] \\ &= \frac{\text{sgn}(\theta_k + \frac{\pi}{M} - \phi_\rho)}{2\pi} \int_0^{\pi - |\theta_k + \frac{\pi}{M} - \phi_\rho|} \left(\frac{\sin^2\theta}{\sin^2\theta + \lambda\Delta \sin^2(\theta_k + \frac{\pi}{M} - \phi_\rho)}\right)^t d\theta - \\ &\quad \frac{\text{sgn}(\theta_k - \frac{\pi}{M} - \phi_\rho)}{2\pi} \int_0^{\pi - |\theta_k - \frac{\pi}{M} - \phi_\rho|} \left(\frac{\sin^2\theta}{\sin^2\theta + \lambda\Delta \sin^2(\theta_k - \frac{\pi}{M} - \phi_\rho)}\right)^t d\theta. \end{aligned} \tag{2.31}$$

Using (2.72) of Appendix, the average $\overline{\mathcal{P}}(k) = E[\tilde{\mathcal{P}}(k;\Delta)]$ of (2.31) over $\Delta$ can be expressed as

$$\begin{aligned}\overline{\mathcal{P}}(k) = &\frac{\mathrm{sgn}(\theta_k + \frac{\pi}{M} - \phi_\rho)}{2\pi}\overline{\mathcal{G}}\left(\pi - |\theta_k + \frac{\pi}{M} - \phi_\rho|, \sqrt{\lambda \sin^2(\theta_k + \frac{\pi}{M} - \phi_\rho)}, t, B, \psi\right) \\ &- \frac{\mathrm{sgn}(\theta_k - \frac{\pi}{M} - \phi_\rho)}{2\pi}\overline{\mathcal{G}}\left(\pi - |\theta_k - \frac{\pi}{M} - \phi_\rho|, \sqrt{\lambda \sin^2(\theta_k - \frac{\pi}{M} - \phi_\rho)}, t, B, \psi\right)\end{aligned} \tag{2.32}$$

which is applicable to FDDQ only. For FDD and TDD systems, $\overline{\mathcal{P}}(k) = \tilde{\mathcal{P}}(k;1)$. Using (2.32), the average BEP for Gray coded $M$-PSK signal set with finite-rate, imperfect feedback is

$$\overline{P}_{\mathrm{b},PSK} = \frac{1}{\log_2(M)} \sum_{k=1}^{M-1} d(k)\overline{\mathcal{P}}(k), \tag{2.33}$$

where $d(k)$ is the weight spectrum of Gray code, derived in [37], which is reproduced here as

$$d(k) = 2\left|\frac{k}{M} - \left\lfloor \frac{k}{M} \right\rceil\right| + 2\sum_{i=2}^{\log_2(M)} \left|\frac{k}{2^i} - \left\lfloor \frac{k}{2^i} \right\rceil\right|, \tag{2.34}$$

where $\lfloor x \rceil$ rounds $x$ to the closest integer. With $M = 2$, $\Delta = 1$, $\phi_\rho = 0$ and $\rho_e = 1$ (i.e., $\rho = \rho_d$ for a delayed feedback case), (2.33), with the help of (2.31), coincides with the results presented in [16]. We also note that the average BEP expressions in [16] can be derived in a very simple way using the methodology presented here.

### 2.4.2 $M_1 \times M_2$-Rectangular QAM Constellation

Let us denote $s_m[k] = s_{m,x}[k] + j s_{m,y}[k]$, $m = 0, 1, \ldots, M-1$, $x = 0, 1, \ldots, M_1 - 1$, $y = 0, 1, \ldots, M_2 - 1$, where the $M$-QAM constellation is of size $M = M_1 M_2$. Here $s_{m,x}[k] = a_{m,x}[k]d$, and $s_{m,y}[k] = a_{m,y}[k]d$, where $a_{m,x}[k] = -(M_1 - 1) + 2x$ (i.e., $a_{m,x}[k]d$ is the in-phase $M_1$-PAM constellation symbol) and $a_{m,y}[k] = -(M_2 - 1) + 2y$ (i.e., $a_{m,y}[k]d$ is the quadrature-phase $M_2$- PAM constellation symbol). The minimum distance of the constellation is $2d$. For simplicity, we define, for $x = 0, 1, \ldots, M_1 - 1$ and $y = 0, 1, \ldots, M_2 - 1$, the parameter $\gamma_{x,y}$ as

$$\gamma_{x,y} \triangleq \frac{2d^2}{\mathcal{F}(|s_m[k]|)} = \frac{2d^2\Lambda}{\sigma_n^2 + \Omega(1 - |\rho|^2)|s_m[k]|^2}. \tag{2.35}$$

#### 2.4.2.1 Average Symbol Error Probability

Let us denote by $\mathcal{P}_{C,x,y}(\beta\Delta)$ the probability of correctly receiving $s_{m,x}[k]+js_{m,y}[k]$, conditioned on $\beta$ and $\Delta$. For $x = 1, 2 \ldots, M_1 - 2$, $y = 1, 2, \ldots, M_2 - 2$, $\mathcal{P}_{C,x,y}(\beta\Delta)$ can be expressed as

$$\begin{aligned}\mathcal{P}_{C,x,y}(\beta\Delta) &= \text{Prob}(s_{m,x}[k] - d \le r_I[k] < s_{m,x}[k] + d|\beta\Delta) \times \\ &\quad \text{Prob}(s_{m,y}[k] - d \le r_Q[k] < s_{m,y}[k] + d|\beta\Delta) = \\ &\quad \Big\{Q(\mathsf{t}_1(x,y)\sqrt{\beta\Delta}) - Q(\mathsf{t}_2(x,y)\sqrt{\beta\Delta})\Big\} \times \\ &\quad \Big\{Q(\mathsf{t}_3(x,y)\sqrt{\beta\Delta}) - Q(\mathsf{t}_4(x,y)\sqrt{\beta\Delta})\Big\}, \end{aligned} \tag{2.36}$$

where

$$Q(x) = \frac{1}{\sqrt{2\pi}} \int_x^\infty \exp(-u^2/2)\, du$$

and

$$\mathsf{t}_1(x,y) = (a_{m,x}[k] - 1 - a_{m,x}[k]\mu_I + a_{m,y}[k]\mu_Q)\sqrt{\gamma_{x,y}}\,, \tag{2.37}$$

$$\mathsf{t}_2(x,y) = (a_{m,x}[k] + 1 - a_{m,x}[k]\mu_I + a_{m,y}[k]\mu_Q)\sqrt{\gamma_{x,y}}\,, \tag{2.38}$$

$$\mathsf{t}_3(x,y) = (a_{m,y}[k] - 1 - a_{m,x}[k]\mu_Q - a_{m,y}[k]\mu_I)\sqrt{\gamma_{x,y}}\,, \tag{2.39}$$

$$\mathsf{t}_4(x,y) = (a_{m,y}[k] + 1 - a_{m,x}[k]\mu_Q - a_{m,y}[k]\mu_I)\sqrt{\gamma_{x,y}}\,. \tag{2.40}$$

For ease of referencing, expressions for $\mathcal{P}_{C,x,y}(\beta\Delta)$ for other values of $x$ and $y$ are given in Table 2.1. Let us define by $\overline{\mathcal{P}}_{C,x,y} \triangleq E[\mathcal{P}_{C,x,y}(\beta\Delta)]$ the probability of correct reception of $s_{m,x}[k] + js_{m,y}[k]$, averaged over $\beta$ and $\Delta$. Notice that, each of the $\mathcal{P}_{C,x,y}(\beta\Delta)$ expressions in Table 2.1 can be expressed as linear combinations of $Q(a\sqrt{\beta\Delta}) \times Q(b\sqrt{\beta\Delta})$ for real values of $a$ and $b$. To derive $\overline{\mathcal{P}}_{C,x,y}$, we must determine $E[Q(a\sqrt{\beta\Delta}) \times Q(b\sqrt{\beta\Delta})]$, averaged over the distributions of $\beta$ and $\Delta$. Similar to the PSK analysis of Section 2.4.1.1 we notice that keeping the order of integration, first over $\beta$ and then over $\Delta$, results in efficient evaluation of the

expressions. To this end, we define the following functions:

$$\mathcal{H}_1(a,b,\Delta,t) \triangleq E[Q(a\sqrt{\beta\Delta})Q(b\sqrt{\beta\Delta})] \tag{2.41}$$
$$= \begin{cases} \mathcal{J}_1(|a|,|b|,\Delta,t) & \text{if } a\geq 0, b\geq 0 \\ \mathcal{K}_1(|a|,\Delta,t)-\mathcal{J}_1(|a|,|b|,\Delta,t) & \text{if } a\geq 0, b<0 \\ \mathcal{K}_1(|b|,\Delta,t)-\mathcal{J}_1(|a|,|b|,\Delta,t) & \text{if } a<0, b\geq 0 \\ 1-\mathcal{K}_1(|a|,\Delta,t)-\mathcal{K}_1(|b|,\Delta,t)+ & \\ \qquad\qquad \mathcal{J}_1(|a|,|b|,\Delta,t) & \text{if } a<0, b<0\,, \end{cases},$$

$$\mathcal{J}_1(a,b,y,t) = E[Q(a\sqrt{y\beta})Q(b\sqrt{y\beta})] \quad \text{for } a,b,y\geq 0, \tag{2.42}$$
$$\mathcal{K}_1(a,y,t) = E[Q(a\sqrt{y\beta})] \quad \text{for } a,y\geq 0, \tag{2.43}$$
$$\mathcal{H}(a,b,t,B,\psi) = E[\mathcal{H}_1(a,b,\Delta,t)] \quad \text{for } a,\ b \text{ real}, \tag{2.44}$$
$$\mathcal{J}(a,b,t,B,\psi) = E[\mathcal{J}_1(a,b,\Delta,t)] \quad \text{for } a,b\geq 0, \tag{2.45}$$
$$\mathcal{K}(a,t,B,\psi) = E[\mathcal{K}_1(a,\Delta,t)] \quad \text{for } a\geq 0, \tag{2.46}$$

$$\mathcal{R}_1(a,y,t) \triangleq E[Q(a\sqrt{y\beta})]$$
$$= \begin{cases} \mathcal{K}_1(|a|,y,t) & \text{if } a,y\geq 0\,, \\ 1-\mathcal{K}_1(|a|,y,t) & \text{if } a<0, y\geq 0\,, \end{cases} \tag{2.47}$$
$$\text{and} \quad \mathcal{R}(a,t,B,\psi) = E[\mathcal{R}_1(a,\Delta,t)]$$
$$= \begin{cases} \mathcal{K}(|a|,t,B,\psi) & \text{if } a\geq 0\,, \\ 1-\mathcal{K}(|a|,t,B,\psi) & \text{if } a<0 \end{cases} \tag{2.48}$$

where, in Appendix, expressions for (2.42), (2.43), (2.45) and (2.46) are given in (2.56), (2.71), (2.64) and (2.74), respectively. Using (2.41) and (2.37)-(2.40), each row in Table 2.1 can be averaged over $\beta$ to arrive at $\tilde{\mathcal{P}}_{C,x,y}(\Delta)$, $x = 0,1,\ldots,M_1-1$, $y = 0,1,\ldots,M_2-1$. Upon further averaging $\tilde{\mathcal{P}}_{C,x,y}(\Delta)$, with the help of (2.44), over $\Delta$ of (2.19), we arrive at $\overline{\mathcal{P}}_{C,x,y}$ for FDDQ. For FDD and TDD schemes, note that $\overline{\mathcal{P}}_{C,x,y} = \tilde{\mathcal{P}}_{C,x,y}(1)$. For convenience, $\overline{\mathcal{P}}_{C,x,y}$ are tabulated in Table 2 for

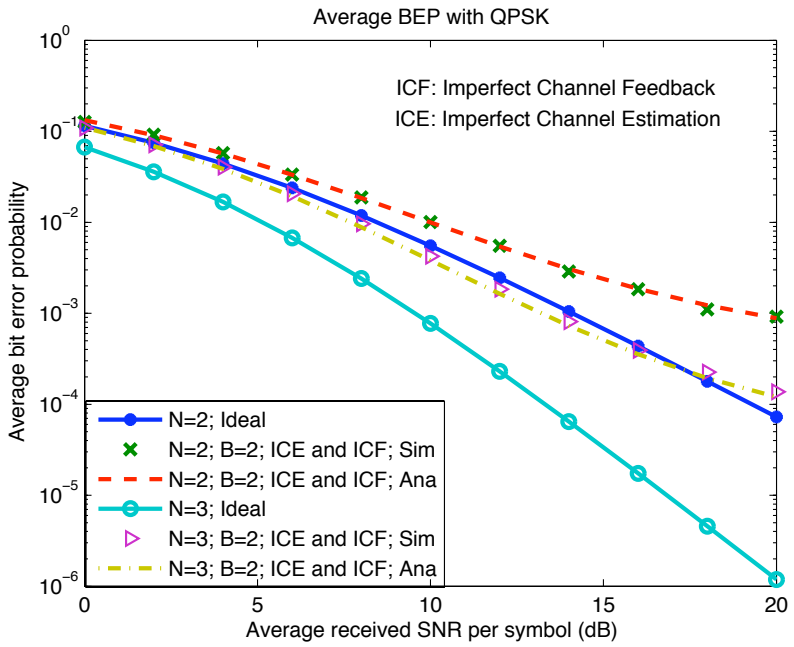


Figure 2.1 Average BEP performance of QPSK modulation with imperfect channel estimation, feedback delay, and feedback channel quantization. Here, we assume $t = 2$ and 3 antennas, with $B = 2$ feedback bits, $\rho_d = 0.99$ and average received SNR of the pilot channel $\gamma_p = 30$ dB.

FDDQ. Using them, the average SEP can be written as

$$\begin{aligned} \overline{P}_{s,QAM} &= \frac{1}{M}\sum_{x=0}^{M_1-1}\sum_{y=0}^{M_2-1}(1-\overline{\mathcal{P}}_{C,x,y}) \\ &= 1-\frac{1}{M}\sum_{x=0}^{M_1-1}\sum_{y=0}^{M_2-1}\overline{\mathcal{P}}_{C,x,y}. \end{aligned} \tag{2.49}$$

With $\kappa = 1$ and $\rho = 1$ (i.e., with perfect channel estimation), it is easy to show that (2.49) coincides with the results presented in [25].

#### 2.4.2.2 Average Bit Error Probability

In this section, we present average BEP analysis of Gray coded $M_1 \times M_2$-QAM constellation. We follow the same Gray code labeling approach as considered in [34], which is briefly described as follows. We define $k_1 = \log_2(M_1)$,

Table 2.1 For each $x \in \{0, 1, \ldots, M_1 - 1\}$ and $y \in \{0, 1, \ldots, M_2 - 1\}$, conditioned on $\beta$ and $\Delta$, the probability of correct reception of the symbol $s_m[k]]$ is tabulated on the third column. In the above table $\hat{\gamma} = \sqrt{\gamma_{x,y}\beta\Delta}$.

| $x$ | $y$ | $P_{C,x,y}(\beta\Delta) =$ Prob $\left(s_{m,x}[k] + js_{m,y}[k] \text{ received successfully} \middle| \beta\Delta\right)$ |
|---|---|---|
| $\{1, \ldots, M_1 - 2\}$ | $\{1, \ldots, M_2 - 2\}$ | $\text{Prob}(s_{m,x}[k] - d \le r_I[k] < s_{m,x}[k] + d \vert \beta\Delta) \times$ $\text{Prob}(s_{m,y}[k] - d \le r_Q[k] < s_{m,y}[k] + d \vert \beta\Delta) =$ $\left\{Q\left([a_{m,x}[k] - 1 - a_{m,x}[k]\mu_I + a_{m,y}[k]\mu_Q]\,\hat{\gamma}\right) - Q\left([a_{m,x}[k] + 1 - a_{m,x}[k]\mu_I + a_{m,y}[k]\mu_Q]\,\hat{\gamma}\right)\right\} \times$ $\left\{Q\left([a_{m,y}[k] - 1 - a_{m,x}[k]\mu_Q - a_{m,y}[k]\mu_I]\,\hat{\gamma}\right) - Q\left([a_{m,y}[k] + 1 - a_{m,x}[k]\mu_Q - a_{m,y}[k]\mu_I]\,\hat{\gamma}\right)\right\}$ |
| $\{1, \ldots, M_1 - 2\}$ | $\{0\}$ | $\text{Prob}(s_{m,x}[k] - d \le r_I[k] < s_{m,x}[k] + d \vert \beta\Delta) \times$ $\text{Prob}(-\infty < r_Q[k] < s_{m,y}[k] + d \vert \beta\Delta) =$ $Q\left(-[a_{m,y}[k] + 1 - a_{m,x}[k]\mu_Q - a_{m,y}[k]\mu_I]\,\hat{\gamma}\right) \times$ $\left\{Q\left([a_{m,x}[k] - 1 - a_{m,x}[k]\mu_I + a_{m,y}[k]\mu_Q]\,\hat{\gamma}\right) - Q\left([a_{m,x}[k] + 1 - a_{m,x}[k]\mu_I + a_{m,y}[k]\mu_Q]\,\hat{\gamma}\right)\right\}$ |
| $\{1, \ldots, M_1 - 2\}$ | $\{M_2 - 1\}$ | $\text{Prob}(s_{m,x}[k] - d \le r_I[k] < s_{m,x}[k] + d \vert \beta\Delta) \times$ $\text{Prob}(s_{m,y}[k] - d \le r_Q[k] < \infty \vert \beta\Delta) =$ $Q\left([a_{m,y}[k] - 1 - a_{m,x}[k]\mu_Q - a_{m,y}[k]\mu_I]\,\hat{\gamma}\right) \times$ $\left\{Q\left([a_{m,x}[k] - 1 - a_{m,x}[k]\mu_I + a_{m,y}[k]\mu_Q]\,\hat{\gamma}\right) - Q\left([a_{m,x}[k] + 1 - a_{m,x}[k]\mu_I + a_{m,y}[k]\mu_Q]\,\hat{\gamma}\right)\right\}$ |
| $\{0\}$ | $\{1, \ldots, M_2 - 2\}$ | $\text{Prob}(-\infty < r_I[k] < s_{m,x}[k] + d \vert \beta\Delta) \times$ $\text{Prob}(s_{m,y}[k] - d \le r_Q[k] < s_{m,y}[k] + d \vert \beta\Delta) =$ $Q\left(-[a_{m,x}[k] + 1 - a_{m,x}[k]\mu_I + a_{m,y}[k]\mu_Q]\,\hat{\gamma}\right) \times$ $\left\{Q\left([a_{m,y}[k] - 1 - a_{m,x}[k]\mu_Q - a_{m,y}[k]\mu_I]\,\hat{\gamma}\right) - Q\left([a_{m,y}[k] + 1 - a_{m,x}[k]\mu_Q - a_{m,y}[k]\mu_I]\,\hat{\gamma}\right)\right\}$ |
| $\{M_1 - 1\}$ | $\{1, \ldots, M_2 - 2\}$ | $\text{Prob}(s_{m,x}[k] - d \le r_I[k] < \infty \vert \beta\Delta) \times$ $\text{Prob}(s_{m,y}[k] - d \le r_Q[k] < s_{m,y}[k] + d \vert \beta\Delta) =$ $Q\left([a_{m,x}[k] - 1 - a_{m,x}[k]\mu_I + a_{m,y}[k]\mu_Q]\,\hat{\gamma}\right) \times$ $\left\{Q\left([a_{m,y}[k] - 1 - a_{m,x}[k]\mu_Q - a_{m,y}[k]\mu_I]\,\hat{\gamma}\right) - Q\left([a_{m,y}[k] + 1 - a_{m,x}[k]\mu_Q - a_{m,y}[k]\mu_I]\,\hat{\gamma}\right)\right\}$ |
| $\{0\}$ | $\{0\}$ | $\text{Prob}(-\infty < r_I[k] < s_{m,x}[k] + d \vert \beta\Delta) \times$ $\text{Prob}(-\infty < r_Q[k] < s_{m,y}[k] + d \vert \beta\Delta) =$ $Q\left(-[a_{m,x}[k] + 1 - a_{m,x}[k]\mu_I + a_{m,y}[k]\mu_Q]\,\hat{\gamma}\right)$ $Q\left(-[a_{m,y}[k] + 1 - a_{m,x}[k]\mu_Q - a_{m,y}[k]\mu_I]\,\hat{\gamma}\right)$ |
| $\{M_1 - 1\}$ | $\{0\}$ | $\text{Prob}(s_{m,x}[k] - d \le r_I[k] < \infty \vert \beta\Delta) \times$ $\text{Prob}(-\infty < r_Q[k] < s_{m,y}[k] + d \vert \beta\Delta) =$ $Q\left([a_{m,x}[k] - 1 - a_{m,x}[k]\mu_I + a_{m,y}[k]\mu_Q]\,\hat{\gamma}\right)$ $Q\left(-[a_{m,y}[k] + 1 - a_{m,x}[k]\mu_Q - a_{m,y}[k]\mu_I]\,\hat{\gamma}\right)$ |
| $\{0\}$ | $\{M_2 - 1\}$ | $\text{Prob}(-\infty < r_I[k] < s_{m,x}[k] + d \vert \beta\Delta) \times$ $\text{Prob}(s_{m,y}[k] - d \le r_Q[k] < \infty \vert \beta\Delta) =$ $Q\left(-[a_{m,x}[k] + 1 - a_{m,x}[k]\mu_I + a_{m,y}[k]\mu_Q]\,\hat{\gamma}\right)$ $Q\left([a_{m,y}[k] - 1 - a_{m,x}[k]\mu_Q - a_{m,y}[k]\mu_I]\,\hat{\gamma}\right)$ |
| $\{M_1 - 1\}$ | $\{M_2 - 1\}$ | $\text{Prob}(s_{m,x}[k] - d \le r_I[k] < \infty \vert \beta\Delta) \times$ $\text{Prob}(s_{m,y}[k] - d \le r_Q[k] < \infty \vert \beta\Delta) =$ $Q\left([a_{m,x}[k] - 1 - a_{m,x}[k]\mu_I + a_{m,y}[k]\mu_Q]\,\hat{\gamma}\right)$ $Q\left([a_{m,y}[k] - 1 - a_{m,x}[k]\mu_Q - a_{m,y}[k]\mu_I]\,\hat{\gamma}\right)$ |

Table 2.2 For each $x \in \{0, 1, \ldots, M_1 - 1\}$ and $y \in \{0, 1, \ldots, M_2 - 1\}$ the average probability of correct reception of the symbol $s_m[k] = s_{m,x}[k] + j s_{m,y}[k]$ is tabulated on the third column for an $M_1 \times M_2$ rectangular QAM constellation with FDDQ scheme. The functions $\mathtt{t}_1(x,y), \mathtt{t}_2(x,y), \mathtt{t}_3(x,y), \mathtt{t}_4(x,y)$ are defined in Section (2.4.2.1). The function $\mathcal{H}(a,b,t,B,\psi)$ is defined in (2.44), whereas the function $\mathcal{R}(a,t,B,\psi)$ is defined in (2.48). Expressions for $\overline{\mathcal{P}}_{C,x,y}$ for FDD and TDD schemes can easily be obtained by replacing $\mathcal{H}(a,b,t,B,\psi)$ by $\mathcal{H}_1(a,b,1,t)$ of (2.41) and $\mathcal{R}(a,t,B,\psi)$ by $\mathcal{R}_1(a,1,t)$ of (2.47).

| $x$ | $y$ | $\overline{\mathcal{P}}_{C,x,y} = E\left[\mathcal{P}_{C,x,y}(\beta\Delta)\right]$ |
|---|---|---|
| $\{1, 2, \ldots, M_1 - 2\}$ | $\{1, 2, \ldots, M_2 - 2\}$ | $\mathcal{H}\left(\mathtt{t}_1(x,y), \mathtt{t}_3(x,y), t, B, \psi\right) -$<br>$\mathcal{H}\left(\mathtt{t}_1(x,y), \mathtt{t}_4(x,y), t, B, \psi\right) -$<br>$\mathcal{H}\left(\mathtt{t}_2(x,y), \mathtt{t}_3(x,y), t, B, \psi\right) +$<br>$\mathcal{H}\left(\mathtt{t}_2(x,y), \mathtt{t}_4(x,y), t, B, \psi\right)$ |
| $\{1, 2, \ldots, M_1 - 2\}$ | $\{0\}$ | $\mathcal{R}\left(\mathtt{t}_1(x,y), t, B, \psi\right) -$<br>$\mathcal{H}\left(\mathtt{t}_1(x,y), \mathtt{t}_4(x,y), t, B, \psi\right) -$<br>$\mathcal{R}\left(\mathtt{t}_2(x,y), t, B, \psi\right) +$<br>$\mathcal{H}\left(\mathtt{t}_2(x,y), \mathtt{t}_4(x,y), t, B, \psi\right)$ |
| $\{1, 2, \ldots, M_1 - 2\}$ | $\{M_2 - 1\}$ | $\mathcal{H}\left(\mathtt{t}_1(x,y), \mathtt{t}_3(x,y), t, B, \psi\right) -$<br>$\mathcal{H}\left(\mathtt{t}_2(x,y), \mathtt{t}_3(x,y), t, B, \psi\right)$ |
| $\{0\}$ | $\{1, 2, \ldots, M_2 - 2\}$ | $\mathcal{R}\left(\mathtt{t}_3(x,y), t, B, \psi\right) -$<br>$\mathcal{R}\left(\mathtt{t}_4(x,y), t, B, \psi\right) -$<br>$\mathcal{H}\left(\mathtt{t}_2(x,y), \mathtt{t}_3(x,y), t, B, \psi\right) +$<br>$\mathcal{H}\left(\mathtt{t}_2(x,y), \mathtt{t}_4(x,y), t, B, \psi\right)$ |
| $\{M_1 - 1\}$ | $\{1, 2, \ldots, M_2 - 2\}$ | $\mathcal{H}\left(\mathtt{t}_1(x,y), \mathtt{t}_3(x,y), t, B, \psi\right) -$<br>$\mathcal{H}\left(\mathtt{t}_1(x,y), \mathtt{t}_4(x,y), t, B, \psi\right)$ |
| $\{0\}$ | $\{0\}$ | $1 - \mathcal{R}\left(\mathtt{t}_4(x,y), t, B, \psi\right) -$<br>$\mathcal{R}\left(\mathtt{t}_2(x,y), t, B, \psi\right) +$<br>$\mathcal{H}\left(\mathtt{t}_2(x,y), \mathtt{t}_4(x,y), t, B, \psi\right)$ |
| $\{M_1 - 1\}$ | $\{0\}$ | $\mathcal{R}\left(\mathtt{t}_1(x,y), t, B, \psi\right) -$<br>$\mathcal{H}\left(\mathtt{t}_1(x,y), \mathtt{t}_4(x,y), t, B, \psi\right)$ |
| $\{0\}$ | $\{M_2 - 1\}$ | $\mathcal{R}\left(\mathtt{t}_3(x,y), t, B, \psi\right) -$<br>$\mathcal{H}\left(\mathtt{t}_2(x,y), \mathtt{t}_3(x,y), t, B, \psi\right)$ |
| $\{M_1 - 1\}$ | $\{M_2 - 1\}$ | $\mathcal{H}\left(\mathtt{t}_1(x,y), \mathtt{t}_3(x,y), t, B, \psi\right)$ |

$k_2 = \log_2(M_2)$, and the sets $\mathcal{X} = \{0, 1, \ldots, M_1 - 1\}$ and $\mathcal{Y} = \{0, 1, \ldots, M_2 - 1\}$. The vector $(a_{k_1-1}, a_{k_1-2}, \ldots, a_0)$ is the Gray code mapping for the in-phase signal $s_{m,x}[k]$, and $(b_{k_2-1}, b_{k_2-2}, \ldots, b_0)$ is the Gray code mapping for the quadrature-phase signal $s_{m,y}[k]$. For $i = 0, \ldots, k_1 - 1$, let us define the following sets: $X_1(i) = \{x : (x \bmod 2^{i+2}) = 2^i + l, l = 0, \ldots, 2^i - 1\} \cup \{x : (x \bmod 2^{i+2}) = 2^{i+1} + l, l = 0, \ldots, 2^i - 1\}$ and $X_0(i) = \{x : (x \bmod 2^{i+2}) = l, l = 0, \ldots, 2^i - 1\} \cup \{x : (x \bmod 2^{i+2}) = 3 \times 2^i + l, l = 0, \ldots, 2^i - 1\}$. In a similar manner, for $j = 0, \ldots, k_2 - 1$, we can define the sets $Y_1(j)$ and $Y_0(j)$. $Y_1(j) = \{y : (y \bmod 2^{j+2}) = 2^j + l, l = 0, \ldots, 2^j - 1\} \cup \{y : (y \bmod 2^{j+2}) = 2^{j+1} + l, l = 0, \ldots, 2^j - 1\}$ and $Y_0(j) = \{y : (y \bmod 2^{j+2}) = l, l = 0, \ldots, 2^j - 1\} \cup \{y : (y \bmod 2^{j+2}) = 3 \times 2^j + l, l = 0, \ldots, 2^j - 1\}$. Using these sets, the decision statistic for each bit $a_i$, $i = 0, \ldots, k_1 - 1$, is given by the disjoint union of intervals on the $x$-axis [34], and is expressed as

$$\widehat{a}_i = \begin{cases} 1 & \text{if } r_I[k] \in \\ & \cup_{x \in X_1(i)} \Big[ -\infty . \mathbf{1}_{\{x=0\}} + (s_{m,x}[k] - d), (s_{m,x}[k] + d) + \infty . \mathbf{1}_{\{x=M_1-1\}} \Big) \\ 0 & \text{otherwise,} \end{cases} \tag{2.50}$$

where $\mathbf{1}_{\{x\}} = 1$ if '$x$' is true and $\mathbf{1}_{\{x\}} = 0$ if '$x$' is false. In a similar manner, for bit $b_j$, $j = 0, \ldots, k_2 - 1$, it is given by the following disjoint union of intervals on the $y$-axis

$$\widehat{b}_j = \begin{cases} 1 & \text{if } r_Q[k] \in \\ & \cup_{y \in Y_1(j)} \Big[ -\infty . \mathbf{1}_{\{y=0\}} + (s_{m,y}[k] - d), (s_{m,y}[k] + d) + \infty . \mathbf{1}_{\{y=M_2-1\}} \Big) \\ 0 & \text{otherwise.} \end{cases} \tag{2.51}$$

Following the approach presented in [32], it is straightforward to show that the average BEP for bit $a_j$, $j = 0, \ldots, k_1 - 1$, with FDDQ is given by

$$\begin{aligned} P_b(a_j) \;=\; & \frac{1}{M} \sum_{x_0 \in X_0(j)} \sum_{x_1 \in X_1(j)} \sum_{y \in \mathcal{Y}} \\ & \Big\{ \mathcal{R}\left( \left[ -\infty . \mathbf{1}_{\{x_1=0\}} + a_{m,x_1}[k] - 1 - a_{m,x_0}[k]\mu_I + a_{m,y}[k]\mu_Q \right] \sqrt{\gamma_{x_0,y}}, t, B, \psi \right) - \\ & \mathcal{R}\left( \left[ \infty . \mathbf{1}_{\{x_1=M_1-1\}} + a_{m,x_1}[k] + 1 - a_{m,x_0}[k]\mu_I + a_{m,y}[k]\mu_Q \right] \sqrt{\gamma_{x_0,y}}, t, B, \psi \right) \Big\} \end{aligned} \tag{2.52}$$

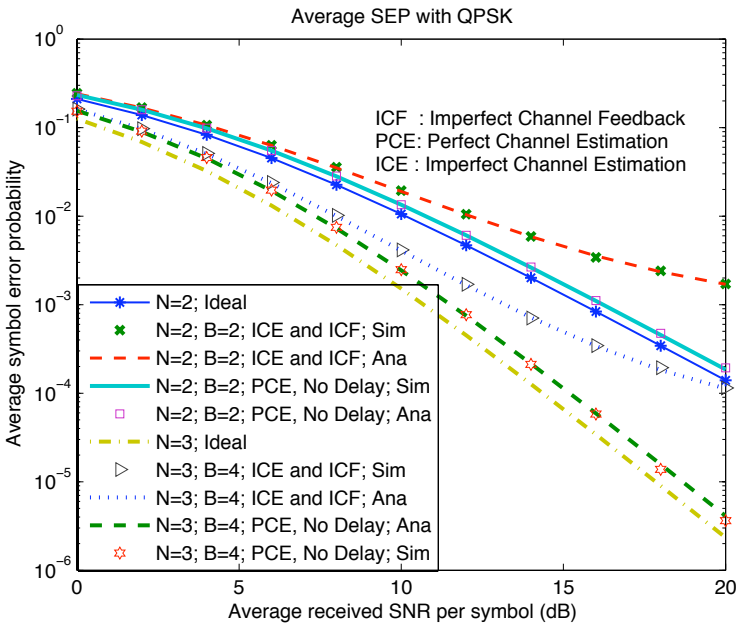


Figure 2.2 Average SEP performance of QPSK modulation with imperfect feedback. Here $t = 2$ and 3 antennas, with $B \in \{2, 4\}$ feedback bits, $\rho_d = 0.99$, and received SNR of the pilot channel $\gamma_p = 30$ dB.

$$+\frac{1}{M}\sum_{x_1\in X_1(j)}\sum_{x_0\in X_0(j)}\sum_{y\in\mathcal{Y}}$$
$$\Big\{\mathcal{R}\left(\left[-\infty.\mathbf{1}_{\{x_0=0\}}+a_{m,x_0}[k]-1-a_{m,x_1}[k]\mu_I+a_{m,y}[k]\mu_Q\right]\sqrt{\gamma_{x_1,y}},t,B,\psi\right)-$$
$$\mathcal{R}\left(\left[\infty.\mathbf{1}_{\{x_0=M_1-1\}}+a_{m,x_0}[k]+1-a_{m,x_1}[k]\mu_I+a_{m,y}[k]\mu_Q\right]\sqrt{\gamma_{x_1,y}},t,B,\psi\right)\Big\},$$

where $\mathcal{R}(a,t,B,\psi)$ is defined in (2.48). In (2.52), the first triple summation captures the probability of transmitting $s_{m,x_0}[k]+js_{m,y}[k]$ and demodulating $s_{m,x_1}[k]+js_{m,y}[k]$, whereas the second triple summation captures the probability of transmitting $s_{m,x_1}[k]+js_{m,y}[k]$ and demodulating $s_{m,x_0}[k]+js_{m,y}[k]$. Similarly, the average BEP for $b_j$, $j=0,\ldots,k_2-1$, with FDDQ is

$$P_b(b_j) = \frac{1}{M}\sum_{y_0\in Y_0(j)}\sum_{y_1\in Y_1(j)}\sum_{x\in\mathcal{X}} \tag{2.53}$$
$$\Big\{\mathcal{R}\left(\left[-\infty.\mathbf{1}_{\{y_1=0\}}+a_{m,y_1}[k]-1-a_{m,x}[k]\mu_Q-a_{m,y_0}[k]\mu_I\right]\sqrt{\gamma_{x,y_0}},t,B,\psi\right)-$$
$$\mathcal{R}\left(\left[\infty.\mathbf{1}_{\{y_1=M_2-1\}}+a_{m,y_1}[k]+1-a_{m,x}[k]\mu_Q-a_{m,y_0}[k]\mu_I\right]\sqrt{\gamma_{x,y_0}},t,B,\psi\right)\Big\}$$

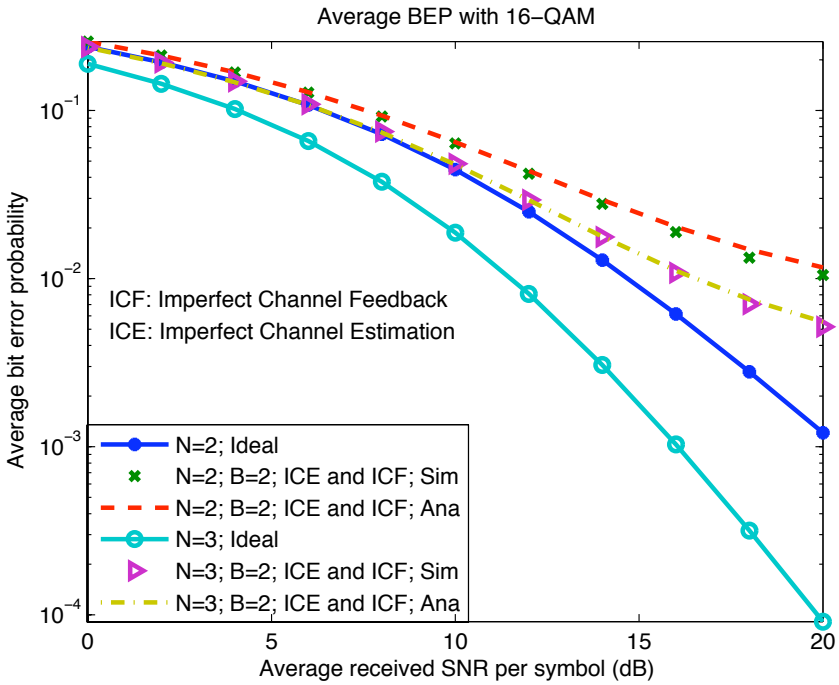


Figure 2.3 Average BEP performance of Gray coded 16-QAM modulation with imperfect channel estimation, feedback delay, and channel quantization. Here, we assume $t = 2$ and 3 antennas, with $B = 2$ feedback bits, $\rho_d = 0.99$ and average received SNR of the pilot channel $\gamma_p = 30$ dB.

$$+\frac{1}{M}\sum_{y_1\in Y_1(j)}\sum_{y_0\in Y_0(j)}\sum_{x\in\mathcal{X}}$$
$$\Big\{\mathcal{R}\left(\left[-\infty.\mathbf{1}_{\{y_0=0\}}+a_{m,y_0}[k]-1-a_{m,x}[k]\mu_Q-a_{m,y_1}[k]\mu_I\right]\sqrt{\gamma_{x,y_1}},t,B,\psi\right)-$$
$$\mathcal{R}\left(\left[\infty.\mathbf{1}_{\{y_0=M_2-1\}}+a_{m,y_0}[k]+1-a_{m,x}[k]\mu_Q-a_{m,y_1}[k]\mu_I\right]\sqrt{\gamma_{x,y_1}},t,B,\psi\right)\Big\}.$$

For FDD and TDD schemes, the average BEP can be obtained by replacing $\mathcal{R}(a,t,B,\psi)$ by $\mathcal{R}_1(a,1,t)$ of (2.47). Finally, the average BEP can be obtained as

$$\overline{P}_{\mathrm{b},QAM}=\frac{1}{\log_2(M)}\left\{\sum_{j=0}^{k_1-1}P_b(a_j)+\sum_{j=0}^{k_2-1}P_b(b_j)\right\}. \tag{2.54}$$

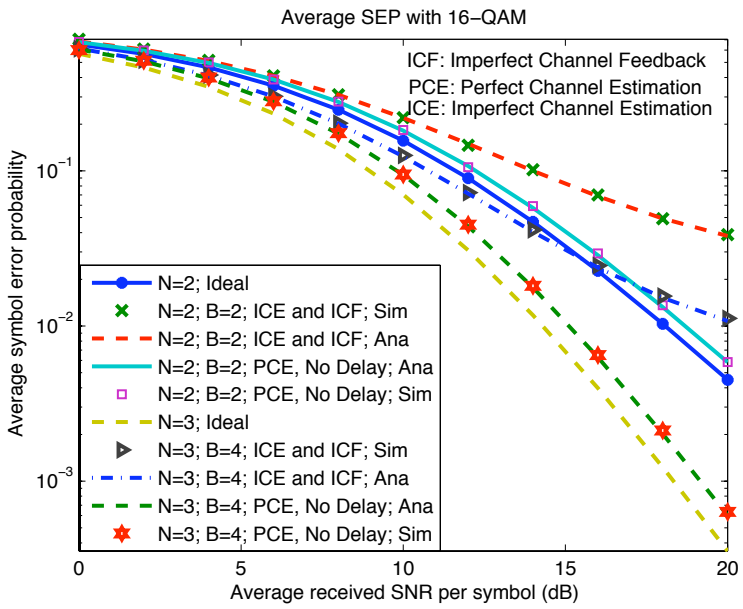


Figure 2.4 Average SEP performance of 16-QAM modulation with imperfect feedback. Here, $t \in \{2, 3\}$, with $B \in \{2, 4\}$ bits, $\rho_d = 0.99$ and average received SNR of the pilot $\gamma_p = 30$ dB.

## 2.5 Results and Discussion

In this section, we present numerical (obtained through the presented analysis) and simulation results quantifying the combined effects of ICE, feedback delay and channel quantization. In all the plots in this section, we employ the well-known Jakes model [2] for the time correlation of the fading process. That is, we set $\rho_d = J_0(2\pi f_d D)$, where $J_0(x)$ is the zeroth order Bessel function [103], $f_d$ is the maximum Doppler frequency which is related to the carrier frequency $f_c$ and the terminal velocity $\mathsf{v}$ as $f_d = \mathsf{v} f_c/c$, and $D$ is the feedback delay. We set $f_c = 2$ GHz, $\mathsf{v} = 34.5$ Kmph, and $D = 0.5$ msec, so that $\rho_d = 0.99$. For expository purpose, we assume MMSE channel estimation (as detailed in Section 2.3.3) with pilot SNR $\gamma_p \in \{15, 30\}$ dB. Then, from (2.14), the combined correlation coefficient is

$$\rho = \rho_d \sqrt{\frac{\gamma_p}{1+\gamma_p}}.$$

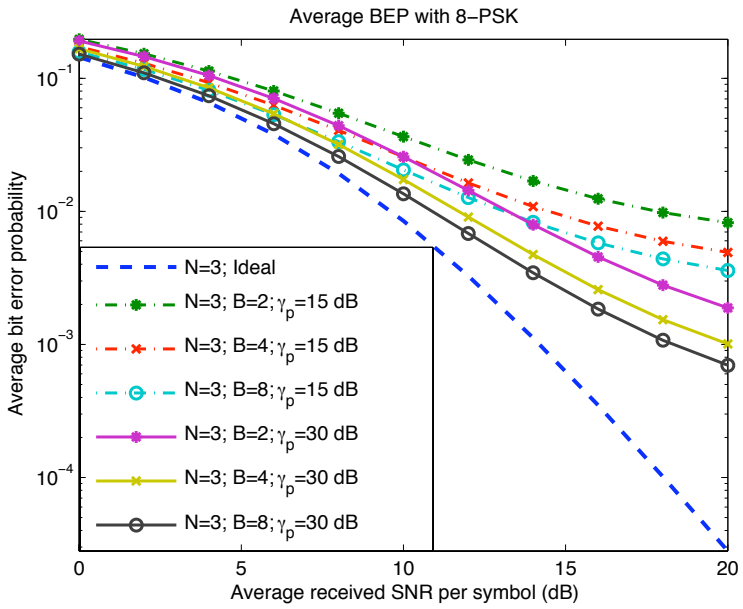


Figure 2.5 Average BEP performance of Gray coded 8-PSK modulation as a function of the number of feedback bits $B \in \{2, 4, 8\}$ and the average pilot SNR $\gamma_p \in \{15, 30\}$ dB, for a fixed delay with $\rho_d = 0.99$. Here, we set $t = 3$ antennas.

Fig. 2.1 shows the average BEP performance of Gray-coded QPSK modulation with $t = 2$ and 3 antennas, $B = 2$ bits, and $\gamma_p = 30$ dB. For comparison, we also plot the ideal performances (i.e., with PCE, no feedback delay, and unquantized feedback). The simulation results in Fig. 2.1 match accurately with the numerical results, thus validating the presented analytical framework. Average SEP performance of QPSK modulation with $t = 2$ and 3 antennas, and with $B = 2$ and 4 bits is presented in Fig. 2.2. Along with the simulation results corroborating the analysis, Fig. 2.2 also shows the ideal SEP curves, and the performance with perfect channel estimation and delay-less finite-rate feedback. Fig. 2.2 shows that imperfect channel estimation and feedback delay cause more degradation to the error performance compared to channel quantization alone. For example, with $t = 2$ antennas and $B = 2$ bits at an SNR of 20 dB, the SEP with ICE and feedback delay is an order of magnitude worse than the SEP with PCE and no feedback delay. Fig. 2.2 also shows that this performance gap increases when the number

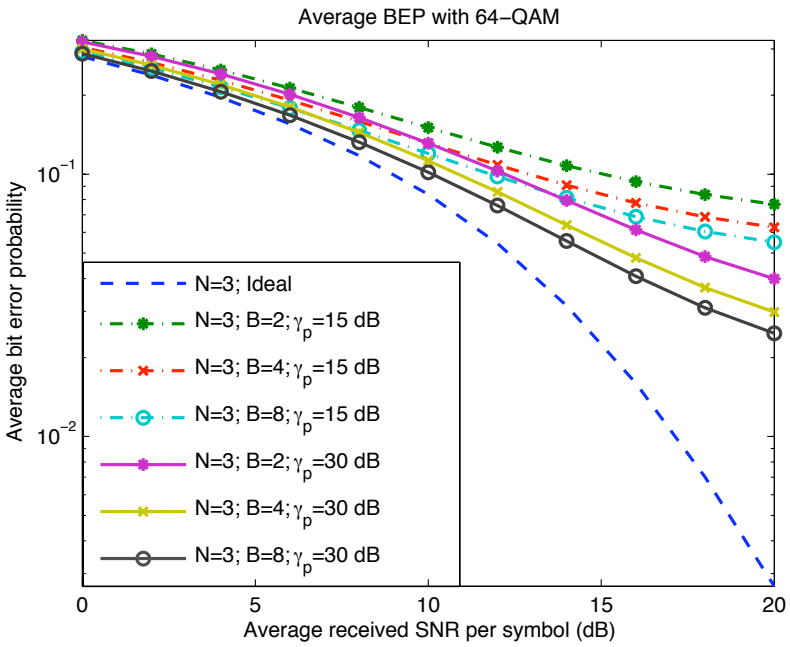


Figure 2.6 Average BEP performance of Gray coded 64-QAM modulation as a function of the number of feedback bits $B \in \{2, 4, 8\}$ and the average pilot SNR $\gamma_p \in \{15, 30\}$ dB, for a fixed feedback delay with $\rho_d = 0.99$. Here, we set $t = 3$ antennas.

of antennas is increased by one, and the number of feedback bits is increased by two. With Gray-coded 16-QAM modulation, Figs. 2.3 and 2.4, respectively, show the average BEP and SEP performances.

Similar to Fig. 2.1, in Fig. 2.3, we use $t = 2$ and 3 antennas with $B = 2$ bits, whereas, similar to Fig. 2.2, in Fig. 2.4, we employ $t = 2$ and 3 antennas with $B = 2$ and 4 bits. From Figs. 2.3 and 2.4, we conclude that imperfect channel feedback degrades the average SEP performance more compared to the average BEP performance. Figs. 2.3 and 2.4 also show that the performance degradation of 16-QAM with imperfect channel feedback is qualitatively similar to that of QPSK in Figs. 2.1 and 2.2.

The effects of pilot SNR and the feedback quantization bits on the average BEP performances of 8-PSK and 64-QAM are investigated in Figs. 2.5 and

2.6, respectively. In Figs. 2.5 and 2.6, we fix the number of antennas at 3, choose $B \in \{2, 4, 8\}$ and $\gamma_p \in \{15, 30\}$ dB. From Figs. 2.5 and 2.6 we observe that at high SNR, for a given combination of $B$ and $\gamma_p$, increasing the pilot SNR is more beneficial to improving the average BEP performance than increasing the number of feedback bits. This can be explained by the fact that imperfect channel estimation introduces error floor at high SNR, which can only be reduced by increasing the accuracy of channel estimation quality.

For example, in Fig. 2.5, with $(B, \gamma_p) = (2, 15)$, increasing $B$ to 8 while keeping $\gamma_p$ at 15 dB improves the BEP by a factor of two, whereas even by keeping $B$ at 2 and increasing $\gamma_p$ to 30 dB improves the BEP by a factor of four. From Fig. 2.6, a similar observation can be made *which emphasizes the importance of accurate channel quality estimation compared to the feedback quality improvement with more bits.* For a fixed value of $B = 8$ bits, Fig. 2.7 plots the average SEP of 32-QAM, $M \in (4 \times 8)$, by varying number of transmit antennas $t \in \{2, 3, 4\}$ and pilot symbol SNR $\gamma_p \in \{15, 30\}$ dB. From Fig. 2.7, we notice that, at high SNR, for a fixed $(t, \gamma_p)$ increasing the pilot SNR has a more direct effect in reducing the error floor than increasing the number of antennas. This is due to the fact that, at high SNR, error floor makes having an additional antenna less attractive from diversity perspective.

Finally, by fixing $\gamma_p$ at 30 dB, in Fig. 2.8 we study the average SEP of 8-PSK by varying number of transmit antennas $t \in \{3, 4\}$ and number of feedback bits $B \in \{2, 4, 8\}$. As expected, Fig. 2.8 shows that for a given number of antennas increasing the number of feedback bits monotonically improves the error performance. However, Fig. 2.8 also suggests that it is more beneficial to have a high feedback bit budget for a smaller number of antennas than to have more antennas with a smaller bit budget. Although extensive set of simulations are performed to confirm the analysis, for clarity, in Figs. 2.5, 2.6, 2.7, 2.8, and 2.9 we presented only the analytical results.

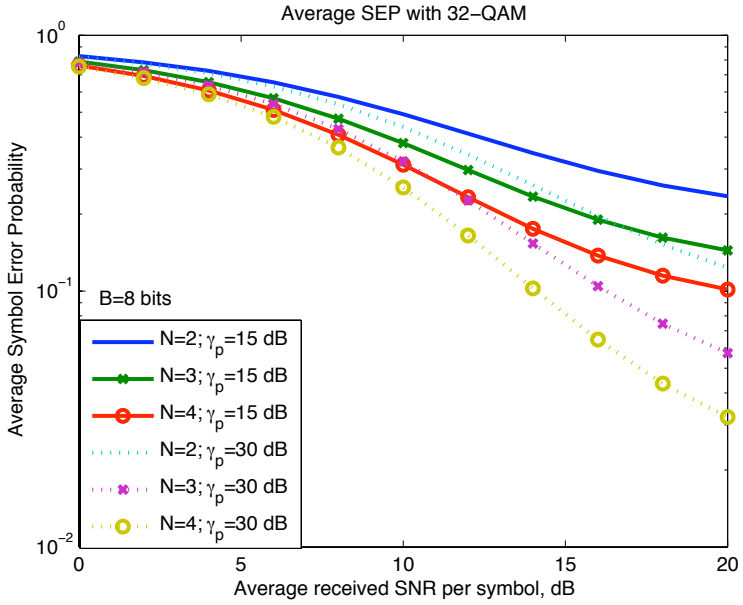


Figure 2.7 Average SEP performance of 32-QAM modulation as a function of the number of antennas $t \in \{2, 3, 4\}$ and the average pilot SNR $\gamma_p \in \{15, 30\}$ dB, for a fixed feedback delay with $\rho_d = 0.99$. Here, we set $B = 8$ bits.

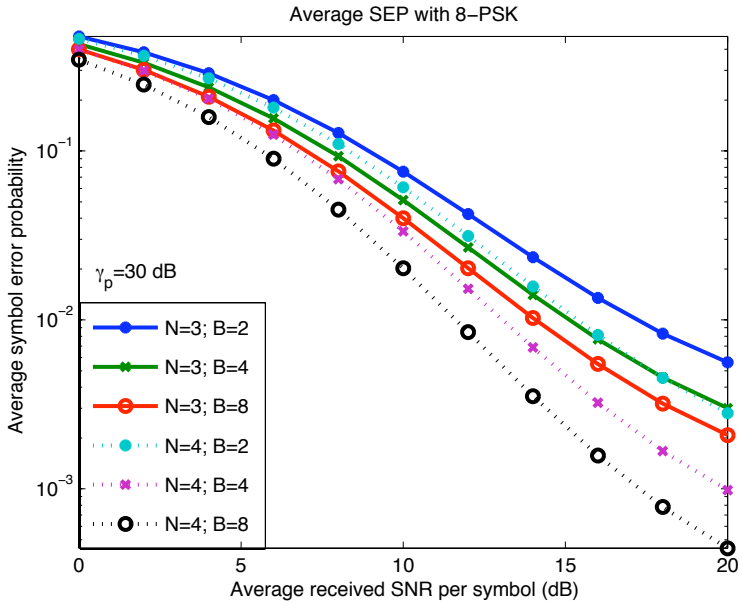


Figure 2.8 Average SEP performance of 8-PSK modulation as a function of the number of antennas $t \in \{3, 4\}$ and $B \in \{2, 4, 8\}$. Here, we set $\gamma_p = 30$ dB.

## 2.6 Conclusion

In this chapter we have considered transmit beamforming for MISO systems on spatially independent Rayleigh fading channels with imperfect channel feedback. We characterized the feedback imperfections in terms of noisy channel estimation, feedback delay, and finite rate channel quantization. A general framework, valid for any two-dimensional constellation and frequency division duplexing with and without channel quantization and time domain duplexing schemes, was presented to account for the feedback imperfections. The error probability analysis is complemented by the simulation results. We demonstrated, through numerical and simulation results, that channel estimation inaccuracy and feedback delay are more detrimental to the error performance compared to the effects of finite-rate channel quantization.

An important feature of the modeling, proposed in this chapter, is that the receiver is assumed to have no knowledge of the estimation and delay related error terms as well as the corresponding correlation co-efficients. In the next chapter we take a critical look at these assumptions and develop a system where the receiver knows the delay related error term while still unaware of the estimation related error term.

## 2.7 Appendix

In this appendix, we derive expressions for (2.42), (2.43), (2.45) and (2.46). We begin with (2.45),

$$\begin{aligned} \mathcal{J}(a,b,t,B,\psi) &\triangleq E\left[Q\left(a\sqrt{\beta\Delta}\right)Q\left(b\sqrt{\beta\Delta}\right)\right] \qquad (2.55)\\ &= \int_{y} f_{\Delta}(y)\,dy \int_{x=0}^{\infty} Q(a\sqrt{xy})\,Q(b\sqrt{xy})\,f_{\beta}(x)\,dx, \end{aligned}$$

where, in (2.55), $a, b \geq 0$, the pdf of $\beta$ is given by (2.8), the pdf of $\Delta$ is given by (2.19), $t$ is the number of transmit antennas, and $B$ is the number of feedback bits.

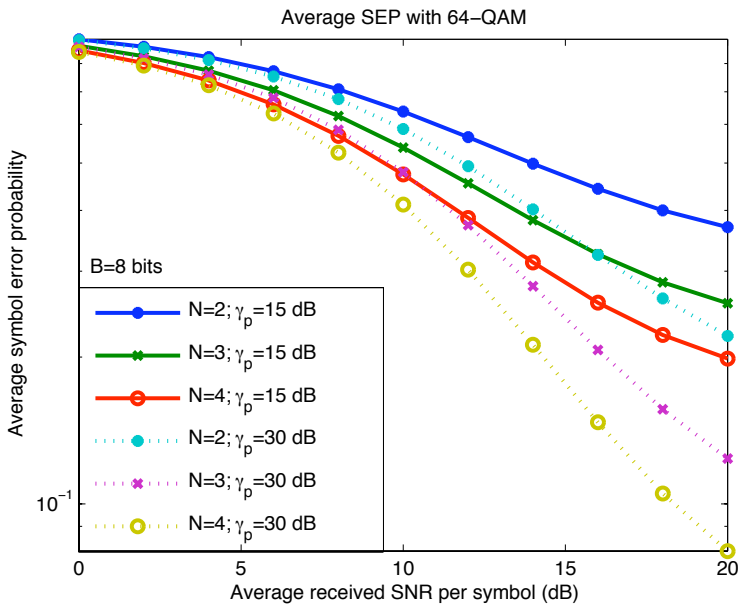


Figure 2.9 Average SEP performance of 64-QAM modulation as a function of the number of antennas $t \in \{2, 3, 4\}$ and the average pilot SNR $\gamma_p \in \{15, 30\}$ dB, for a fixed feedback delay with $\rho_d = 0.99$. Here, we set $B = 8$ bits.

Let us first focus on the inner integral of (2.55), which can be simplified as follows: Let $a_1 = a\sqrt{y}$ and $b_1 = b\sqrt{y}$, and using integration by-parts, we have

$$\begin{aligned}
\mathcal{J}_1(a,b,y,t) &\triangleq \int_{x=0}^{\infty} Q(a_1\sqrt{x})Q(b_1\sqrt{x})f_\beta(x)dx = \\
&\left[Q(a\sqrt{x})Q(b\sqrt{x})F_\beta(x)\right]_{x=0}^{\infty} + \frac{b_1}{2\sqrt{2\pi}}\int_{x=0}^{\infty} F_\beta(x)Q(a_1\sqrt{x})e^{-\frac{b_1^2 x}{2}}x^{-\frac{1}{2}}dx + \\
&\quad \frac{a_1}{2\sqrt{2\pi}}\int_{x=0}^{\infty} F_\beta(x)Q(b_1\sqrt{x})e^{-\frac{a_1^2 x}{2}}x^{-\frac{1}{2}}dx \\
&= \frac{b_1}{2\sqrt{2\pi}}\int_{x=0}^{\infty} F_\beta(x)Q(a_1\sqrt{x})e^{-\frac{b_1^2 x}{2}}x^{-\frac{1}{2}}dx + \\
&\quad \frac{a_1}{2\sqrt{2\pi}}\int_{x=0}^{\infty} F_\beta(x)Q(b_1\sqrt{x})e^{-\frac{a_1^2 x}{2}}x^{-\frac{1}{2}}dx \\
&= \mathcal{M}(a,b,y,t) + \mathcal{M}(b,a,y,t) \qquad (2.56)
\end{aligned}$$

where

$$\mathcal{M}(a,b,y,t) \triangleq \frac{b_1}{2\sqrt{2\pi}} \int_{x=0}^{\infty} F_\beta(x) Q(a_1\sqrt{x}) e^{-\frac{b_1^2 x}{2}} x^{-\frac{1}{2}} dx. \tag{2.57}$$

To simplify the derivation we use the following alternate representation for the Gaussian $Q$-function [12]:

$$Q(x) = \frac{1}{\pi} \int_{\theta=0}^{\frac{\pi}{2}} \exp\left(-\frac{x^2}{2\sin^2\theta}\right) d\theta \quad x \geq 0, \tag{2.58}$$

and $F_\beta(x)$ of (2.9), $\mathcal{M}(a,b,y,t)$ of (2.57) can be simplified as

$$\begin{aligned}
\mathcal{M}(a,b,y,t) &= \frac{b_1}{2\sqrt{2\pi}} \int_{x=0}^{\infty} Q(a_1\sqrt{x}) e^{-\frac{b_1^2 x}{2}} x^{-\frac{1}{2}} dx - \\
&\frac{b_1}{2\sqrt{2\pi}} \sum_{j=0}^{t-1} \frac{1}{j!} \int_{x=0}^{\infty} Q(a_1\sqrt{x}) e^{-(\frac{b_1^2}{2}+1)x} x^{j-\frac{1}{2}} dx \\
&= \frac{b_1}{2\pi\sqrt{2\pi}} \int_0^{\pi/2} d\theta \int_{x=0}^{\infty} e^{-\left(\frac{b_1^2}{2}+\frac{a_1^2}{2\sin^2\theta}\right)x} x^{-\frac{1}{2}} dx - \\
&\frac{b_1}{2\pi\sqrt{2\pi}} \sum_{j=0}^{t-1} \frac{1}{j!} \int_0^{\pi/2} d\theta \int_{x=0}^{\infty} e^{-\left(\frac{b_1^2}{2}+\frac{a_1^2}{2\sin^2\theta}+1\right)x} x^{j-\frac{1}{2}} dx \\
&= \frac{1}{2\pi} \int_0^{\pi/2} d\theta \sqrt{\frac{b_1^2\sin^2\theta}{b_1^2\sin^2\theta + a_1^2}} - \\
&\sum_{j=0}^{t-1} \frac{1}{j!} \frac{\Gamma\left(j+\frac{1}{2}\right) 2^{j+\frac{1}{2}}}{2\pi\sqrt{2\pi}} \int_0^{\pi/2} d\theta b_1 \left(\frac{\sin^2\theta}{b_1^2\sin^2\theta + 2\sin^2\theta + a_1^2}\right)^{j+\frac{1}{2}} \\
&= \frac{1}{2\pi} \int_0^{\pi/2} d\theta \sqrt{\frac{b^2\sin^2\theta}{b^2\sin^2\theta + a^2}} - \sum_{j=0}^{t-1} \frac{1}{j!} \frac{b\Gamma\left(j+\frac{1}{2}\right) 2^{j+\frac{1}{2}}}{2\pi\sqrt{2\pi}} \times \\
&\int_0^{\pi/2} d\theta \left(\frac{\sin^2\theta}{a^2+b^2\sin^2\theta}\right)^{j+\frac{1}{2}} \sqrt{y}\left[y + \frac{2\sin^2\theta}{a^2+b^2\sin^2\theta}\right]^{-\left(j+\frac{1}{2}\right)}.
\end{aligned} \tag{2.59}$$

Upon using (2.56), (2.57) and (2.59) in (2.55), we have

$$\mathcal{J}(a,b,t,B,\psi) = \int_y f_\Delta(y)\mathcal{M}(a,b,y,t)dy + \int_y f_\Delta(y)\mathcal{M}(b,a,y,t)dy. \tag{2.60}$$

In the absence of feedback quantization (i.e., as $B \to \infty$ and $\psi \to 0$), recall that we have $f_\Delta(y) = \delta(y-1)$. Then, (2.60) reduces to

$$\mathcal{J}(a,b,t,\infty,0) = \mathcal{M}(a,b,1,t) + \mathcal{M}(b,a,1,t), \tag{2.61}$$

which is also equal to $\mathcal{J}_1(a,b,1,t)$ of (2.42). For finite $B$, using (2.19) for the pdf of $\Delta$, we have

$$\mathcal{J}(a,b,t,B,\psi) = 2^B(t-1)\int_{1-\psi}^{1}(1-y)^{t-2}\left\{\mathcal{M}(a,b,y,t)+\mathcal{M}(b,a,y,t)\right\}dy. \tag{2.62}$$

To further simplify (2.62), let us define

$$\mathcal{M}_1(a,b,\psi,t) \triangleq \int_{1-\psi}^{1}(1-y)^{t-2}\mathcal{M}(a,b,y,t)dy \tag{2.63}$$

so that (2.62) is

$$\mathcal{J}(a,b,t,B,\psi) = 2^B(t-1)\left\{\mathcal{M}_1(a,b,\psi,t)+\mathcal{M}_1(b,a,\psi,t)\right\}. \tag{2.64}$$

Using (2.59) in (2.63), we obtain

$$\begin{aligned}\mathcal{M}_1(a,b,\psi,t) &= \frac{1}{2\pi}\int_{1-\psi}^{1}(1-y)^{t-2}\int_0^{\pi/2}\sqrt{\frac{b^2\sin^2\theta}{b^2\sin^2\theta+a^2}}dyd\theta \;- \\ &\quad \sum_{j=0}^{t-1}\frac{1}{j!}\frac{b\Gamma\left(j+\frac{1}{2}\right)2^{j+\frac{1}{2}}}{2\pi\sqrt{2\pi}}\times\int_0^{\pi/2}d\theta\left(\frac{\sin^2\theta}{a^2\sin^2\theta+b^2}\right)^{j+\frac{1}{2}} \\ &\quad \int_{1-\psi}^{1}dy(1-y)^{t-2}\sqrt{y}\left[y+\frac{2\sin^2\theta}{a^2\sin^2\theta+b^2}\right]^{-\left(j+\frac{1}{2}\right)}. \end{aligned}\tag{2.65}$$

Owing to the fact that $\int_{1-\psi}^{1} f_\Delta(y)dy = 1$, the first double integral of (2.65) reduces to

$$\begin{aligned}\int_{1-\psi}^{1}(1-y)^{t-2}\int_0^{\pi/2}\sqrt{\frac{b^2\sin^2\theta}{b^2\sin^2\theta+a^2}}dyd\theta &= \frac{1}{2^B(t-1)}\int_0^{\pi/2}\sqrt{\frac{b^2\sin^2\theta}{b^2\sin^2\theta+a^2}}d\theta \\ &= \frac{1}{2^B(t-1)}\frac{ab}{(a^2+b^2)}\,{}_2F_1\left(1,1;\frac{3}{2};\frac{b^2}{a^2+b^2}\right)\end{aligned}\tag{2.66}$$

where ${}_2F_1(\cdot,\cdot;\cdot;\cdot)$ is the hypergeometric function [103], and we have used [12, Eqn. (5.17)] to simplify the integral in (2.66). On the other hand, to simplify the inner integral of (2.65) let us consider the following result [35] for positive integer values of $m$:

$$\begin{aligned}\mathcal{D}_1(\psi,\alpha,m,n) &\triangleq \int_{1-\psi}^{1}\sqrt{y}(1-y)^m(y+\alpha)^{-n}dy \\ &= \sum_{l=0}^{m}(-1)^l\binom{m}{l}\int_{1-\psi}^{1}y^{l+\frac{1}{2}}(y+\alpha)^{-n}dy \\ &= \sum_{l=0}^{m}\frac{(-1)^l\binom{m}{l}\alpha^{-n}}{(l+\frac{3}{2})}\Big\{{}_2F_1\left(l+\frac{3}{2},n;l+\frac{5}{2};\frac{-1}{\alpha}\right)- \\ &\quad (1-\psi)^{l+\frac{3}{2}}\,{}_2F_1\left(l+\frac{3}{2},n;l+\frac{5}{2};\frac{\psi-1}{\alpha}\right)\Big\}. \qquad (2.67)\end{aligned}$$

Using (2.67), the inner integral of (2.65) simplifies to

$$\int_{1-\psi}^{1}dy(1-y)^{t-2}\sqrt{y}\left[y+\frac{2\sin^2\theta}{a^2\sin^2\theta+b^2}\right]^{-\left(j+\frac{1}{2}\right)}=\mathcal{D}_1\left(\psi,\frac{2\sin^2\theta}{a^2\sin^2\theta+b^2},t-2,j+\frac{1}{2}\right). \qquad (2.68)$$

Using (2.66) and (2.68), (2.65) simplifies to

$$\begin{aligned}\mathcal{M}_1(a,b,\psi,t) &= \frac{1}{\pi 2^{B+1}(t-1)}\frac{ab}{(a^2+b^2)}\,{}_2F_1\left(1,1;\frac{3}{2};\frac{b^2}{a^2+b^2}\right)- \\ &\quad \sum_{j=0}^{t-1}\frac{1}{j!}\frac{b\Gamma\left(j+\frac{1}{2}\right)2^{j+\frac{1}{2}}}{2\pi\sqrt{2\pi}}\times \\ &\quad \int_0^{\pi/2}d\theta\left(\frac{\sin^2\theta}{a^2\sin^2\theta+b^2}\right)^{j+\frac{1}{2}}\times\mathcal{D}_1\left(\psi,\frac{2\sin^2\theta}{a^2\sin^2\theta+b^2},t-2,j+\frac{1}{2}\right). \qquad (2.69)\end{aligned}$$

Finally, using (2.69) in (2.64), we arrive at a single-integral based formula for $\mathcal{J}(a,b,t,B,\psi)$. To simplify (2.43) and (2.46), now consider the following random variable

$$\mathcal{G}(\Delta,\phi,b,t)=\int_{\theta=0}^{\phi}\left(\frac{\sin^2\theta}{\sin^2\theta+b^2\Delta}\right)^t d\theta \qquad (2.70)$$

with the pdf of $\Delta$ as defined in (2.19). Note that the function $\mathcal{K}_1(a,y,t)$ of (2.43) for $a, y \geq 0$ can be expressed in terms of (2.70) as

$$\begin{aligned}\mathcal{K}_1(a,y,t) &= E[Q(a\sqrt{y\beta})] \\ &= \frac{1}{\pi}\int_0^{\frac{\pi}{2}} \left(\frac{\sin^2\theta}{\sin^2\theta + ya^2/2}\right)^t d\theta = \frac{1}{\pi}\mathcal{G}\left(y, \frac{\pi}{2}, \frac{a}{\sqrt{2}}, t\right). \end{aligned} \quad (2.71)$$

The average of (2.70) over $\Delta$ can be performed as follows

$$\begin{aligned}\overline{\mathcal{G}}(\phi,b,t,B,\psi) &\triangleq E\left[\mathcal{G}(\Delta,\phi,b,t)\right] \\ &= 2^B(t-1)\int_{y=1-\psi}^{1}(1-y)^{t-2}\mathcal{G}(y,\phi,b,t)dy \\ &= 2^B(t-1)\int_{\theta=0}^{\phi}\left(\frac{\sin^2\theta}{b^2}\right)^t\int_{y=1-\psi}^{1}(1-y)^{t-2}\left(y+\frac{\sin^2\theta}{b^2}\right)^{-t}dyd\theta \\ &= 2^B(t-1)\int_{\theta=0}^{\phi}\left(\frac{\sin^2\theta}{b^2}\right)^t\mathcal{D}_2\left(\psi, \frac{\sin^2\theta}{b^2}, t-2, t\right)d\theta, \end{aligned} \quad (2.72)$$

where

$$\begin{aligned}&\mathcal{D}_2(\psi,\alpha,m,n) \triangleq \int_{1-\psi}^{1}(1-y)^m(y+\alpha)^{-n}dy \\ &= \frac{-\alpha^n}{1+m}\,{}_2F_1\left(1,n;2+m;-\frac{1}{\alpha}\right) - \frac{\alpha^{1-n}(1+\alpha)^m}{n-1}\,{}_2F_1\left(1-n,-m;2-n;\frac{\alpha}{\alpha+1}\right) \\ &+\frac{(1+\alpha)^m(1+\alpha-\psi)^{1-n}}{n-1}\,{}_2F_1\left(1-n,-m;2-n;\frac{1+\alpha-\psi}{\alpha+1}\right), \end{aligned} \quad (2.73)$$

and the simplification is due to [35]. As a result, we have, for $a > 0$,

$$\begin{aligned}\mathcal{K}(a,t,B,\psi) &= E\left[\mathcal{K}_1(a,\Delta,t)\right] \\ &= \frac{1}{\pi}E\left[\mathcal{G}\left(\Delta,\frac{\pi}{2},\frac{a}{\sqrt{2}},t\right)\right] = \frac{1}{\pi}\overline{\mathcal{G}}\left(\frac{\pi}{2},\frac{a}{\sqrt{2}},t,B,\psi\right) \end{aligned} \quad (2.74)$$

which is (2.46).

**Acknowledgement**

The text of this chapter, in part, has *appeared* in:

- Y. Isukapalli, R. Annavajjala, and B. D. Rao, "Performance analysis of transmit beamforming for MISO systems with imperfect feedback," *IEEE Transactions on Communications*, vol. 57, no. 1, pp. 222-231, Jan. 2009.

- Y. Isukapalli, R. Annavajjala, and B. D. Rao, "Average SEP and BEP analysis of transmit beamforming for MISO systems with imperfect feedback and M-PSK constellation," *IEEE Symp. on Pers. Indoor and Mobile Radio Comm. (PIMRC)*, Athens, Greece, pp. 1-5, Sep. 2007.

# 3 A Distinction between Delay Related Error and Estimation Related Error

In the previous chapter we modeled the estimation errors and feedback delay in a similar manner, i.e., the error terms due to estimation and delay are assumed to be unknown and hence both were part of receiver thermal noise when the performance analysis is carried out. This chapter revolves around the idea that *delay related error term can be known* at the receiver while the *estimation related error term can not be known* at the receiver. Thus the modeling proposed here highlights the distinction between errors that arise due to channel estimation from those that arise due to feedback delay and represents an important departure from past work. Employing a *packet fading model*, since the channel is constant for the whole block, the channel estimation error (as well as the known delay error term) is also constant for the whole block requiring a more careful approach to carrying out the performance analysis.

With the new modeling we address the problem of analyzing the effect of imperfect feedback in a slowly varying spatially independent Rayleigh fading wireless channel on the average packet error probability (PEP) of transmit beamforming multiple input single output systems. PEP is an important error statistic for slowly fading wireless communication system designers. We also develop the tools relevant for deriving analytical expressions for the PEP, one such important

tool is the analytically tractable approximation to the Gaussian $Q$-function, which helps in the evaluation of the expectation of higher powers ($\geq 3$) of $Q$-function. Analytical expression is derived for the PEP with BPSK signaling. The derived approximated closed-form analytical expression is complemented by simulations.

## 3.1 Introduction

Multiplicative fading is a major source of performance degradation in a multipath wireless environment. Channel coding and interleaving can offer some protection from the negative effects of fading. However, in some wireless systems data has to be organized into small packets, which are confined to fixed time slots, with or without interleaving. One popular example of such a system is the slotted multiple access scheme. It is important for the system designers to know the impact of fading on the performance. An important metric for studying the performance of a non-interleaved wireless packet data transmission is the average packet error probability (PEP) [38]-[53]. Packet error probability is also increasingly becoming an important *quality-of-service* parameter for the wireless networking community since it determines how frequently the information packet has to be re-transmitted [54]-[59].

Extensive analytical results quantifying the impact of fading on average symbol and error probability (SEP/BEP) are available for various modulation schemes [12]. However, in slow fading situations, there is no mapping between the average SEP/BEP and the average PEP. Consequently knowing average SEP/BEP does not help in understanding the average PEP. Analysis of average PEP is a more complicated problem compared to the analysis of average SEP/BEP. Analytical quantification of packet error probability has received considerable attention in the literature [38]-[53]. Closed-form expressions for PEP have been derived for the non-coherent FSK modulation. The non-coherent FSK's SEP, conditioned on the channel, is an exponential function and taking expectation of the higher powers

of conditional SEP w.r.t. the fading random variable is analytically tractable. However, closed-form expressions are not available for coherent BPSK and other constellations. Conditional PEP (conditioned on a function of the wireless channel) for a scheme such as coherent BPSK results in integer powers of the Gaussian-$Q$ function. This makes the analysis challenging because in order to derive the average PEP expression, one has to integrate the integer powers of the Gaussian-Q function w.r.t. the random variable that captures the fading environment, an analytically difficult exercise. We also note that, to the best of our knowledge, the effect of channel estimation errors on PEP has not been considered in the literature. In this chapter we consider the problem of deriving analytical expressions for PEP of a multiple input single output (MISO) system with various forms of practical imperfections. We later show that this problem captures various commonly interested performance analysis of wireless systems as special cases.

The first form of feedback imperfection considered is channel estimation error. As explained in the previous chapter, it is now a common practice to model the actual channel and its estimate as a jointly Gaussian random process, with an error term that is orthogonal to the channel estimate [28, 60, 62, 76]. The error term associated with a particular channel estimate is unknown to the receiver and hence it becomes part of noise when the performance analysis is carried out. If the channel under consideration is varying at symbol level, or if the performance criteria is average symbol/bit error probability (as was the case in the previous chapter), then the variance of the error term will be simply added (along with the symbol dependency) to the variance of the receiver noise resulting in an effective noise term with variance equaling the sum of variance of receiver noise and the variance of the estimation error term ( [28, 60], and the references therein). In this chapter, we also follow the standard model of joint Gaussianity between the channel and its estimate, but *adapt it to the packet fading model*. An important difference is that in a packet fading model the error term is constant for the entire packet while each symbol experiences a different noise sample requiring new analytical

tools.

The second form of feedback imperfection we address is the delay between constructing the beamforming vector at the receiver and using it at the transmitter. Another well accepted formulation [16, 18, 62], [64]-[70] is to treat the impact of feedback delay in a manner similar to estimation errors, i.e., actual channel and its delayed version are assumed to be jointly Gaussian with an unknown (to the receiver) error term that is orthogonal to the delayed version. Since the delay related error term is unknown to the receiver, similar to estimation related error term, during performance analysis it becomes part of noise thus removing any conceptual distinction between the mismatch in beamforming due to feedback delay and estimation errors. Though much of the past work on feedback delay [16, 18, 62], [64]-[70] effectively make the delay related error term part of receiver noise, alternate options were considered (primarily in the context of adaptive modulation) in [71]-[78]. However, it is important to note that much of the work in [64]-[78] treated estimation errors and feedback delay in a similar manner, i.e., either both the error terms are assumed to be known or unknown to the receiver. In this chapter, based on feedback system considerations we feel it is appropriate to treat the errors due to feedback delay to be known at the receiver, while the errors due to estimation errors are un-known at the receiver. This modeling approach is adopted in this work and it shows that the impact of feedback delay on beamforming MISO system performance can be less severe and is also conceptually quite different from channel estimation errors.

The third form of feedback imperfection considered in this chapter, namely finite-rate quantization of the channel [22]-[25]. To summarize, the contributions presented in this chapter are threefold: an accurate characterization of estimation errors in a packet fading context, a new modeling of feedback delay which shows improved performance for a beamforming MISO system and conceptually distinguishes it from estimation errors, and derivation of an analytical expression quantifying the impact of channel estimation errors, feedback delay and channel

quantization on the average packet error probability. All these contributions further the understanding of feedback communication systems. As a side benefit, the analytical tools developed promise to be of general interest with broad applicability.

The rest of this chapter is organized as follows. A general framework for the modeling of imperfect feedback in the packet fading context is presented in Section 3.2. An analytical expression for the average packet error probability with un-coded BPSK constellation is derived in Section 3.3. Numerical and simulation results are presented in Section 3.4. We conclude this chapter in Section 3.5.

Important variables: $t$-number of transmit antennas, $\ell$-packet index, $k$-symbol index in the packet, $N$-number of symbols in a packet, $\tilde{\rho}_e$ estimation related correlation co-efficient, $\rho_e$-magnitude of $\tilde{\rho}_e$, $\tilde{\rho}_d$ delay related correlation co-efficient, $\rho_d$-magnitude of $\tilde{\rho}_d$, $B$-number of feedback bits, $\gamma_b$-SNR per bit, $\mathbf{h}_\ell$-actual channel of $\ell^{th}$ packet, $\widehat{\mathbf{h}}_\ell$-estimated channel of $\ell^{th}$ packet.

## 3.2 System Model

We consider a multiple input single output system with $t$ antennas at the transmitter and one antenna at the receiver. Let $\mathbf{h}_\ell$ be the channel between the transmitter and the receiver for the $\ell^{th}$ packet. $\mathbf{h}_\ell$ is modeled as a spatially i.i.d. frequency-flat Rayleigh fading channel which is constant for all the $N$ un-coded symbols in packet $\ell$. The vector valued channel $\mathbf{h}_\ell \sim \mathcal{NC}(\mathbf{0}, \mathbf{I})$. Furthermore, it is assumed that the channel varies from packet to packet but exhibits a significant correlation. The justification for feedback overhead, in systems such as the ones considered here, comes from the fact that the low-rate uplink channel is able to provide an improved link quality between transmitter and receiver. For feedback systems it is important that the wireless channel varies slowly, otherwise the mismatch between the beamforming vector and the actual channel will result in a significant performance degradation.

Ideally, the channel should be treated as continuously changing, implying that $\tilde{\rho}_d$ actually varies across a packet. However, assuming continuous variation of channel across all the symbols makes the problem analytically more challenging to the extent of making the analysis intractable. Assuming channel to remain constant for the packet (or block) is a fairly common assumption in many journal publications [79]- [83] (and numerous papers that cite them). Using the popular and well accepted Clark's model [2], we provide a simple example to validate the assumption of channel remaining constant for a packet and exhibiting correlation across the packets. According to Clark's model, the correlation, $R(\tau)$, between channel samples with a lag of $\tau$ is given by

$$R(\tau) = J_0(2\pi f_m \tau)$$

where $J_0()$ is the $0^{th}$ order Bessel function of the first kind, $f_m = v/\lambda$, $v$ is the velocity of mobile, and $\lambda$ is the carrier wavelength.

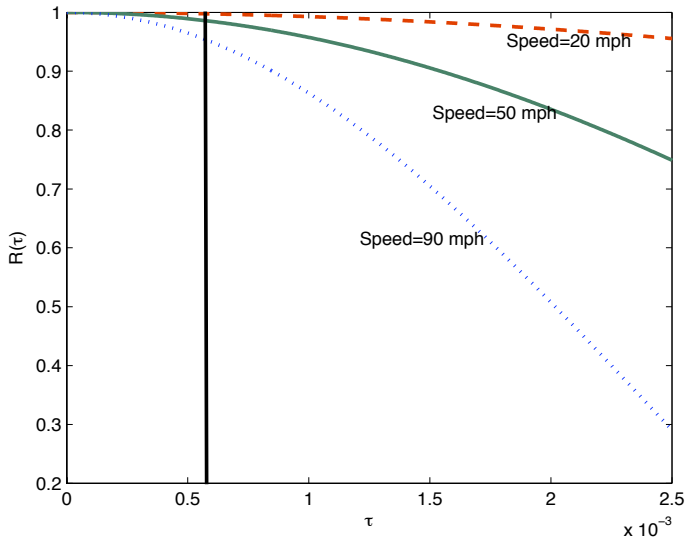


Figure 3.1 Correlation between two channel samples separated by a lag of $\tau$.

In Fig. 3.1, we plot the correlation $R(\tau)$ as a function of lag $\tau$. For this simulation, we follow the GSM system parameters as listed in page. 67 of [1]. Carrier frequency is assumed to be 900 MHz. Fig. **??** has three curves showing the

correlation for different mobile speeds (20, 50, and 90 mph). The solid black line is drawn at 0.57 milliseconds, which is the packet length of user (one of the eight served in a TDMA fashion) in a GSM system. At 20 mph speed, the correlation is nearly constant in the time-interval of interest (0.57 milliseconds). As the speed of mobile increases, at 90 mph, the correlation noticeably changes with-in a packet. So at relatively smaller speeds we can assume that the channel effectively remain constant for the entire packet. Another important point is that, the correlation calculated based on Clark's model assumes that a large number of multipath are coming from all directions around the mobile. However, in most of the cases there will only be a few multipath, and they generally arrive from a narrow angular space. Hence the correlation values suggested by Clark's model should be treated as the worst case scenario. The correlation in many real world situations is considerably higher than Clark model's estimate. In summary, smaller packet size combined with low mobility can justify the assumption of channel remaining constant for the duration of the packet and exhibiting a correlation across the packets.

The transmitted $k^{th}$ symbol in the packet $\ell$ is denoted by $s_\ell[k]$ and $E[|s_\ell[k]|^2] = E_s$. Let $\mathbf{w}_\ell$ be the unit norm beamforming vector (BV) at the transmitter for the packet $\ell$. Then, the $k^{th}$ received signal in the packet $\ell$ is given by

$$y_\ell[k] = \mathbf{h}_\ell^H \, \mathbf{w}_\ell \, s_\ell[k] + \eta_\ell[k], \quad k = 1, 2, \cdots, N \tag{3.1}$$

where $\eta_\ell[k]$ is the thermal noise that effects the $k^{th}$ symbol of $\ell^{th}$ packet, $\eta_\ell[k] \sim \mathcal{NC}\,(0, \sigma_n^2)$. We now discuss in detail the three forms of feedback imperfections and develop a general model, applicable for the packet fading context, that captures channel estimation errors, feedback delay, and finite-rate channel quantization for transmit beamforming MISO systems.

### 3.2.1 Channel Estimation Errors - Packet Fading Context

Let $\widehat{\mathbf{h}}_\ell$ be the estimate of $\mathbf{h}_\ell$. We assume that $\mathbf{h}_\ell$ and $\widehat{\mathbf{h}}_\ell$ are jointly Gaussian, a reasonable assumption for many practical estimation techniques (

[28,60,63,65] and the references therein). The jointly Gaussian assumption allows us to relate them as follows:

$$\mathbf{h}_\ell = \frac{\tilde{\rho}_e}{\sqrt{\Lambda}}\,\widehat{\mathbf{h}}_\ell + \sqrt{1-\rho_e^2}\,\boldsymbol{\varepsilon}_{\ell\,e} \tag{3.2}$$

where $\boldsymbol{\varepsilon}_{\ell\,e} \sim \mathcal{NC}\,(\mathbf{0},\mathbf{I})$, $\widehat{\mathbf{h}}_\ell \sim \mathcal{NC}\,(\mathbf{0},\Lambda\mathbf{I})$, and $\tilde{\rho}_e = \rho_e\, e^{j\phi_{\rho_e}}$ is the complex correlation coefficient that determines the degree of accuracy in channel estimation. The closer $\rho_e$ is to one, the more accurate is the channel estimate. $\tilde{\rho}_e$ can be assumed to be known at the receiver. Assuming instantaneous feedback and no channel quantization, the beamforming vector to be used at the transmitter is given by

$$\mathbf{w}_\ell = \frac{\widehat{\mathbf{h}}_\ell}{\|\widehat{\mathbf{h}}_\ell\|}\,. \tag{3.3}$$

The $k^{th}$ received signal of the $\ell^{th}$ packet with the BV given in (3.3) and $\mathbf{h}_\ell$ given in (3.2) is

$$\begin{aligned} y_\ell[k] &= \mathbf{h}_\ell^H\,\mathbf{w}_\ell\,s_\ell[k] + \eta_\ell[k] \\ &= \left(\frac{\tilde{\rho}_e}{\sqrt{\Lambda}}\,\widehat{\mathbf{h}}_\ell + \sqrt{1-\rho_e^2}\,\boldsymbol{\varepsilon}_{\ell\,e}\right)^H \frac{\widehat{\mathbf{h}}_\ell}{\|\widehat{\mathbf{h}}_\ell\|}\,s_\ell[k] + \eta_\ell[k] \\ &= \frac{\bar{\tilde{\rho}}_e}{\sqrt{\Lambda}}\,\|\widehat{\mathbf{h}}_\ell\|\,s_\ell[k] + \left(\sqrt{1-\rho_e^2}\,\tilde{\varepsilon}_{\ell\,e}\,s_\ell[k] + \eta_\ell[k]\right) \end{aligned} \tag{3.4}$$

where

$$\tilde{\varepsilon}_{\ell\,e} = \frac{\boldsymbol{\varepsilon}_{\ell\,e}^H\widehat{\mathbf{h}}_\ell}{\|\widehat{\mathbf{h}}_\ell\|} \sim \mathcal{NC}\,(0,1)\,.$$

In the above equation $\tilde{\varepsilon}_{\ell\,e}$ is unknown to the receiver and hence the receiver can not compensate for the phase rotation caused due to $\tilde{\varepsilon}_{\ell\,e}$.

In previous chapter, the performance criteria was average SEP/BEP and as a consequence the estimation error term simply got absorbed into the thermal noise and increased its variance (along with introducing a symbol dependency). In the packet fading model the estimation error term $\tilde{\varepsilon}_{\ell\,e}$ is constant and impacts the entire packet (while each symbol experiences a different noise sample) and hence it can not be simply lumped into the additive noise term. As will be evident from the next section, not lumping the estimation error term into white noise also makes

the analysis more complicated. Nevertheless, it has to be dealt with since PEP is a more appropriate performance metric to capture the impact of estimation errors in slow fading channels.

### 3.2.2 Feedback Delay with Imperfect Channel Estimation

In the above discussion, a simplistic assumption of feedback being available instantly was made at the transmitter. In reality there is a delay and to account for this it is assumed that the beamforming vector for the current packet $\ell$ is derived from the channel estimate of the previous packet $(\ell - 1)$. Since there is a time lag between forming the BV at the receiver and its use at the transmitter, the BV $\mathbf{w}_\ell$ depends on $\widehat{\mathbf{h}}_{\ell-1}$ as opposed to the current channel estimate $\widehat{\mathbf{h}}_\ell$. Assuming that the channel estimate and its delayed version are jointly Gaussian, we can relate them as follows:

$$\widehat{\mathbf{h}}_\ell = \tilde{\rho}_d \, \widehat{\mathbf{h}}_{\ell-1} + \sqrt{(1-\rho_d^2)\Lambda} \, \boldsymbol{\varepsilon}_{\ell\, d} \tag{3.5}$$

where $\widehat{\mathbf{h}}_\ell \sim \mathcal{NC}\,(\mathbf{0}, \Lambda\mathbf{I})$ and $\tilde{\rho}_d = \rho_d \, e^{j\phi_{\rho_d}}$ is the complex correlation co-efficient between $\widehat{\mathbf{h}}_\ell$ and $\widehat{\mathbf{h}}_{\ell-1}$, $\boldsymbol{\varepsilon}_{\ell\, d} \sim \mathcal{NC}\,(\mathbf{0}, \mathbf{I})$ is the error term due to delay and is assumed to be uncorrelated with $\widehat{\mathbf{h}}_{\ell-1}$. The delay correlation co-efficient $\tilde{\rho}_d$ is assumed to be known to the receiver and measures the impact of delay. With the help of (3.2) and (3.5), the actual channel $\mathbf{h}_\ell$ in terms of delayed version of the estimated channel $\widehat{\mathbf{h}}_{\ell-1}$ can be written as

$$\mathbf{h}_\ell = \tilde{\rho}_e \left\{ \frac{\tilde{\rho}_d}{\sqrt{\Lambda}} \, \widehat{\mathbf{h}}_{\ell-1} + \sqrt{1-\rho_d^2} \, \boldsymbol{\varepsilon}_{\ell\, d} \right\} + \sqrt{1-\rho_e^2} \, \boldsymbol{\varepsilon}_{\ell\, e} \, . \tag{3.6}$$

With the inclusion of estimation errors along with the feedback delay, the beamforming vector (still un-quantized) is given by

$$\mathbf{w}_\ell = \frac{\widehat{\mathbf{h}}_{\ell-1}}{\|\widehat{\mathbf{h}}_{\ell-1}\|} \, . \tag{3.7}$$

The beamforming vector $\mathbf{w}_\ell$ indicates that the BV is formed with the help of channel estimate from the previous packet $(\ell - 1)$ and is used to transmit the data

and pilot sequences as part of packet $\ell$. With this formulation, the $k^{th}$ received symbol of the packet $\ell$ can be written as

$$\begin{aligned} y_\ell[k] &= \mathbf{h}_\ell^H \mathbf{w}_\ell \, s_\ell[k] + \eta_\ell[k] \\ &= \left( \tilde{\rho}_e \left\{ \frac{\tilde{\rho}_d}{\sqrt{\Lambda}} \widehat{\mathbf{h}}_{\ell-1} + \sqrt{1-\rho_d^2}\, \boldsymbol{\varepsilon}_{\ell\, d} \right\} + \sqrt{1-\rho_e^2}\, \boldsymbol{\varepsilon}_{\ell\, e} \right)^H \frac{\widehat{\mathbf{h}}_{\ell-1}}{\|\widehat{\mathbf{h}}_{\ell-1}\|} s_\ell[k] + \eta_\ell[k] \\ &= \bar{\tilde{\rho}}_e \left\{ \frac{\bar{\tilde{\rho}}_d \|\widehat{\mathbf{h}}_{\ell-1}\|}{\sqrt{\Lambda}} + \sqrt{1-\rho_d^2}\, \acute{\varepsilon}_{\ell\, d} \right\} s_\ell[k] + \underbrace{\sqrt{1-\rho_e^2}\, \acute{\varepsilon}_{\ell\, e}\, s_\ell[k] + \eta_\ell[k]}_{\text{Unknown to the Receiver}} \end{aligned} \tag{3.8}$$

where

$$\begin{aligned} \acute{\varepsilon}_{\ell\, d} &= \frac{\boldsymbol{\varepsilon}_{\ell\, d}^H \widehat{\mathbf{h}}_{\ell-1}}{\|\widehat{\mathbf{h}}_{\ell-1}\|} \sim \mathcal{NC}\left(0,1\right), \\ \acute{\varepsilon}_{\ell\, e} &= \frac{\boldsymbol{\varepsilon}_{\ell\, e}^H \widehat{\mathbf{h}}_{\ell-1}}{\|\widehat{\mathbf{h}}_{\ell-1}\|} \sim \mathcal{NC}\left(0,1\right). \end{aligned}$$

For a particular packet both $\acute{\varepsilon}_{\ell\, d}$ and $\acute{\varepsilon}_{\ell\, e}$ are constant. The distributions of both $\acute{\varepsilon}_{\ell\, d}$ and $\acute{\varepsilon}_{\ell\, e}$ indicate their random nature over packets.

As explained in the previous section the estimation related error term $\acute{\varepsilon}_{\ell\, e}$ is unknown to the receiver and hence the phase rotation caused by $\acute{\varepsilon}_{\ell\, e}$ can not be compensated. The role of delay related error term $\acute{\varepsilon}_{\ell\, d}$, which determines the penalty due to the feedback delay, will depend on the modeling assumptions. Notice that if there is no feedback delay, then $\tilde{\rho}_d = 1$ and the error term vanishes. If $\acute{\varepsilon}_{\ell\, d}$ is also assumed to be unknown, then it can be treated in a manner similar to estimation error. In particular, if the performance metric is SEP/BEP, or if the channel is varying at a symbol level as opposed to packet level, then $\acute{\varepsilon}_{\ell\, d}$ can be merged into the receiver noise greatly simplifying the analysis [16, 18], [64]-[70]. A closer examination, as explained below, indicates that there is a distinction between estimation error related term and the delay related term and so lumping them together is a questionable simplification.

We propose a model/approach to handle this error that we believe more accurately captures the impact of delay on feedback system performance. The model is based on the following system assumption: there is a pilot sequence

before every packet of data and that the beamforming vector (3.7) is based on the channel estimate from the previous packet. Under this assumption, the receiver will be knowing both $\widehat{\mathbf{h}}_\ell$ and $\widehat{\mathbf{h}}_{\ell-1}$ and hence it knows the error term due to delay $\varepsilon_{\ell d}$, c.f. 3.5 (and subsequently $\acute{\varepsilon}_{\ell d}$). As shown later, this simple change in the approach impacts the performance of the system considerably and indicates more clearly the conceptual distinction between the imperfections resulting from delay and estimation. However this modeling also makes the problem of performance analysis more complicated. Note that even if the receiver knows $\acute{\varepsilon}_{\ell d}$, it can not compensate for all the loss caused due to delay. Its performance lies in between a system with no feedback delay ($\rho_d = 1$), and a system where the receiver does not know $\acute{\varepsilon}_{\ell d}$, ($0 < \rho_d < 1$) and is lumped into the receiver noise. By changing the way beamforming vector is formed, the receiver is able to know the delay related error term $\acute{\varepsilon}_{\ell d}$, on the other hand it is impossible to know the estimation related error term $\acute{\varepsilon}_{\ell e}$.

### 3.2.3 Quantization of Delayed Version of Channel Estimate

In the previous two sections we assumed that the channel state information is exactly conveyed to the transmitter. In practice, the receiver estimates the channel, and quantizes it into one of $\mathcal{C} = 2^B$ code words in the codebook which is known to both transmitter and receiver. The index, which is represented by $B$ bits, of the code word corresponding to the channel estimate is fed back to the transmitter. We assume that the feedback channel is error free [22]-[27]. The beamforming vector formed by quantizing delayed version of the channel estimate is given by

$$\mathbf{w}_\ell = \mathcal{Q}\left[\frac{\widehat{\mathbf{h}}_{\ell-1}}{\|\widehat{\mathbf{h}}_{\ell-1}\|}\right] \tag{3.9}$$

where $\mathcal{Q}$ is the quantization function, here we assume a VQ based codebook ( [25, 26]). Using (3.6) and (3.9), the $k^{th}$ received signal of the packet $\ell$ is:

$$y_\ell[k] \;=\; \mathbf{h}_\ell^H \mathbf{w}_\ell \, s_\ell[k] + \eta_\ell[k]$$

$$
\begin{aligned}
&= \left(\tilde{\rho}_e \left\{ \frac{\tilde{\rho}_d}{\sqrt{\Lambda}} \widehat{\mathbf{h}}_{\ell-1} + \sqrt{1-\rho_d^2}\, \boldsymbol{\varepsilon}_{\ell d} \right\} + \sqrt{1-\rho_e^2}\, \boldsymbol{\varepsilon}_{\ell e} \right)^H \left( \mathcal{Q}\left[ \frac{\widehat{\mathbf{h}}_{\ell-1}}{\|\widehat{\mathbf{h}}_{\ell-1}\|} \right] \right) \\
&\quad s_\ell[k] + \eta_\ell[k] \\
&= \bar{\tilde{\rho}}_e \left( \frac{\bar{\tilde{\rho}}_d}{\sqrt{\Lambda}} \underline{\vartheta_{\ell-1}} \, \|\widehat{\mathbf{h}}_{\ell-1}\| + \sqrt{1-\rho_d^2}\, \hat{\varepsilon}_{\ell d} \right) s_\ell[k] + \sqrt{1-\rho_e^2}\, \hat{\varepsilon}_{\ell e}\, s_\ell[k] + \eta_\ell[k],
\end{aligned}
\tag{3.10}
$$

where

$$
\begin{aligned}
\hat{\varepsilon}_{\ell d} &= \boldsymbol{\varepsilon}_{\ell d}^H \left( \mathcal{Q}\left[ \widehat{\mathbf{h}}_{\ell-1} / \|\widehat{\mathbf{h}}_{\ell-1}\| \right] \right), \qquad \hat{\varepsilon}_{\ell d} \sim \mathcal{NC}\,(0,1)\,, \\
\hat{\varepsilon}_{\ell e} &= \boldsymbol{\varepsilon}_{\ell e}^H \left( \mathcal{Q}\left[ \widehat{\mathbf{h}}_{\ell-1} / \|\widehat{\mathbf{h}}_{\ell-1}\| \right] \right), \qquad \hat{\varepsilon}_{\ell e} \sim \mathcal{NC}\,(0,1)\,, \\
\vartheta_{\ell-1} &= \left( \widehat{\mathbf{h}}_{\ell-1} / \|\widehat{\mathbf{h}}_{\ell-1}\| \right)^H \left( \mathcal{Q}\left[ \widehat{\mathbf{h}}_{\ell-1} / \|\widehat{\mathbf{h}}_{\ell-1}\| \right] \right).
\end{aligned}
\tag{3.11}
$$

We now take a closer look at the additional changes to the $k^{th}$ symbol in the received packet $\ell$ because of use of a quantized beamforming vector. The received signal with and without quantized BV is given by (3.12) and (3.13) respectively

$$
\overbrace{y_\ell[k]}^{\text{Un-Quantized BV (3.7)}} = \underbrace{\bar{\tilde{\rho}}_e \left\{ \frac{\bar{\tilde{\rho}}_d}{\sqrt{\Lambda}} \|\widehat{\mathbf{h}}_{\ell-1}\| + \sqrt{1-\rho_d^2}\, \acute{\varepsilon}_{\ell d} \right\}}_{\text{known to the Receiver}} s_\ell[k] + \underbrace{\sqrt{1-\rho_e^2}\, \acute{\varepsilon}_{\ell e}\, s_\ell[k] + \eta_\ell[k]}_{\text{Unknown to the Receiver}},
\tag{3.12}
$$

$$
\overbrace{y_\ell[k]}^{\text{Quantized BV (3.9)}} = \underbrace{\bar{\tilde{\rho}}_e \left( \frac{\bar{\tilde{\rho}}_d}{\sqrt{\Lambda}} \underline{\vartheta_{\ell-1}} \, \|\widehat{\mathbf{h}}_{\ell-1}\| + \sqrt{1-\rho_d^2}\, \hat{\varepsilon}_{\ell d} \right)}_{\tilde{\psi}_\ell = \psi_\ell\, e^{j\,\phi_{\psi_\ell}} \text{ (Known to the Receiver)}} s_\ell[k] + \underbrace{\sqrt{1-\rho_e^2}\, \hat{\varepsilon}_{\ell e}\, s_\ell[k] + \eta_\ell[k]}_{\text{Unknown to the Receiver}}.
\tag{3.13}
$$

The above two equations mainly defer in three places. The effective error terms with un-quantized BV are $\acute{\varepsilon}_{\ell d}$ and $\acute{\varepsilon}_{\ell e}$ and the effective error terms with quantized BV are $\hat{\varepsilon}_{\ell d}$ and $\hat{\varepsilon}_{\ell e}$.

All these effective error terms are different in an instantaneous sense, but all of them are CSCG random variables with same mean and variance. Since we are interested in average PEP we can conclude that quantization did not have any effect in this aspect. The main effect of quantization on the PEP comes from

$\vartheta_{\ell-1}$ (underlined term in $\tilde{\psi}_\ell$). $\vartheta_{\ell-1}$ is the inner product between the unquantized and quantized BV and the statistical characterization of $\tilde{\Delta} \triangleq |\vartheta_{\ell-1}|^2$ will be important for the performance analysis. Since finding the exact pdf of $\tilde{\Delta}$ is rather difficult, [25, 26] upper bounded $\tilde{\Delta}$ (i.e., lower bounded the average error performance) by a r.v $\Delta$, whose pdf is given by

$$p_\Delta(x) = 2^B(t-1)(1-x)^{t-2}, \quad 1-\omega < x < 1 \tag{3.14}$$

where $\omega = 2^{-B/(t-1)}$. In what follows, we use $\Delta$ in place of $\tilde{\Delta}$. Because of our modeling assumptions, the receiver knows $\tilde{\rho}_d$, $\tilde{\rho}_e$, $\widehat{\mathbf{h}}_\ell$, $\widehat{\mathbf{h}}_{\ell-1}$, and $\mathcal{Q}\left[\widehat{\mathbf{h}}_{\ell-1}/\|\widehat{\mathbf{h}}_{\ell-1}\|\right]$, so it knows $\tilde{\psi}_\ell$ which enables coherent detection of the transmitted symbol.

## 3.3 Average Packet Error Probability

Since the feedback delay related error term and estimation related error term are constant for the entire packet, average packet error probability, a metric that requires averaging over the packet index $\ell$ thereby capturing the effect of imperfect feedback in transmit beamforming MISO systems, provides a meaningful way to study performance analysis. Also as pointed out in the introduction, for slotted multiple access schemes and as a quality of service parameter for the MAC layer of wireless networks, analytical understanding of PEP is important from system design point of view. Existing results primarily are PEP with non-coherent FSK modulation and so not readily applicable.

In this section we present the analysis of the average packet error probability of an un-coded packet of $N$ BPSK symbols with imperfect feedback. We first begin with the decision statistic required for the detection of $k^{th}$ symbol of $\ell^{th}$ packet and then focus on the PEP. The coherent detection of transmitted symbol is based on $r_\ell[k]$, obtained from $y_\ell[k]$ in (3.13).

$$\begin{aligned} r_\ell[k] &= e^{-j\,\phi_{\psi_\ell}}\, y_\ell[k] \\ &= \left(\psi_\ell + \sqrt{1-\rho_e^2}\,\breve{\varepsilon}_{\ell\,e}\right) s_\ell[k] + \breve{\eta}_\ell[k], \end{aligned} \tag{3.15}$$

$$\begin{aligned}
\psi_\ell &= \left|\bar{\tilde{\rho}}_e \left( \frac{\bar{\tilde{\rho}}_d}{\sqrt{\Lambda}}\, \vartheta_{\ell-1}\, \|\widehat{\mathbf{h}}_{\ell-1}\| + \sqrt{1-\rho_d^2}\, \hat{\varepsilon}_{\ell\, d} \right) \right|, \qquad (3.16)\\
\breve{\varepsilon}_{\ell\, e} &= e^{-j\, \phi_{\psi_\ell}}\, \hat{\varepsilon}_{\ell\, e} \sim \mathcal{NC}\,(0,1)\,,\\
\breve{\eta}_\ell[k] &= e^{-j\, \phi_{\psi_\ell}}\, \eta_\ell[k] \sim \mathcal{NC}\left(0, \sigma_n^2\right).
\end{aligned}$$

Notice that in the above equation, $\psi_\ell$ and $\breve{\varepsilon}_{\ell\, e}$ do not depend on $[k]$ indicating that these two terms are fixed for the entire packet, whereas the notation for the white noise is $\breve{\eta}_\ell[k]$ indicating a different noise sample for each symbol.

To highlight the differences with the previous chapter, we now briefly contrast the decision variable (DV) in (3.15) to that of the the DV we used in the previous chapter. The performance metric in the previous chapter was average SEP/BEP and the DV in the previous chapter was given as

$$r[k] = \kappa s[k] + \xi[k], \qquad (3.17)$$

where $\kappa$ is an *unknown* complex constant number(note that in this chapter we assume the knowledge of $\tilde{\rho}_e$, the estiamtion related correlation coefficient, and $\tilde{\rho}_d$, the delay related correlation coefficient, at the receiver) and $\xi$ is conditionally (conditioned on both fading and quantization of channel) CSCG random variable. In the previous chapter to derive analytical expression average SEP/BEP, we had to account for the fact that the transmitted symbol is scaled and rotated as well as the noise is symbol dependent. The DV (3.15) in this chapter is more complicated. All the symbols of $\ell^{th}$ block are scaled by a known random variable $\psi_\ell$. Note that knowledge of $\psi_\ell$ at the receiver is possible due to the modeling assumptions presented. Also, all the symbols of $\ell^{th}$ block experience the same channel estimation related error term $\breve{\varepsilon}_{\ell\, e}$.

Since we are restricting our attention to the BPSK constellation, the receiver uses the real part (for thresholding) of $r_\ell[k]$ to decode the transmitted symbol as

$$\begin{aligned}
\tilde{r}_\ell[k] &= \text{Real}\,(r_\ell[k]) = \kappa\, s_\ell[k] + \hat{\eta}_\ell[k],\\
\kappa &= \psi_\ell + \sqrt{(1-\rho_e^2)/2}\, \hat{\boldsymbol{\varepsilon}}_{\ell er}\,, \quad \psi_\ell > 0, \quad -\infty < \kappa < \infty, \qquad (3.18)
\end{aligned}$$

$\hat{\boldsymbol{\varepsilon}}_{\ell er}$ and $\hat{\eta}_\ell$ are both real random variables with $\hat{\boldsymbol{\varepsilon}}_{\ell er} = \text{Real}\,(\hat{\boldsymbol{\varepsilon}}_{\ell e}) \sim \mathcal{N}\,(0,1)$ and $\hat{\eta}_\ell[k] = \text{Real}\,(\breve{\eta}_\ell[k]) \sim \mathcal{N}\,(0, \sigma_n^2/2)$. As pointed out earlier $\hat{\boldsymbol{\varepsilon}}_{\ell er}$ is a fixed constant for a particular packet, and viewed over a number of packets it is a statistical quantity. The derivation of an analytical expression for PEP is quite involved and here we outline the important steps in the derivation.

1. Derivation of pdf for $\kappa$: The signal scaling random variable in the decision statistic $\tilde{r}_\ell[k]$ is $\kappa$. So the pdf of $\kappa$ is important for the analysis of PEP. The derivation of the pdf of $\kappa$ is complicated by its dependency on the three forms of imperfection. Details of the derivation can be found in Subsection 3.3.1.

2. Expectation of the Gaussian $Q$-function and its higher powers w.r.t the random variable $\kappa$: Much of the analytical complexity in the performance analysis (PEP) revolves around the evaluation of expectations of the Gaussian $Q$-function and its higher powers w.r.t the random variable $\kappa$ in closed-form. For the first two powers of the Gaussian $Q$-function, we are able to evaluate the expectation using the exact form of the Gaussian $Q$-function. For higher powers ($\geq 3$), we make use of an approximation of the Gaussian $Q$-function and evaluate its expectation w.r.t $\kappa$. Details are in Subsection 3.3.2.2.

### 3.3.1 Derivation of pdf for $\kappa$

The signal scaling term $\kappa$ in the decision statistic $\tilde{r}_\ell[k]$ is given in (3.18):

$$\kappa = \psi_\ell + \sqrt{(1-\rho_e^2)/2}\,\hat{\boldsymbol{\varepsilon}}_{\ell er}\,, \quad \psi_\ell > 0, \quad -\infty < \kappa < \infty.$$

Conditioned on $\psi_\ell$, the conditional pdf of $\kappa$ is given by

$$p_\kappa(z|\psi_\ell = x) \;=\; \frac{1}{\sqrt{\pi(1-\rho_e^2)}}\, e^{-\frac{(z-x)^2}{1-\rho_e^2}}.$$

and the pdf of $\kappa$ can be obtained as

$$\begin{aligned} p_\kappa(z) &= \int_{-\infty}^{\infty} p_\kappa(z,x)dx \\ &= \int_{-\infty}^{\infty} p_\kappa(z|x)\, p_{\psi_\ell}(x)\, dx \end{aligned} \tag{3.19}$$

The evaluation of (3.19) requires the pdf of $\psi_\ell$ which is derived in Section 3.6.1 of the Appendix and the final expression is given in (3.66). Note that if there are no estimation errors in the model, or if the performance criteria is average symbol/bit error probability [61], or if the performance criteria is average packet error probability with any constellation other than BPSK, then the pdf of $\psi_\ell$ becomes central to the performance analysis. Here, not only is the pdf of $\psi_\ell$ required, the extra step discussed in (3.19) has to be carried out for the pdf of $\kappa$. Substituting the pdf of $\psi_\ell$ in (3.19), we obtain

$$p_\kappa(z) = \sum_{l=0}^{n} \sum_{p=0}^{2n-l-1} \sum_{g=0}^{\delta} \left\{ \mathcal{K}_{p_1} f_{a2}(l,p,g,\mathcal{L},z) + \mathcal{K}_{p_2} f_{b2}(l,p,g,\mathcal{L},z) \right\} \tag{3.20}$$

where the variable and the corresponding defining equation are listed as pairs: $n$ - (3.46), $\delta$ - (3.57), $\mathcal{L}$ - (3.54), $\mathcal{K}_{p_1}$ - (3.60), and $\mathcal{K}_{p_2}$ - (3.61), and

$$\begin{aligned} f_{b2}(l,p,g,\mathcal{L},z) &= \frac{2\,\mathcal{L}^{n-l-g}\, e^{-\frac{z^2}{1-\rho_e^2}}}{\rho_e^{2(n-l-g)}\,\Gamma(n-l-g)\,\sqrt{\pi(1-\rho_e^2)}} \times \\ &\qquad \int_0^\infty x^{2(n-l-g)-1}\, e^{\frac{-x^2\left[\rho_e^2+\mathcal{L}(1-\rho_e^2)\right]}{\rho_e^2(1-\rho_e^2)}+\frac{2xz}{1-\rho_e^2}}\, dx\,. \end{aligned}$$

To evaluate the above integral we use the following identity [35]

$$\int_0^\infty x^{v-1} e^{-\beta x^2-\gamma x}\, dx = (2\beta)^{-v/2}\,\Gamma(v)\, e^{\frac{\gamma^2}{8\beta}}\, D_{-v}\left(\frac{\gamma}{\sqrt{2\beta}}\right). \tag{3.21}$$

In the present context

$$\begin{aligned} \beta &= \frac{\rho_e^2+\mathcal{L}(1-\rho_e^2)}{\rho_e^2\,(1-\rho_e^2)}, \\ \gamma &= -\frac{2z}{1-\rho_e^2}, \\ v &= 2(n-l-g)\,. \end{aligned}$$

$f_{b2}(l,p,g,\mathcal{L},z)$ can now be written as

$$f_{b2}(l,p,g,\mathcal{L},z) = \mathcal{H}_1\, e^{-z^2\,\mathcal{H}_2}\, D_{-2(n-l-g)}\left(-z\,\mathcal{H}_3\right), \quad -\infty < z < \infty \tag{3.22}$$

where

$$\mathcal{H}_1 = \frac{\mathcal{L}^{n-l-g}\,(1-\rho_e^2)^{n-l-g}\,\Gamma(2[n-l-g])}{2^{n-l-g-1}\,\Gamma(n-l-g)\,(\rho_e^2+\mathcal{L}(1-\rho_e^2))^{n-l-g}\,\sqrt{\pi(1-\rho_e^2)}}\,, \quad (3.23)$$

$$\mathcal{H}_2 = \frac{\rho_e^2+2\mathcal{L}(1-\rho_e^2)}{2(1-\rho_e^2)(\rho_e^2+\mathcal{L}(1-\rho_e^2))}\,, \quad (3.24)$$

$$\mathcal{H}_3 = \frac{\sqrt{2}\,\rho_e}{\sqrt{(1-\rho_e^2)(\rho_e^2+\mathcal{L}(1-\rho_e^2))}}\,, \quad (3.25)$$

and $D_{\tilde{p}}(\tilde{l})$ is the parabolic cylinder function [35]. Finally

$$f_{a2}(l,p,g,\mathcal{L},z) = f_{b2}(l,p,g,1,z)\,, \quad (3.26)$$

which completes all the steps required to compute $p_\kappa(z)$ in (3.20).

The analytical expression for $p_\kappa(z)$ is confirmed using simulations (histogram approach is used to get the simulated version of $\kappa$'s pdf) in Fig. 3.7 for number of transmit antennas $t \in \{2,3\}$, delay correlation co-efficient $\rho_d \in \{0.98, 0.94\}$, and estimation error correlation co-efficient $\rho_e \in \{0.95, 0.91\}$. The number of feedback bits $B$ which determines the quantization codebook size is fixed at 4. From the Fig. 3.7 it can be seen that the tail of the pdf increases as the number of antennas increase, also the tail increases as the correlation increases.

### 3.3.2 Analytical Expression for Packet Error Probability

Conditioned on $\kappa$, the packet error probability (the probability that at least one symbol in the packet is received incorrectly) is given by

$$\begin{aligned} P_{B,\ell}(\gamma_b,\rho_e,t,N) &= 1-\{1-p_{b,\ell}\}^N \\ &= 1-\sum_{m=0}^{N}\binom{N}{m}(-1)^m\,(p_{b,\ell})^m \end{aligned}$$

where $p_{b,\ell}$ is the error probability of a symbol in the $\ell^{th}$ packet (calculated with the help of decision statistic $\tilde{r}_\ell[k]$)[1] Note that since $\kappa$ is fixed for the entire packet (while

[1]Similar to [45], the above equation can be easily modified to the scenario of a block channel coded system that can correct an arbitrary number of errors.

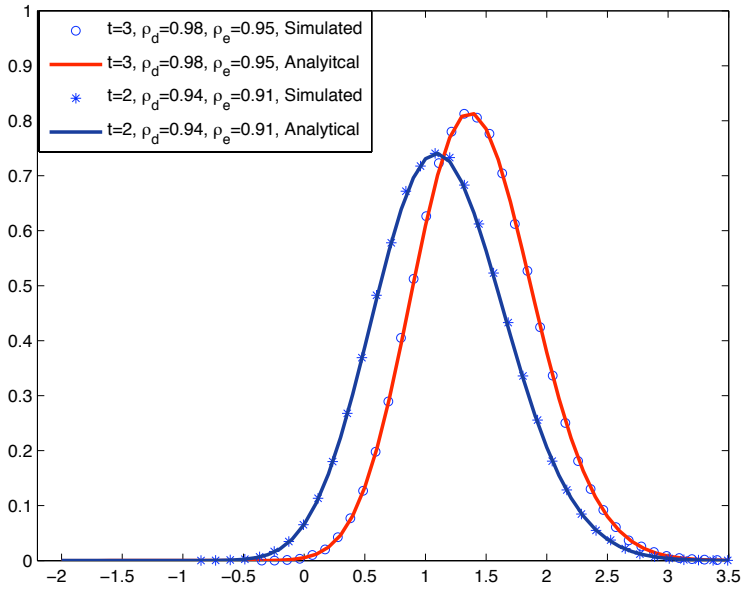


Figure 3.2 Verification of the pdf for the signal scaling term $\kappa$ defined in (3.18), number of transmit antennas $t \in \{2, 3\}$, delay correlation co-efficient $\rho_d \in \{0.98, 0.94\}$, and estimation error correlation co-efficient $\rho_e \in \{0.95, 0.91\}$, number of feedback bits $B = 4$.

the noise sample is different for each symbol), all the symbols have the same error probability. The average packet error probability is given by

$$\begin{aligned} \tilde{P}_B(\gamma_b, \rho_e, t, N) &= E_\ell \left[ P_{B,\ell}(\gamma_b, \rho_e, t, N) \right] \\ &= 1 - \sum_{m=0}^{N} \binom{N}{m} (-1)^m E_\ell \left[ (p_{b,\ell})^m \right]. \end{aligned} \tag{3.27}$$

Accounting for the fact that '$\kappa$' can be negative with a non-trivial probability, with BPSK constellation, $E_\ell \left[ (p_{b,\ell})^m \right]$ can be written as

$$\begin{aligned} E_\ell \left[ (p_{b,\ell})^m \right] &= A_p E_\ell \left[ Q^m \left( \sqrt{2\gamma_b \, z_1} \right) \right] + (1 - A_p) \, E_\ell \left\{ 1 - Q \left( \sqrt{2\gamma_b \, z_2} \right) \right\}^m \\ &= A_p \, E_{z_1} \left[ Q^m \left( \sqrt{2\gamma_b \, z_1} \right) \right] + \\ &\quad (1 - A_p) \sum_{w=0}^{m} (-1)^w \, E_{z_2} \left\{ Q^w \left( \sqrt{2\gamma_b \, z_2} \right) \right\} \end{aligned} \tag{3.28}$$

where

$$Q(x) = \frac{1}{\sqrt{2\pi}} \int_{u=x}^{\infty} \exp\left(-\frac{u^2}{2}\right) du$$

is the standard Gaussian tail function [12] and $A_p$ is the area under the positive side of pdf $p_\kappa(z)$. i.e.,

$$A_p = \int_0^\infty p_\kappa(z) dz.$$

Note that in the evaluation of $E_\ell\left[(p_{b,\ell})^m\right]$, one can integrate w.r.t $z$ directly, however, Since $-\infty < \kappa < \infty$, for clarity in presentation we chose to express $E_\ell\left[(p_{b,\ell})^m\right]$ as shown in (3.28). In (3.28), $\gamma_b$ is the SNR of a symbol in the packet and

$$\begin{aligned} z_1 &= \kappa^2, \qquad 0 < \kappa < \infty, \\ z_2 &= \kappa^2, \qquad -\infty < \kappa < 0. \end{aligned}$$

Using transformation of random variables, the pdfs of $z_1$ and $z_2$, needed to evaluate (3.28), can be shown to be given by (3.69) and (3.70) respectively. For readability purpose the pdfs of $z_1$ (3.69) and $z_2$ (3.70) are given at the end of Section 3.6.1 of the Appendix. To evaluate (3.28), we need to find an expression for $A_p$ and evaluate the expectations of the Gaussian $Q$-function and its higher powers w.r.t the random variable $\kappa$. These steps are described below.

#### 3.3.2.1 Evaluation of $A_p$

A closed-form expression for $A_p$ can be evaluated as

$$\begin{aligned} A_p &= \int_0^\infty p_\kappa(z) dz = 1 - \int_0^\infty p_\kappa(-z) dz, \\ &= \sum_{l=0}^{n} \sum_{p=0}^{2n-l-1} \sum_{g=0}^{\delta} \left\{ \mathcal{K}_{p_1} f_{ap1}(l,p,g,\mathcal{L},z) + \mathcal{K}_{p_2} f_{ap2}(l,p,g,\mathcal{L},z) \right\}, \quad (3.29) \end{aligned}$$

$$f_{ap2}(l,p,g,\mathcal{L},z) = 1 - \mathcal{H}_1 \int_0^\infty e^{-z^2 \mathcal{H}_2} D_{-2(n-l-g)}\left(\mathcal{H}_3\, z\right) dz.$$

Let

$$z = \sqrt{x}, \quad dz = \frac{1}{2} x^{-\frac{1}{2}} dx.$$

$$
\begin{aligned}
f_{ap2}(l,p,g,\mathcal{L},z) &= 1-\frac{\mathcal{H}_1}{2}\int_0^{\infty} x^{-\frac{1}{2}}\, e^{-x\,\mathcal{H}_2}\, D_{-2(n-l-g)}\left(\mathcal{H}_3\sqrt{x}\right) dx, \\
&= 1-\frac{\mathcal{H}_1\, 2^{-(n-l-g+1)}\,\sqrt{\pi}}{\Gamma(n-l-g+1)} \\
&\quad {}_2F_1\left(n-l-g,\frac{1}{2};n-l-g+1;\frac{4\mathcal{H}_2-\mathcal{H}_3^2}{4\mathcal{H}_2+\mathcal{H}_3^2}\right) \qquad (3.30)
\end{aligned}
$$

where ${}_2F_1(\cdot,\cdot;\cdot;\cdot)$ is the hypergeometric function. To evaluate the above integral we used [35]

$$
\begin{aligned}
\int_0^{\infty} x^{-\frac{\beta}{2}+1}\, e^{-xc}\, D_{-\nu}\left(2(kx)^{\frac{1}{2}}\right) dx &= \frac{2^{1-\beta-\frac{\nu}{2}}\,\sqrt{\pi}\,\Gamma(\beta)}{\Gamma\left(\frac{\nu+\beta+1}{2}\right)}(c+k)^{-\frac{\beta}{2}} \\
&\quad {}_2F_1\left(\frac{\nu}{2},\frac{\beta}{2};\frac{\nu+\beta+1}{2};\frac{c-k}{c+k}\right), \qquad (3.31) \\
&\quad \left[\mathrm{Re}\,(c+k)>0, \quad \mathrm{Re}\left(\frac{c}{k}\right)>0\right].
\end{aligned}
$$

In (3.29)

$$f_{ap1}(l,p,g,\mathcal{L},z) = f_{ap2}(l,p,g,1,z).$$

#### 3.3.2.2 Evaluating the expectations of the Gaussian $Q$-functions in (3.28)

In this subsection we evaluate the expectations of the Gaussian $Q$-function and its higher powers w.r.t the random variable $\kappa$. As explained in the previous subsection, the random variable $\kappa$ is now split into two random variables $z_1$ (capturing the positive part of $\kappa$) and $z_2$ (capturing the negative part of $\kappa$) in closed-form. For $m \in \{1,2\}$ ($m$ being the power of the Gaussian $Q$-function), we evaluate the expectation using the exact form of the Gaussian $Q$-function. For higher powers ($m \geq 3$), we make use of an approximation of the Gaussian $Q$-function and evaluate its expectation w.r.t $z_1$ and $z_2$. We start with $A_p\, E_{z_1}\left[Q^m\left(\sqrt{2\,\gamma_b\, z_1}\right)\right]$, $m = 1\,\text{and}\,2$, required to compute (3.28):

$$
\begin{aligned}
A_p\, E_{z_1}\left[Q^m\left(\sqrt{2\,\gamma_b\, z_1}\right)\right] &= \int_{z_1=0}^{\infty} Q^m\left(\sqrt{2\,\gamma_b\, z_1}\right)\left[A_p\, p_{z_1}(z_1)\right] dz_1 \\
&= \int_{z_1=0}^{\infty} Q^m\left(\sqrt{2\,\gamma_b\, z_1}\right)\left[\hat{p}_1(z_1)+\hat{p}_2(z_1)\right]\, dz_1. \qquad (3.32)
\end{aligned}
$$

For $m = 1$, $A_p\, E_{z_1}\left[Q^m\left(\sqrt{2\,\gamma_b\, z_1}\right)\right]$ can be written as

$$\begin{aligned} A_p\, E_{z_1}\left[Q\left(\sqrt{2\,\gamma_b\, z_1}\right)\right] &= \int_{z_1=0}^{\infty} Q\left(\sqrt{2\,\gamma_b\, z_1}\right)\hat{p}_1(z_1)\,dz_1 + \\ &\quad \int_{z_1=0}^{\infty} Q\left(\sqrt{2\,\gamma_b\, z_1}\right)\hat{p}_2(z_1)\,dz_1\,, \\ &= \mathcal{G}_1\left(\frac{\pi}{2}\right) + \mathcal{G}_2\left(\frac{\pi}{2}\right) \end{aligned} \tag{3.33}$$

where $\mathcal{G}_1(\varphi)$ and $\mathcal{G}_2(\varphi)$ are derived in Section 3.6.2 of the Appendix. For $m = 1$ and 2, in Section 3.6.2 of the Appendix we exploit the fact that the first and second powers of the Gaussian $Q$-function are parameterized by $\varphi = \frac{\pi}{2}$ and $\varphi = \frac{\pi}{4}$ respectively in the function $\tilde{Q}(x)$ given below [12], i.e., $\tilde{Q}\left(\frac{\pi}{2}\right) = Q(x)$ and $\tilde{Q}\left(\frac{\pi}{4}\right) = Q^2(x)$

$$\tilde{Q}(x) = \frac{1}{\pi}\int_{\theta=0}^{\varphi} e^{\left(-\frac{x^2}{2\sin^2\theta}\right)}d\theta, \quad x \geq 0. \tag{3.34}$$

Following the above steps and Section 3.6.2 of the Appendix, it can be shown that

$$\begin{aligned} A_p\, E_{z_1}\left\{Q^2\left(\sqrt{2\gamma_b z_1}\right)\right\} &= \mathcal{G}_1\left(\frac{\pi}{4}\right) + \mathcal{G}_2\left(\frac{\pi}{4}\right), \\ (1-A_p)\, E_{z_2}\left\{Q\left(\sqrt{2\gamma_b z_2}\right)\right\} &= \mathcal{G}_1\left(\frac{\pi}{2}\right) - \mathcal{G}_2\left(\frac{\pi}{2}\right), \\ (1-A_p)\, E_{z_2}\left\{Q^2\left(\sqrt{2\gamma_b z_2}\right)\right\} &= \mathcal{G}_1\left(\frac{\pi}{4}\right) - \mathcal{G}_2\left(\frac{\pi}{4}\right). \end{aligned}$$

Exact expressions for $A_p\, E_{z_1}\left[Q^m\left(\sqrt{2\,\gamma_b\, z_1}\right)\right]$ and $(1-A_p)\, E_{z_2}\left[Q^m\left(\sqrt{2\,\gamma_b\, z_2}\right)\right]$, for $m \geq 3$, are difficult to derive. With the help of results presented in Section 3.6.3 of the Appendix, the following series representation can be given for an analytically tractable form for $Q^m(x)$. We begin with the approximated form for $Q(x)$ (from Section 3.6.3)

$$\begin{aligned} Q(x) &\approx e^{\frac{-x^2}{2}}\sum_{\tilde{m}=0}^{m_a} c_{\tilde{m}}\, x^{\tilde{m}}\,, \\ c_{\tilde{m}} &= \frac{(-1)^{\tilde{m}+2}(A)^{\tilde{m}+1}}{B\sqrt{\pi}\,(\sqrt{2})^{\tilde{m}+2}\,(\tilde{m}+1)!}\,. \end{aligned}$$

where $A = 1.98$, $B = 1.135$, and $m_a = 10$ [84]. $Q^m(x)$ can be written as

$$Q^m(x) \approx e^{\frac{-mx^2}{2}}\sum_{k_1=0}^{m\,m_a} c_{k_1}\, x^{k_1}\,, \tag{3.35}$$

The co-efficients $c_{k_1}$ can be calculated in an easy manner using the fourier transform properties in a programming language like MATLAB. The expectations of the $Q$ approximation with respect to $z_1$ and $z_2$ are carried out in Section 3.6.4 of the Appendix and the final expressions are given by (3.110) and (3.115).

### 3.3.3 Special Cases of the PEP Expression in (3.27)

In this section we briefly discuss a few special cases of the PEP expression given in (3.27).

1. With block length $N = 1$ and assuming that the delay related error term known at the receiver, the PEP expression (3.27) coincides with the analytical expression for average SEP in our conference paper [61]. The results in [61] are for $M_1 \times M_2$-QAM constellation, by choosing $M_1 = 1$ and $M_2 = 1$ the results for BPSK constellation can be obtained. In previous chapter both the delay and estimation error related terms are not known at the receiver.

   According to the formulation in this chapter, delay related term is known at the receiver while the estimation related error term is not known. In [61] we derived closed-form average SEP expressions for $M_1 \times M_2$-QAM constellation assuming that the delay related error term is known at the receiver. Another important change between the previous chapter and the present chapter is that in previous chapter we do not assume the knowledge of $\rho_e$ and $\rho_d$ but in this chapter we assume that both $\rho_e$ and $\rho_d$ are known. The derivation (assuming that $\rho_e$ is not known at the receiver) of average SEP expression for $M_1 \times M_2$-QAM constellation from our paper [61] is summarized in Section 3.6.5 of the Appendix.

   The average SEP expression for BPSK, based on (3.27) (i.e., by substituting $N = 1$ in (3.27) and after some simplification) is given by

$$P_{_{SEP}} = 2\mathcal{G}_1\left(\frac{\pi}{2}\right) + (1 - A_p)\,,$$

   $\mathcal{G}_1(\varphi)$ is defined in Section 3.6.2 of the Appendix.

2. PEP expression in (3.27) can also be applied to systems where the delay related error term is not known at the receiver. In (3.27) with $\rho_d = 1$ and changing the value of $\rho_e$ such that it captures both estimation related correlation co-efficient and delay related correlation co-efficient[2] PEP in (3.27) gives the performance of a system where the delay related error term is not known at the receiver.

3. By making the block length $N = 1$, and assuming that the delay related error term is not known at the receiver, the PEP expression (3.27) coincides with the results presented in [62] (for BPSK constellation).

4. By making $\rho_e = 1$, $\rho_d = 1$, and assuming perfect quantization, with $t = 1$ the results in an approximated analytical expression for PEP with BPSK. Except for a few modulation schemes (such as non-coherent FSK[3]), PEP is generally studied with the help of computer simulations, and to the best of our knowledge this approximated analytical form (3.27) is the first available in the literature.

5. With arbitrary $t$ and perfect feedback ($\rho_e = 1$, $\rho_d = 1$, and $B = \infty$), (3.27) gives the average packet error probability with $t$ degrees of diversity.

6. By making appropriate changes to the PEP expression in (3.27), one can obtain an analytical understanding into the effects of fading, i.e., we can study the effects of channel estimation errors alone, or delay alone, or channel quantization alone, or other possible combinations of feedback imperfection.

   We believe the general framework (and the closed-form pdfs of random variables) to derive PEP presented in this chapter can be leveraged to analytically study the average packet error probability in other system settings as well.

[2] As explained in the previous chapter and in [62], when both estimation and delay related noise terms are absorbed into the receiver noise, then the effective correlation co-efficient becomes the product of delay only correlation co-efficient and estimation only correlation co-efficient.

[3] Or other modulation schemes where the conditional BEP/SEP expressions result in an exponential function.

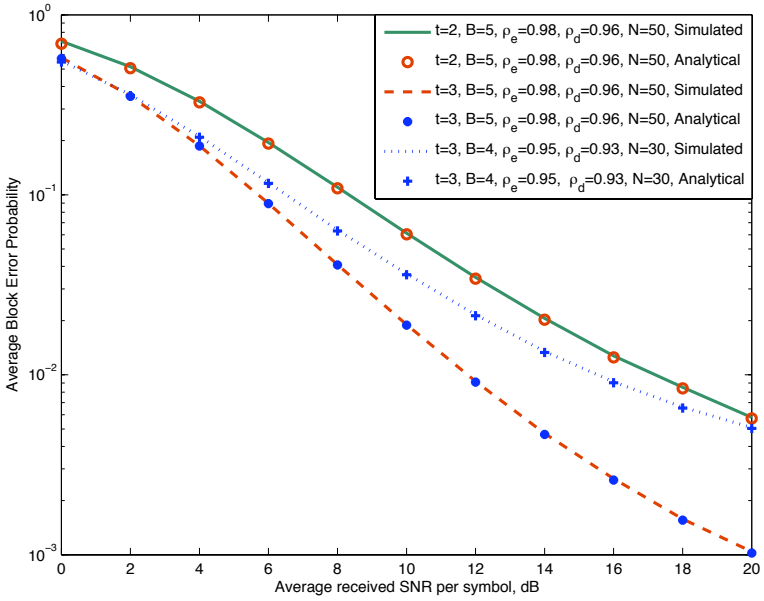


Figure 3.3 Effect of imperfections in feedback (estimation, delay and quantization) on the average packet error probability: packet size $N \in \{30, 50\}$, $t \in \{2, 3\}$, $\rho_e \in \{0.98, 0.95\}$, $\rho_d \in \{0.96, 0.93\}$, and number of feedback bits $B \in \{4, 5\}$.

## 3.4 Simulation Results

In this section we present a sample simulation to verify the accuracy of the derived analytical expression for the average packet error probability and also show the effectiveness of the modeling of feedback delay. Fig. 3.3 shows the accuracy of derived analytical expression (in the form of an approximated infinite series) for average packet error probability of transmit beamforming with imperfect feedback of a packet of $N \in \{30, 50\}$ un-coded BPSK symbols with $t \in \{2, 3\}$ transmit antennas, the estimation error correlation co-efficient $\rho_e \in \{0.98, 0.95\}$, the feedback delay related correlation co-efficient $\rho_d \in \{0.96, 0.93\}$, and number of feedback bits $B \in \{4, 5\}$. As pointed out earlier, the first two powers of $Q$-function are evaluated exactly. For higher powers ($m \geq 3$ in (3.28)), we calculate the expectation w.r.t to the tractable approximation of the $Q$-function given in (3.101). Fig. 3.3

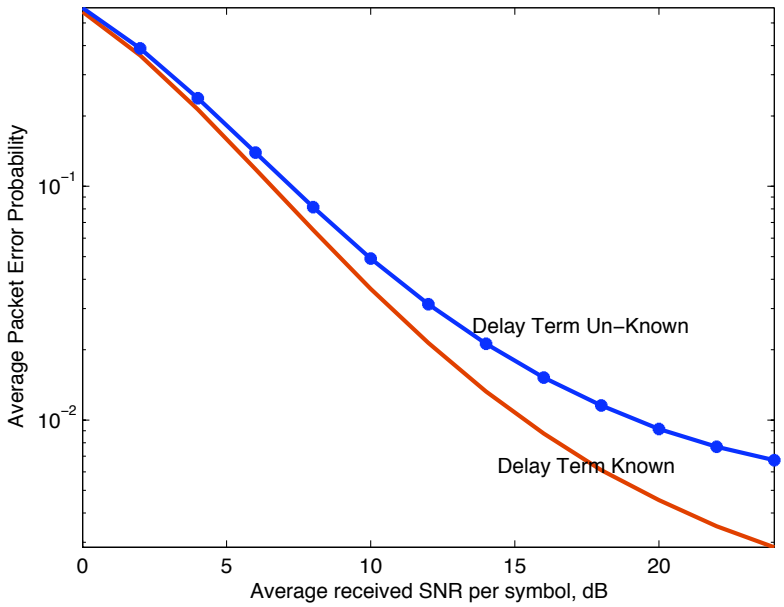


Figure 3.4 Impact of delay related error term: number of transmit antennas $t = 3$, packet size $N = 30$, $\rho_e = 0.97$, $\rho_d = 0.9$, and $B = 4$.

further validates the tightness of the approximation of Gaussian $Q$-function in Section 3.6.3. According to the popular Clark's model [2], the correlation between channel samples with a lag of $\tau$ is given by $R(\tau) = J_0(2\pi f_m \tau)$ where $J_k()$ is the $k^{th}$ order Bessel function of the first kind, $f_m = v/\lambda$, $v$ is the velocity of mobile, and $\lambda$ is the carrier wavelength. $\rho_d = 0.96$ correspond to a Doppler frequency of 80 Hz, and a delay of 5 milliseconds. At a carrier frequency of 900 MHz, Doppler frequency of 80 Hz translates into 60 mph of mobile speed. In Fig. 3.3, by fixing $N = 50$, $\rho_d = 0.98$, $\rho_e = 0.96$, and $B = 5$, improvement in performance can be seen as the number of antennas are increased from $t = 2$ to $t = 3$.

As discussed in the modeling of imperfect feedback, one of the contributions of this chapter is the modeling aspect of feedback delay. The impact of the knowledge of delay related error term (at the receiver) on the performance can be seen in Fig.3.4. With all system parameters being the same, the solid curve shows the performance of the system with delay related error term assumed known to the

receiver as in this chapter. The dotted curve shows the performance of the system when the receiver is assumed to not know the delay related error term as has been done in the past. Apart from being conceptually distinct from estimation error related error term, the delay related error term as modeled in the chapter shows improved system performance. The past modeling [62] (and references therein) simplifies the analysis but can lead to erroneous conclusions on system performance. The simulation parameters for Fig.3.4 are: Number of transmit antennas $t = 3$, packet size $N = 30$, estimation related correlation co-efficient $\rho_e = 0.97$, delay related correlation co-efficient $\rho_d = 0.99$, and number of feedback bits $B = 4$.

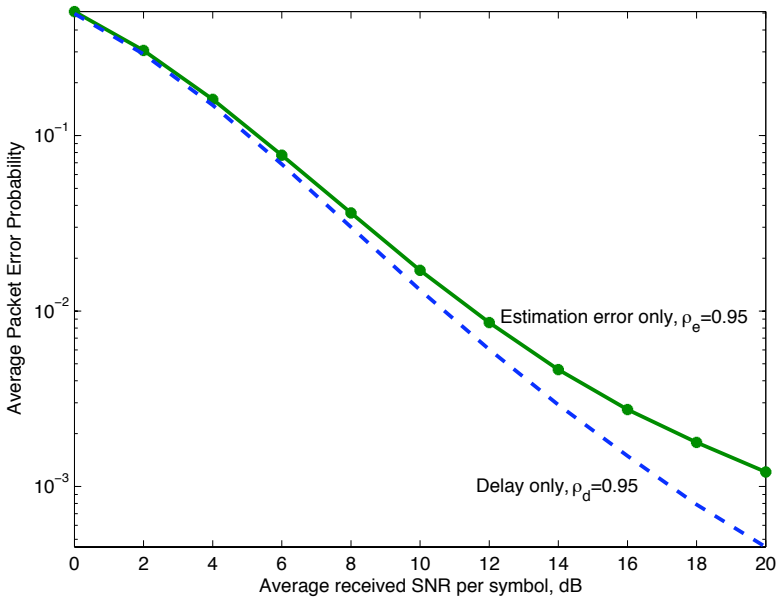


Figure 3.5 Contrast between delay only system and estimation error only system: number of feedback bits $B = 4$, block length $N = 30$, $\rho_e = 0.95$ and $\rho_d = 0.95$.

Fig.3.5 contrasts the effect due to feedback delay alone and due to estimation errors alone. The solid dotted curve shows PEP due to estimation errors alone with $\rho_e = 0.95$ and the dotted curve shows the PEP due to feedback delay alone with $\rho_d = 0.95$. Clearly the performance due to estimation errors alone is worse than performance due to delay alone. In this figure the feedback delay error

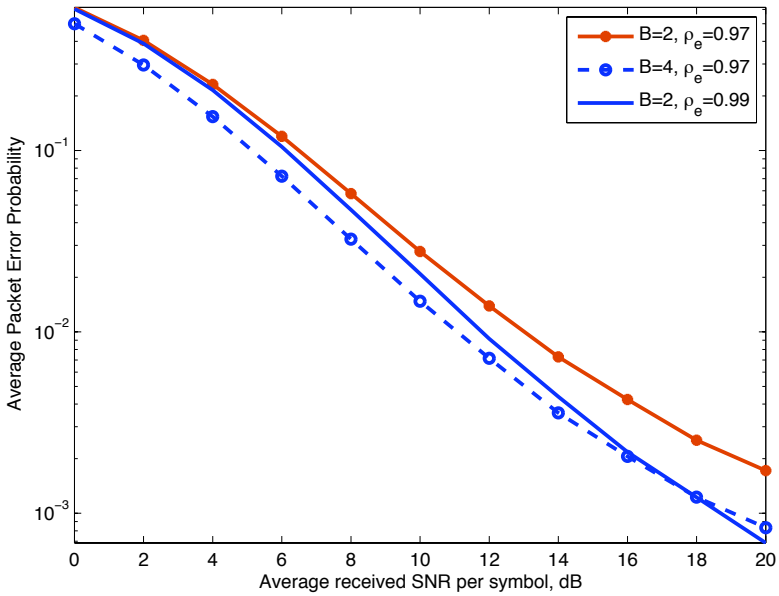


Figure 3.6 Trade-off between channel estimation errors and channel quantization: number of transmit antennas $t = 3$, block size $N = 30$, and delay related correlation coefficient $\rho_d = 0.97$.

term is known at the receiver thus it is able to perform better. If the feedback delay is not modeled in the way explained in this chapter, then both curves would be same. The important message from this figure is: if a trade-off is possible it is better to put more resources into reducing estimation errors as opposed to trying to reduce the feedback delay.

In Fig.3.5- number of feedback bits $B = 4$ and the block length $N = 30$. In Fig.3.6 we consider a possible trade-off between the number of feedback bits and the channel estimation quality. Quality of channel estimation depends on number of pilots and the pilot SNR [62]. If the forward link budget is constrained then increasing the number of feedback bits, which in turn improves the quality of channel quantization, can help in achieving a performance which is equivalent to increasing the pilot SNR. Similarly if the feedback link is constrained then pilot SNR can be increased to achieve an improvement in performance. Fig.3.6

illustrates this observation. In Fig.3.6- number of transmit antennas $t = 3$, block size $N = 30$, and delay related correlation coefficient $\rho_d = 0.97$.

## 3.5 Conclusion

We considered the problem of analyzing the average packet error probability, an important quality-of-service parameter, of closed loop MISO systems with imperfect feedback. The feedback imperfections include channel estimation errors, feedback delay and finite-rate channel quantization. Modeling of channel estimation errors in the packet fading context makes use of the fact that the channel estimate and the related error term are constant for the entire packet.

The modeling approach distinguishes between errors due to channel estimation (*un-known to the receiver*) from those due to feedback delay (*known to the receiver*). Knowledge of delay related error term at the receiver helps in improved performance compared to a system without the knowledge of delay error term. An approximated analytical expression for the PEP of an un-coded (or a simple block channel coded) packet of BPSK symbols is derived. An important tool in the derivation of the PEP expression is the analytically tractable approximation for the Gaussian Q-function, derived in Section 3.3.2 of the Appendix.

The general expressions derived are quite complex and not easily amenable to interpretation. Nevertheless, the steps taken in this chapter are necessary and hopefully will prove to be useful for future work that has greater interpretability. Special cases of interest are discussed. The derived closed-form analytical expression is validated by simulations. Simulation results have also been used to contrast the relative effects of the three forms of feedback imperfections on the average packet error probability. Sections 2 and 3 studied the impact of imperfect under different assumptions, however, both chapters have dealt with only spatially independent scenario. In the next chapter we study the imperfect feedback in a spatial correlation context.

## 3.6 Appendix

### 3.6.1 Derivation of the pdf for $\psi_\ell$

In this section of the Appendix we derive the pdf of the random variable $\psi_\ell$

$$\psi_\ell \;=\; \left|\bar{\tilde{\rho}}_e \left( \bar{\tilde{\rho}}_d \, \vartheta_{\ell-1} \, \frac{\|\widehat{\mathbf{h}}_{\ell-1}\|}{\sqrt{\Lambda}} + \sqrt{1-\rho_d^2}\, \hat{\varepsilon}_{\ell\, d} \right) \right| .$$

$\psi_\ell$ has the parameters associated with all three forms of feedback imperfection. $\tilde{\rho}_e$ determines the estimation quality, $\tilde{\rho}_d$ determines the effect due to delay, $\sqrt{1-\rho_d^2}\,\hat{\varepsilon}_{\ell\, d}$ is the error term due to feedback delay that is known to the receiver (because of the modeling approach presented in Section 3.2.2), and $\vartheta_{\ell-1}$ is the inner product between the estimated and delayed channel direction and its quantized version. Because of the analytical complexity involved in deriving $p_{\psi_\ell}$, the pdf of $\psi_\ell$, we begin with first writng $\psi_\ell$ as

$$\begin{aligned} \psi_\ell &= \rho_e \, \varphi \,, \\ \varphi &= \left|\bar{\tilde{\rho}}_d \, \vartheta_{\ell-1} \, \frac{\|\widehat{\mathbf{h}}_{\ell-1}\|}{\sqrt{\Lambda}} + \sqrt{1-\rho_d^2}\, \hat{\varepsilon}_{\ell\, d} \right| . \end{aligned} \tag{3.36}$$

**pdf of $\varphi^2$ :**

We first derive $p_{\varphi^2}(z)$, pdf of $\varphi^2$ and then use a simple transformation to get the pdf of $\psi_\ell$. In $\varphi$,

$$\frac{\|\widehat{\mathbf{h}}_{\ell-1}\|}{\sqrt{\Lambda}} \;\sim\; \frac{2\, x^{2t-1} e^{-x^2}}{\Gamma(t)} \,, \quad x \geq 0 \,, \tag{3.37}$$

$$\hat{\varepsilon}_{\ell\, d} \;\sim\; \mathcal{NC}\,(0,1)\,, \tag{3.38}$$

and the pdf of $\Delta = |\vartheta_{\ell-1}|^2$ (later in the derivation we will be needing the pdf of $\Delta$ not $\vartheta_{\ell-1}$) is

$$\begin{aligned} p_\Delta(x) &= 2^B (t-1)(1-x)^{t-2}, \quad 1-\omega < x < 1, \\ \omega &= 2^{-\frac{B}{t-1}} \,. \end{aligned} \tag{3.39}$$

Note that $\varphi$ has three random variables ($\vartheta_{\ell-1}$, $\|\widehat{\mathbf{h}}_{\ell-1}\|$, and $\hat{\varepsilon}_{\ell\,d}$) in it and all three are independent of each other. To begin with assume that $\vartheta$ is a constant (we will relax this assumption at a later stage).

If $X_1$ and $X_2$ are statistically independent Gaussian random variables, each one with same variance $\sigma^2$ and with the non-centrality parameter $s^2 = m_1^2 + m_2^2$ ($m_1$ and $m_2$ are the means of $X_1$ and $X_2$ respectively), then the non-central chi-squared distribution, $Z = X_1^2 + X_2^2$ is given by

$$p(z|s) = \frac{1}{2\sigma^2} e^{-\frac{\left(s^2+z\right)}{2\sigma^2}}\, \boldsymbol{I}_0\left(\frac{\sqrt{z}\,s}{\sigma^2}\right) \tag{3.40}$$

where $\boldsymbol{I}_0(x)$ is the modified bessel function of $0^{th}$ order [35]. Let

$$\sigma \;=\; \sqrt{\frac{1-\rho_d^2}{2}}\,, \tag{3.41}$$

$$s^2 \;\triangleq\; y = \frac{\rho_d^2\,\Delta\,\|\widehat{\mathbf{h}}_{\ell-1}\|^2}{\Lambda}\,. \tag{3.42}$$

After a simple transformation, the conditional pdf of $y$ is given by

$$p(y|\Delta) = \frac{e^{-y/(\rho_d^2\,\Delta)}\,y^{t-1}}{(\rho_d^2\Delta)^t\,\Gamma(t)}\,, \qquad y \geq 0. \tag{3.43}$$

With $\sigma$ defined in (3.41) and $y$ defined in (3.42), (3.40) can be applied to the present context to get $p_{\varphi^2}(z|y,\Delta)$, the conditional pdf of $\varphi^2$

$$p_{\varphi^2}(z|y,\Delta) \;=\; \frac{1}{2\sigma^2}\,e^{-\frac{(y+z)}{2\sigma^2}}\,\boldsymbol{I}_0\left(\frac{\sqrt{zy}}{\sigma^2}\right).$$

The conditional pdf of $\varphi^2$ is given by

$$\begin{aligned}
p_{\varphi^2}(z|\Delta) &= \int_{-\infty}^{\infty} p_{\varphi^2}(z|y,\Delta)\,p(y|\Delta)\,dy \\
&= \int_{-\infty}^{\infty}\left(\frac{1}{2\sigma^2}\,e^{-\frac{(y+z)}{2\sigma^2}}\,\sum_{\tilde{k}=0}^{\infty}\frac{(zy)^{\tilde{k}}}{4^{\tilde{k}}\sigma^{4\tilde{k}}\,(\tilde{k}!)^2}\right)\left(\frac{e^{-y/(\rho_d^2\Delta)}y^{t-1}}{(\rho_d^2\,\Delta)^t\,\Gamma(t)}\right)dy \\
p_{\varphi^2}(z|\Delta) &= \lambda\,e^{-\frac{z}{2\sigma^2}}\sum_{\tilde{k}=0}^{\infty}\mathcal{L}(\tilde{k})\,z^{\tilde{k}}, \qquad z>0
\end{aligned} \tag{3.44}$$

where

$$\begin{aligned}
\lambda &= \frac{(1-\rho_d^2)^{t-1}}{\Gamma(t)\,[1-\rho_d^2\,(1-\Delta)]^t}\,, \\
\mathcal{L}(\tilde{k}) &= \frac{\Gamma(\tilde{k}+t)\rho_d^{2\tilde{k}}\Delta^{\tilde{k}}}{(1-\rho_d^2)^{\tilde{k}}\,[1-\rho_d^2\,(1-\Delta)]^{\tilde{k}}\;(\tilde{k}!)^2}\,.
\end{aligned}$$

In the above derivation we used the infinite series representation for $\boldsymbol{I}_0(x)$:

$$\boldsymbol{I}_\alpha(x) = \sum_{\bar{k}=0}^{\infty} \frac{(x/2)^{\alpha+2\bar{k}}}{\bar{k}!\,\Gamma(\alpha+\bar{k}+1)}\,,$$

and the following identity [35]

$$\int_0^\infty x^n e^{-\omega x}\,dx = n!\,\omega^{-(n+1)}. \tag{3.45}$$

We can further simplify $p_{\varphi^2}(z|\Delta)$ given in (3.44) by writing the infinte series as

$$\begin{aligned}
\sum_{\tilde{k}=0}^{\infty} \mathcal{L}(\tilde{k})\, z^{\tilde{k}} &= \sum_{\tilde{k}=0}^{\infty} (\tilde{k}+t-1)\cdots(\tilde{k}+1)\,\frac{\beta^{\tilde{k}}}{\tilde{k}!} \\
&= \frac{d^n}{d\beta^n}\left(\sum_{\tilde{k}=0}^{\infty}\frac{\beta^{\tilde{k}+n}}{\tilde{k}!}\right) \\
&= \frac{d^n}{d\beta^n}\left(\beta^n e^\beta\right) = e^\beta\left(\sum_{l=0}^{n} n_{c\,l}\, n_{p\,l}\,\beta^{n-l}\right)
\end{aligned}$$

where

$$\begin{aligned}
n &= t-1\,, \\
n_{c\,l} &= \frac{n!}{l!(n-l)!}\,, \\
n_{p\,l} &= \frac{n!}{(n-l)!}\,, \\
\beta &= \frac{\rho_d^2\,\Delta\, z}{(1-\rho_d^2)\left[1-\rho_d^2\,(1-\Delta)\right]}\,.
\end{aligned} \tag{3.46}$$

After some simplification $p_{\varphi^2}(z|\Delta)$ can be written as

$$\begin{aligned}
p_{\varphi^2}(z|\Delta) &= \frac{(1-\rho_d^2)^n}{\Gamma(t)\left[1-\rho_d^2\,(1-\Delta)\right]^{n+1}}\, e^{-\frac{z}{2\sigma^2}+\beta} \sum_{l=0}^{n} n_{c\,l}\, n_{p\,l}\,\beta^{n-l} \\
&= \frac{(1-\rho_d^2)^n\; e^{-z/\left[1-\rho_d^2(1-\Delta)\right]}}{\Gamma(t)\left[1-\rho_d^2\,(1-\Delta)\right]^{n+1}} \sum_{l=0}^{n} n_{c\,l}\left\{n_{p\,l}\Gamma(l+1)\right\}\frac{z^{n-l}}{\Gamma(l+1)}\left(\frac{\rho_d^2}{1-\rho_d^2}\right)^{n-l} \\
&= \frac{(1-\rho_d^2)^n}{\left[1-\rho_d^2\,(1-\Delta)\right]^n} \sum_{l=0}^{n} n_{c\,l}\, f_l(z)\left\{\frac{\rho_d^2\,\Delta}{1-\rho_d^2}\right\}^{n-l}
\end{aligned} \tag{3.47}$$

where

$$f_l(z) = \frac{e^{-z/\left[1-\rho_d^2(1-\Delta)\right]}\, z^{n-l}}{\left[1-\rho_d^2\,(1-\Delta)\right]^{n-l+1}\,\Gamma(n-l+1)}\,, \quad 0 \le l \le n.$$

For sanity check the area under the pdf $p_{\varphi^2}(z|\Delta)$ can be verified to be one. To begin with note that

$$\int_0^\infty f_l(z)dz = 1 \tag{3.48}$$

$$\begin{aligned}
\int_0^\infty p_{\varphi^2}(z|\Delta)\,dz &= \int_0^\infty \frac{(1-\rho_d^2)^n}{\left[1-\rho_d^2\,(1-\Delta)\right]^n} \sum_{l=0}^{n} n_{c\,l}\, f_l(z) \left(\frac{\rho_d^2\Delta}{1-\rho_d^2}\right)^{n-l} \\
&= \frac{(1-\rho_d^2)^n}{\left[1-\rho_d^2\,(1-\Delta)\right]^n} \sum_{l=0}^{n} n_{c\,l} \left(\frac{\rho_d^2\,\Delta}{1-\rho_d^2}\right)^{n-l} \\
&= \frac{(1-\rho_d^2)^n}{\left[1-\rho_d^2\,(1-\Delta)\right]^n} \left(1+\frac{\rho_d^2\,\Delta}{1-\rho_d^2}\right)^{n} = 1.
\end{aligned}$$

We now look at the case where $\Delta$ is random. The pdf for $\Delta$ is given in (3.14). We now integrate out the randomness due to $\Delta$ to get $p_{\varphi^2}(z)$, the pdf of $\varphi^2$.

$$\begin{aligned}
p_{\varphi^2}(z) &= \int_{-\infty}^{\infty} p_{\varphi^2}(z|\Delta) p_\Delta(\Delta)\,d\Delta \\
&= \int_{1-\omega}^{1} \left( \frac{(1-\rho_d^2)^n}{\left[1-\rho_d^2\,(1-\Delta)\right]^n} \sum_{l=0}^{n} n_{c\,l}\, f_l(z) \left\{\frac{\rho_d^2\,\Delta}{1-\rho_d^2}\right\}^{n-l} \right) \times \\
&\qquad \left(2^B\, n\,(1-\Delta)^{n-1}\right) d\Delta \\
&= 2^B n (1-\rho_d^2)^n \sum_{l=0}^{n} \frac{n_{c\,l}\, z^{n-l}}{\Gamma(n-l+1)} \left\{\frac{\rho_d^2}{1-\rho_d^2}\right\}^{n-l} \times \\
&\qquad \underbrace{\int_{1-\omega}^{1} \frac{e^{-z/\left[1-\rho_d^2(1-\Delta)\right]}\,(\Delta)^{n-l}\,(1-\Delta)^{n-1}}{\left[1-\rho_d^2\,(1-\Delta)\right]^{2n-l+1}}\,d\Delta}_{J(z)}\,.
\end{aligned} \tag{3.49}$$

In order to evaluate $J(z)$, let

$$\frac{1}{\left[1-\rho_d^2\,(1-\Delta)\right]} = \alpha\,,$$

which implies

$$\Delta = \frac{\alpha\rho_d^2 - \alpha + 1}{\alpha\rho_d^2}$$

and

$$d\Delta = -\frac{d\alpha}{\alpha^2\rho_d^2}\,.$$

$$
\begin{aligned}
J(z) &= \int_{1-\omega}^{1} \frac{e^{-z/\left[1-\rho_d^2(1-\Delta)\right]}\,\Delta^{n-l}\,(1-\Delta)^{n-1}}{\left[1-\rho_d^2\,(1-\Delta)\right]^{n-l+1}}\,d\Delta \\
&= \frac{(-1)^n\,(\rho_d^2-1)^{n-l}}{(\rho_d^2)^{2n-l}} \int_{\frac{1}{1-\rho_d^2\omega}}^{1} e^{-z\alpha}\left(\frac{1}{\rho_d^2-1}+\alpha\right)^{n-l}(1-\alpha)^{n-1}d\alpha \\
&= \frac{(-1)^n\,(\rho_d^2-1)^{n-l}}{(\rho_d^2)^{2n-l}} \int_{\frac{1}{1-\rho_d^2\omega}}^{1} e^{-z\alpha} \sum_{p=0}^{2n-l-1} c_p\,\alpha^p\,d\alpha\,. \qquad (3.50)
\end{aligned}
$$

The co-efficients $c_p$ are calculated as follows. Let $F(x)$ be a function defined as follows:

$$
\begin{aligned}
F(x) &= (d+x)^s\,(1-x)^r = \sum_{h=0}^{s+r} c_h\,x^h, \\
c_h &= \frac{1}{h!}\frac{d^h\,(F(x))}{dx^h}\bigg|_{x=0} = \frac{1}{h!}\sum_{q=0}^{h}\left(\begin{array}{c} h \\ q \end{array}\right) L_r\,L_s(-1)^{h-q}d^{s-q}, \qquad (3.51) \\
L_r &= \frac{r!}{(r-h+q)!} \quad \text{if } r \geq (h-q) \quad \text{else } L_r = 0, \\
L_s &= \frac{s!}{(s-q)!} \quad \text{if } s \geq q \quad \text{else } L_s = 0.
\end{aligned}
$$

In the present context,

$$
\begin{aligned}
x &= \alpha, \\
s &= n-l, \\
r &= n-1, \\
d &= \frac{1}{\rho_d^2-1}. \qquad (3.52)
\end{aligned}
$$

With the help of the above function, $J(z)$ can now be expressed as

$$
J(z) = \frac{(-1)^n\,(\rho_d^2-1)^{n-l}}{(\rho_d^2)^{2n-l}} \sum_{p=0}^{2n-l-1} c_p\,I_p \qquad (3.53)
$$

where $c_p$ is calculated with the help of (3.51) and $I_p$ can be evaluated as

$$
\begin{aligned}
I_p &= \int_{\frac{1}{1-\rho^2\omega}}^{1} e^{-z\alpha}\,\alpha^p\,d\alpha \\
&= \left[-e^{-z\alpha}\left(\frac{\alpha^p}{z}+\sum_{g=1}^{p}\frac{p\,(p-1)\cdots(p-g+1)}{z^{g+1}}\alpha^{p-g}\right)\right]_{\frac{1}{1-\rho_d^2\omega}}^{1}
\end{aligned}
$$

$$= \sum_{g=0}^{p} \frac{p_{p\,g}\left[e^{-z\mathcal{L}}\mathcal{L}^{p-g} - e^{-z}\right]}{z^{g+1}}$$

where

$$\mathcal{L} = \frac{1}{1-\rho_d^2\,\omega} \tag{3.54}$$

where $\omega$ is defined in (3.39). Substituting (3.53) in (3.49), the final closed form for pdf $p_{\varphi^2}(z)$ is given by

$$\begin{aligned} p_{\varphi^2}(z) &= \frac{2^B n(1-\rho_d^2)^n}{\rho_d^{2n}} \sum_{l=0}^{n} \frac{(-1)^l\, n_{c\,l}\, z^{n-l}}{\Gamma(n-l+1)} \sum_{p=0}^{2n-l-1} c_p \left( \sum_{g=0}^{p} \frac{p_{p\,g}\left[e^{-z\mathcal{L}}\,\mathcal{L}^{p-g} - e^{-z}\right]}{z^{g+1}} \right) \\ &= \sum_{l=0}^{n} \sum_{p=0}^{2n-l-1} \sum_{g=0}^{\delta} \left\{ \mathcal{K}_{p_1} \tilde{f}_1(l,p,g,\mathcal{L},z) + \mathcal{K}_{p_2} \tilde{f}_2(l,p,g,\mathcal{L},z) \right\} + \mathcal{R}_{n,z} \end{aligned} \tag{3.55}$$

where

$$\mathcal{R}_{n,z} = \sum_{l=0}^{n} \sum_{p=n-l}^{2n-l-1} \sum_{g=n-l}^{p} \frac{\mathcal{K}_{p_3}(-1)^l\, n_{c\,l}\; c_p\, p_{p\,g}\left[e^{-z\mathcal{L}}\,\mathcal{L}^{p-g} - e^{-z}\right]}{\Gamma(n-l+1)\, z^{g-n+l+1}}, \tag{3.56}$$

$$\delta = \begin{cases} p & \text{if } p \le n-l-1 \\ n-l-1 & \text{if } p \ge n-l \end{cases}, \tag{3.57}$$

$$\tilde{f}_2(l,p,g,\mathcal{L},z) = \frac{\mathcal{L}^{n-l-g}\, e^{-\mathcal{L}\,z}\, z^{n-l-g-1}}{\Gamma(n-l-g)}, \tag{3.58}$$

$$\tilde{f}_1(l,p,g,\mathcal{L},z) = \tilde{f}_2(l,p,g,1,z), \tag{3.59}$$

$$\mathcal{K}_{p_1} = \frac{c_p\, 2^B\, n\,(1-\rho_d^2)^n\,(-1)^{l+1}\, n_{c\,l}\,\Gamma(n-l-g)\, p_{p\,g}}{\rho_d^{2n}\Gamma(n-l+1)}, \tag{3.60}$$

$$\mathcal{K}_{p_2} = -\mathcal{K}_{p_1}\mathcal{L}^{p-n+l}, \tag{3.61}$$

$$\mathcal{K}_{p_3} = \frac{2^B n(1-\rho_d^2)^n}{\rho_d^{2n}}, \tag{3.62}$$

and $c_p$'s can be calculated with the help of (3.51). $\mathcal{L}$ is defined in (3.54).

**Simplification of $p_{\varphi^2}(z)$:**

Note that the form of $p_{\varphi^2}(z)$ given in (3.55) is separated into two parts, terms with powers of $z$ in the numerator and terms with powers of $z$ in the denominator. $\mathcal{R}_{n,z}$ defined in (3.56) captures the terms with powers of $z$ in the

denominator. The negative exponent of $z$ in $\mathcal{R}_{n,z}$ will make the performance analysis intractable. We now take a closer look and analytically prove that $\mathcal{R}_{n,z} = 0$.

$$\mathcal{R}_{n,z} = \mathcal{K}_{p_3} \sum_{l=0}^{n} \sum_{p=n-l}^{2n-l-1} \sum_{g=n-l}^{p} \frac{(-1)^l \, n_{c\,l} \; c_p \, p_{p\,g} \left[ e^{-z\mathcal{L}} \, \mathcal{L}^{p-g} - e^{-z} \right]}{\Gamma(n-l+1) \, z^{g-n+l+1}} \, .$$

Let

$$g - n + l = e$$

and

$$p - n + l = f \, .$$

$$\mathcal{R}_{n,z} = \mathcal{K}_{p_3} \sum_{l=0}^{n} \sum_{f=0}^{n-1} \sum_{e=0}^{f} \frac{(-1)^l \, n_{c\,l} \; c_{f+n-l} \, (n-l+f)!}{(n-l)! \, (f-e)!} \, \frac{e^{-z\,\mathcal{L}} \mathcal{L}^{f-e} - e^{-z}}{z^{e+1}} . \quad (3.63)$$

From previous discussion

$$\begin{aligned} c_p &= \frac{1}{p!} \sum_{q=0}^{p} \left( \begin{array}{c} p \\ q \end{array} \right) L_r \, L_s (-1)^{p-q} \, d^{s-q} \\ L_r &= \frac{r!}{(r-h+q)!} \quad \text{if } \; r \geq (h-q) \quad \text{else } \; L_r = 0 \\ L_s &= \frac{s!}{(s-q)!} \quad \text{if } \; s \geq q \quad \text{else } \; L_s = 0 \end{aligned}$$

$s = n - l$, $r = n - 1$, and $d = \frac{1}{\rho_d^2 - 1}$. We now look at the co-efficient $c_{n-l+f}$, which are evaluated with the help of (3.51)

$$\begin{aligned} c_{n-l+f} &= \frac{1}{(n-l+f)!} \sum_{q=0}^{n-l+f} \left( \begin{array}{c} n-l+f \\ q \end{array} \right) L_r \, L_s \, (-1)^{n-l+f-q} \, d^{s-q} \\ L_r &\neq 0 \quad \text{if } \; n-1 \geq (n-l+f-q) \quad \text{else } \; L_r = 0 \\ L_s &\neq 0 \quad \text{if } \; n-l \geq q \quad \text{else } \; L_s = 0 \end{aligned}$$

The two in-equalities in $L_r$ and $L_s$ in the above equations are satisfied only if $q = n - l$, then $c_{n-l+f}$ is

$$c_{n-l+f} = \frac{(n-1)! \, (-1)^f}{f!(n-f-1)!} \, . \quad (3.64)$$

The important point in the above equation is that $c_{n-l+f}$ is independent of $l$. We can now write $\mathcal{R}_{n,z}$ in (3.63) as

$$\begin{aligned}\mathcal{R}_{n,z} &= \mathcal{K}_{p_3}\sum_{l=0}^{n}(-1)^l\, n_{c\,l}\sum_{f=0}^{n-1}\frac{(n-l+f)!}{(n-l)!}\,\mathcal{T}(f)\\ &= \mathcal{K}_{p_3}\sum_{l=0}^{n}(-1)^l\, n_{c\,l}\,\mathcal{W}(f)\end{aligned}$$

where

$$\begin{aligned}\mathcal{T}(f) &= \sum_{e=0}^{f}\frac{c_{f+n-l}\,\left[e^{-zL}L^{f-e}-e^{-z}\right]}{(f-e)!\,z^{e+1}}\,,\\ \mathcal{W}(f) &= \sum_{f=0}^{n-1}\frac{(n-l+f)!}{(n-l)!}\,\mathcal{T}(f)\\ &= \sum_{f=0}^{n-1}m_f\,l^f\end{aligned}$$

where $m_f$'s are constants that are independent of index $l$, as shown in the next step we do not need to calculate them explicitly. $\mathcal{R}_{n,z}$ can now be written as

$$\mathcal{R}_{n,z} = \mathcal{K}_{p_3}\sum_{f=0}^{n-1}m_f\underbrace{\sum_{l=0}^{n}(-1)^l\, n_{c\,l}\,l^f}_{\mathcal{C}_f}\,.$$

By using the following property of binomial co-efficients

$$\sum_{k=0}^{n}(-1)^k\, n_{c\,k}\,l^{b-1}=0,\quad n\geq b\geq 1,$$

it is clear that

$$\mathcal{C}_f=0,\;\; n-1\geq f\geq 0,$$

and subsequently $\mathcal{R}_{n,z}=0$. This result is important because the presence of negative exponents of $z$ in the pdf make the performance analysis difficult. The final simplified form of pdf $p_{\varphi^2}(z)$ can now be written as

$$p_{\varphi^2}(z) = \sum_{l=0}^{n}\sum_{p=0}^{2n-l-1}\sum_{g=0}^{\delta}\left\{\mathcal{K}_{p_1}f_1(l,p,g,\mathcal{L},z)+\mathcal{K}_{p_2}f_2(l,p,g,\mathcal{L},z)\right\} \quad (3.65)$$

where (variable - definition): $n$ - (3.46), $\delta$ - (3.57), $\mathcal{L}$ - (3.54), $\mathcal{K}_{p_1}$ - (3.60), $\mathcal{K}_{p_2}$ - (3.61), $f_1(,,,,)$ - (3.59), and $f_2(,,,,)$ - (3.58).

**pdf of $\psi_\ell$ :**

Note that the random variable that is of interest to us $\psi_\ell$. From earlier discussion $\psi_\ell$ is related to $\varphi$ as $\psi_\ell = \rho_e \varphi$. (3.65) is the pdf of $\varphi^2$. Using transformation of random variables, $p_{\psi_\ell}$, the pdf of $\psi_\ell$ can be shown to be given by

$$p_{\psi_\ell}(x) = \sum_{l=0}^{n} \sum_{p=0}^{2n-l-1} \sum_{g=0}^{\delta} \left\{ \mathcal{K}_{p_1} f_{a1}(l,p,g,\mathcal{L},x) + \mathcal{K}_{p_2} f_{a2}(l,p,g,\mathcal{L},x) \right\}, x > 0\,, \tag{3.66}$$

$$f_{a2}(l,p,g,\mathcal{L},x) = \frac{2\,\mathcal{L}^{n-l-g}\, e^{-\frac{\mathcal{L}\,x^2}{\rho_e^2}}\, x^{2(n-l-g)-1}}{\rho_e^{2(n-l-g)}\,\Gamma(n-l-g)}. \tag{3.67}$$

$$f_{a1}(l,p,g,\mathcal{L},x) = f_{a2}(l,p,g,1,x) \tag{3.68}$$

where (variable - definition): $n$ - (3.46), $\delta$ - (3.57), $\mathcal{L}$ - (3.54), $\mathcal{K}_{p_1}$ - (3.60), and $\mathcal{K}_{p_2}$ - (3.61).

**pdfs of $z_1$ and $z_2$ :**

$z_1$ and $z_2$ are the random variables defined in Section 3.3.2, here we present the expressions for the pdfs of $z_1$ and $z_2$.

$$p_{z_1}(z_1) = \sum_{l=0}^{n} \sum_{p=0}^{2n-l-1} \sum_{g=0}^{\delta} \left\{ \mathcal{K}_{p_1} f_{s1}(l,p,g,\mathcal{L},z_1) + \mathcal{K}_{p_2} f_{s2}(l,p,g,\mathcal{L},z_1) \right\}, \tag{3.69}$$

$$f_{s2}(l,p,g,\mathcal{L},z_1) = \frac{\mathcal{H}_1}{2\,A_p}\, {z_1}^{-\frac{1}{2}}\, e^{-z_1 \mathcal{H}_2}\, D_{-2(n-l-g)}\left(-\sqrt{z_1}\,\mathcal{H}_3\right),$$

$$f_{s1}(l,p,g,\mathcal{L},z_1) = f_{s2}(l,p,g,1,z_1)\,.$$

$$p_{z_2}(z_2) = \sum_{l=0}^{n} \sum_{p=0}^{2n-l-1} \sum_{g=0}^{\delta} \left\{ \mathcal{K}_{p_1} f_{s3}(l,p,g,\mathcal{L},z_2) + \mathcal{K}_{p_2} f_{s4}(l,p,g,\mathcal{L},z_2) \right\}, \tag{3.70}$$

$$f_{s4}(l,p,g,\mathcal{L},z_1) = \frac{\mathcal{H}_1}{2\,(1-A_p)}\, {z_2}^{-\frac{1}{2}}\, e^{-z_2 \mathcal{H}_2}\, D_{-2(n-l-g)}\left(\sqrt{z_2}\,\mathcal{H}_3\right),$$

$$f_{s3}(l,p,g,\mathcal{L},z_1) = f_{s4}(l,p,g,1,z_1)\,.$$

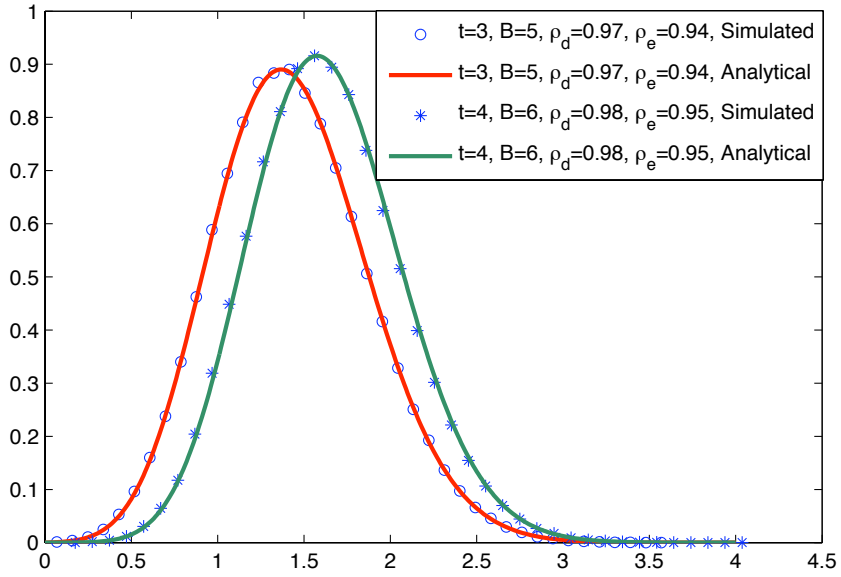


Figure 3.7 Verification of the pdf for the signal scaling term $\psi_\ell$ defined in (3.66), number of transmit antennas $t \in \{3, 4\}$, delay correlation co-efficient $\rho_d \in \{0.97, 0.98\}$, and estimation error correlation co-efficient $\rho_e \in \{0.94, 0.95\}$, number of feedback bits $B \in \{5, 6\}$.

where the variables and the corresponding defining equation are listed as pairs: $\mathcal{L}$ - (3.54), $\mathcal{K}_{p_1}$ - (3.60), $\mathcal{K}_{p_2}$ - (3.61), $\mathcal{H}_1$ - (3.23), $\mathcal{H}_2$ - (3.24), and $\mathcal{H}_3$ - (3.25), and $D_{\tilde{p}}(\tilde{l})$ is the parabolic cylinder function. Parabolic cylinder function has many representations, for analytical simplicity we choose to work with the following representation [35]:

$$D_{\tilde{p}}(\tilde{l}) = 2^{\frac{\tilde{p}}{2}}\, e^{-\frac{\tilde{l}^2}{4}} \left\{ \frac{\sqrt{\pi}}{\Gamma\left(\frac{1-\tilde{p}}{2}\right)}\ {}_1F_1\left(-\frac{\tilde{p}}{2}, \frac{1}{2}; \frac{\tilde{l}^2}{2}\right) - \frac{\sqrt{2\pi}\,\tilde{l}}{\Gamma\left(\frac{-\tilde{p}}{2}\right)}\ {}_1F_1\left(\frac{1-\tilde{p}}{2}, \frac{3}{2}; \frac{\tilde{l}^2}{2}\right) \right\} \quad (3.71)$$

where ${}_1F_1(\cdot,\cdot;\cdot)$ is the confluent hypergeometric function of the first kind. Using the representation in (3.71) for the parabolic cylinder function, (3.69) and (3.70) can be written as

$$\begin{aligned} p_{z_1}(z_1) &= \frac{\hat{p}_1(z_1) + \hat{p}_2(z_1)}{A_p}, \quad z_1 > 0, \\ p_{z_2}(z_2) &= \frac{\hat{p}_1(z_2) - \hat{p}_2(z_2)}{(1 - A_p)}, \quad z_2 > 0, \end{aligned}$$

$$\hat{p}_1(x) = \sum_{l=0}^{n} \sum_{p=0}^{2n-l-1} \sum_{g=0}^{\delta} \left\{ \mathcal{K}_{p_1} f_{\hat{s}5}(l,p,g,\mathcal{L},x) + \mathcal{K}_{p_2} f_{\hat{s}6}(l,p,g,\mathcal{L},x) \right\}, \tag{3.72}$$

$$f_{\hat{s}6}(l,p,g,\mathcal{L},x) = \mathcal{R}_1 \, x^{-\frac{1}{2}} \, e^{-x\mathcal{R}_h} \, {}_1F_1\left(\mathcal{R}_n, \frac{1}{2}; x\,\mathcal{R}_c\right), \quad x > 0, \tag{3.73}$$

$$\mathcal{R}_1 = \frac{\mathcal{H}_1 \sqrt{\pi}}{2^{n-l-g+1}\,\Gamma\left(\frac{1+2(n-l-g)}{2}\right)}, \tag{3.74}$$

$$\mathcal{R}_h = \frac{(4\mathcal{H}_2 + \mathcal{H}_3^2)}{4}, \tag{3.75}$$

$$\mathcal{R}_n = n - l - g\,, \tag{3.76}$$

$$\mathcal{R}_c = \frac{\mathcal{H}_3^2}{2}, \tag{3.77}$$

$$f_{\hat{s}5}(l,p,g,\mathcal{L},x) = f_{\hat{s}6}(l,p,g,1,x)\,. \tag{3.78}$$

$$\hat{p}_2(x) = \sum_{l=0}^{n} \sum_{p=0}^{2n-l-1} \sum_{g=0}^{\delta} \left\{ \mathcal{K}_{p_1} f_{\hat{s}7}(l,p,g,\mathcal{L},x) + \mathcal{K}_{p_2} f_{\hat{s}8}(l,p,g,\mathcal{L},x) \right\}, \tag{3.79}$$

$$f_{\hat{s}8}(l,p,g,\mathcal{L},x) = \mathcal{R}_2 \, e^{-x\,\mathcal{R}_h} \, {}_1F_1\left(\mathcal{R}_{n2}, \frac{3}{2}; x\,\mathcal{R}_c\right), \quad x > 0, \tag{3.80}$$

$$\mathcal{R}_2 = \frac{\mathcal{H}_1\,\mathcal{H}_3\sqrt{2\pi}}{2^{n-l-g+1}\,\Gamma\left(n-l-g\right)}, \tag{3.81}$$

$$\mathcal{R}_{n2} = n - l - g + \frac{1}{2}\,, \tag{3.82}$$

$$f_{\hat{s}7}(l,p,g,\mathcal{L},x) = f_{\hat{s}8}(l,p,g,1,x)\,. \tag{3.83}$$

### 3.6.2 Closed Form Expressions for $\mathcal{G}_1(\varphi)$ and $\mathcal{G}_2(\varphi)$

In this section of the Appendix we derive the analytical expressions for $\mathcal{G}_1(\varphi)$ and $\mathcal{G}_2(\varphi)$, which are used in the evaluation of $A_p E\left[Q^m\left(\sqrt{2\,\gamma_b\,z_1}\right)\right]$ and $(1-A_p)E\left[Q^m\left(\sqrt{2\,\gamma_b\,z_2}\right)\right]$, where $m \in \{1,2\}$.

#### 3.6.2.1 Derivation of $\mathcal{G}_1(\varphi)$

$$\mathcal{G}_1(\varphi) = \int_{\tilde{y}=0}^{\infty} \tilde{Q}\left(\sqrt{2\,\gamma_b\,\tilde{y}}\right) \hat{p}_1(\tilde{y})\,d\tilde{y}, \tag{3.84}$$

$$= \sum_{l=0}^{n} \sum_{p=0}^{2n-l-1} \sum_{g=0}^{\delta} \left\{ \mathcal{K}_{p_1} f_{c1}(l,p,g,\mathcal{L},\varphi) + \mathcal{K}_{p_2} f_{c2}(l,p,g,\mathcal{L},\varphi) \right\} \quad (3.85)$$

where (variable - definition): $n$ - (3.46), $\delta$ - (3.57), $\mathcal{L}$ - (3.54), $\mathcal{K}_{p_1}$ - (3.60), $\mathcal{K}_{p_2}$ - (3.61), $\tilde{Q}(x)$ - (3.34), and $\hat{p}_1(x)$ - (3.72).

$$\begin{aligned} f_{c2}(l,p,g,\mathcal{L},\varphi) &= \int_{\tilde{y}=0}^{\infty} \tilde{Q}\left(\sqrt{2\,\gamma_b\,\tilde{y}}\right)\, f_{\hat{s}6}(l,p,g,\mathcal{L},\tilde{y})\, d\tilde{y} \\ &= \mathcal{R}_1 \int_{\tilde{y}=0}^{\infty} \tilde{Q}\left(\sqrt{2\,\gamma_b\,\tilde{y}}\right)\, \tilde{y}^{-\frac{1}{2}}\, e^{-\tilde{y}\,\mathcal{R}_h}\; {}_1F_1\left(\mathcal{R}_n, \frac{1}{2}; \tilde{y}\,\mathcal{R}_c\right) d\tilde{y} \\ &= \frac{\mathcal{R}_1}{\pi} \int_{\theta=0}^{\varphi} d\theta \int_{\tilde{y}=0}^{\infty} \tilde{y}^{-\frac{1}{2}}\, e^{-\tilde{y}\left(\frac{\gamma_b}{\sin^2\theta}+\mathcal{R}_h\right)}\; {}_1F_1\left(\mathcal{R}_n, \frac{1}{2}; \tilde{y}\,\mathcal{R}_c\right) d\tilde{y} \end{aligned} \quad (3.86)$$

where (variable - definition): $f_{\hat{s}6}(,,,,)$ - (3.73), $\mathcal{R}_1$ - (3.74), $\mathcal{R}_h$ - (3.75), $\mathcal{R}_n$ - (3.76), and $\mathcal{R}_c$ - (3.77). With $\tilde{y}\,\mathcal{R}_c = x$, (3.86) becomes

$$f_{c2}(l,p,g,\mathcal{L},\varphi) = \frac{\mathcal{R}_1}{\pi\,\mathcal{R}_c^{\frac{3}{2}}} \int_{\theta=0}^{\varphi} d\theta \int_{x=0}^{\infty} x^{-\frac{1}{2}}\, e^{-x\,\mathcal{S}}\; {}_1F_1\left(\mathcal{R}_n, \frac{1}{2}; x\right) dx \quad (3.87)$$

where

$$\mathcal{S} = \frac{\gamma_b}{\sin^2\theta\,\mathcal{R}_c} + \frac{\mathcal{R}_h}{\mathcal{R}_c}\,. \quad (3.88)$$

Notice that $\mathcal{S} > 1$ for $\rho_e < 1$. To evaluate the above equation, we use the identity given below [35]:

$$\int_{r=0}^{\infty} r^{c-1}\, e^{-r\,d}\; {}_1F_1\,(a,c;r)\, dr = \Gamma(c)\, d^{-c}\, \left(\frac{d-1}{d}\right)^{-a} = \Gamma(c)\, d^{-c}\left(1-d^{-1}\right)^{q}, \quad \mathrm{Re}\, c > 0,\ \mathrm{Re}\, d > 1. \quad (3.89)$$

In the present context, in (3.109),

$$\begin{aligned} c &= \frac{1}{2}, \\ d &= \mathcal{S}, \\ q &= -\mathcal{R}_n. \end{aligned}$$

With the help of above identity, (3.87) becomes

$$f_{c2}(l,p,g,\mathcal{L},\varphi) \;=\; \mathcal{M}\int_{\theta=0}^{\varphi} d^{-c}\,\left(1-d^{-1}\right)^{q}\,d\theta$$

where

$$\begin{aligned} d^{-1} &= \mathcal{R}_d\left(\frac{\sin^2\theta}{\sin^2\theta+c_1}\right),\\ \mathcal{M} &= \frac{\mathcal{R}_1\,\Gamma\left(\frac{1}{2}\right)}{\pi\,\mathcal{R}_c^{\frac{3}{2}}},\\ \mathcal{R}_d &= \frac{\mathcal{R}_c}{\mathcal{R}_h}, \end{aligned}$$

and

$$c_1 = \frac{\gamma_b}{\mathcal{R}_h}. \tag{3.90}$$

By using the generalized binomial series expansion,

$$\begin{aligned} (1-x)^q &= \sum_{\tilde{n}=0}^{\infty}\frac{(-1)^{\tilde{n}}\,\bar{p}_{k,\tilde{n}}}{\tilde{n}!}\,(x)^{\tilde{n}},\\ \bar{p}_{k,\tilde{n}} &= q\,(q-1)\,\cdots\,(q-\tilde{n}+1). \end{aligned}$$

$f_{c2}(l,p,g,\mathcal{L},\varphi)$ can now be written in a series of steps as [4]

$$\begin{aligned} f_{c2}(l,p,g,\mathcal{L},\varphi) &= \mathcal{M}\int_{\theta=0}^{\varphi}\sum_{\tilde{n}=0}^{\infty}\frac{\mathcal{R}_d^{\tilde{n}+\frac{1}{2}}\,(-1)^{\tilde{n}}\,\bar{p}_{k,\tilde{n}}}{\tilde{n}!}\tilde{d}^{\tilde{n}+c}d\theta\\ &= \mathcal{M}\int_{\theta=0}^{\varphi}\sum_{\tilde{n}=0}^{\infty}\frac{\mathcal{R}_d^{\tilde{n}+\frac{1}{2}}\,(-1)^{\tilde{n}}\,\bar{p}_{k,\tilde{n}}}{\tilde{n}!}\Big(1-(1-\tilde{d})\Big)^{\tilde{n}+c}d\theta\\ &= \mathcal{M}\int_{\theta=0}^{\varphi}\sum_{\tilde{n}=0}^{\infty}\frac{\mathcal{R}_d^{\tilde{n}+\frac{1}{2}}\,(-1)^{\tilde{n}}\,\bar{p}_{k,\tilde{n}}}{\tilde{n}!}\sum_{\bar{n}=0}^{\infty}\frac{(-1)^{\bar{n}}\,\bar{b}_{k,\bar{n}}}{\bar{n}!}\Big(1-\tilde{d}\Big)^{\bar{n}}d\theta \end{aligned}$$

$$\begin{aligned} &= \mathcal{M}\int_{\theta=0}^{\varphi}\sum_{\tilde{n}=0}^{\infty}\frac{\mathcal{R}_d^{\tilde{n}+\frac{1}{2}}\,(-1)^{\tilde{n}}\,\bar{p}_{k,\tilde{n}}}{\tilde{n}!}\sum_{\bar{n}=0}^{\infty}\frac{(-1)^{\bar{n}}\,\bar{b}_{k,\bar{n}}}{\bar{n}!}\sum_{\bar{n}_1=0}^{\bar{n}}(-1)^{\bar{n}_1}\begin{pmatrix}\bar{n}\\ \bar{n}_1\end{pmatrix}\tilde{d}^{\bar{n}_1}d\theta\\ &= \mathcal{M}\sum_{\tilde{n}=0}^{\infty}\frac{\mathcal{R}_d^{\tilde{n}+\frac{1}{2}}\,(-1)^{\tilde{n}}\,\bar{p}_{k,\tilde{n}}}{\tilde{n}!}\sum_{\bar{n}=0}^{\infty}\frac{(-1)^{\bar{n}}\,\bar{b}_{k,\bar{n}}}{\bar{n}!}\sum_{\bar{n}_1=0}^{\bar{n}}(-1)^{\bar{n}_1}\begin{pmatrix}\bar{n}\\ \bar{n}_1\end{pmatrix}\mathcal{D}\,(\varphi,c_1,\bar{n}_1) \end{aligned} \tag{3.91}$$

[4] Note that the convergence of the above series is not a problem since $d^{-1}<1$.

where

$$\begin{aligned}
\bar{b}_{k,\bar{n}} &= (\tilde{n}+c)\,(\tilde{n}+c-1)\cdots(\tilde{n}+c-\bar{n}+1)\,, \\
\tilde{d} &= \frac{\sin^2\theta}{\sin^2\theta+c_1}\,, \\
\mathcal{D}\,(\varphi,c_1,\bar{n}_1) &= \int_{\theta=0}^{\varphi}\tilde{d}\,d\theta = \int_{\theta=0}^{\varphi}\left(\frac{\sin^2\theta}{\sin^2\theta+c_1}\right)^{\bar{n}_1}d\theta \qquad (3.92)\\
&= \pi\Bigg\{\frac{\varphi}{\pi}-\frac{T}{\pi}\sqrt{\frac{c_1}{1+c_1}}\sum_{k=0}^{\bar{n}_1-1}\left(\begin{array}{c}2k\\k\end{array}\right)\frac{1}{[4(1+c_1)]^k} \\
&\quad -\frac{2}{\pi}\sqrt{\frac{c_1}{1+c_1}}\sum_{k=0}^{\bar{n}_1-1}\sum_{j=0}^{k-1}\left(\begin{array}{c}2k\\j\end{array}\right)\frac{(-1)^{j+k}}{[4(1+c_1)]^k}\frac{\sin[(2k-2j)T]}{2k-2j}\Bigg\},\ 0\le\ \varphi\le 2\pi \qquad (3.93)
\end{aligned}$$

where

$$\begin{aligned}
T &= \frac{1}{2}\tan^{-1}\left(\frac{2\sqrt{c_1(1+c_1)}\sin 2\varphi}{(1+2\,c_1)\cos 2\varphi-1}\right)+ \\
&\quad \frac{\pi}{2}\left[1-2\sqrt{c_1(1+c_1)}\sin 2\varphi\left(\frac{(1+2\,c_1)\cos 2\varphi}{2}\right)\right].
\end{aligned}$$

Equation (3.91) gives the final expression for $f_{c2}(l,p,g,\mathcal{L},\varphi)$. To complete the calculation of $\mathcal{G}_1(\varphi)$in (3.85) we still need $f_{c1}(l,p,g,\mathcal{L},\varphi)$ which is given by

$$f_{c1}(l,p,g,\mathcal{L},\varphi) = f_{c2}(l,p,g,1,\varphi)\,.$$

**Derivation of $\mathcal{G}_2(\varphi)$**

$$\begin{aligned}
\mathcal{G}_2(\varphi) &= \int_{\tilde{y}=0}^{\infty}\tilde{Q}\left(\sqrt{2\,\gamma_b\,\tilde{y}}\right)\hat{p}_2(\tilde{y})\,d\tilde{y}, \qquad (3.94)\\
&= \sum_{l=0}^{n}\sum_{p=0}^{2n-l-1}\sum_{g=0}^{\delta}\left\{\mathcal{K}_{p_1}f_{d1}(l,p,g,\mathcal{L},\varphi)+\mathcal{K}_{p_2}f_{d2}(l,p,g,\mathcal{L},\varphi)\right\} \qquad (3.95)
\end{aligned}$$

where (variable - definition): $n$ - (3.46), $\delta$ - (3.57), $\mathcal{L}$ - (3.54), $\mathcal{K}_{p_1}$ - (3.60), $\mathcal{K}_{p_2}$ - (3.61), $\tilde{Q}(x)$ - (3.34), and $\hat{p}_2(x)$ - (3.79), and

$$\begin{aligned} f_{d2}(l,p,g,\mathcal{L},\varphi) &= \int_{\tilde{y}=0}^{\infty} \tilde{Q}\left(\sqrt{2\,\gamma_b\,\tilde{y}}\right)\, f_{\hat{s}8}(l,p,g,\mathcal{L},\tilde{y})\,d\tilde{y} \\ &= \mathcal{R}_2 \int_{\tilde{y}=0}^{\infty} \tilde{Q}\left(\sqrt{2\,\gamma_b\,\tilde{y}}\right)\, e^{-\tilde{y}\,\mathcal{R}_h}\; {}_1F_1\left(\mathcal{R}_{n2},\,\frac{3}{2};\,\tilde{y}\,\mathcal{R}_c\right) d\tilde{y} \\ &= \frac{\mathcal{R}_2}{\pi} \int_{\theta=0}^{\varphi} d\theta \int_{\tilde{y}=0}^{\infty} e^{-\tilde{y}\left(\frac{\gamma_b}{\sin^2\theta}+\mathcal{R}_h\right)}\; {}_1F_1\left(\mathcal{R}_{n2},\frac{3}{2};\tilde{y}\,\mathcal{R}_c\right) d\tilde{y} \quad (3.96) \end{aligned}$$

where (variable - definition): $f_{\hat{s}8}(,,,,)$ - (3.80), $\mathcal{R}_2$ - (3.81), $\mathcal{R}_h$ - (3.75), $\mathcal{R}_{n2}$ - (3.82), and $\mathcal{R}_c$ - (3.77). With $\tilde{y}\,\mathcal{R}_c = x$,

$$f_{d2}(l,p,g,\mathcal{L},\varphi) = \frac{\mathcal{R}_2}{\pi\,\mathcal{R}_c} \int_{\theta=0}^{\varphi} d\theta \int_{x=0}^{\infty} e^{-x\mathcal{S}}\; {}_1F_1\left(\mathcal{R}_{n2},\frac{3}{2};x\right) dx,$$

$\mathcal{S}$ is defined in (3.88). $f_{d2}(l,p,g,\mathcal{L},\varphi)$ can be evaluated using the following infinite series expansion for the Gauss hypergeometric function

$$\begin{aligned} {}_1F_1\,(a,b;r)\,dr &= \sum_{\bar{m}=0}^{\infty} \frac{a_{\bar{m}}\,r^{\bar{m}}}{b_{\bar{m}}\,\bar{m}!}\,, \\ a_{\bar{m}} &= 1.\,a_1\,(a_1+1)\cdots(a_1+\bar{m}-1), \qquad a_1 = \mathcal{R}_{n2}\,, \\ b_{\bar{m}} &= 1.\,b_1\,(b_1+1)\cdots(b_1+\bar{m}-1), \qquad b_1 = \frac{3}{2}\,. \end{aligned}$$

With the above series representation, $f_{d2}(l,p,g,\mathcal{L},\varphi)$ can now be written as

$$\begin{aligned} f_{d2}(l,p,g,\mathcal{L},\varphi) &= \frac{\mathcal{R}_2}{\pi\,\mathcal{R}_c} \sum_{\bar{m}=0}^{\infty} \frac{a_{\bar{m}}}{b_{\bar{m}}} \int_{\theta=0}^{\varphi} d\theta \int_{x=0}^{\infty} \frac{e^{-x\,\mathcal{S}}\,x^{\bar{m}}}{\bar{m}!}\,dx, \\ &= \frac{\mathcal{R}_2}{\pi\,\mathcal{R}_c} \sum_{\bar{m}=0}^{\infty} \frac{a_{\bar{m}}}{b_{\bar{m}}} \int_{\theta=0}^{\varphi} \mathcal{S}^{-(\bar{m}+1)} d\theta, \\ &= \frac{\mathcal{R}_2}{\pi\,\mathcal{R}_c} \sum_{\bar{m}=0}^{\infty} \frac{a_{\bar{m}}}{b_{\bar{m}}}\,\mathcal{R}_d^{\bar{m}+1}\,\mathcal{D}\,(\varphi,c_1,\bar{m}+1) \qquad (3.97) \end{aligned}$$

where $\mathcal{D}\,(\varphi,c_1,\bar{m}+1)$ is defined in (3.92) and $c_1$ is defined in (3.90). Finally $f_{d1}(l,p,g,\mathcal{L},\varphi)$ is given by

$$f_{d1}(l,p,g,\mathcal{L},\varphi) = f_{d2}(l,p,g,1,\varphi).$$

### 3.6.3 An Analytically Tractable Approximation for the Gaussian $Q$-Function

In this section of the Appendix we propose an approximation for the Gaussian $Q$-function that enables simpler evaluation of important communication system performance metrics. The approximation enables derivation of closed-form expressions for metrics such as average symbol, bit and packet error probabilities which are known to be analytically involved as they require computation of the expectation of $Q$-function and its integer powers, for any $m$ of Nakagami-$m$ fading. The tightness of the approximation is verified by simulations. The usefulness of the approximation is demonstrated by obtaining a simple closed-form expression for the average symbol error probability of differentially encoded QPSK in Nakagami-$m$ fading. This result is used in Section 3.3.2 for the evaluation of packet error probability.

#### 3.6.3.1 Introduction

The Gaussian $Q$-function plays an important role in the performance analysis of many communication problems [85]. Obtaining closed form expressions for a number of wireless communication performance metrics, particularly average symbol, bit and block error probabilities of various digital communication schemes typically involve taking the expectation of the Gaussian $Q$-function and its integer powers with respect to a random variable that captures the fading environment and is quite involved [12]. The analytical problems associated with evaluating expectation of the $Q$-function spurred the interest in finding alternate representations, as well as approximations that are both tight and analytically simple in form [12], [86]-[90] (and the references therein). The appeal of the alternate representation of the $Q$-function,

$$Q(x) = \frac{1}{\pi} \int_{\theta=0}^{\pi/2} e^{\left(-\frac{x^2}{2\sin^2\theta}\right)} d\theta, \quad x \geq 0,$$

$$Q^2(x) = \frac{1}{\pi} \int_{\theta=0}^{\pi/4} e^{\left(-\frac{x^2}{2\sin^2\theta}\right)} d\theta, \quad x \geq 0,$$

presented in detail in [12], is limited to the first two powers of the $Q$-function and it requires a double integration to get the expectation of the $Q$-function with respect to a standard Nakagami-$m$ distribution, $m$ being the Nakagami fading parameter ($m = 1$ represents the popular Rayleigh fading environment). Among the approximations, to the best of our knowledge, the one presented in [90] performs well in terms of how accurately it resembles the actual $Q$-function combined with its relatively simple form. As pointed out in [91], there are better approximations for $Q$-function compared to that in [90]. However, the approximation in [90] is sufficient for the purposes of this work.

Our interest in approximating the $Q$-function is two fold, one is the accuracy and the second is the simplicity of the form that lets further performance analysis of fading communication systems possible in an easy manner. The form of approximation given in [90] is still not easy to integrate and is limited to a restricted $m$ of Nakagami-$m$ distributions. In this section of the Appendix, building upon the approximation in [90], we suggest a modified approximation which is simple and is easily integrable with respect to any $m$ of a Nakagami-$m$ fading distribution in closed-form while preserving the tightness of the approximation.

#### 3.6.3.2 Approximation for the Gaussian $Q$-Function

The approximation for $Q$-function given in [90] is

$$Q(x) \approx \frac{\left(1 - e^{\frac{-Ax}{\sqrt{2}}}\right) e^{\frac{-x^2}{2}}}{B\sqrt{2\pi}x}, \tag{3.98}$$

where $A = 1.98$ and $B = 1.135$[5]. The accuracy with which (3.98) represents the actual $Q$-function is quite remarkable. However, the presence of $x$ in the denominator of (3.98) makes it difficult to evaluate $E\left[Q^N(x)\right]$ in many scenarios. Higher integer powers of the $Q$-function appear in the evaluation of average block

[5]Please refer to [90] for a discussion on the selection of $A$ and $B$

error probabilities. It is straightforward to show that if the maximum integer power of the Gaussian $Q$-function in the performance metric[6] is $N$, then with (3.98) replacing the actual $Q$-function, closed-form expression for $E[Q^N(x)]$ in Nakagami-$m$ fading is possible only for $m > \frac{N}{2}$. For the performance metric of average SEP (ASEP) for a differentially encoded QPSK in Nakagami-$m$ studied in [90], the maximum integer power of $Q$-function is 4 and so the analytical results are limited to $m > 2$. Unfortunately this limitation implies that important cases such as the popular Rayleigh fading ($m = 1$) are not covered.

Building on the approximation given in [90], we develop a slightly modified version of (3.98) that will avoid the presence of $x$ in the denominator and is easily integrable for any $m$. We begin with Taylor series expansion of $e^{\frac{-Ax}{\sqrt{2}}}$

$$e^{\frac{-Ax}{\sqrt{2}}} = \sum_{n=0}^{\infty} \frac{(-Ax)^n}{\sqrt{2}^{\,n}\, n!}\,. \tag{3.99}$$

Substituting (3.99) in (3.98) and truncating the series we arrive at

$$\begin{aligned} Q(x) &\approx \frac{\left(1 - e^{\frac{-Ax}{\sqrt{2}}}\right) e^{\frac{-x^2}{2}}}{B\sqrt{2\pi}x} \\ &\approx e^{\frac{-x^2}{2}} \sum_{n=1}^{n_a} c_n\, x^{n-1}\,, \\ c_n &= \frac{(-1)^{n+1}(A)^n}{B\sqrt{\pi}\,(\sqrt{2})^{n+1}\, n!}\,. \end{aligned} \tag{3.100}$$

In (3.100) we truncated the infinite series by taking the first $n_a$ terms. The presence of $(\sqrt{2}^{\,n+1}\, n!)$ in the denominator of (3.100) ensures that as $n$ increases $c_n$ approaches zero quickly. So we can approximate the complete infinite series with a relatively small $n_a$. Obtaining (3.100) requires only a minor modification to (3.98) but is very important from a performance metric evaluation point of view. The analytical simplicity of (3.100) is significant, (3.100) doesn't have $x$ in the denominator, and the expression is a simple finite weighted summation of the terms of the form $x^\alpha\, e^{-\frac{x^2}{2}}$, $\alpha \geq 0$, which are easily integrable for any $m$ of a Nakagami-$m$ distribution. This simplicity also extends to powers of the $Q$-function. Let $N$ be

[6] with $x$ appearing inside the square root of the $Q$-function's argument ($Q(\sqrt{w\,x}\,)$) as is the case in [90].

the maximum integer power of $Q$-function in the performance metric, then using multinomial expansion, we can write $Q^N(x)$ as

$$\begin{aligned} Q^N(x) &\approx e^{\frac{-Nx^2}{2}} \left(c_1 + c_2\, x + \cdots + c_{n_a}\, x^{n_a-1}\right)^N, \\ &= \sum_{k_1,k_2,\ldots,k_{n_a}} K_M\, C_M\, x^{f_m}\, e^{\frac{-Nx^2}{2}}, \end{aligned} \tag{3.101}$$

the summation is over all sequences of nonnegative integers $k_1, \ldots, k_{n_a}$ such that $k_1 + \cdots + k_{n_a} = N$. In (3.101)

$$K_M = \frac{N!}{(k_1)!(k_2)!\ldots(k_{n_a})!}, \tag{3.102}$$

$$C_M = (c_1)^{k_1}(c_2)^{k_2}\ldots(c_{n_a})^{k_{n_a}}, \tag{3.103}$$

$$f_m = k_2 + 2k_3 + \cdots + (n_a - 1)k_{n_a}. \tag{3.104}$$

Notice that the final form for the approximation of $Q^N(x)$, given in (3.101), is still a simple finite linear combination of terms of the form $x^\alpha e^{-\frac{N}{2}x^2}$, $\alpha \geq 0$. So it is relatively easy to evaluate $E[Q^N(x)]$ for any $m$ of a Nakagami-m distribution. Also we believe that due to the nature of the term $x^\alpha e^{-\frac{N}{2}x^2}$ and the availability of a vast number of integration tables [35], $E[Q^N(x)]$ can be evaluated for a wide range of other distributions as well. Note that with the help of generalized binomial expansion, it is also possible to express the tighter $Q$-approximations given in [86] (eq. 9 and 13) in a form that is suitable for integration w.r.t a Nakagami-$m$ distribution. However from the perspective of understanding the performance of communication systems we find (3.101) to be both simple and close enough to the results obtained by the actual $Q$-function.

We now examine how accurately (3.101) represents the actual $Q$-function. For $N \in \{3, 4, 5\}$, where $N$ is the exponent of the Gaussian $Q$-function, Fig. 1 shows that the approximation to the Gaussian $Q$-function given in (3.101) can be seen to be quite tight. The approximation in (3.101) obviously depends on $n_a$. With $N = 4$, Fig. 2 plots the additional loss incurred as we further approximated (3.98) to arrive at (3.100). From Fig. 2 we observe that $n_a = 8$ is a reasonable choice as the additional loss is almost zero.

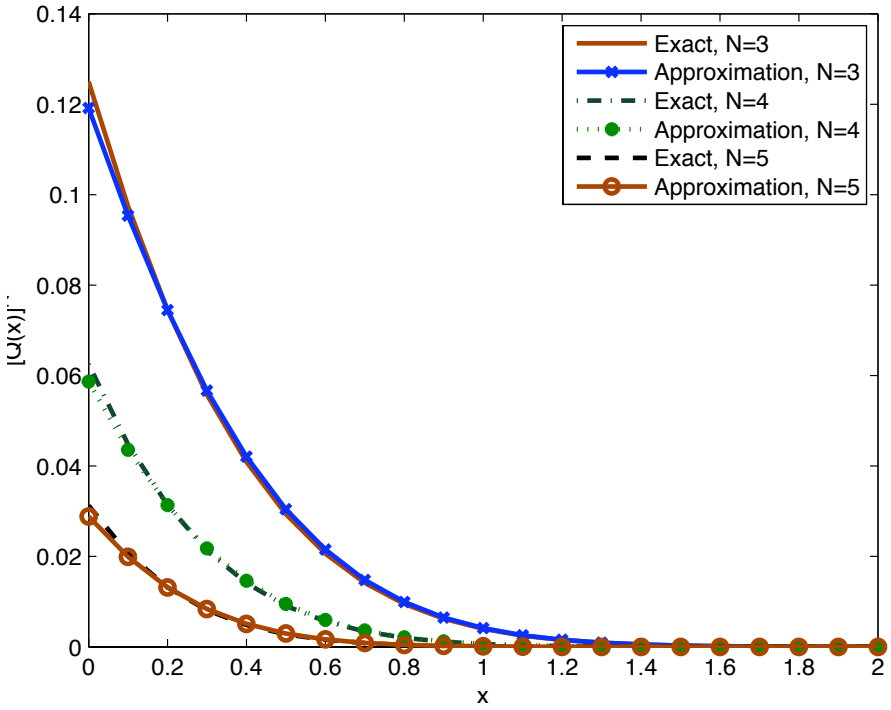


Figure 3.8 Verification of the accuracy of the Gaussian $Q$-function approximation given in (3.101).

#### 3.6.3.3 Average SEP of Differentially Encoded QPSK

To demonstrate the usefulness of the approximation developed, we determine the expression for the Average SEP of Differentially Encoded QPSK. Conditioned on the fading related parameter $\gamma$, the SEP of differentially encoded QPSK (DE-QPSK) is given by [12]

$$P_s(\gamma_s, m, \gamma) = 4Q\left(\sqrt{\gamma}\right) - 8Q^2\left(\sqrt{\gamma}\right) + 8Q^3\left(\sqrt{\gamma}\right) - 4Q^4\left(\sqrt{\gamma}\right). \tag{3.105}$$

The pdf of $\gamma$ is given by

$$p_\gamma(\gamma) = \frac{m^m\,\gamma^{m-1}}{\gamma_s^m\,\Gamma(m)}\,e^{-\frac{m\gamma}{\gamma_s}}, \tag{3.106}$$

where $\gamma_s$ is the SNR per symbol. Averaging over fading, with the help of (3.101) and (3.106), the average SEP is given by

$$P_s(\gamma_s, m) = E_\gamma\left[P_s(\gamma_s, m, \gamma)\right]$$

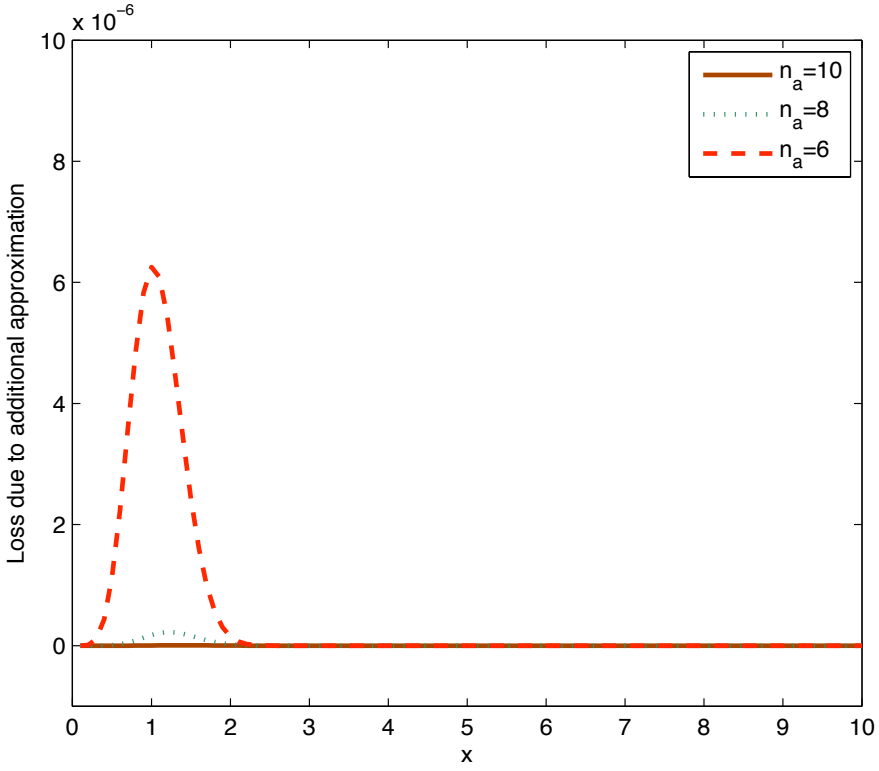


Figure 3.9 Additional loss due to further approximation of (3.98) to arrive at (3.100), $N = 4$.

$$
\begin{aligned}
&= E_\gamma\left[4\,Q\left(\sqrt{\gamma}\right) - 8\,Q^2\left(\sqrt{\gamma}\right) + 8\,Q^3\left(\sqrt{\gamma}\right) - 4\,Q^4\left(\sqrt{\gamma}\right)\right] \\
&= 4\,\mathcal{F}\left(\gamma_s, m, 1\right) - 8\,\mathcal{F}\left(\gamma_s, m, 2\right) + 8\,\mathcal{F}\left(\gamma_s, m, 3\right) \\
&-4\,\mathcal{F}\left(\gamma_s, m, 4\right)
\end{aligned} \tag{3.107}
$$

where

$$
\begin{aligned}
&\mathcal{F}\left(\gamma_s, m, N\right) = E_\gamma\left[Q^N\left(\sqrt{\gamma}\right)\right] \\
&= \sum_{k_1,k_2,\ldots,k_{n_a}} \frac{m^m K_M C_M}{\gamma_s^m \Gamma(m)} \int_0^\infty \gamma^{\frac{f_m+2m-2}{2}} e^{-\left(\frac{N}{2}+\frac{m}{\gamma_s}\right)\gamma} d\gamma, \\
&= \sum_{k_1,k_2,\ldots,k_{n_a}} \frac{m^m K_M C_M \Gamma\left(\frac{f_m}{2}+m\right) 2^{\frac{f_m}{2}+m} \gamma_s^{\frac{f_m}{2}}}{\Gamma(m)\,\left(N\,\gamma_s + 2m\right)^{\frac{f_m}{2}+m}}
\end{aligned} \tag{3.108}
$$

where $K_M$, $C_M$ and $f_m$ are defined in (3.102), (3.103), and (3.104) respectively and $\Gamma(.)$ is the standard Gamma function. To simplify the above expression we

used the identity [35]

$$\int_0^\infty x^p e^{-\omega x}\, dx = \Gamma(p+1)\, \omega^{-(p+1)}\,, \quad \omega > 0\,, \quad p > -1\,. \tag{3.109}$$

Without approximating the $Q$-function, the single integral based expression given for ASEP of DE-QPSK in [12] is only valid for integer values of $m$. With the $Q$-approximation of [90], as pointed out earlier, the complicated ASEP expression for DE-QPSK given in [90] is valid for $m > 2$, and it involves the confluent hypergeometric function ${}_1F_1$. The final ASEP expression derived in this section of the Appendix (3.107) is valid for any $m$ of Nakagami-$m$ fading and is a simple finite series. In Fig. 3 it can be seen that the analytical form of average SEP given in (3.107) matches well with the simulated average SEP for different values of $m$.

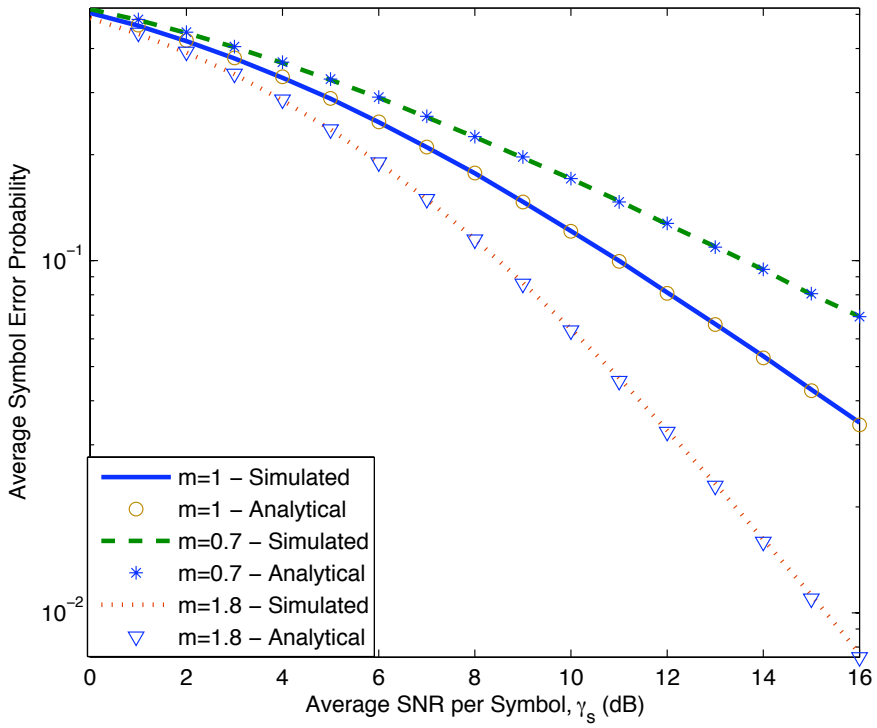


Figure 3.10 Comparison of simulated and analytical (3.107) average SEP of DE-QPSK, $m$ is the Nakagami-$m$ fading parameter.

In conclusion, a principal reason for approximating the Gaussian $Q$-function is to have a simple form for the $Q$-function that facilitates further mathe-

matical analysis of communication system's performance. Through a modification to the approximation given in [90], the new approximation (3.101) proposed in this Appendix preserves the tightness of the approximation in [90] yet allowing the closed-form analytical expression for $E[Q^N(x)]$ for any $m$ of a Nakagami-$m$ fading distribution. Average SEP of DE-QPSK in Nakagami-$m$ fading is evaluated using the proposed approximation and its accuracy is validated by simulations.

### 3.6.4 Evaluation of 3.28 for $m \geq 3$

In this section, for $m \geq 3$, with the help of the analytically tractable approximation of $Q(x)$ given in (3.101), we derive closed-form expressions for $A_p\, E\left[Q^m\left(\sqrt{2\,\gamma_b\, z_1}\right)\right]$ and $(1-A_p)\, E\left[Q^m\left(\sqrt{2\,\gamma_b\, z_2}\right)\right]$.

$$\begin{aligned} A_p\, E\left[Q^m\left(\sqrt{2\,\gamma_b\, z_1}\right)\right] &= A_p \int_{z_1=0}^{\infty} Q^m\left(\sqrt{2\,\gamma_b\, z_1}\right) p_{z_1}(z_1)\, dz_1 \\ &= \int_{z_1=0}^{\infty} Q^m\left(\sqrt{2\,\gamma_b\, z_1}\right) \hat{p}_1(z_1)\, dz_1 + \\ &\quad \int_{z_1=0}^{\infty} Q^m\left(\sqrt{2\,\gamma_b\, z_1}\right)\, \hat{p}_2(z_1)\, dz_1 \\ &= U_1(\gamma_b) + U_2(\gamma_b) \end{aligned} \tag{3.110}$$

where $p_{z_1}(z_1)$, $\hat{p}_1(z_1)$, and $\hat{p}_2(z_1)$ are defined in (3.69), (3.72), and (3.79) respectively and

$$U_1(\gamma_b) = \sum_{l=0}^{n} \sum_{p=0}^{2n-l-1} \sum_{g=0}^{\delta} \left\{\mathcal{K}_{p_1} f_{e1}(l,p,g,\mathcal{L}) + \mathcal{K}_{p_2} f_{e2}(l,p,g,\mathcal{L})\right\}, \tag{3.111}$$

$$\begin{aligned} f_{e2}(l,p,g,\mathcal{L}) &= \mathcal{R}_1 \int_{z_1=0}^{\infty} Q^m\left(\sqrt{2\,\gamma_b\, z_1}\right)\, {z_1}^{-\frac{1}{2}}\, e^{-z_1\,\mathcal{R}_h}\; {}_1F_1\left(\mathcal{R}_n,\, \frac{1}{2};\, z_1\,\mathcal{R}_c\right) dz_1 \\ &= \mathcal{R}_1 \int_{z_1=0}^{\infty} \sum_{k_1=0}^{\infty} c_{k_1}\, (2\,\gamma_b)^{\frac{k_1}{2}}\, {z_1}^{\frac{k_1-1}{2}}\, e^{-z_1(m\,\gamma_b+\mathcal{R}_h)}\; {}_1F_1\left(\mathcal{R}_n,\, \frac{1}{2};\, z_1\,\mathcal{R}_c\right) dz_1 \\ &= \mathcal{R}_1 \sum_{k_1=0}^{\infty} c_{k_1} (2\,\gamma_b)^{\frac{k_1}{2}}\, \mathcal{F}\left(\mathcal{R}_n, \frac{1}{2}, k_1+\frac{1}{2}, \mathcal{R}_c,\, m\gamma_b+\mathcal{R}_h\right) \end{aligned}$$

where (variable - definition): $n$ - (3.46), $\delta$ - (3.57), $\mathcal{L}$ - (3.54), $\mathcal{K}_{p_1}$ - (3.60), $\mathcal{K}_{p_2}$ - (3.61), $\mathcal{R}_1$ - (3.74), $\mathcal{R}_h$ - (3.75), $\mathcal{R}_n$ - (3.76), and $\mathcal{R}_c$ - (3.77), and

$$\begin{aligned}\mathcal{F}\left(a,b,\alpha,k,s\right) &= \int_{x=0}^{\infty} x^{\alpha-1}e^{-s\,x}\,{}_1F_1\left(a,b;k\,x\right)\,dx \\ &= \Gamma(\alpha)\,s^{-\alpha}\,{}_2F_1\left(a,\alpha\,;b\,;ks^{-1}\right), \quad [\alpha>0,\,|s|>|k|] \end{aligned} \tag{3.112}$$

To complete the calculation of $U_1(\gamma_b)$ in (3.111) we still need $f_{e1}(l,p,g,\mathcal{L})$ which is given by

$$f_{e1}(l,p,g,\mathcal{L}) = f_{e2}(l,p,g,1)\,.$$

We now focus on $U_2(\gamma_b)$ in (3.110):

$$U_2(\gamma_b) = \sum_{l=0}^{n}\sum_{p=0}^{2n-l-1}\sum_{g=0}^{\delta}\left\{\mathcal{K}_{p_1}f_{e3}(l,p,g,\mathcal{L})+\mathcal{K}_{p_2}f_{e4}(l,p,g,\mathcal{L})\right\}, \tag{3.113}$$

$$\begin{aligned} f_{e4}(l,p,g,\mathcal{L}) &= \int_{z_1=0}^{\infty} Q^m\left(\sqrt{2\,\gamma_b\,z_1}\right)\,\hat{p}_2(z_1)\,dz_1 \\ &= \mathcal{R}_2\int_{z_1=0}^{\infty} Q^m\left(\sqrt{2\,\gamma_b\,z_1}\right)\,e^{-z_1\,\mathcal{R}_h}\,{}_1F_1\left(\mathcal{R}_{n2},\,\frac{3}{2};\,z_1\,\mathcal{R}_c\right)dz_1 \\ &= \mathcal{R}_2\int_{z_1=0}^{\infty}\sum_{k_1=0}^{\infty} c_{k_1}(2\,\gamma_b)^{\frac{k_1}{2}}\,z_1^{\frac{k_1}{2}}\,e^{-z_1(m\gamma_b+\mathcal{R}_h)}\,{}_1F_1\left(\mathcal{R}_{n2},\,\frac{3}{2};\,z_1\,\mathcal{R}_c\right)dz_1 \\ &= \mathcal{R}_2\sum_{k_1=0}^{\infty} c_{k_1}(2\,\gamma_b)^{\frac{k_1}{2}}\,\mathcal{F}\left(\mathcal{R}_{n2},\frac{3}{2},\frac{k_1}{2}+1\,,\mathcal{R}_c,\,m\gamma_b+\mathcal{R}_h\right) \end{aligned} \tag{3.114}$$

where (variable - definition): $\mathcal{R}_2$ - (3.81), and $\mathcal{R}_{n2}$ - (3.82). To complete $U_2(\gamma_b)$ in (3.113), $f_{e3}(l,p,g,\mathcal{L})$ is given by

$$f_{e3}(l,p,g,\mathcal{L}) = f_{e4}(l,p,g,1)\,.$$

Substituting (3.111) and (3.113) in (3.110) gives the final closed form expression for $A_p\,E\left[Q^m\left(\sqrt{2\,\gamma_b\,z_1}\right)\right]$. It is straightforward to show that

$$(1-A_p)\,E\left[Q^m\left(\sqrt{2\,\gamma_b\,z_2}\right)\right] = U_1(\gamma_b)-U_2(\gamma_b)\,. \tag{3.115}$$

### 3.6.5 Average SEP- Delay Error Known at the Receiver

With appropriate changes to (3.15) the decision variable (DV), with $N = 1$, and assuming that the receiver does not know $\rho_e$, can be shown to be given by

$$r[k] = \bar{\rho_e}\sqrt{\Omega}s_m[k] + \tilde{v}[k], \tag{3.116}$$

where, conditioned on $|s_m[k]|$ and $z$, $\tilde{v}[k]$ is a zero-mean CSCG r.v with variance

$$\frac{\sigma_n^2 + |s_m[k]|^2(1-|\rho_e|^2)\Omega}{z}.$$

Here $z = |\varphi|^2$. Closed form expression for the pdf of $z$ is given by (3.65). Note that the DV in (3.116) is made to be consistent (notation wise) with the results in Chapter 2, where we studied the issue of average BEP and SEP under the assumption that both the delay and estimation related error terms are unknown at the receiver. In this section the receiver knows the delay related error term.

#### 3.6.5.1 Average Symbol Error Probability of $M$-QAM Constellation

The DV at the demodulator can be expressed in a parametric form as

$$r[k] = \kappa s_m[k] + \xi[k] = r_I[k] + jr_Q[k], \tag{3.117}$$

where $\kappa = \bar{\rho_e}\sqrt{\Omega} \triangleq \mu_I + j\mu_Q$, and $\xi[k]$, conditioned on $|s_m[k]|$ and $z$, is a CSCG r.v with variance $\mathcal{F}(|s_m[k]|)/z$, where $\mathcal{F}(x) = (\sigma_n^2 + (1-|\rho_e|^2)x^2\Omega)$. Key steps in the derivation of average SEP are given below.

Let $s_m[k] = s_{m,x}[k] + js_{m,y}[k]$, $m = 0, 1, \ldots, M-1$, $x = 0, 1, \ldots, M_1 - 1$, $y = 0, 1, \ldots, M_2 - 1$, where $s_{m,x}[k] = a_{m,x}[k]d$, and $s_{m,y}[k] = a_{m,y}[k]d$, where $a_{m,x}[k] = -(M_1 - 1) + 2x$ and $a_{m,y}[k] = -(M_2 - 1) + 2y$. For simplicity, let us define the parameter

$$\gamma_{x,y} \triangleq \frac{2d^2}{\mathcal{F}(|s_m[k]|)} = \frac{2d^2}{\sigma_n^2 + \Omega(1-|\rho_e|^2)|s_m[k]|^2}.$$

Let $\mathcal{P}_{x,y}(z)$ be the probability of correctly receiving $s_{m,x}[k] + js_{m,y}[k]$, conditioned on $z$. For $x = 1, 2 \ldots, M_1 - 2$, $y = 1, 2, \ldots, M_2 - 2$, $\mathcal{P}_{x,y}(z)$ can be expressed as

$\mathcal{P}_{x,y}(z) = \text{Prob}(s_{m,x}[k] - d \leq r_I[k] < s_{m,x}[k] + d|z) \times \text{Prob}(s_{m,y}[k] - d \leq r_Q[k] < s_{m,y}[k] + d|z)$,

$$\mathcal{P}_{x,y}(z) = \left\{Q(\mathtt{t}_1(x,y)\sqrt{z}) - Q(\mathtt{t}_2(x,y)\sqrt{z}\,)\right\} \times \left\{Q(\mathtt{t}_3(x,y)\sqrt{z}) - Q(\mathtt{t}_4(x,y)\sqrt{z}\,)\right\}, \tag{3.118}$$

where

$$Q(x) = \frac{1}{\sqrt{2\pi}} \int_x^\infty \exp(-u^2/2)du$$

and $\mathtt{t}_1(x,y)$, $\mathtt{t}_2(x,y)$, $\mathtt{t}_3(x,y)$, and $\mathtt{t}_4(x,y)$ are defined in (2.37)-(2.40).

As explained in Chapter 2, we can similarly define the probability of correctly receiving for all $x = 0, 1, \ldots, M_1 - 1$ and $y = 0, 1, \ldots, M_2 - 1$. Notice that, each of the $\mathcal{P}_{x,y}(z)$ can be expressed as linear combinations of $Q(a\sqrt{z}\,) \times Q(b\sqrt{z}\,)$ for real values of $a$ and $b$. Let $\overline{\mathcal{P}}_{x,y} \triangleq E[\mathcal{P}_{x,y}(z)]$. To derive $\overline{\mathcal{P}}_{x,y}$, we must determine $E[Q(a\sqrt{z}\,) \times Q(b\sqrt{z}\,)]$. To this end, we define $\mathcal{H}(a,b,t,B,\rho_d)$ and $\mathcal{R}(a,t,B,\rho_d)$.

$$\mathcal{H}(a,b,t,B,\rho_d) \triangleq E[Q(a\sqrt{z})Q(b\sqrt{z})] \tag{3.119}$$

$$= \begin{cases} \mathcal{J}(a,b,t,B,\rho_d) & \text{if } a \geq 0, b \geq 0 \\ 2\mathcal{J}(|a|,0,t,B,\rho_d) - \mathcal{J}(a,|b|,t,B,\rho_d) & \text{if } a \geq 0, b < 0 \\ 2\mathcal{J}(0,|b|,t,B,\rho_d) - \mathcal{J}(|a|,b,t,B,\rho_d) & \text{if } a < 0, b \geq 0 \\ 1 - 2\mathcal{J}(|a|,0,t,B,\rho_d) - 2\mathcal{J}(0,|b|,t,B,\rho_d) & \\ \quad + \mathcal{J}(|a|,|b|,t,B,\rho_d) & \text{if } a < 0, b < 0 \end{cases}$$

$$\mathcal{R}(a,t,B,\rho_d) \triangleq E[Q(a\sqrt{z}\,)] = \begin{cases} 2\mathcal{J}(a,0,t,B,\rho_d) & \text{if } a \geq 0 \\ 1 - 2\mathcal{J}(|a|,0,t,B,\rho_d) & \text{if } a < 0. \end{cases}$$

Closed form expression for $\mathcal{J}(a,b,t,B,\rho_d)$, derived in the next subsection, is given in (3.121) (with the help of pdf of $z$ given in (3.65)). For all other values $x$ and $y$, $\overline{\mathcal{P}}_{x,y}$ can be derived similarly. The average SEP can be written as

$$\mathrm{P}_S = 1 - \frac{1}{M} \sum_{x=0}^{M_1-1} \sum_{y=0}^{M_2-1} \overline{\mathcal{P}}_{x,y}. \tag{3.120}$$

We now present a sample simulation to verify the accuracy of the derived analytical expression. Fig.3.11 shows the average SEP performance of $4 \times 4$ QAM with $t = 4$

antennas, $B = 4$ feedback bits, the delay only correlation co-efficient $\rho_d = 0.98$, estimation only correlation co-efficient $\rho_e = 0.995$ and $\Omega = 1$. It can be seen that the analytical expression accurate match the simulations.

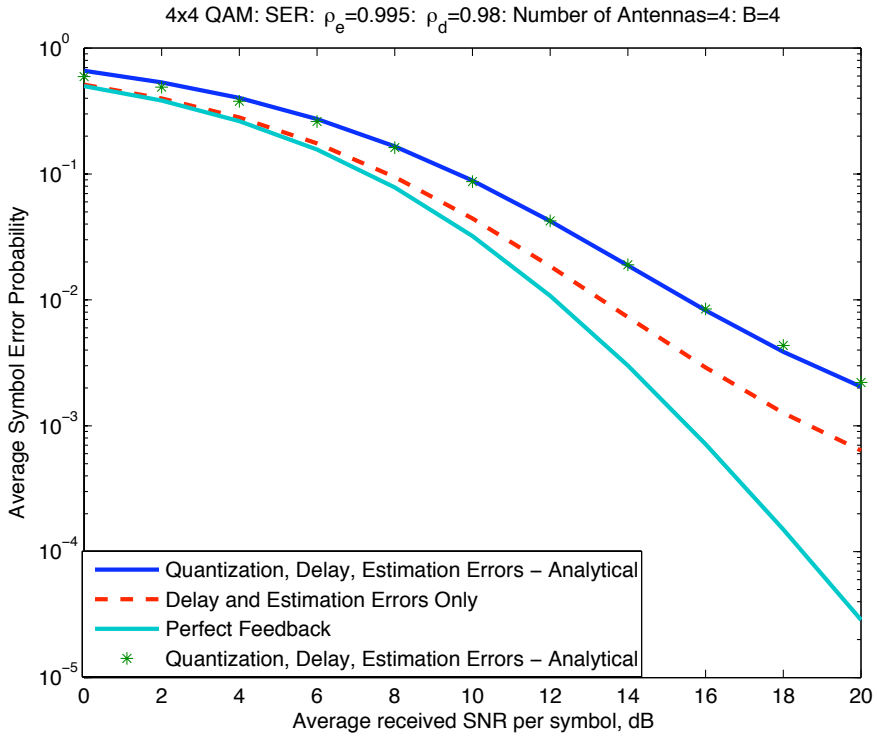


Figure 3.11 Combined effects of channel estimation error, feedback delay and channel quantization on average SEP of $4 \times 4$-QAM: $t = 4$ antennas, $B = 4$ feedback bits, delay only correlation co-efficient $\rho_d = 0.98$, and estimation only correlation co-efficient $\rho_e = 0.995$.

### 3.6.5.2 Closed Form for $\mathcal{J}(a, b, t, B, \rho_d)$

$$\begin{aligned} \mathcal{J}(a,b,t,B,\rho_d) &= E[Q(a\sqrt{z})Q(b\sqrt{z})] \qquad (3.121) \\ &= \sum_{l=0}^{n} \sum_{p=0}^{2n-l-1} \sum_{g=0}^{\delta} \left\{ \mathcal{K}_{p_1} \mathcal{G}(a,b,n,l+g,1) + \mathcal{K}_{p_2} \mathcal{G}(a,b,n,l+g,L) \right\}, \end{aligned}$$

$$\mathcal{G}(a,b,n,l,L) = \int_{z=0}^{\infty} Q(a\sqrt{z})Q(b\sqrt{z}) f_2(l,g,z)dz \qquad (3.122)$$

$$
\begin{aligned}
&= \left[Q(a\sqrt{z})Q(b\sqrt{z})F_2(l,L,z)\right]_{z=0}^{\infty} + \\
&\quad \frac{b}{2\sqrt{2\pi}} \int_{z=0}^{\infty} F_2(l,L,z)Q(a\sqrt{z})e^{-\frac{b^2 z}{2}} z^{-\frac{1}{2}} dz + \\
&\quad \frac{a}{2\sqrt{2\pi}} \int_{z=0}^{\infty} F_2(l,L,z)(z)Q(b\sqrt{z})e^{-\frac{a^2 z}{2}} z^{-\frac{1}{2}} dz \\
&= \mathcal{X}(a,b,n,l,L) + \mathcal{X}(b,a,n,l,L), \qquad (3.123)
\end{aligned}
$$

$$
\mathcal{X}(a,b,n,l,L) \triangleq \frac{b}{2\sqrt{2\pi}} \int_{z=0}^{\infty} F_2(l,L,z)Q(a\sqrt{z})e^{-\frac{b^2 z}{2}} z^{-\frac{1}{2}} dz, \qquad (3.124)
$$

$$
\begin{aligned}
F_2(l,L,z) &= \int_0^z f_2(l,g,z)\, dz \\
&= 1 - e^{-zL} \sum_{j=0}^{n-l-1} \frac{L^j}{\Gamma(j+1)} z^j \quad z \geq 0.
\end{aligned}
$$

Upon using

$$
Q(z) = (1/\pi) \int_{\theta=0}^{\pi/2} \exp\left(-\frac{z^2}{2\sin^2\theta}\right) d\theta \quad z \geq 0,
$$

$\mathcal{X}(a,b,n,l,L)$ can be simplified as

$$
\begin{aligned}
\mathcal{X}(a,b,n,l,L) &= \frac{b}{2\sqrt{2\pi}} \int_{z=0}^{\infty} Q(a\sqrt{z})e^{-\frac{b^2 z}{2}} z^{-\frac{1}{2}} dz - \\
&\qquad \frac{b}{2\sqrt{2\pi}} \sum_{j=0}^{n-l-1} \frac{L^j}{j!} \int_{z=0}^{\infty} Q(a\sqrt{z})e^{-(\frac{b^2}{2}+L)z} z^{j-\frac{1}{2}} dz \\
&= \frac{b}{2\pi\sqrt{2\pi}} \int_0^{\pi/2} d\theta \int_{z=0}^{\infty} e^{-\left(\frac{b^2}{2}+\frac{a^2}{2\sin^2\theta}\right)z} z^{-\frac{1}{2}} dz - \\
&\qquad \frac{b}{2\pi\sqrt{2\pi}} \sum_{j=0}^{n-l-1} \frac{L^j}{j!} \int_0^{\pi/2} d\theta \int_{z=0}^{\infty} e^{-\left(\frac{b^2}{2}+\frac{a^2}{2\sin^2\theta}+L\right)z} z^{j-\frac{1}{2}} dz \\
&= \frac{1}{2\pi} \int_0^{\pi/2} \left(\frac{b^2\sin^2\theta}{b^2\sin^2\theta + a^2}\right)^{\frac{1}{2}} d\theta - \\
&\qquad \sum_{j=0}^{n-l-1} \frac{L^j}{j!} \frac{b\Gamma\left(j+\frac{1}{2}\right)2^{j+\frac{1}{2}}}{2\pi\sqrt{2\pi}} \int_0^{\pi/2} \left(\frac{\sin^2\theta}{b^2\sin^2\theta + 2L\sin^2\theta + a^2}\right)^{j+\frac{1}{2}} d\theta
\end{aligned}
$$

$$= \frac{ab}{2\pi(a^2+b^2)}\,{}_2F_1\left(1,1;\frac{3}{2};\frac{b^2}{a^2+b^2}\right) - \sum_{j=0}^{n-l-1}\frac{L^j}{j!}\frac{b\Gamma\left(j+\frac{1}{2}\right)2^{j+\frac{1}{2}}}{2\pi\sqrt{2\pi}}\frac{1}{(a^2+b^2+2L)^{j+1}} \times\frac{\sqrt{\pi}\,a}{2}\frac{\Gamma(j+1)}{\Gamma(j+\frac{3}{2})}\,{}_2F_1\left(1,j+1;j+\frac{3}{2};\frac{b^2+2L}{a^2+b^2+2L}\right). \quad (3.125)$$

**Acknowledgement**

The text of this chapter, in part, has *appeared* in:

- Y. Isukapalli and B. D. Rao, "Analyzing the effect of channel estimation errors on the average block error probability of a MISO transmit beamforming system," *IEEE Global Telecom. (Globecom) Conf.*, New Orleans, LA, pp. 1-6, Dec. 2008.

- Y. Isukapalli and B. D. Rao, "An analytically tractable approximation for the Gaussian Q-function," *IEEE Communications Letters*, vol. 12, no. 9, pp. 669-671, Sep. 2008.

- Y. Isukapalli and B. D. Rao, "Performance analysis of finite rate feedback MISO systems in the presence of estimation errors and delay," *IEEE Asilomar Conf. on Sig. Syst. and Comp.*, CA, pp. 1931-1935, Oct. 2007

The text of this chapter, in part, is *under review* in:

- Y. Isukapalli and B. D. Rao, "Packet error probability of a transmit beamforming system with imperfect feedback," submitted, *IEEE Transactions on Signal Processing*, submitted, May 2009, revised, Jul. 2009.

# 4 Spatial Correlation: Codebook Design and Performance Analysis

In this chapter we shift our focus to spatially correlated channels. In the previous chapters modeling and analysis was carried out for spatially independent channels. The spatially independent assumption is justified for rich-scattering environment, otherwise there will be correlation across the antennas.

We present an optimum codebook design algorithm that minimizes the loss in average symbol error probability (SEP) of a spatially correlated channels under both perfect and imperfect channel estimate assumptions. Towards the goal of designing an optimum codebook that minimizes average SEP (ASEP) loss due to finite-rate channel quantization, we derive the distortion function as a first order approximation of the instantaneous SEP loss. Utilizing high resolution quantization theory and assuming perfect channel estimation at the receiver, we analyze the loss in ASEP for spatially independent and correlated finite-rate feedback transmit beamforming system with rectangular $M_1 \times M_2$-QAM constellation. We then consider the high-SNR regime and show that the loss associated with quantizing the spatially independent channels is related to the loss associated with quantizing the spatially correlated channels by a scaling constant given by the determinant of the correlation matrix. Simulation results illustrate the effectiveness of the new codebook design and validate the derived analytical expressions for ASEP loss.

We also present a novel codebook design algorithm that minimizes the loss in ergodic capacity. Simulation results show that the new codebook designed

under the consideration of estimation errors and feedback delay clearly outperforms the codebook designed under ideal conditions. Analysis for the loss in ergodic capacity for spatially independent channels with channel estimation errors and delay is presented and validated through simulations.

## 4.1 Introduction

Under ideal channel estimation and no feedback delay assumptions, the effect of limited feedback on the ergodic capacity is a well studied concept. Average Symbol Error Probability, another important communication system performance metric, has received much less attention. For a limited set of constellations and for independent and identically distributed (i.i.d.) fading channels it has been analyzed utilizing an approximation to the statistical distribution of the key random variable that characterizes the system performance. Specifically for spatially i.i.d. channels both [25] and [26] characterized the absolute amplitude square of the inner product between the channel direction and its quantized version as a truncated beta distribution and used it to study effect of quantization on ASEP. Similar to the capacity analysis, ASEP analysis for correlated channels using such statistical methods have not met with much success. [92] discussed the importance of using right metric for codebook design. However, [92] did not provide codebook construction based on the average bit error probability (metric considered in [92]) criteria. The importance of the choice of performance metric and the effect of mismatch in the channel statistics assumptions are the main focus of this chapter.

We first begin with the design of codebooks that are optimum for minimizing the average symbol error probability loss assuming perfect channel knowledge at the receiver. For this scenario, we then make use of the source coding based framework developed in [93] to analyze the ASEP loss in correlated Rayleigh fading channels with rectangular QAM constellation. The application of the theory in [93] to this problem is quite involved because of the complicated dependency of

the objective function on the random variables involved as well as the nature of the constellation ($M_1 \times M_2$-QAM). The impact of the performance metric on the performance of the quantizer is highlighted by comparing the performance with past quantizer designs which utilize capacity loss as a metric. The quantizer design problem in the presence of channel estimation errors is also addressed and compared to the designs that assume perfect channel knowledge at the receiver.

The second component of this chapter is about the optimum codebook design and loss analysis of ergodic capacity. Under ideal conditions an optimum codebook design for ergodic capacity loss is presented in [26]. A grassmannian codebook design for correlated channels with perfect channel estimation and no delay is proposed in [94]. In the context of determining a transmit weighting matrix that improves the performance of orthogonal space-time block codes, a mean-squared error criteria is used to design codebook for channels with feedback delay and feedback channel bit errors [95]. With randomized vector codebook, the ergodic capacity for spatially i.i.d. channels with estimation errors and finite-rate quantization is studied in [96] and [97].

In this part of our work we focus on optimum vector quantization (VQ) algorithm that is directly related to the loss in ergodic capacity of a spatially and temporally correlated channel with estimation errors and feedback delay. Following the approach taken in [13] and [26], a new design criteria is developed and a Lloyd-type VQ design algorithm is proposed to design the quantization codebook. The codebook design for spatially i.i.d. channel with estimation errors and delay then becomes a special case of the correlated case. With this codebook, analysis for loss in ergodic capacity is presented for the spatially i.i.d. scenario with estimation errors and delay. In this chapter the estimation and delay related error terms are modeled similarly, i.e., both are unknown to the receiver.

The rest of this chapter is organized as follows. In Section 4.2 we introduce the system model. Optimum transmit beamforming vector under both perfect and imperfect channel estimate scenarios and optimum codebook design specific

to minimizing the loss in average symbol error probability are developed in Section 4.3. The average SEP loss expressions for spatially independent and correlated channels are derived for rectangular $M_1 \times M_2$-QAM modulation in Section 4.4. Results related to the codebook design and performance analysis of ergodic capacity are presented in Section 4.5. We conclude this chapter in Section 4.6.

Important variables: $t$-number of transmit antennas, $B$-number of feedback bits, $\rho$- Average signal-to-noise ratio per symbol.

## 4.2 System Model

We consider a multiple input single output (MISO) system with $t$ antennas at the transmitter and one antenna at the receiver. The wireless channel $\mathbf{h} \in \mathbb{C}^{t\times 1}$ between the transmitter and the receiver is modeled as a correlated frequency-flat Rayleigh fading channel with spatial distribution given by $\mathbf{h} \sim \mathcal{NC}\big(\mathbf{0}, \mathbf{\Sigma}_{\rm h}\big)$[1]. Let $\mathbf{w} \in \mathbb{C}^{t\times 1}$ be the unit norm beamforming vector (BV) at the transmitter. Then, the received signal is given by

$$y = \mathbf{h}^H \mathbf{w}\, s_m + \eta\,, \tag{4.1}$$

where $\eta \sim \mathcal{NC}\big(0, 1\big)$. For simplicity the time indices are ignored in the above equation. The transmitted two dimensional modulation symbol is denoted by $s_m$ with $E[|s_m|^2] = \rho$. Note that $\rho$ represents the SNR. The channel is estimated at the receiver and is partially available at the transmitter through a finite-rate feedback link of $B$ bits per CSI update. More specifically, a quantization codebook $\mathcal{W} = \big\{\widehat{\mathbf{v}}_1, \cdots, \widehat{\mathbf{v}}_C\big\}$, composed of $C = 2^B$ unit-norm transmit BV's is assumed to be known to both the receiver and the transmitter. Based on the channel estimate, the receiver selects the best code point $\widehat{\mathbf{v}}$ from the codebook and sends the corresponding index back to the transmitter through an error free link [22], [25], [26], [93], [94], and [101].

[1] We normalize the channel covariance matrix such that the mean of the eigenvalues equals to one, i.e., $Trace(\mathbf{\Sigma}_{\rm h}) = t$.

## 4.3 Optimum Transmit Beamforming Vector and Codebook Design

In this section, under the assumption of perfect and imperfect estimates of the channel at the receiver, we design the optimum codebook matched to the distortion function, the average SEP loss.

### 4.3.1 Perfect Channel Estimation

Assuming perfect knowledge of the channel vector $\mathbf{h}$, the optimum transmit BV, a well-known result, is given by the channel direction vector

$$\mathbf{v} = \frac{\mathbf{h}}{\|\mathbf{h}\|}.$$

In a low rate feedback link based system, the receiver selects the code point $\widehat{\mathbf{v}}$ that is closest to $\mathbf{v}$. Assuming no errors in the feedback link, the unit-norm vector $\widehat{\mathbf{v}}$ is employed as the BV at the transmitter. The received signal can now be written as

$$\begin{aligned} y &= \langle \mathbf{h}, \widehat{\mathbf{v}} \rangle s_m + \eta \\ &= \sqrt{\alpha} \langle \mathbf{v}, \widehat{\mathbf{v}} \rangle s_m + \eta \end{aligned} \tag{4.2}$$

where

$$\alpha = \|\mathbf{h}\|^2$$

and

$$\langle \mathbf{x}, \mathbf{y} \rangle = \mathbf{x}^H \mathbf{y}.$$

#### 4.3.1.1 Distortion Function - Average SEP of Rectangular QAM

In this subsection, we derive the *non-mean-squared distortion* function, the average SEP loss for a rectangular $M_1 \times M_2$-QAM constellation of size $M = M_1 M_2$. The transmitting symbol $s_m = s_x + j s_y$, $m = 0, 1, \ldots, M-1$, $x = 0, 1, \ldots, M_1 - 1$, $y = 0, 1, \ldots, M_2 - 1$. Here $s_x = a_x d$, and $s_y = a_y d$, where $a_x = -(M_1 - 1) + 2x$ (i.e., $a_x d$ is the in-phase $M_1$-PAM constellation symbol)

and $a_y = -(M_2 - 1) + 2y$ (i.e., $a_y d$ is the quadrature-phase $M_2$-PAM constellation symbol). Average symbol error probability without channel quantization for the in-phase $M_1$-PAM is given by [12]

$$P_{PM_1} = 2\left(1 - \frac{1}{M_1}\right) E\left[Q\left(\sqrt{\lambda\,\alpha}\right)\right] \tag{4.3}$$

where

$$Q(x) = \frac{1}{\sqrt{2\pi}} \int_x^\infty \exp(-u^2/2)\, du\,,$$

$$\lambda = \rho\,\phi\,,$$

and

$$\phi = \frac{6}{M_1^2 + M_2^2 - 2}\,.$$

The ASEP for Quadrature $M_2$-PAM is given by (4.3), with $M_1$ replaced by $M_2$.

$$P_{PM_2} = 2\left(1 - \frac{1}{M_2}\right) E\left[Q\left(\sqrt{\lambda\,\alpha}\right)\right]$$

The ASEP of $M_1 \times M_2$-QAM with perfect feedback is given by

$$P_{P-QAM} = P_{PM_1} + P_{PM_2} - P_{PM_1}\, P_{PM_2}.$$

The ASEP with finite-rate channel quantization for $M_1$-PAM is given by,

$$P_{QM_1} = 2\left(1 - \frac{1}{M_1}\right) E\left[Q\left(\sqrt{\lambda\,\alpha\,|\langle \mathbf{v}, \widehat{\mathbf{v}}\rangle|^2}\right)\right]. \tag{4.4}$$

The ASEP for $M_2$-PAM with channel quantization is given by (4.4), with $M_1$ replaced by $M_2$.

$$P_{QM_2} = 2\left(1 - \frac{1}{M_2}\right) E\left[Q\left(\sqrt{\lambda\,\alpha\,|\langle \mathbf{v}, \widehat{\mathbf{v}}\rangle|^2}\right)\right].$$

The ASEP of $M_1 \times M_2$-QAM with finite-rate quantization is given by

$$P_{Q-QAM} = P_{QM_1} + P_{QM_2} - P_{QM_1}\, P_{QM_2}.$$

The finite-rate quantization results in an increase in the average symbol error probability, which is given by

$$P_{Loss} = P_{Q-QAM} - P_{P-QAM}.$$

The instantaneous SEP loss due to finite-rate CSI quantization is taken to be the system distortion function $D_{\mathrm{Q}}(\mathbf{v},\, \widehat{\mathbf{v}}\,;\, \alpha)$. Removing the expectation in $P_{Loss}$ gives the instantaneous loss in average SEP and it can be expanded as

$$\begin{aligned} D_{\mathrm{Q}}(\mathbf{v},\, \widehat{\mathbf{v}}\,;\, \alpha) \;\; = \;\; & \left[Q\left(\sqrt{\lambda\alpha|\langle \mathbf{v}, \widehat{\mathbf{v}}\rangle|^2}\right) - Q\left(\sqrt{\lambda\alpha}\right)\right] 2\left(2 - \frac{1}{M_1} - \frac{1}{M_2}\right) - \\ & \left[\left\{Q\left(\sqrt{\lambda\alpha|\langle \mathbf{v}, \widehat{\mathbf{v}}\rangle|^2}\right)\right\}^2 - \left\{Q\left(\sqrt{\lambda\alpha}\right)\right\}^2\right] \times \\ & 4\left(1 - \frac{1}{M_1} - \frac{1}{M_2} + \frac{1}{M_1 M_2}\right). \end{aligned}$$

After some simplification $D_{\mathrm{Q}}(\mathbf{v},\, \widehat{\mathbf{v}}\,;\, \alpha)$ can now be written as

$$\begin{aligned} D_{\mathrm{Q}}(\mathbf{v}, \widehat{\mathbf{v}}\,;\, \alpha) \;\; \triangleq \;\; & \left[Q\left(\sqrt{\lambda\alpha|\langle \mathbf{v}, \widehat{\mathbf{v}}\rangle|^2}\right) - Q\left(\sqrt{\lambda\alpha}\right)\right] \times \\ & \left[A + C\left(Q\left(\sqrt{\lambda\alpha}\right) + Q\left(\sqrt{\lambda\alpha|\langle \mathbf{v}, \widehat{\mathbf{v}}\rangle|^2}\right)\right)\right] \end{aligned} \tag{4.5}$$

where

$$A = 2\left(2 - \frac{1}{M_1} - \frac{1}{M_2}\right), \tag{4.6}$$

and

$$C = -4\left(1 - \frac{1}{M_1} - \frac{1}{M_2} + \frac{1}{M_1 M_2}\right). \tag{4.7}$$

Under high resolution assumption, the quantized beamforming vector $\widehat{\mathbf{v}}$ is close to $\mathbf{v}$, and the inner product $|\langle \mathbf{v}, \widehat{\mathbf{v}}\rangle|$ is close to one. In this case, the distortion function $D_{\mathrm{Q}}\big(\mathbf{v}, \widehat{\mathbf{v}}\,;\, \alpha\big)$ can be approximated using a first order Taylor series expansion w.r.t. the random variable $|\langle \mathbf{v}, \widehat{\mathbf{v}}\rangle|^2$. After some manipulations, the distortion function can be written as

$$\begin{aligned} D_{\mathrm{Q}}(\mathbf{v},\, \widehat{\mathbf{v}}\,;\, \alpha) \;\; \approx \;\; & \exp\left(-\frac{\lambda\,\alpha}{2}\right) \cdot \sqrt{\frac{\lambda\,\alpha}{8\pi}} \times \\ & \left[A + 2C\,Q\left(\sqrt{\lambda\alpha}\right)\right]\left(1 - |\langle \mathbf{v}, \widehat{\mathbf{v}}\rangle|^2\right). \end{aligned} \tag{4.8}$$

In this thesis, we only consider the case with same distance $d$ in both in-phase and quadrature-phase. The analysis can be easily extended to the case where the distances are not the same.

#### 4.3.1.2 Optimum Codebook Design for Rectangular QAM with Perfect Channel Estimate

The codebook is designed to minimize the average SEP loss. The cost function for SEP loss given in (4.8) is different compared to the ergodic capacity loss function employed in [26]. However, the general vector quantization (VQ) framework can still be used with appropriate modification. The criteria in this case is given by

$$\max_{\mathcal{Q}(.)} E|\langle\tilde{\alpha}\mathbf{v},\, \mathcal{Q}(\mathbf{h})\rangle|^2,$$
$$\mathcal{Q}(\mathbf{h}) = \hat{\mathbf{v}} \tag{4.9}$$

where

$$\tilde{\alpha}^2 = \exp\left(-\frac{\lambda\,\alpha}{2}\right)\sqrt{\frac{\lambda\,\alpha}{8\pi}}\left[A + 2C\,Q\left(\sqrt{\lambda\alpha}\right)\right].$$

With this new design criterion, the codebook is designed by iterating the two conditions of Lloyd algorithm, the nearest neighbor-hood condition and centroid condition, until convergence. More details on the algorithm design can be found in [26]. It should be noted that similar to the case of capacity loss, because of the form of the SEP loss function, the codebook designed for spatially i.i.d. channel for the SEP distortion is also optimum for the capacity loss function. A drawback with the new codebook is that the codebook has to be designed for each operating SNR, constellation and correlation matrix.

Fig. 4.1 shows the ASEP resulting from using codebooks optimized for ergodic capacity loss and average SEP loss when evaluated using the ASEP metric. Note that optimum codebook implies that there is a separate codebook for each SNR point. The gains with the optimum codebook designed for SEP loss are evident in Fig. 4.1. As seen in Fig. 4.1 there is a gain of 1.2dB at an SNR of 15dB, with number of transmit antennas $t = 3$ and the feedback bits $B = 4$, between using the codebook optimized for ASEP loss and the codebook optimized for average capacity loss. The gain is increasing with SNR indicating that at medium-high SNR it is important to use the optimum codebook designed specifically for minimizing

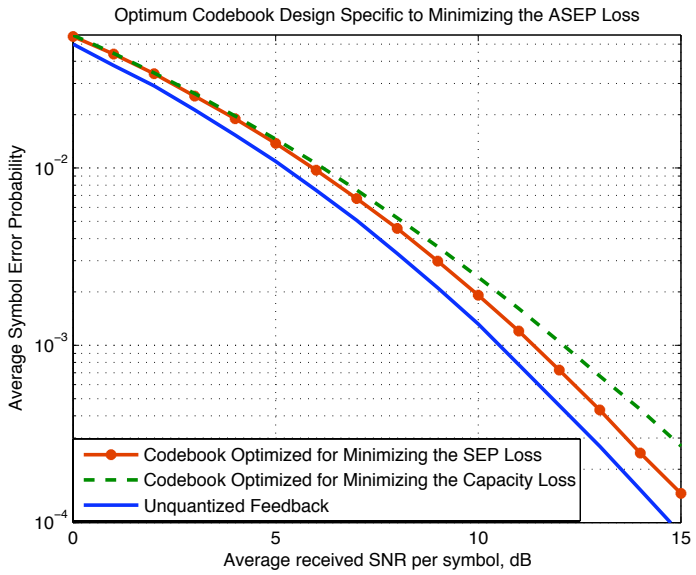


Figure 4.1 Comparison between the codebook optimized to minimize the average capacity loss and ASEP loss with BPSK constellation, number of transmit antennas $t = 3$, and the number of feedback bits $B = 4$.

ASEP loss. The spatial correlation matrix in Fig. 4.1 is assumed to have a Toeplitz structure with the first row being $[1,\ 0.9,\ 0.81]$. In Section 4.4 we quantify the loss due to quantization under i.i.d. and correlated scenarios assuming perfect channel estimation at the receiver and the optimum codebook designed in this section.

### 4.3.2 Erroneous Channel Estimation

With channel estimation errors, the optimum transmit beamforming vector is no longer given by the channel direction vector. We consider design of a codebook that takes into account the statistics of the channel estimate. The effect of estimation errors are abstracted using the modeling approach as in [100]. This modeling results in the channel estimate, $\widetilde{\mathbf{h}}$ and the actual channel, $\mathbf{h}$, being related in the following manner:

$$\mathbf{h} = \widetilde{\mathbf{h}} + \mathbf{n} \tag{4.10}$$

where

$$\widetilde{\mathbf{h}} \sim \mathcal{NC}\left(\mathbf{0}, \mathbf{\Sigma}_{\mathrm{im}}\right),$$

$$\mathbf{\Sigma}_{\mathrm{im}} = \mathbf{\Sigma}_{\mathrm{ce}}\mathbf{\Sigma}_{\mathrm{ee}}^{-1}\mathbf{\Sigma}_{\mathrm{ec}}$$

and the uncorrelated error term

$$\mathbf{n} \sim \mathcal{NC}\left(\mathbf{0}, \mathbf{\Sigma}_{\mathrm{n}}\right),$$

$$\mathbf{\Sigma}_{\mathrm{n}} = \mathbf{\Sigma}_{\mathrm{h}} - \mathbf{\Sigma}_{\mathrm{ce}}\mathbf{\Sigma}_{\mathrm{ee}}^{-1}\mathbf{\Sigma}_{\mathrm{ec}}.$$

$\mathbf{\Sigma}_{\mathrm{h}}$ and $\mathbf{\Sigma}_{\mathrm{ee}}$ are the autocorrelation matrices of $\mathbf{h}$ and $\widetilde{\mathbf{h}}$ respectively, $\mathbf{\Sigma}_{\mathrm{ce}}$ and $\mathbf{\Sigma}_{\mathrm{ec}}$ are the cross-correlation matrices. The correlation between the two processes indicates the quality of the channel estimate. This modeling can be justified for pilot based channel estimation schemes.

With estimation errors, the received signal with an arbitrary unit norm beamforming vector $\mathbf{w}$ is given by

$$\begin{aligned} y &= \left(\widetilde{\mathbf{h}} + \mathbf{n}\right)^H \mathbf{w}\, s_m + \eta \\ &= \widetilde{\mathbf{h}}^H \mathbf{w}\, s_m + \zeta \end{aligned} \tag{4.11}$$

where conditioned on $\mathbf{w}$ and assuming that $s_m$ belongs to PSK constellation,

$$\zeta \sim \mathcal{NC}\left(0, 1 + \rho\, \mathbf{w}^H \mathbf{\Sigma}_{\mathrm{n}} \mathbf{w}\right).$$

The appearance of signal term in the noise is due to the fact that only the channel estimate $\widetilde{\mathbf{h}}$ is available at the receiver instead of actual channel $\mathbf{h}$. Selection of $\mathbf{w}_{opt}$, the optimum BV, is based on maximizing the following received SNR

$$\begin{aligned} \mathbf{w}_{opt} &= \arg\max_{\|\mathbf{w}\|=1} \left( \frac{\rho\, \mathbf{w}^H \widetilde{\mathbf{h}} \widetilde{\mathbf{h}}^H \mathbf{w}}{1 + \rho\, \mathbf{w}^H \mathbf{\Sigma}_{\mathrm{n}} \mathbf{w}} \right) \\ &= \arg\max_{\|\mathbf{w}\|=1} \left( \frac{\mathbf{w}^H \widetilde{\mathbf{h}} \widetilde{\mathbf{h}}^H \mathbf{w}}{\mathbf{w}^H \mathbf{\Sigma}_{\mathrm{d}} \mathbf{w}} \right) \end{aligned}$$

where

$$\mathbf{\Sigma}_{\mathrm{d}} = \rho \mathbf{\Sigma}_{\mathrm{n}} + \mathbf{I}.$$

The solution to the above maximization problem is given by

$$\mathbf{w}_{opt} = \frac{\boldsymbol{\Sigma}_{\mathrm{d}}^{-1}\widetilde{\mathbf{h}}}{\|\boldsymbol{\Sigma}_{\mathrm{d}}^{-1}\widetilde{\mathbf{h}}\|}\,. \tag{4.12}$$

With this selection of the beamforming vector, the received SNR $\rho_e$ is given by

$$\begin{aligned} \rho_e &= \rho\,\omega\,, \\ \omega &= \widetilde{\mathbf{h}}^H \boldsymbol{\Sigma}_{\mathrm{d}}^{-1}\widetilde{\mathbf{h}}\,. \end{aligned} \tag{4.13}$$

#### 4.3.2.1 Distortion Function - Average SEP of BPSK Constellation

In this section, to illustrate how the codebook design changes because of estimation errors, we focus on BPSK constellation. The extension of codebook design for rectangular QAM constellation is relatively straightforward. The average symbol error probability with un-quantized version of optimum beamforming vector given in (4.12) is

$$P_{_P} = E\left[Q\left(\sqrt{2\rho\,\omega}\right)\right], \tag{4.14}$$

The ASEP with quantized feedback (i.e., $\mathbf{w} = \widehat{\mathbf{v}}$ ) is given by,

$$P_{_Q} = E\left[Q\left(\sqrt{2\rho\,\tau}\right)\right] \tag{4.15}$$

where

$$\tau = \frac{\widehat{\mathbf{v}}^H\,\widetilde{\mathbf{h}}\,\widetilde{\mathbf{h}}^H\,\widehat{\mathbf{v}}}{\widehat{\mathbf{v}}^H\,\boldsymbol{\Sigma}_{\mathrm{d}}\,\widehat{\mathbf{v}}}\,.$$

Under high resolution assumption, the instantaneous loss in SEP due to quantization can be approximated by taking the first order Taylor series expansion of $P_{_P} - P_{_Q}$( (4.14)-(4.15)) w.r.t. the variable $\tau$ around $\omega$ as

$$\begin{aligned} D_{\text{Q-BPSK}}(\mathbf{v},\,\widehat{\mathbf{v}};\,\omega) &= \left[Q\left(\sqrt{2\rho\,\tau}\right) - Q\left(\sqrt{2\rho\,\omega}\right)\right] \\ &\approx \exp\left(-\rho\,\omega\right)\sqrt{\frac{\rho\,\omega}{4\pi}}\;(\omega-\tau)\,. \end{aligned}$$

#### 4.3.2.2 Optimum Codebook Design for BPSK with Estimation Errors

The design criteria is to minimize the average symbol error probability loss

$$\min_{\mathcal{Q}(.)} E\left(\frac{\widehat{\mathbf{v}}^H \mathbf{\Sigma}_{\mathrm{v}} \widehat{\mathbf{v}}}{\widehat{\mathbf{v}}^H \mathbf{\Sigma}_{\mathrm{d}} \widehat{\mathbf{v}}}\right)$$

where

$$\mathbf{\Sigma}_{\mathrm{v}} = \exp\left(-\rho\,\omega\right)\,\sqrt{\omega}\left\{\omega\,\mathbf{\Sigma}_{\mathrm{d}} - \widetilde{\mathbf{h}}\,\widetilde{\mathbf{h}}^H\right\}.$$

We now briefly discuss the two conditions of Lloyd algorithm.

*Nearest Neighborhood Condition*: Beginning with an arbitrary set of unit vectors $\widehat{\mathbf{v}}_i,\ i = 1, \cdots, C$ forming the codebook $\mathcal{W}$, the optimum Voronoi Regions $\mathcal{R}_i,\ i = 1, \cdots, C$ are found from the following condition

$$\mathcal{R}_i = \left\{\mathbf{v} \in \mathbb{C}^t : \frac{\widehat{\mathbf{v}}_i^H \mathbf{\Sigma}_{\mathrm{v}} \widehat{\mathbf{v}}_i}{\widehat{\mathbf{v}}_i^H \mathbf{\Sigma}_{\mathrm{d}} \widehat{\mathbf{v}}_i} \leq \frac{\widehat{\mathbf{v}}_j^H \mathbf{\Sigma}_{\mathrm{v}} \widehat{\mathbf{v}}_j}{\widehat{\mathbf{v}}_j^H \mathbf{\Sigma}_{\mathrm{d}} \widehat{\mathbf{v}}_j}, \forall j \neq i\right\}.$$

*Centroid Condition*: The codebook $\mathcal{W}$ is updated in this step. For a given partition $\mathcal{R}_i$ obtained from the previous step, the new set of beamforming vectors satisfy

$$\begin{aligned}
\widehat{\mathbf{v}}_i &= \arg \min_{\|\widehat{\mathbf{v}}\|=1, \widehat{\mathbf{v}} \in \mathcal{R}_i} E\left\{\frac{\widehat{\mathbf{v}}^H \mathbf{\Sigma}_{\mathrm{v}} \widehat{\mathbf{v}}}{\widehat{\mathbf{v}}^H \mathbf{\Sigma}_{\mathrm{d}} \widehat{\mathbf{v}}}\right\} \\
&= \arg \min_{\|\widehat{\mathbf{v}}\|=1, \widehat{\mathbf{v}} \in \mathcal{R}_i} \left\{\frac{\widehat{\mathbf{v}}^H \mathbf{\Sigma}_{\mathrm{m}} \widehat{\mathbf{v}}}{\widehat{\mathbf{v}}^H \mathbf{\Sigma}_{\mathrm{d}} \widehat{\mathbf{v}}}\,\middle|\, \mathbf{v} \in \mathcal{R}_i\right\},\ i = 1, \cdots, C
\end{aligned}$$

where

$$\mathbf{\Sigma}_{\mathrm{m}} = E(\mathbf{\Sigma}_{\mathrm{v}}).$$

In the implementation of the algorithm $\mathbf{\Sigma}_{\mathrm{m}}$ has to be estimated from the training unit norm vectors belonging to $\mathcal{R}_i$. The generalized eigenvalue equation for $\mathbf{\Sigma}_{\mathrm{d}}$ and $\mathbf{\Sigma}_{\mathrm{m}}$ is

$$\mathbf{\Sigma}_{\mathrm{m}} \mathbf{F} = \Lambda \mathbf{\Sigma}_{\mathrm{d}} \mathbf{F}$$

where

$$\Lambda = \mathrm{diag}\left(\lambda_1, \cdots, \lambda_t\right),$$

and

$$\mathbf{F} = \left(\mathbf{f}_1, \cdots, \mathbf{f}_t\right).$$

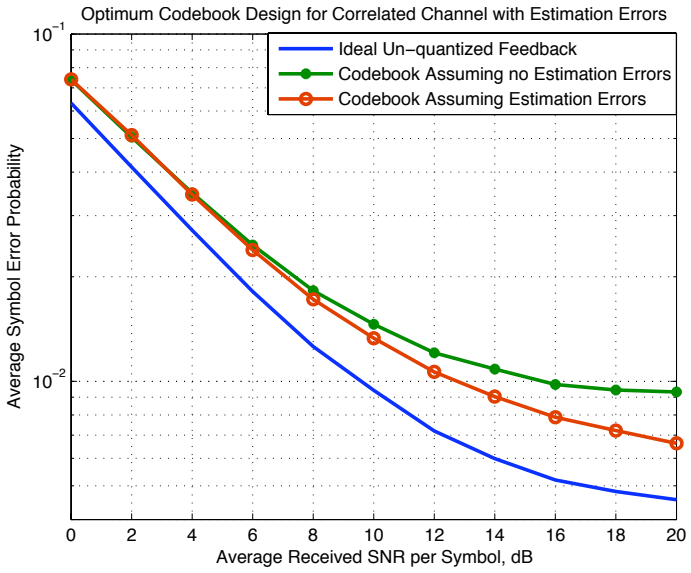


Figure 4.2 Effectiveness of codebook design that takes channel estimation errors into account as compared to codebook designed specific to ASEP loss but ignoring estimation errors - BPSK constellation, number of transmit antennas $t = 3$, and the number of feedback bits $B = 4$.

Assuming that $\lambda_1 > \lambda_2 \cdots > \lambda_t$, the solution to minimization function is given by $\mathbf{f}_t$ suitably normalized as

$$\widehat{\mathbf{v}}_i = \frac{\mathbf{f}_t}{\|\mathbf{f}_t\|}.$$

The above two conditions are iterated until convergence. Note that compared to the perfect channel estimation scenario, the encoding process is also different. Fig. 4.2 shows the effectiveness of designing the codebook (for each SNR point) taking estimation errors into account. For the results shown in Fig. 4.2, $\mathbf{\Sigma}_{\mathrm{h}}$ is simulated following the correlation model in [104]: A linear antenna array with antenna spacing of half wavelength, angle of arrival $\phi = 0^\circ$ and an uniform angular spread of $[-\pi/5, \pi/5]$. $\mathbf{\Sigma}_{\mathrm{im}}$ is simulated in a similar fashion with an uniform angular spread of $[-\pi/5.5, \pi/5.5]$ and the resulting correlation matrix is scaled by 0.7582. Note that the various auto and cross correlation matrices are included in $\mathbf{\Sigma}_{\mathrm{im}}$, so they are not specified separately. The noise correlation matrix is given by

$\mathbf{\Sigma}_{\mathrm{n}} = \mathbf{\Sigma}_{\mathrm{h}} - \mathbf{\Sigma}_{\mathrm{im}}$.

## 4.4 Average SEP Loss Analysis

To obtain insights into the performance of quantized feedback schemes developed, we make use of the analytical results based on high resolution theory developed in [93]. Though the optimum codebook under both perfect and imperfect channel estimates were developed above, due to analytical tractability reasons, the ASEP loss analysis is carried out only under the assumption that perfect channel estimate is available at the receiver. In the last subsection, we consider the high-SNR regime for an insight into the effect of quantization on a correlated channel. We only present the end results and the details are relegated to the Appendices. For the purpose of completeness, in Section 4.7.1 of the Appendix we briefly summarize the asymptotic distortion analysis of the generalized vector quantizer results that are relevant for the analysis of average SEP loss of $M_1 \times M_2$-QAM constellation. The distortion analysis results presented are really lower bounds that become more accurate as the number of feedback bits increase.

### 4.4.1 Distortion Analysis for Spatially i.i.d. Channels

The final expression for the loss in ASEP of a spatially i.i.d. MISO system with rectangular QAM is given by

$$\begin{aligned} D_{\text{Q-iid}} \;=\; & \left( \frac{\sqrt{\lambda}(t-1)A\, 2^{t-1}\Gamma\left(t+\frac{1}{2}\right)}{\sqrt{\pi}\, t!\, (\lambda+2)^{\left(t+\frac{1}{2}\right)}} \right) \cdot 2^{-\frac{B}{t-1}} + \\ & \left[ \frac{\lambda(t-1)\, C\, \Gamma\left(t+\frac{1}{2}\right)}{4\pi\, (1+\lambda)^{t+1}\, \Gamma\left(t+\frac{3}{2}\right)} \right] \cdot \\ & {}_2F_1\left(1, t+1; t+\frac{3}{2}; \frac{1}{1+\kappa}\right) \cdot 2^{-\frac{B}{t-1}}, \end{aligned} \tag{4.16}$$

$A$ and $C$ are defined in (4.6) and (4.7), ${}_2F_1(\cdot,\cdot;\cdot;\cdot)$ is the hypergeometric function [103], and

$$\kappa = \frac{\lambda}{\lambda+2}\,.$$

Important steps in the derivation of above equation are given in Section 4.7.2 of the Appendix.

### 4.4.2 Distortion Analysis for Spatially Correlated Channels

Assuming that the optimum codebook is used, the ASEP loss of a spatially correlated MISO system is given by

$$\begin{aligned} D_{\text{Q-cor}} &= \left[\beta_1\big(t,\lambda,\mathbf{\Sigma}_{\text{h}}\big)\, T_{\mathcal{D}} + \beta_2\big(t,\lambda,\mathbf{\Sigma}_{\text{h}}\big)\sqrt{\frac{\lambda}{2}}\, T_{\mathcal{E}}\right]\cdot \\ &\quad \gamma_t^{-1}\cdot\left|\mathbf{\Sigma}_{\text{h}}\right|^{-1}\cdot 2^{-\frac{B}{t-1}} \end{aligned} \tag{4.17}$$

where

$$\beta_1\big(t,\lambda,\mathbf{\Sigma}_{\text{h}}\big) = \left(\int_{\mathbf{v}:\,\mathbf{g}(\mathbf{v})=0} \Big(\frac{\lambda}{2} + \mathbf{v}^{\mathsf{H}}\mathbf{\Sigma}_{\text{h}}^{-1}\,\mathbf{v}\Big)^{\frac{(1-t)(t+\frac{1}{2})}{t}} d\,\mathbf{v}\right)^{\frac{t}{t-1}},$$

and

$$\begin{aligned} \beta_2\big(t,\lambda,\mathbf{\Sigma}_{\text{h}}\big) = \Bigg(\int_{\mathbf{v}:\,\mathbf{g}(\mathbf{v})=0} &\Big(\lambda + \mathbf{v}^{\mathsf{H}}\mathbf{\Sigma}_{\text{h}}^{-1}\,\mathbf{v}\Big)^{\frac{(1-t)(t+1)}{t}}\cdot \\ &{}_2F_1\Big(1,t+1;t+\frac{3}{2};\frac{1}{1+\nu}\Big)^{\frac{t-1}{t}} d\,\mathbf{v}\Bigg)^{\frac{t}{t-1}}. \end{aligned}$$

$T_{\mathcal{D}}$, $T_{\mathcal{E}}$, and $\nu$ are defined in (4.48), (4.49), and (4.50) respectively. The derivation details of the above equation can be found in Section 4.7.3 of the Appendix.

### 4.4.3 Mismatched Distortion Analysis for Correlated Channels

As pointed out in Section 4.3.1.2, if the codebook designed for capacity is used for average symbol error probability analysis there will be a loss due to the mismatch in codebook design. From the results in [98], the loss due to mismatch can be calculated as

$$D_{\text{Low-mm}} = 2^{-\frac{B}{t-1}}\int_{\mathbb{Q}} I_{\text{c,opt}}^{\text{w,mm}}(\mathbf{v})\,[\lambda_{cap}(\mathbf{v})]^{\frac{1}{t-1}}\; p\big(\mathbf{v}\big)\, d\,\mathbf{v}, \tag{4.18}$$

$I_{\text{c,opt}}^{\text{w,mm}}$ is the constrained, weighted, and mismatched inertial profile. Due to the nature of mismatch[2], using the results in [98, 99], it is easy to show that $I_{\text{c,opt}}^{\text{w,mm}}$ is

[2]The mismatched distortion function is a scaled version of the true optimal distortion function, hence the optimal Voronoi shapes remains same.

same as $I^{\mathrm{w}}_{\mathrm{c,\,opt}}(\mathbf{v})$ given by (4.47). $\lambda_{cap}$, the point density function of the capacity loss metric (clearly sub-optimal for ASEP metric), is given by (eq.(30) in [99]) and $p(\mathbf{v})$ is given by (4.45). Even if the codebook is designed specific to minimizing the average SEP loss, a mismatch (e.g. by using codebook designed for a different SNR) is still possible. By selecting different system parameters (SNR, correlation matrix, constellation type) for point density function and the constrained and weighted inertial profile, (4.18) can also be used to analytically characterize the loss due to the usage of a wrong codebook.

### 4.4.4 Distortion Analysis in High-SNR Regime

The analytical expressions for SEP loss of $M_1 \times M_2$-ary QAM constellation for transmit beamforming of a MISO system are given by (4.16) and by (4.17) for spatially i.i.d. and correlated cases. The equations are lengthy and complex providing limited insight into the system behavior. In high-SNR regime it is easy to see that $\kappa \approx 1$. For spatially i.i.d. MISO fading channels, the average distortion, $D_{\text{Q-H-SNR-iid}}$, under high-SNR assumption can be simplified as

$$\begin{aligned} D_{\text{Q-H-SNR-iid}} \;=\; & \left( \frac{2^{t-1}\,(t-1)\,A\,\Gamma\left(t+\frac{1}{2}\right)}{\sqrt{\pi}\,t!\,\phi^t} \right) \cdot 2^{-\frac{B}{t-1}} \rho^{-t} + \\ & \left[ \frac{(t-1)\,C\,\Gamma\left(t+\frac{1}{2}\right)}{4\pi\,\Gamma\left(t+\frac{3}{2}\right)\,\phi^t} \right] \cdot \\ & {}_2F_1\left(1, t+1; t+\frac{3}{2}; \frac{1}{2}\right) 2^{-\frac{B}{t-1}}\,\rho^{-t}\,. \end{aligned} \tag{4.19}$$

From the above equation it is clear that the diversity order is '$t$' and increasing the number of feedback bits has an exponential impact on the system distortion function, notice that this fact is true even without the high-SNR assumption. The rest of the terms in (4.19) depend on the number of transmitting antennas and the size of the rectangular QAM constellation. For spatially correlated channel, the functions $\beta_1\big(t, \lambda, \mathbf{\Sigma}_{\mathrm{h}}\big)$ and $\beta_2\big(t, \lambda, \mathbf{\Sigma}_{\mathrm{h}}\big)$ are difficult to evaluate. However, we can evaluate them in closed-form under high SNR assumption as follows:

$$\beta_{1-H-SNR}\big(t, \lambda, \mathbf{\Sigma}_{\mathrm{h}}\big) = \lambda^{-\left(t+\frac{1}{2}\right)}\, 2^{\left(t+\frac{1}{2}\right)}\, \gamma_t^{\frac{t}{t-1}},$$

and

$$\beta_{2-H-SNR}\big(t,\lambda,\mathbf{\Sigma}_{\rm h}\big) = 2\,\lambda^{-(t+1)}\,\gamma_t^{\frac{t}{t-1}}$$

where $\beta_{1-H-SNR}$ and $\beta_{2-H-SNR}$ are high-SNR versions of $\beta_1$ and $\beta_2$. After some manipulations we arrive at an interesting simple relation between the ASEP loss associated with spatially correlated and i.i.d. channel scenarios as

$$D_{\text{Q-H-SNR-iid}} = |\mathbf{\Sigma}_{\rm h}|\, D_{\text{Q-H-SNR-cor}}. \tag{4.20}$$

In the correlated case the loss is a simple scaling of the loss associated with i.i.d. case, the scaling factor being the determinant of the correlation matrix. Note that this analysis is quite general in the sense that we can have an arbitrary correlation structure across the antennas. The quantization parameter $B$, and number of antennas, $t$, both appear in the exponent for the correlated scenario under general and high-SNR regimes. In the correlated scenario, the additional loss in ASEP due to quantization is independent of the constellation size. The diversity order is also not effected as a result of quantization. For both i.i.d. and correlated channels, in high-SNR regime, the ASEP without quantization can be written in terms of ASEP with quantization and ASEP loss due to quantization as follows:

$$\begin{aligned} P_{_{P-QAM}} &\approx c_1\,\rho^{-t}\left(1+c_2\,2^{-\frac{B}{t-1}}\right) \\ &= c_1\,(\rho-\Delta\rho)^{-t} \end{aligned}$$

where

$$\Delta\rho = \left[1-\left(1+c_2\,2^{-\frac{B}{t-1}}\right)^{-\frac{1}{t}}\right]\rho\,.$$

$\Delta\rho$ can be viewed as the SNR penalty caused by the finite-rate quantization of the CSI, $c_1$ and $c_2$ are constants. Note that exact values of $c_1$ and $c_2$ can be calculated but are not relevant for the present discussion. The insights from the above equation are as follows: The system performance in terms of SEP is more sensitive to the finite-rate channel quantization in the high-SNR regime and in order to maintain the same SNR penalty due to finite-rate feedback, the quantization resolution

$B$ has to increase as the system average SNR increases. Since $\Delta\rho/\rho \ll 1$, after some manipulation, we can obtain a relation for number of feedback bits $B$ as

$$\begin{aligned} \frac{B}{t-1} &= -\log_2\left[\left(1-\Delta\rho/\rho\right)^{-t}-1\right)/c_2\right] \\ &\approx -\log_2(\Delta\rho)+\log_2(\rho)-\log_2(t)+\log_2(c_2), \end{aligned}$$

which means for a fixed number of antennas $t$, in order to maintain a fixed SNR loss $\Delta\rho$,

$$B \approx (t-1)\log_2(\rho)+c\,.$$

### 4.4.5 Simulation Results

A sample simulation in Fig. 4.3 plots the average SEP loss due to the finite-rate quantization of the channel direction versus feedback rate $B$, for a $3\times 1$ MISO system over perfectly estimated spatially i.i.d. and correlated Rayleigh fading channels with different rectangular $M_1 \times M_2$-QAM constellations at system SNRs $\rho = 10$dB, and 24dB, respectively. Codebooks are designed by using optimal criterion, suitable for minimizing ASEP loss, as explained in Section 4.3.1.2. The spatially correlated channel is simulated by the correlation model in [104]: A linear antenna array with antenna spacing of half wavelength, angle of arrival $\phi = 0^\circ$ and uniform angular-spread in $[-30^\circ, 30^\circ]$.

Fig. 4.3 shows the analytical and simulation plots for both spatially i.i.d. and correlated channels. The analytical expression for i.i.d. is closed-form, and for correlated channel the expression is closed-form under high SNR assumption. The simulation and analytical results match well as the number of feedback bits increase. The distortion function we have is a first order approximation and this approximation becomes accurate as the number of feedback bits increase. Also note that the analytical expression for distortion is not optimum but a lower bound on the optimum, which becomes more tight as the number of feedback bits increases.

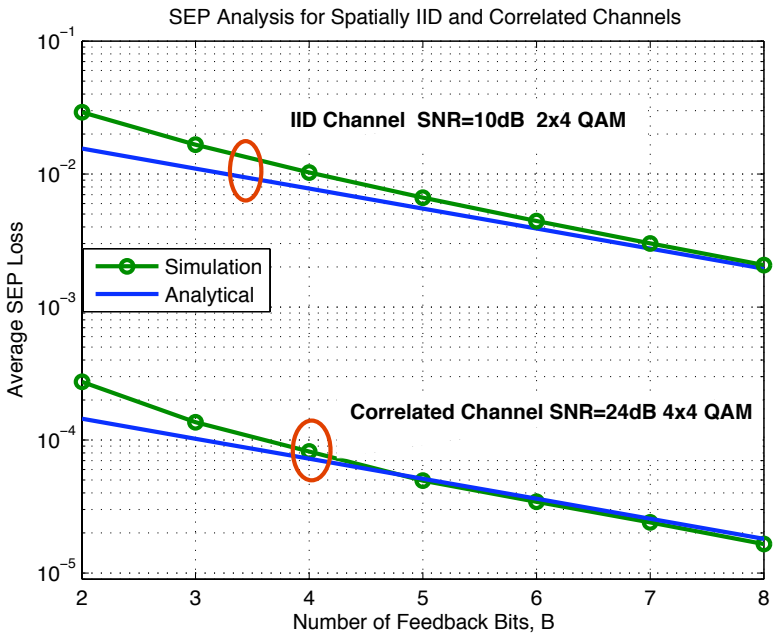


Figure 4.3 ASEP loss due to finite-rate quantization with $M_1 \times M_2$-QAM constellation for both spatially i.i.d. and spatially correlated channels, number of transmit antennas $t = 3$.

## 4.5 Results on Ergodic Capacity

In this section we present the contributions of the thesis in our study of ergodic capacity under imperfect feedback constraints. The system model and the optimum beamforming vector given in (4.12) are applicable for ergodic capacity also. However, the system distortion function and the codebook design algorithm have to be adapted for ergodic capacity. We begin with the distortion function relevant for ergodic capacity analysis.

### 4.5.1 Distortion Function

To minimize the effect of quantization errors, one is naturally led to a vector quantization framework and finding an optimum codebook of $C = 2^B$ beamforming vectors (please note the notation here, $C$ represents number of codepoints in the codebook). We now discuss the design of such a codebook. The beamform-

ing vector after quantization is given by

$$\mathbf{w} = \widehat{\mathbf{v}} = \mathcal{Q}\left(\mathbf{w}_{opt}\right), \tag{4.21}$$

where $\mathcal{Q}$ is the quantization function to be described in the next subsection. The lower bound on the ergodic capacity with optimum beamforming vector $\mathbf{w}_{opt}$ is given by

$$C_W = E\left[\log_2\left(1 + \frac{\rho \mathbf{w}_{opt}^H \widetilde{\mathbf{h}}\,\widetilde{\mathbf{h}}^H \mathbf{w}_{opt}}{1 + \rho\, \mathbf{w}_{opt}^H \mathbf{\Sigma}_{\mathrm{n}} \mathbf{w}_{opt}}\right)\right]. \tag{4.22}$$

With $\widehat{\mathbf{v}}$ (note that $\widehat{\mathbf{v}}$ is the quantized version of optimum beamforming vector) from (4.21) plugged into (4.22),

$$C_Q = E\left[\log_2\left(1 + \frac{\rho\, \|\widetilde{\mathbf{h}}\|^2 |\vartheta|^2}{1 + \rho\, \widehat{\mathbf{v}}^H \mathbf{\Sigma}_{\mathrm{n}} \widehat{\mathbf{v}}}\right)\right], \tag{4.23}$$

where

$$\vartheta = \widehat{\mathbf{v}}^H \mathbf{v}$$

and

$$\mathbf{v} = \frac{\widetilde{\mathbf{h}}}{\|\widetilde{\mathbf{h}}\|}.$$

The additional loss in ergodic capacity (there is already some loss because of estimation errors and delay) due to channel quantization, is given by

$$\begin{aligned} C_L &= C_W - C_Q \\ &= E\left[\log_2\left(\frac{\omega + \rho\, \omega\, \widehat{\mathcal{V}}}{1 + \rho \cdot \left(\widehat{\mathcal{V}} + \alpha \cdot |\vartheta|^2\right)}\right)\right], \end{aligned} \tag{4.24}$$

where

$$\alpha = \|\widetilde{\mathbf{h}}\|^2$$

and

$$\widehat{\mathcal{V}} = \widehat{\mathbf{v}}^H \mathbf{\Sigma}_{\mathrm{n}} \widehat{\mathbf{v}}.$$

Note that $C_L$ quantifies the loss due to quantization alone precisely, and unlike $C_W$ and $C_Q$, $C_L$ is not a bound.

### 4.5.2 Optimum Codebook Design

The criteria for designing the codebook is to minimize the loss in ergodic capacity $C_L$ (4.24). However, $C_L$ in the above form is not very convenient because it complicates the centroid finding step in the VQ design and some modification is necessary. After some manipulation, the loss term $C_L$ can be written as

$$C_L = -E\,\log_2\left[1-\left(1-\left(\frac{1+\rho\cdot\left(\widehat{\mathcal{V}}+\alpha\cdot|\vartheta|^2\right)}{\omega+\rho\,\omega\,\widehat{\mathcal{V}}}\right)\right)\right].$$

After taking the first order approximation using

$$-\log(1-x) \backsimeq x,$$

the approximated loss, $C_{LA}$, can be written as

$$\begin{aligned} C_{LA} &= \frac{1}{\ln 2}E\left(\frac{\omega-1+\rho\,\left(\widehat{\mathcal{V}}(\omega-1)-\alpha|\vartheta|^2\right)}{\omega+\rho\,\omega\,\widehat{\mathcal{V}}}\right) \\ &= \frac{1}{\ln 2}E\left(\frac{\widehat{\mathbf{v}}^H\mathbf{\Sigma}_{\mathrm{v}}\widehat{\mathbf{v}}}{\widehat{\mathbf{v}}^H\mathbf{\Sigma}_{\mathrm{d}}\widehat{\mathbf{v}}}\right), \end{aligned} \tag{4.25}$$

where

$$\mathbf{\Sigma}_{\mathrm{v}} = \left\{\frac{(\omega-1)\mathbf{I}+\rho(\omega-1)\mathbf{\Sigma}_{\mathrm{n}}-\rho\alpha\mathbf{v}\mathbf{v}^H}{\omega}\right\}, \tag{4.26}$$

$$\mathbf{\Sigma}_{\mathrm{d}} = \rho\mathbf{\Sigma}_{\mathrm{n}}+\mathbf{I}.$$

It will be shown that this form $C_{LA}$ results in a convenient VQ design. The above approximation is important as the codebook design will be developed using $C_{LA}$. The approximation is well justified in the high SNR and high resolution (higher $C$) regime.

**Codebook Design Criterion**: Design a quantizer $\mathcal{Q}$ ( $\mathcal{Q}:\mathbb{C}^t\rightarrow\mathcal{W}$) to minimize $C_{LA}$, which can be written as

$$\min_{\mathcal{Q}(.)} E\left(\frac{\widehat{\mathbf{v}}^H\mathbf{\Sigma}_{\mathrm{v}}\widehat{\mathbf{v}}}{\widehat{\mathbf{v}}^H\mathbf{\Sigma}_{\mathrm{d}}\widehat{\mathbf{v}}}\right)$$

where $\widehat{\mathbf{v}}=\mathcal{Q}(\mathbf{v})$, $\|\widehat{\mathbf{v}}\|=1$ and $\widehat{\mathbf{v}}\in\mathcal{W}$. The above vector quantization problem (a modified form of Lloyd algorithm) has a monotonic convergence property.

**Codebook Design Algorithm**: Lloyd algorithm has two conditions, the Nearest Neighborhood Condition and Centroid Condition. The details of these two conditions are discussed below. Generate a large sample set of vectors $\mathbf{v}$, which are the normalized vectors of the delayed channel estimates.

*Nearest Neighborhood Condition*: Beginning with an arbitrary set of unit vectors $\widehat{\mathbf{v}}_i,\ i = 1, \cdots, C$ forming the codebook $\mathcal{W}$, the optimum Voronoi Regions $\mathcal{R}_i,\ i = 1, \cdots, C$ are found from the following condition

$$\mathcal{R}_i = \left\{ \mathbf{v} \in \mathbb{C}^t : \frac{\widehat{\mathbf{v}}_i^H \mathbf{\Sigma}_{\mathrm{v}} \widehat{\mathbf{v}}_i}{\widehat{\mathbf{v}}_i^H \mathbf{\Sigma}_{\mathrm{d}} \widehat{\mathbf{v}}_i} \leq \frac{\widehat{\mathbf{v}}_j^H \mathbf{\Sigma}_{\mathrm{v}} \widehat{\mathbf{v}}_j}{\widehat{\mathbf{v}}_j^H \mathbf{\Sigma}_{\mathrm{d}} \widehat{\mathbf{v}}_j}, \forall j \neq i \right\}$$

$\mathcal{R}_i$ contains all the training unit norm vectors $\mathbf{v}$ satisfying the above condition. In the above condition, $\mathbf{\Sigma}_{\mathrm{v}}$ as defined in (4.26) contains $\mathbf{v}$ (as indicated earlier, $\mathbf{v} = \widetilde{\mathbf{h}}/\|\widetilde{\mathbf{h}}\|$).

*Centroid Condition*: The codebook $\mathcal{W}$ is updated in this step. For a given partition $\mathcal{R}_i$ obtained from the previous step, the new set of beamforming vectors satisfy

$$\begin{aligned} \widehat{\mathbf{v}}_i &= \arg \min_{\|\widehat{\mathbf{v}}\|=1, \widehat{\mathbf{v}} \in \mathcal{R}_i} E \left\{ \frac{\widehat{\mathbf{v}}^H \mathbf{\Sigma}_{\mathrm{v}} \widehat{\mathbf{v}}}{\widehat{\mathbf{v}}^H \mathbf{\Sigma}_{\mathrm{d}} \widehat{\mathbf{v}}} \right\},\ i = 1, \cdots, C \\ &= \arg \min_{\|\widehat{\mathbf{v}}\|=1, \widehat{\mathbf{v}} \in \mathcal{R}_i} \left\{ \frac{\widehat{\mathbf{v}}^H \mathbf{\Sigma}_{\mathrm{m}} \widehat{\mathbf{v}}}{\widehat{\mathbf{v}}^H \mathbf{\Sigma}_{\mathrm{d}} \widehat{\mathbf{v}}} \middle| \mathbf{v} \in \mathcal{R}_i \right\},\ i = 1, \cdots, C, \end{aligned}$$

where $\mathbf{\Sigma}_{\mathrm{m}} = E(\mathbf{\Sigma}_{\mathrm{v}})$. In the implementation of the algorithm $\mathbf{\Sigma}_{\mathrm{m}}$ has to be estimated from the training unit norm vectors belonging to $\mathcal{R}_i$. To solve the above minimization problem consider the generalized eigenvalue equation for $\mathbf{\Sigma}_{\mathrm{d}}$ and $\mathbf{\Sigma}_{\mathrm{m}}$

$$\mathbf{\Sigma}_{\mathrm{m}} \mathbf{F} = \Lambda \mathbf{\Sigma}_{\mathrm{d}} \mathbf{F},$$

where

$$\begin{aligned} \mathbf{F}^H \mathbf{\Sigma}_{\mathrm{d}} \mathbf{F} &= \mathbf{I}, \\ \mathbf{F}^H \mathbf{\Sigma}_{\mathrm{m}} \mathbf{F} &= \Lambda = \mathrm{diag}\left(\lambda_1, \cdots, \lambda_t\right), \\ \mathbf{F} &= \left(\mathbf{f}_1, \cdots, \mathbf{f}_t\right). \end{aligned}$$

Assuming that $\lambda_1 > \lambda_2 \cdots > \lambda_t$, the solution to minimization function is given by $\mathbf{f}_t$. In the above form, $\mathbf{f}_t$ may not be a unit vector, while running the algorithm, $\mathbf{f}_t$

can be normalized to make it a unit vector and it has no effect on the minimization. The $i^{th}$ new codeword is given by

$$\widehat{\mathbf{v}}_i = \frac{\mathbf{f}_t}{\|\mathbf{f}_t\|}.$$

The above two conditions are iterated until the convergence.

Compared to the optimum codebook design presented in [26], apart from some changes in additive and multiplicative factors, the primary change due to the presence of estimation error and delay is that, in the centroid condition, the new codebook design depends on the joint eigen decomposition of both signal and noise correlation matrices. In contrast, the centroid condition in [26] requires eigen decomposition of only the signal correlation matrix. Similar to [26] a new codebook has to be designed for each SNR point. However, the codebook design is an off-line process so it is not a computational burden on MS. Ideally speaking, even minor changes in the noise or signal correlation matrices require a completely new codebook.

### 4.5.3 Encoding: Beamforming Vector Selection

The optimum encoding process (selection of the code point index to be sent to the transmitter) is defined as follows

$$\widehat{\mathbf{v}} = \arg\max_{\widehat{\mathbf{v}}_i \in \mathcal{W}} \frac{|\langle \widehat{\mathbf{v}}_i, \mathbf{v} \rangle|^2}{\widehat{\mathbf{v}}_i^H \mathbf{\Sigma}_{\mathrm{d}} \widehat{\mathbf{v}}_i}$$

By this encoding process, the unit norm sphere $\mathcal{S}_t = \{\mathbf{v} \in \mathbb{C}^t\}$, is partitioned into $C$ regions $\mathcal{R}_i, i = 1, ..., C$, where

$$\mathcal{R}_i = \left\{ \mathbf{v} \in \mathcal{S}_t : \frac{\widehat{\mathbf{v}}_i^H \mathbf{\Sigma}_{\mathrm{v}} \widehat{\mathbf{v}}_i}{\widehat{\mathbf{v}}_i^H \mathbf{\Sigma}_{\mathrm{d}} \widehat{\mathbf{v}}_i} \leq \frac{\widehat{\mathbf{v}}_j^H \mathbf{\Sigma}_{\mathrm{v}} \widehat{\mathbf{v}}_j}{\widehat{\mathbf{v}}_j^H \mathbf{\Sigma}_{\mathrm{d}} \widehat{\mathbf{v}}_j}, \forall j \neq i \right\}$$

The above encoding process is optimum in the sense that it maximizes the received SNR. Compared to [26] the encoding process is also different. Since estimation errors and delay were not considered, in [26] only the numerator part is used in the encoding.

### 4.5.4 Spatially i.i.d. Channel - Loss Analysis

Analyzing the loss for correlated channels with estimation errors, delay (EED) and quantization is a complicated problem and analytic tractability remains elusive at this time. However, we have had success with the loss in ergodic capacity for the less general but still important spatially i.i.d. channel with EED and channel quantization. A closed-form analytical expression for the combined loss due to the three forms of feedback imperfection (estimation errors, delay and channel quantization) is derived in this section for the spatial i.i.d. channel.

***Notation***: In this subsection, $\gamma_s$ denotes the SNR and $\rho$ denotes the correlation coefficient.

Without EED and channel quantization (i.e., transmitter has $\mathbf{h}/\|\mathbf{h}\|$), the ergodic capacity is given by

$$C_{ideal} = E\left[\log_2\left(1 + \|\mathbf{h}\|^2\gamma_s\right)\right].$$

It can be shown that for the spatially i.i.d. channel, $\mathbf{\Sigma}_{\text{hh}} = \mathbf{I}$ and $\mathbf{\Sigma}_{\text{im}} = |\rho|^2\mathbf{I}$, $0 < |\rho| < 1$. More specifically $\rho$ can be shown as the product of estimation related correlation coefficient $\rho_e$, and delay related correlation co-efficient $\rho_d$ (Chapter 2). With these values the lower bound on ergodic capacity as given in (4.23) becomes

$$C_{quant} \;=\; E\left[\log_2\left(1 + \|\mathbf{h}\|^2\gamma_s^f\,\theta\right)\right], \tag{4.27}$$

where

$$\gamma_s^f = \frac{|\rho|^2\gamma_s}{1 + (1 - |\rho|^2)\gamma_s},$$

and

$$\theta = |\vartheta|^2.$$

The loss in ergodic capacity with un-quantized channel without EED and the quantized channel with EED is given by (4.28). Note that this loss formulation is different (but more general) from the one in spatially correlated with EED scenario. The loss function in correlated channel case is defined as the further loss

due to quantization. Where as for i.i.d., $C_{L-iid}$ implies the overall loss due to EED and quantization.

$$\begin{aligned} C_{ideal} - C_{quant} &= E\left[\log_2\left(1+\|\mathbf{h}\|^2\gamma_s\right)\right] - E\left[\log_2\left(1+\|\mathbf{h}\|^2\gamma_s^f\vartheta\right)\right] \\ C_{L-iid} &= -E\left[\log_2\left(\frac{1+\|\mathbf{h}\|^2\gamma_s^f\vartheta}{1+\|\mathbf{h}\|^2\gamma_s}\right)\right] \\ &= -E\left[\log_2\left(1-\frac{\|\mathbf{h}\|^2(\gamma_s-\gamma_s^f\vartheta)}{1+\|\mathbf{h}\|^2\gamma_s}\right)\right]. \end{aligned} \tag{4.28}$$

By using the Taylor series expansion

$$-\log(1-x) = \sum_{k=1}^{\infty}\frac{x^k}{k},$$

(4.28) can be written as

$$\begin{aligned} C_{L-iid} &= \frac{1}{\ln 2}\sum_{k=1}^{\infty}\frac{1}{k}E\left[\frac{\|\mathbf{h}\|^2(\gamma_s-\gamma_s^f\vartheta)}{1+\|\mathbf{h}\|^2\gamma_s}\right]^k \\ &= \frac{1}{\ln 2}\sum_{k=1}^{\infty}\frac{1}{k}E\left(\left[\frac{\|\mathbf{h}\|^2\gamma_s}{1+\|\mathbf{h}\|^2\gamma_s}\right]^k\right)E(\beta^k), \end{aligned} \tag{4.29}$$

where

$$\beta = 1-\xi\theta,$$
$$\xi = \frac{\gamma_s^f}{\gamma_s}.$$

It is easy to see that $\xi < 1$ and $\xi = 1$ *if and only if* there is no delay and no estimation error. In (4.29), the independence of the quantization related term and channel norm related term is due to the fact that the channel is spatially i.i.d. The codebook design for this scenario is a special case of the previously considered spatially correlated case. Note that optimum codebook design specific to the loss in ergodic capacity is studied in [26]. An approximate pdf for $\theta$, is given as

$$f_\theta(x) = 2^B(t-1)(1-x)^{t-2}, \quad 1-\psi < x < 1, \tag{4.30}$$

where $\psi = 2^{-B/(t-1)}$. The first expectation in (4.29) can be evaluated as [102]

$$E\left(\left[\frac{\|\mathbf{h}\|^2\gamma_s}{1+\|\mathbf{h}\|^2\gamma_s}\right]^k\right) = \frac{\Gamma(k+t)}{\Gamma(t)}\gamma_s^k\,{}_2F_0\left(t+k,k;;-\gamma_s\right), \tag{4.31}$$

where ${}_2F_0(,,;;)$ is the generalized hypergeometric function. Using change of variables the pdf of $\beta$ can be shown to be

$$f_\beta(x) = \frac{2^B(t-1)}{\xi^{t-1}}\left(\xi - 1 + x\right)^{t-2}, \quad 1-\xi < x < 1-\xi+\xi\psi.$$

$E\left(\beta^k\right)$ can be evaluated as follows:

$$E\left(\beta^k\right) = \frac{2^B(t-1)}{\xi^{t-1}}\int_{1-\xi}^{1-\xi+\xi\psi} x^k\left(\xi-1+x\right)^{t-2}dx \tag{4.32}$$

$$= \frac{2^B(t-1)(\xi-1)^{t-2}}{\xi^{t-1}(k+1)}\Big[(\tau)^{k+1}\,{}_2F_0\left(-t+2,k+1;2+k;1+\frac{\xi\psi}{1-\xi}\right) - (1-\xi)^{k+1}\,{}_2F_0\left(-t+2,k+1;2+k;1\right)\Big], \tag{4.33}$$

where

$$\tau = 1-\xi+\xi\psi.$$

Substituting (4.31) and (4.33) in (4.29) gives the final closed-form expression for $C_{L-iid}$.

### 4.5.5 Simulation Results

The effectiveness of the new codebook design algorithm can be seen in Fig. 4.4. It plots the (simulated) lower bound on ergodic capacity due to the finite rate quantization of the CSI with estimation errors and feedback delay. Simulation parameters: $t = 3$, $B \in \{4, 6\}$, the spatially correlated channel, $\mathbf{\Sigma}_{\text{hh}}$, is simulated by the correlation model in [104]: A linear antenna array with antenna spacing of half wavelength, angle of arrival $\phi = 0^\circ$ and an uniform angular spread of $[-\pi/5, \pi/5]$. $\mathbf{\Sigma}_{\text{im}}$ is simulated in a similar fashion with an uniform angular spread of $[-\pi/5.5, \pi/5.5]$ and the resulting correlation matrix is scaled by 0.7582. Note that the various auto and cross correlation matrices are included in $\mathbf{\Sigma}_{\text{im}}$, so they are not specified separately. The noise correlation is given by $\mathbf{\Sigma}_{\text{n}} = \mathbf{\Sigma}_{\text{hh}} - \mathbf{\Sigma}_{\text{im}}$.

The new codebook clearly outperforms the codebook designed without taking the EED into account [26]. The difference between the two codebooks is not much in the low SNR regime. However, there is a considerable gap in the high

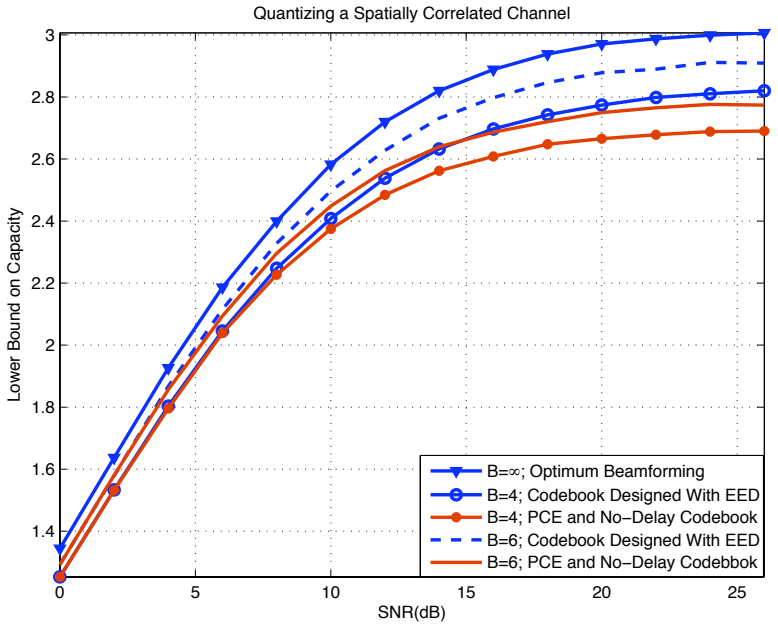


Figure 4.4 Performance of new codebook deigned by considering both noise and signal correlation matrices: simulation parameters: number of antennas $t = 3$, number of feedback bits $B \in \{4, 6\}$.

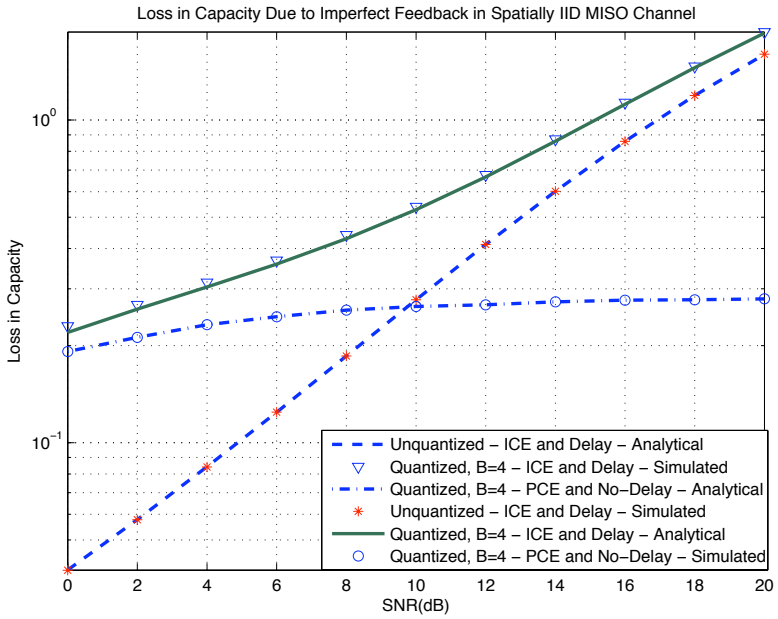


Figure 4.5 Effect of feedback imperfections on ergodic capacity of spatially i.i.d. channel, compared to Fig. 4.4, this Fig plots the loss in ergodic capacity due to EED and channel quantization.

SNR regime. Since the signal part leaks into the noise, all the curves flatten out at high SNRs. Increasing the number of feedback bits improves the performance. Though the loss analysis for correlated channels with EED is not presented, based on the source coding perspective provided in [93], it can be shown that the loss is proportional to $2^{-B/(t-1)}$. The calculation of the constant before this exponent is a non-trivial problem.

In Fig. 4.5 both the analytical and simulated curves are plotted for the loss in ergodic capacity due to estimation errors, delay and finite rate quantization. The analytical curves are in agreement with the simulations. Simulation parameters: $t = 3$, $|\rho|^2 = 0.989$, and $B = 4$. In the evaluation of analytical expression for loss (4.29) only the first 40 terms in the series were considered. The penalty of having the three forms of imperfection (solid green line) is quite severe on the system performance. The figure also shows loss due to quantization alone and EED alone. The loss due to quantization alone is seen to be much less compared to the loss due to EED alone.

## 4.6 Conclusion

In this chapter we considered the problem of designing an optimum codebook that minimizes the loss in average SEP and analyzing the effect of finite-rate feedback on the ASEP of a transmit beamforming MISO system with rectangular QAM utilizing a high-resolution source coding perspective. We derived the distortion function as a first order approximation of the instantaneous SEP loss and used it to design optimum codebook under both perfect and imperfect channel estimate assumptions. Assuming perfect channel estimation at the receiver, no feedback delay and under high resolution assumptions, we provided analytical expressions for loss in ASEP due to finite-rate channel quantization for spatially independent and correlated channels. We then considered the high-SNR regime and showed that the loss associated with the spatially i.i.d. case is the loss associated with the

spatially correlated case scaled by the determinant of the correlation matrix. The simulation results are in agreement with the analytical expressions. The presented framework of analysis can be extended to analyze the loss in SEP or BEP of other two dimensional linear modulation schemes.

In the presence of estimation errors and delay, for the optimum transmit beamforming, a new codebook design algorithm minimizing the ergodic loss is also proposed. Simulations clearly show that the new codebook (designed for ergodic capacity) outperforms the optimum codebook designed for perfect channel estimation and no-delay case. For spatially i.i.d. scenario, a closed-form analytical expression for the loss in ergodic capacity is derived and validated through simulations.

## 4.7 Appendix

### 4.7.1 High Resolution Theory

It is assumed that the source variable $\mathbf{h}$ is a two-vector tuple, $(\mathbf{v}, \alpha)$, where vector $\mathbf{v} \in \mathbb{Q}$ represents the actual quantization variable of dimension $2t$ and $\alpha \in \mathbb{Z}$ is the additional side information of dimension 1. The *side information* $\alpha$ is available at the receiver but not at the transmitter. The encoding or the quantization process is denoted as $\widehat{\mathbf{v}} = \mathcal{Q}(\mathbf{v}, \alpha)$. The distortion introduced by a finite-rate quantizer is defined as

$$D = E\Big[D_{\mathrm{Q}}\big(\mathbf{v}, \widehat{\mathbf{v}}\,;\, \alpha\big)\Big]$$

where $D_{\mathrm{Q}}\big(\mathbf{v}, \widehat{\mathbf{v}}\,;\, \alpha\big)$ is a general *non-mean-squared distortion* function between $\mathbf{v}$ and $\widehat{\mathbf{v}}$ that is parameterized by $\alpha$. It is further assumed that function $D_{\mathrm{Q}}$ has a continuous second order derivative $\mathbf{W}_{\alpha}(\mathbf{v})$, the sensitivity matrix, with the $(i,j)^{\text{th}}$ element given by

$$w_{i,j} = \frac{1}{2}\,\frac{\partial^2}{\partial\, v_i \partial\, v_j} D_{\mathrm{Q}}\big(\,\mathbf{v}\,, \widehat{\mathbf{v}}\,;\, \alpha\big)\,\Big|_{\mathbf{v}=\widehat{\mathbf{v}}}\,. \tag{4.34}$$

$\mathbf{W}_{\alpha}(\mathbf{v})$ represents sensitivity matrix of an unconstrained source. However, the beamforming vector has a norm constraint $\|\mathbf{v}\| = 1$, and a phase constraint

$\measuredangle\langle \mathbf{v}, \widehat{\mathbf{v}} \rangle = 0$. We denote the constrained space as $\mathbf{g}(\mathbf{v}) = 0$. Since we are operating in the constrained space, the degrees of freedom in $\mathbf{v}$ reduce from $2t$ to $2t-2$. The sensitivity matrix is replaced by its constrained version $\mathbf{W}_{\mathrm{c},\,\alpha}(\mathbf{v})$ given by

$$\mathbf{W}_{\mathrm{c},\,\alpha}\big(\mathbf{v}\big) = \mathbf{V}_n^T\, \mathbf{W}_{\alpha}\big(\mathbf{v}\big)\, \mathbf{V}_n\,, \tag{4.35}$$

where $\mathbf{V}_n \in \mathbb{R}^{2t \times 2t-2}$ is an orthonormal matrix with its columns constituting an orthonormal basis for the null space $\mathcal{N}\big(\frac{\partial}{\partial \mathbf{v}}\, \mathbf{g}(\mathbf{v})\big)$. Under high resolution assumption, the asymptotic distortion of the generalized finite-rate quantization system can be lower bounded by the following form

$$D_{\mathrm{Low}} = 2^{-\frac{B}{t-1}} \left( \int_{\mathbb{Q}} \big( I^{\mathrm{w}}_{\mathrm{c,opt}}(\mathbf{v})\, p\big(\mathbf{v}\big)\big)^{\frac{t-1}{t}}\; d\,\mathbf{v} \right)^{\frac{t}{t-1}}, \tag{4.36}$$

where $I^{\mathrm{w}}_{\mathrm{c,opt}}\big(\mathbf{v}\big)$ is the constrained average optimal inertial profile defined as [93]

$$I^{\mathrm{w}}_{\mathrm{c,opt}}\big(\mathbf{v}\big) = \int_{\mathbb{Z}} I_{\mathrm{c,opt}}\big(\mathbf{v}\,;\,\alpha\big)\, p\big(\alpha \big|\, \mathbf{v}\big)\; d\,\alpha\,. \tag{4.37}$$

The normalized inertial profile of an optimal quantizer is defined as the minimum inertia of all admissible Voronoi regions. The inertial profile of any Voronoi shape, including the constrained optimal inertial profile, $I_{\mathrm{c,opt}}\big(\mathbf{v}\,;\,\alpha\big)$, can be tightly lower bounded by that of an M-shaped hyper-ellipsoid

$$I_{\mathrm{c,opt}}\big(\mathbf{v}\,;\,\alpha\big) \gtrapprox \frac{t-1}{t} \left( \frac{\big|\mathbf{W}_{\mathrm{c},\alpha}(\mathbf{v})\big|}{\kappa^2_{2t-2}} \right)^{\frac{1}{2t-2}} \tag{4.38}$$

where $|\cdot|$ represents determinant and $\kappa_n$ is the volume of an $n$-dimensional unit sphere.

### 4.7.2 Spatially i.i.d. Channel: Average SEP Loss Analysis

In this section of the Appendix, we make use of the asymptotic distortion bounds presented in Section 4.7.3 and show the main steps in arriving at the loss in average symbol error probability for the $M_1 \times M_2$-QAM constellation. The relevant distortion function $D_{\mathrm{Q}}\big(\mathbf{v}, \widehat{\mathbf{v}}\,;\,\alpha\big)$ is given in (4.8). Due to space limitations, we only outline the important steps and present the final results.

The lower bound on asymptotic distortion given by (4.36), requires the computation of constrained sensitivity matrix (4.35), lower bound on constrained normalized inertial profile of an optimal quantizer (4.38) and the weighted constrained inertial profile (4.37). After some simplification the constrained sensitivity matrix for the distortion function of SEP loss (instantaneous) can be shown to be given by

$$\mathbf{W}_{\mathrm{c},\,\alpha}(\mathbf{v}) \;=\; \exp\left(-\frac{\lambda\,\alpha}{2}\right)\sqrt{\frac{\lambda\,\alpha}{8\pi}}\,\left[A+2C\,Q\left(\sqrt{\lambda\alpha}\right)\right]\cdot\mathbf{I}_{2t-2}. \tag{4.39}$$

For spatially independent and correlated channels, the optimal inertial profile is obtained by substituting (4.39), the constrained sensitivity matrix, into the hyperellipsoidal approximation given by (4.38). The optimal constrained inertial profile is given by

$$\begin{aligned} I_{\mathrm{c},\,\mathrm{opt}}\,(\mathbf{v}\,;\,\alpha) \;&=\; \left(\frac{(t-1)}{t}\,\exp\left(-\frac{\lambda\,\alpha}{2}\right)\gamma_t^{\,-\frac{1}{t-1}}\sqrt{\frac{\lambda\,\alpha}{8\pi}}\right)\cdot \\ &\qquad \left[A+2C\,Q\left(\sqrt{\lambda\alpha}\right)\right] \end{aligned} \tag{4.40}$$

where

$$\gamma_t = \frac{\pi^{t-1}}{(t-1)!}\,.$$

For spatially i.i.d. channel, $\mathbf{h}\sim\mathcal{NC}(\mathbf{0},\,\mathbf{I}_t)$, the random variable $\alpha$ ($\alpha = \|\mathbf{h}\|^2$) has a pdf

$$\begin{aligned} p_\alpha(x) \;&=\; p_{\alpha|\mathbf{v}}\,(x) \\ &=\; \frac{\exp(-x)\,x^{t-1}}{(t-1)!}\,, \qquad x\geq 0\,. \end{aligned} \tag{4.41}$$

Since the channel is spatially independent $\alpha$ does not depend on the channel direction $\mathbf{v}$. Using (4.41) and (4.40) in (4.37), $I_{\mathrm{c,opt}}\big(\mathbf{v}\,;\,\alpha\big)$, the weighted constrained inertial profile coefficient can be obtained.

After some simplification an intermediate step in the derivation, with a change in variable using

$$y = x\left(\frac{\lambda}{2}+1\right),$$

is given by

$$I_{\text{opt}}^{\text{w}}(\mathbf{v}) = D_{\mathcal{A}}\, A\, \Gamma\left(t+\frac{1}{2}\right) + D_{\mathcal{A}}\, 2C \int_0^{\infty} Q\left(\sqrt{\mu y}\right) \exp\left(-y\right)\, y^{t-\frac{1}{2}}\, dy \quad (4.42)$$

where

$$D_{\mathcal{A}} = \frac{\sqrt{\lambda}(t-1)\,\gamma_t^{\,-\frac{1}{t-1}}}{\sqrt{8\pi}\, t!\left(\frac{\lambda}{2}+1\right)^{\left(t+\frac{1}{2}\right)}},$$

and

$$\mu = \frac{2\lambda}{\lambda+2},$$

and $\Gamma(n)$ is the standard Gamma function [103]

$$\Gamma(n) = \int_0^{\infty} e^{-u} u^{n-1} du.$$

We use

$$Q(x) = \frac{1}{\pi} \int_{\theta=0}^{\pi/2} \exp\left(-\frac{x^2}{2\sin^2\theta}\right) d\theta, \quad x \geq 0,$$

an alternative definition of $Q$ function [12], to simplify the second term with integral in (4.42) and arrive at

$$\int_0^{\infty} Q\left(\sqrt{\mu y}\right) \exp\left(-y\right)\, y^{t-\frac{1}{2}}\, dy = \frac{\Gamma\left(t+\frac{1}{2}\right)}{\pi} \int_{\theta=0}^{\pi/2} \left(\frac{\sin^2\theta}{\kappa+\sin^2\theta}\right)^{t+\frac{1}{2}} d\theta \quad (4.43)$$

where

$$\kappa = \frac{\mu}{2}.$$

We make use of [12, Eqn. (5.17)] to arrive at a closed-form expression

$$\int_{\theta=0}^{\pi/2} \left(\frac{\sin^2\theta}{\kappa+\sin^2\theta}\right)^{t+\frac{1}{2}} d\theta = \frac{\sqrt{\kappa\pi}\,\Gamma\left(t+1\right)}{2\left(1+\kappa\right)^{t+1}\Gamma\left(t+\frac{3}{2}\right)}\, {}_2F_1\left(1, t+1; t+\frac{3}{2}; \frac{1}{1+\kappa}\right). \quad (4.44)$$

for the finite integral in (4.43). By substituting the weighted constrained inertial profile coefficient (4.42) and

$$p(\mathbf{v}) = \frac{1}{\gamma_t},$$

into the distortion integral (4.36), the ASEP loss of an i.i.d. MISO system can be shown to be given by (4.16).

### 4.7.3 Spatially Correlated Channel: Average SEP Loss Analysis

In this section of the Appendix, loss in average symbol error probability is evaluated for the spatially correlated scenario. All the steps until the derivation of constrained normalized inertial profile (4.40) are same for both spatially independent and correlated channels. For correlated MISO fading channels $\mathbf{h} \sim \mathcal{NC}\big(\mathbf{0},\, \mathbf{\Sigma}_{\mathrm{h}}\big)$ with channel correlation matrix $\mathbf{\Sigma}_{\mathrm{h}}$ having distinct eigen-values, i.e., [3] $\lambda_{\mathrm{h},1} > \cdots > \lambda_{\mathrm{h},\,t} > 0$. The marginal pdf of $\mathbf{v}$ and conditional distribution of $\alpha|\mathbf{v}$ can be shown to be [102]:

$$p_{\,\mathbf{v}}\,(\mathbf{x}) \;\;=\;\; \gamma_t^{-1}\;|\mathbf{\Sigma}_{\mathrm{h}}|^{-1}\;\left(\mathbf{x}^{\mathsf{H}}\mathbf{\Sigma}_{\mathrm{h}}^{-1}\,\mathbf{x}\right)^{-t}, \tag{4.45}$$

$$p_{\alpha|\mathbf{v}}\,(x) \,=\, \frac{x^{t-1}\left(\mathbf{v}^{\mathsf{H}}\mathbf{\Sigma}_{\mathrm{h}}^{-1}\,\mathbf{v}\right)^{t}\exp\left(-x\,\mathbf{v}^{\mathsf{H}}\mathbf{\Sigma}_{\mathrm{h}}^{-1}\,\mathbf{v}\right)}{(t-1)!}\,. \tag{4.46}$$

By substituting the conditional pdf $p_{\alpha|\mathbf{v}}\,(x)$ given by (4.46) and the constrained normalized inertial profile (4.40) into equation (4.37), the average inertial profile can be obtained as

$$I^{\mathrm{w}}_{\mathrm{c,\,opt}}\big(\mathbf{v}\big) = \left(\frac{\left(\mathbf{v}^{\mathsf{H}}\mathbf{\Sigma}_{\mathrm{h}}^{-1}\,\mathbf{v}\right)^{t}}{\left(\mathbf{v}^{\mathsf{H}}\mathbf{\Sigma}_{\mathrm{h}}^{-1}\,\mathbf{v}+\frac{\lambda}{2}\right)^{t+\frac{1}{2}}}\right)\cdot \left[T_{\mathcal{D}} + \frac{T_{\mathcal{E}}\sqrt{\nu}}{(1+\nu)^{t+1}}\,{}_2F_1\left(1, t+1; t+\frac{3}{2}; \frac{1}{1+\nu}\right)\right] \tag{4.47}$$

where

$$T_{\mathcal{D}} = \frac{\sqrt{\lambda}(t-1)\gamma_t^{-\frac{1}{t-1}}\,A\,\Gamma\left(t+\frac{1}{2}\right)}{\sqrt{8\pi}\,t!}, \tag{4.48}$$

$$T_{\mathcal{E}} = \frac{\sqrt{\lambda}(t-1)\,\gamma_t^{-\frac{1}{t-1}}\,C\,\Gamma\left(t+\frac{1}{2}\right)}{\Gamma\left(t+\frac{3}{2}\right)\sqrt{8}\pi}, \tag{4.49}$$

and

$$\nu = \frac{\lambda}{\left(2\,\mathbf{v}^{\mathsf{H}}\mathbf{\Sigma}_{\mathrm{h}}^{-1}\,\mathbf{v}+\lambda\right)}\,. \tag{4.50}$$

[3] In this chapter, we assume that the channel covariance matrix $\mathbf{\Sigma}_{\mathrm{h}}$ has distinct positive eigen-values. The result can be extended to any covariance matrix that is positive definite. If the channel covariance matrix is singular, the quantization should be carried out in a space with reduced dimension.

Using (4.45) and $I^{\mathrm{w}}_{\mathrm{c,\,opt}}(\mathbf{v})$ in (4.47), with the help of the alternative representation of $Q$ function, the average symbol error probability loss of a spatially correlated transmit beamforing multiple input single output system is given by (4.17).

**Acknowledgement**

The text of this chapter, in part, has *appeared* in:

- Y. Isukapalli, J. Zheng, and B. D. Rao, "Optimum codebook design and average SEP loss analysis of spatially independent and correlated feedback based MISO systems with rectangular QAM constellation," *IEEE Transactions on Signal Processing*, vol. 57, no. 5, pp. 2017-2024 , May 2009.

- Y. Isukapalli and B. D. Rao, "Finite rate feedback for spatially and temporally correlated MISO channels in the presence of estimation errors and feedback delay," *IEEE Global Telecom. (Globecom) Conf.*, Washington D.C., pp. 2791-2795, Nov. 2007.

- Y. Isukapalli, J. Zheng and B. D. Rao, "Average SEP loss analysis of transmit beamforming for finite rate feedback MISO systems with QAM constellation," *IEEE Intern. Conf. on Acous. Speech and Sig. Proc. (ICASSP)*, Hawaii, vol. 3, pp. 1520-6149, Apr. 2007.

# 5 Modeling and Prediction of Wireless Channel

Now we turn our attention to the issue of minimizing the negative impact of feedback delay on the performance of the system. An obvious solution to the problem of feedback delay is to predict the channel and then quantize the predicted channel. In this chapter we study the role of ergodicity in wireless channel prediction. With an eye on developing a better wireless channel simulator we first begin with a general, but non-linear and non-tractable, form of wireless channel model. Under certain assumptions we then consider a simplified and well accepted linear sinusoidal channel model. Following the sinusoidal channel model, conditions under which the ergodic assumption is valid are presented. This sheds insight into when statistical channel models that employ ensemble averaging are appropriate.

Due to the lack of ergodicity in a typical real world wireless channel, Least Squares prediction, an approach based on time averages is motivated as opposed to linear minimum mean squared error channel prediction, an approach based on ensemble averaging. We then study methods such as Forward-Backward and rank reduction for high quality channel prediction. Simulation results are presented to complement the analytical expressions. Simulation results also illustrate the improvement in channel prediction quality.

## 5.1 Introduction

The demand for high data rates with high reliability has intensified the research efforts in wireless systems with channel state information (CSI) at the transmitter. In frequency division duplexing systems the receiver has to feed back the CSI to the transmitter. As seen from the previous chapters, depending on the temporal correlation, the effect of delay between channel estimation and its actual use can degrade the performance of a communication system. Typical communication problems sensitive to the feedback delay include, power control, adaptive modulation, antenna switching schemes, transmit beamforming (the main theme of this thesis) and opportunistic beamforming. Channel prediction can be useful in these scenarios. Channel prediction algorithms can be classified into two broad categories, data driven and statistics driven. Data driven approaches include various Least Squares (LS) based methods and sub-space based modeling methods (MUSIC, ESPRIT, and their variations) [3]. The popular statistical method is the linear minimum mean squared error (LMMSE) method. The LMMSE method uses apriori statistical knowledge and so its performance can be inferior to alternate approaches in the absence of ergodicity. The ergodicity of the underlying model has to be evaluated carefully before employing LMMSE and this chapter addresses the validity of this assumption.

We first begin with a general but non-linear and non-tractable form of wireless channel model. This channel model can be useful to generate realistic channel data. However, for the general channel model any statistical analysis is difficult to carry out. Hence we consider a simplified sinusoidal channel model and with limited scattering, we show that time average is not in general equal to the ensemble average. This gives an insight into the utility of statistical methods for channel prediction that are based on ensemble averaging. LMMSE prediction [4], an algorithm designed under the assumption of ergodicity gives a pessimistic picture about the prediction possibilities and motivate LS prediction, a time-averaging

method which depends only on the temporal properties of the channel. For simplicity we focus on a Single Input and Single Output (SISO) system.

The rest of this chapter is organized as follows. In Section 5.2 we present a general channel model. The main theme of the chapter is prediction and the role of ergodicity of the channel model in prediction, is studied in Section 5.3. Convergence analysis between time average and ensemble average approaches is carried out in Section 5.4. In Section 5.5 we show that the Forward-Backward (FB) prediction reduces the prediction error compared to the Forward-only prediction and rank-reduction is shown to improve prediction when the effective number of multipath is less than the filter order and we conclude this chapter in Section 5.6.

Important variables: $N$- number of clusters (also number of point sources in Section 5.3), $\omega_{max}$- Maximum Doppler frequency, $v$- velocity of the receiver, $R_e(\tau)$- Ensemble autocorrelation, $R_t(\tau)$- Time average autocorrelation, $\rho$- SNR of channel estimate.

## 5.2 A General Multipath Model

As mentioned in the introduction chapter, wireless channel is typically classified into three parts. Path loss or slow fading, shadow fading and fast fading. Slow and shadow fadings generally happen at a much higher time scale than fast fading and hence the focus of system designer is typically more on the fast fading. In this chapter our modeling approach concerns only fast fading. The motivation behind this section is the simulation of a realistic wireless channel.

As shown in Fig. 5.1 a total of $U$ number of multipath are assumed to be arriving at a moving receiver. In the present section we do not consider the fact that the $U$ multipath arrive in groups where each group might follow a particular spatial distribution. The resulting baseband version of the wireless channel can be modeled as

$$h(t) = \sum_{n=1}^{U} \frac{\alpha_n(t)}{d_n(t)} P_n(t)\, e^{j\{\omega_n(t)\, t + \phi_n(t)\}}, \tag{5.1}$$

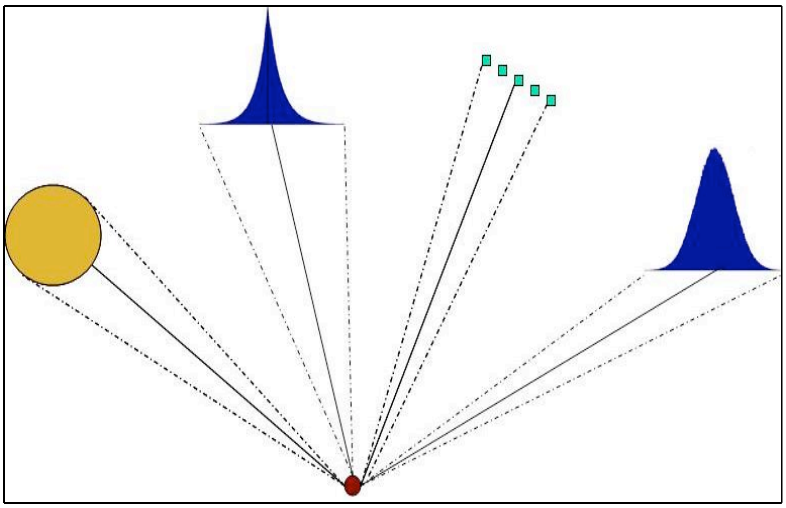

Figure 5.1 A general multipath arrival model.

- $\alpha_n(t)$- Time-varying amplitude: Assuming that the multipath appear as clusters in Section 5.2.1 we present an analytical characterization for the amplitude variation. Assuming equal amplitude for each of the multipath component is a standard assumption. However, in some measurement campaigns it has been noticed that Weibull distribution is a better fit for amplitude of the multipath. In studying the role of ergodicity we assume a Weibull distribution for multipath amplitude.

- $d_n(t)$- Assuming that the vehicle is moving with a velocity of $v$ and an acceleration of $a$, with distance, the power decays as

$$\frac{1}{s_n + vt + \frac{at^2}{2}}.$$

Large scale fading and shadowing are generally parameterized by the distance between the mobile and the base station. Assuming that the small scale fading measurement starts at distance $s_n$, we write the above equation as (5.2) (shown below) to make the distance $s_n$ as part of (along with $v$ and

$a$) fast fading phenomena.

$$\frac{1}{\underbrace{s_n\left(1+\frac{vt+\frac{at^2}{2}}{s_n}\right)}_{d_n(t)}}, \tag{5.2}$$

$d_n(t)$ captures the remaining effect from shadowing and slow fading as a parameter of time $t$, $v$, and $a$. For small $x$, with the help of the following approximation

$$\frac{1}{1+x} \approx e^{-x},$$

one can have a simpler exponential form for $1/d_n(t)$. i.e.,

$$\frac{1}{d_n(t)} \approx e^{-\left(\frac{v+\frac{at}{2}}{s_n}\right)t}. \tag{5.3}$$

- $\phi_n(t)$- Time-varying phase: In a recent paper [105], it is formulated that the phase should be treated as time-varying. Autocorrelation of $\phi_n(t)$ is given as [105]

$$R_\phi(\tau) = e^{-B|\tau|/2} \tag{5.4}$$

where $B$, a receiver related physical parameter, is a positive constant with the dimension of frequency and $\tau$ is the lag.

- $P(t)$- Captures the effect of pulse shaping.

- $\omega_n(t)$- Time-varying Doppler: In the channel modeling literature, it is a common practice to treat the doppler frequency to be tine-invariant in channel modeling literature. However time-varying Doppler makes sense in situations where the plane wave assumption breaks down. It is easy to go back to the time-invariant Doppler from a time-varying Doppler by setting an appropriate parameter to zero. The below equation represents the variation of Doppler when the plane wave assumption breaks down.

$$\omega_n(t) = \omega_{\max}\cos\theta_n - \frac{v\,t\,\omega_{max}\sin^2\theta_n}{s_n} \tag{5.5}$$

where $s_n$ is the distance of the object causing scattering and the mobile. As seen in the above equation as the distance between the mobile and source of scattering (SS) increases the second term can be ignored. However, when the mobile is in acceleration then even if the mobile is away from SS then there will be a time dependent Doppler.

Instead of assuming constant velocity, in this chapter we assume an accelerating vehicle. Closeness to the scatterers and the accelerating vehicle assumptions are valid for modern city environment. With these assumptions the time-varying Doppler frequency is given by the following expression.

$$\omega_n(t) = (\omega_{max} + \omega_a(t)) \cos\theta_n - \frac{\pi\, t \left(v + \frac{a\,t}{2}\right)^2 \sin^2\theta_n}{s_n\, \lambda}, \tag{5.6}$$

$$\omega_a(t) = \frac{\pi\, a\, t}{\lambda}.$$

After incorporating the parameters in (5.1) as defined above, clearly the channel model in (5.1) represents the most general nature of what is popularly known as Clark's model in literature. A recent publication [105] extended the Clark's model for time-varying phase. In this chapter we considered a more general, but highly complex and non-linear, form for the wireless channel. Though analytically intractable, the main motivation for using the channel model in (5.1) is for simulation of wireless communication process in software. We now examine under what assumptions (5.1) can be reduced into an analytically tractable form proposed by the famous Clark model.

- Assuming that the time scale of channel validity is small (of the order of milliseconds) and the distance between the scatterer and the moving receiver is large (of the order of tens of meters) $d_n(t) \approx 1$.
- A constant pulse assumption leads to $P_n(t) = 1$.
- A constant velocity receiver implies that $a = 0$
- $s_n$ is large, i.e., the scattering source is far away from the moving receiver.

- Phase variation is small with in the time scale of operation, leading to $\phi_n(t) = \phi_n$.

Under the above mentioned assumptions the wireless channel takes a simple linear form of sum-of-sinusoids. In the next subsection we consider a popular multipath arrival scenario and propose a simpler way to simulate the wireless channel and develop a model based on stochastic sinusoidal processes.

### 5.2.1 Multipath in Clusters

Simulation of wireless channel has two different domains. One is the software simulation and the other is simulating the wireless channel in hardware. The goal of hardware simulators is to be able to replicate a realistic wireless channel scenario with as minimum number of sinusoids. Hence, there has been considerable amount of research in reproducing the Clark model's statistical properties with as minimum sinusoids as possible [2], [107].

Jakes in his seminal work exploited the symmetrical properties and was able to reproduce the Clark's statistical properties with as few as eight sinusoids. However, Jakes model went through some corrections as it had some statistical inconsistencies [108] and [109]. Recently Grolleau *et al.* [106] published stochastic sinusoidal model where in they accurately reproduced the Clark model's statistical properties with just one sinusoid. In this section we extend the stochastic sinusoidal model to explain the cluster phenomena. We also derive the statistical properties of the amplitude variation of the stochastic sinusoids. An additional advantage of the modeling shown below is simulation of multipath phenomena in hard ware with much fewer sinusoids than the total number of multipath. The model presented here is quite general in nature and it can be shown that Clark's model is a special case of the model presented.

In this section we assume a linearized model, i.e., plane wave, no acceleration at the mobile and constant phase for each multipath. As shown in Fig. 5.1 in various channel measurement campaigns it is observed that the multipath gen-

erally appear in clusters as opposed to point sources. The channel model in (5.1) can now be written as (5.7).

$$h(t) = \sum_{n=1}^{N} \sum_{m=1}^{M} \beta_{nm}\, e^{j\omega_{nm} t} \tag{5.7}$$

where $N$-number of clusters, $M$-number of multipath components in each cluster, i.e., $U = NM$, $\beta_{nm}$ and $\omega_{nm}$ are amplitude and doppler frequencies of $m^{th}$ multipath in the $n^{th}$ cluster:

$$\begin{aligned}
\omega_{nm} &= \omega_{\max} \cos\theta_{nm} \\
\omega_{max} &= 2\pi v/\lambda; \\
\theta_{nm} &= \theta_n + \psi_{nm} \\
\cos\theta_{nm} &= \cos\theta_n \cos\psi_{nm} - \sin\theta_n \sin\psi_{nm}
\end{aligned}$$

Assuming smaller angular spread ($\cos\psi_{nm} \approx 1$ and $\sin\psi_{nm} \approx \psi_{nm}$) we approximate the above equation as

$$\cos\theta_{nm} \approx \cos\theta_n - \psi_{nm} \sin\theta_n. \tag{5.8}$$

With the above approximation $h(t)$ can now be simplified as

$$\begin{aligned}
h(t) &= \sum_{n=1}^{N} \sum_{m=1}^{M} \beta_{nm}\, e^{j\omega_{\max}[\cos\theta_n - \psi_{nm} \sin\theta_n]t}, \\
&= \sum_{n=1}^{N} \beta_n(t)\, e^{j\omega_n t}, \qquad (5.9) \\
\beta_n(t) &= \sum_{m=1}^{M} \beta_{nm}\, e^{-j\omega_{\max} \sin\theta_n \psi_{nm} t} \qquad (5.10)
\end{aligned}$$

where,

- $\beta_{nm}$ is the amplitude of the $m^{th}$ multipath of the $n^{th}$ cluster. Note that the phase is absorbed into the constant amplitude of $1/\sqrt{NM}$, $\beta_{nm} = \frac{\phi_{nm}}{\sqrt{NM}}$.
- $\phi_{nm}$ is the phase of the $m^{th}$ multipath of the $n^{th}$ cluster.

- $\omega_{nm}$ is the Doppler frequency of the $m^{th}$ multipath of the $n^{th}$ cluster.

$$\omega_{nm} = \omega_{max} \cos\theta_{nm}$$

where $\omega_{max}$ is the maximum Doppler frequency.

From (5.9) it can be observed that it is exactly same as Clark's model except that the amplitude is also time varying with a specific structure as given in (5.10). By making the amplitude constant one can easily go back to the Clark's model. Equation (5.9) can also be treated as a generalized form of the stochastic sinusoidal model considered in [106] and this model explains a much richer class of multipath arrival scenarios. There is also an obvious benefit of reduction in the number of sinusoids needed in simulating the channel variation process in hardware.

#### 5.2.1.1 Ensemble Autocorrelation of $\beta_n(t)$- Amplitude Random Process

We now look at the ensemble autocorrelation of the random amplitude variations captured in $\beta_n(t)$.

$$\begin{aligned}
\beta_n(t) &= \sum_{m=1}^{M} \beta_{nm}\, e^{-j\omega_{max}\sin\theta_n\,\psi_{nm}t} \\
R_\beta(\tau) &= E[\beta_n^*(t)\beta_n(t+\tau)] \\
&= E\left[\sum_{m=1}^{M} \beta_{nm}^*\, e^{j\omega_{max}\sin\theta_n\,\psi_{nm}t} \sum_{\tilde{m}=1}^{\tilde{M}} \beta_{n\tilde{m}}\, e^{-j\omega_{max}\sin\theta_n\,\psi_{n\tilde{m}}(t+\tau)}\right] \\
&= \sum_{m=1}^{M} E[e^{-j\omega_{max}\sin\theta_n\,\psi_{nm}\tau}]/M \\
&= \int_{-\pi}^{\pi} e^{-j\omega_c\,\psi_{nm}\tau}\; p(\psi)\, d\psi
\end{aligned}$$

As reported in some measurement campaigns, in this chapter we consider the truncated laplacian pdf (it is straightforward to extend the results to some other distributions)

$$p(\psi) = \frac{e^{-|\sqrt{2}\psi/\sigma|}}{\mathcal{A}}, \quad -\sigma \le \psi \le \sigma$$

where

$$\mathcal{A} = \sqrt{2}\,\sigma\,\left(1 - e^{-\sqrt{2}}\right).$$

$$\begin{aligned} R_\beta(\tau) &= \frac{1}{\mathcal{A}} \int_{-\sigma}^{\sigma} e^{-j\omega_c \psi\tau} e^{-|\sqrt{2}\psi/\sigma|}\, d\psi \\ &= \frac{2}{\mathcal{A}} \int_{0}^{\sigma} \cos(\omega_c \psi\tau) e^{-\sqrt{2}\psi/\sigma}\, d\psi \end{aligned}$$

Making use of

$$\int e^{a\theta} \cos b\theta = \frac{e^{a\theta}\,(a\cos b\theta + b \sin b\theta)}{a^2 + b^2},$$

$$R_\beta(\tau) = \frac{2\sigma^2 e^{-\sqrt{2}}}{\mathcal{A}(2+\omega_c^2\tau^2\sigma^2)} \left[\omega_c\,\tau \sin(\omega_c\,\sigma\tau) - \frac{\sqrt{2}}{\sigma}\cos(\omega_c\,\sigma\tau)\right] + \frac{2\sqrt{2}\sigma}{\mathcal{A}(2+\omega_c^2\tau^2\sigma^2)}\,. \tag{5.11}$$

#### 5.2.1.2 Power Spectral Density

The amplitude random process, $\beta_n(t)$, is a wide sense stationary process and hence the power spectral density is obtained by taking the Fourier transform of the autocorrelation function. Let $\mathcal{F}\{f(x)\}$ represent the Fourier transform of $f(x)$.

$$S_\beta(f) = \mathcal{F}\left\{R_\beta(\tau)\right\}. \tag{5.12}$$

$$\mathcal{F}\left\{\frac{2\sqrt{2}\sigma}{\mathcal{A}(2+\omega_c^2\tau^2\sigma^2)}\right\} = \frac{1}{\mathcal{A}\omega_c}\, e^{-\frac{\sqrt{2}}{\omega_c\,\sigma}|f|}, \tag{5.13}$$

$$\mathcal{F}\left\{\frac{1}{a^2+\tau^2}\right\} = \frac{1}{2a}\, e^{-a|f|}, \tag{5.14}$$

$$\mathcal{F}\left\{\frac{\tau}{a^2+\tau^2}\right\} = \frac{i}{2}\, e^{-a|f|}, \tag{5.15}$$

$$\mathcal{F}\left\{\cos(\omega_c\sigma\tau)\right\} = \frac{1}{2}\left[\delta\left(f - \frac{\omega_c\sigma}{2\pi}\right) + \delta\left(f + \frac{\omega_c\sigma}{2\pi}\right)\right], \tag{5.16}$$

$$\mathcal{F}\left\{\sin(\omega_c\sigma\tau)\right\} = \frac{1}{2j}\left[\delta\left(f - \frac{\omega_c\sigma}{2\pi}\right) - \delta\left(f + \frac{\omega_c\sigma}{2\pi}\right)\right]. \tag{5.17}$$

With the help of Fourier transform properties and (5.13)- (5.17), the final expression (5.12) for the power spectral density can be obtained. The autocorrelation and power spectral densities are useful in generating the amplitude of the stochastic sinusoidal channel model. As shown in [106] one needs the second order statistical properties to generate the channel and [106] uses the circular pattern of arrival.

The autocorrelation and power spectral densities from this chapter can be helpful in generalizing the results in [106] for multipath arriving in a variety of spatial pattern. To summarize the advantage of mathematical simplification of multipath arrival in clusters is primarily useful in building a simpler hardware based wireless simulator. In the next section we study a crucial statistical link between channel prediction based on data driven approaches and the approaches driven by statistics.

## 5.3 Ergodicity of Wireless Channels

In this section we assume a simple, but well accepted, linearized channel model with $N$ number of point sources. We examine the assumption of ergodicity as this is the key to conclusions drawn on impact of delay in feedback based communication systems and channel prediction. The multiplicative complex flat and fast fading process is modeled as [2], [3], and [4] (and references therein).

$$h(t) = \sum_{n=1}^{N} \alpha_n e^{j\omega_n t}, \tag{5.18}$$

where, $\alpha_n = \beta_n e^{j(\phi_n)}$ is the time-varying amplitude, $\phi_n$ is the phase and $\omega_n$ is the Doppler frequency of the $n^{th}$ multipath. $\omega_n = \omega_{max} \cos\theta_n$, where $\omega_{max}$ is the maximum Doppler frequency and $\theta_n$ is the angle of arrival (AOA) of $n^{th}$ multipath. $\omega_{max} = 2\pi v/\lambda$, where $v$ is the velocity of mobile and $\lambda$ is the carrier wavelength. We refer to this model as sinusoidal channel model.

With the help of pilot symbol sequence, the discrete channel is assumed to be estimated by the LS method. Let $\widehat{h}$ represent the estimate of channel $h$, assuming $E[|\widehat{h}|^2] = \rho$ and the noise power to be 1, the signal-to-noise ratio (SNR) of the estimated channel will be $\rho$. The channel is predicted from the estimate $\widehat{h}$ and $\rho$ has considerable impact on the channel prediction.

The coherence time, which plays a crucial role in the conclusions drawn about the effect of the delay between channel estimation and its actual use, is based on the autocorrelation property (an ensemble average) of the channel [16], [62].

Often ergodicity is assumed and ensemble averages are used in lieu of temporal averages. We now look at the ensemble average, $R_e(\tau)$, for the sinusoidal channel model given in (5.18).

$$\begin{aligned}
h(t) &= \sum_{n=1}^{N} \alpha_n e^{j\omega_n t} \\
R_e(\tau) &= E[h^*(t)h(t+\tau)] \\
&= E\left[\sum_{n=1}^{N} \alpha_n^* e^{-j\omega_n t} \sum_{m=1}^{N} \alpha_m e^{j\omega_m (t+\tau)}\right] \\
&= \sum_{n=1}^{N} E[|\alpha_n|^2] E[e^{j\omega_n \tau}] \qquad (\because E[\alpha_n^* \alpha_m] = 0) \\
&= \sum_{n=1}^{N} E[e^{j\omega_n \tau}]/N \\
&= \int_{-\pi}^{\pi} e^{j\omega_{max}\tau \cos\theta}\ p(\theta)\, d\theta
\end{aligned}$$

In the above equation it is assumed that $E[|\alpha_n|^2] = 1/N$, this effectively removes the amplitude distribution from the ensemble average, $R_e(\tau)$. As we will see below, this is not true for time averages. To carry out the integration shown in the above equation we use the following expression [110, page. 331].

$$e^{j\omega_{max}\tau \cos\theta} = J_0(\omega_{max}\tau) + 2\sum_{k=1}^{\infty} j^k J_k(\omega_{max}\tau) \cos k\theta, \tag{5.19}$$

where $J_k()$ is the $k^{th}$ order Bessel function of the first kind and $j = \sqrt{-1}$. Note that if we assume a uniform distribution for the angle of arrival, $\theta \in (0, 2\pi]$, then there is no need for (5.19), the ensemble average is the well known Bessel function. However, in practical scenarios, the angle of arrival can assume different probability density function (pdf)s depending on the environment, (5.19) is helpful in finding the ensemble average in these practical scenarios.

$$\begin{aligned}
R_e(\tau) &= \int_{-\pi}^{\pi} \left( J_0(\omega_{max}\tau) + 2\sum_{k=1}^{\infty} j^k J_k(\omega_{max}\tau) \cos k\theta \right)\ p(\theta)\, d\theta \\
&= J_0(\omega_{max}\tau) + 2\sum_{k=1}^{\infty} j^k J_k(\omega_{max}\tau) \underbrace{\int_{-\pi}^{\pi} \cos k\theta\ p(\theta) d\theta}_{\mathcal{J}(k)}
\end{aligned}$$

It has been reported in the channel measurement papers [114] and in some standard documents that Laplacian distribution is the best fit for the angle of arrival. Substituting Laplacian pdf in $\mathcal{J}(k)$ gives

$$\mathcal{J}(k) = \frac{1}{\sqrt{2}\sigma} \int_{-\pi}^{\pi} \cos k\theta \; e^{-|\sqrt{2}\theta/\sigma|} d\theta,$$

where $\sigma$ is the standard deviation of the angular spread. Making use of

$$\int e^{a\theta} \cos b\theta = \frac{e^{a\theta} \left(a \cos b\theta + b \sin b\theta\right)}{a^2 + b^2},$$

and after some simplification we arrive at

$$\mathcal{J}(k) = \frac{2}{2 + \sigma^2 k^2} \left(1 + e^{-\sqrt{2}\pi/\sigma} (-1)^{k+1}\right)$$

The final form for the ensemble average is given by

$$R_e(\tau) = J_0(\omega_{max}\tau) + \sum_{k=1}^{\infty} j^k \frac{4}{2 + \sigma^2 k^2} J_k(\omega_{max}\tau) \left(1 + e^{-\sqrt{2}\pi/\sigma} (-1)^{k+1}\right). \qquad (5.20)$$

In Fig. 5.1 we plot the absolute value (unlike real valued correlation of Jakes scenario, correlation of Laplacian AOA scenario given by (5.20) is a complex number) of the temporal correlation for different values of standard deviation of AOA. As expected, if the angular spread is small, the correlation is high. For comparison, we also plotted the correlation obtained from the Jakes model (Bessel function). The correlation from Jakes scenario is quite low compared to the correlation of a Laplacian AOA scenario. Number of paths, $N = 10$, and maximum Doppler frequency, $\omega_{max} = 100Hz$ are the parameters assumed in Fig. 5.1. For clarity, the simulated curves are not shown in the Fig. 5.1. We verified that the simulations agree accurately with the analysis. Note that the ensemble average is independent of number of multipath, meaning that ensemble average of even a single path would have resulted in the same correlation as (5.20).

The time average, $R_t(\tau)$, for the sinusoidal channel model, for large sample set, can be shown to be given by

$$\begin{aligned} R_t(\tau) &= \lim_{T\to\infty} \frac{1}{2T} \int_{-T}^{T} h(t) h^*(t-\tau) dt \\ &= \sum_{n=1}^{N} |\alpha_n|^2 e^{j\omega_n \tau}. \end{aligned} \qquad (5.21)$$

Assuming a uniform distribution for AOA, ensemble average of even a single multipath resembles a Bessel curve, but not the time average. Note that unlike, ensemble average, time average is not independent of $N$. If the number of multipath present in a single realization is large (100s) then the ergodic assumption is a valid one. It has been noted in literature that typical number of sinusoids present in an outdoor wireless channel do not exceed more than ten [6]. This means that the real world channel is almost never ergodic, except in a highly rich indoor scattering.

## 5.4 Convergence of Time-Average and Ensemble-Average

To quantify the difference between the ensemble average (5.20) and time average (5.21), we look at the mean-square error (MSE) between them as a function of number of multipath, $N$, maximum Doppler frequency, $\omega_{max}$, the lag, $\tau$, and the parameters describing the angular spread and amplitude distribution of the multipath. As we saw earlier, once we constrain the power of a single multipath $E[|\alpha_n|^2] = 1/N$, then ensemble average is effectively free from the pdf associated with amplitude distribution. As seen in (5.21) the power constraint doesn't eliminate the randomness associated with amplitude in time average. As shown later in this section, the MSE between ensemble and time averages also depends on the pdf of the amplitude of multipath.

Channel measurement papers [114] reported Rayleigh distribution to be a better fit for the amplitude distribution. However, in this chapter we choose to work with Weibull distribution, as it has a flexibility to control the tail properties (can be useful for describing a variety of possible wireless channel scenarios) and the mean by the selection of its parameters and it is mathematically tractable. The pdf of Weibull random variable, $|\alpha_n| = \beta_n$, is given by

$$p(x) = c\, b^{-c} x^{c-1} e^{-(\frac{x}{b})^c} \tag{5.22}$$

The parameters $b$ and $c$ control the moments of the distribution. Note that for $c = 2$, the Weibull pdf becomes a Rayleigh pdf and for $b = 0$ and $c = 1$, Weibull

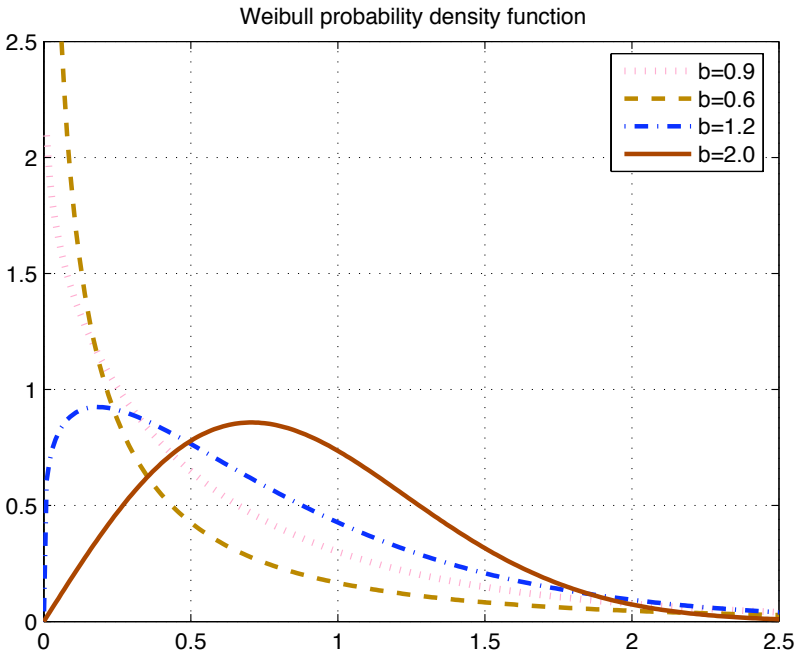


Figure 5.2 Weibull pdf with different $b$'s.

pdf becomes an exponential pdf. Since the power of each multipath has to be equal, $E[|\alpha_n|^2] = 1/N$, $b$ and $c$ have to satisfy

$$b^2\Gamma\left[\frac{2+c}{c}\right] = \frac{1}{N}, \tag{5.23}$$

where

$$\Gamma(n) = \int_0^\infty e^{-u}u^{n-1}du$$

is the standard Gamma function [110]. In Fig. 5.2 we plot the Weibull pdf for different values of $b$, the value of $c$ is determined by (5.23). The important point to note from Fig. 5.2 is that higher $b$ results in a strong tail. We later connect this tail property of $b$ to the MSE between the ensemble and time averages. The MSE, $\mathcal{L}(N, \sigma, b, \omega_{max}, \tau)$, between ensemble and time averages for the realistic channel scenario (Laplacian AOA and Weibull amplitude) is given by

$$\mathcal{L}(N, \sigma, b, \omega_{max}, \tau) \quad = \quad E\left[\left|R_e(\tau) - \sum_{n=1}^{N}|\alpha_n|^2 e^{j\omega_n\tau}\right|^2\right]$$

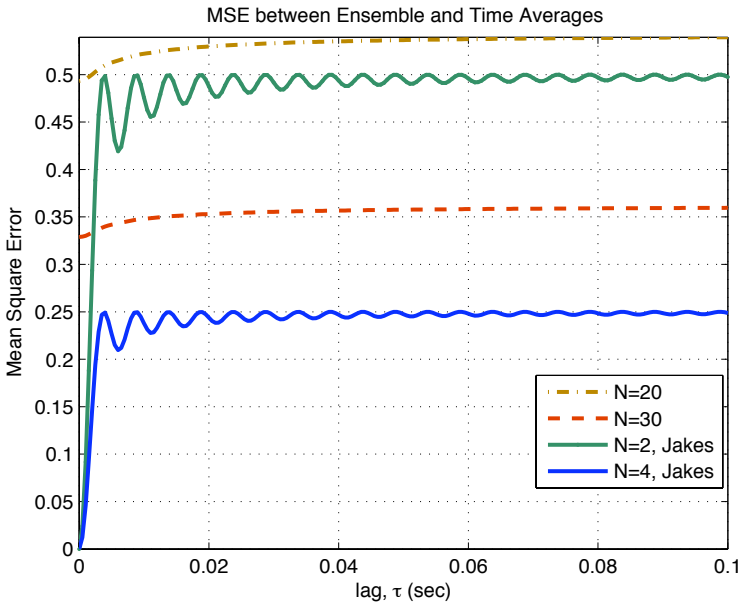


Figure 5.3 Effect of number of paths on mean squared error: the standard deviation of AOA $\sigma = 30$, maximum Doppler frequency, $\omega_{max} = 100Hz$, and the Weibull parameter $b = 0.8$.

$$
\begin{aligned}
&= E\left[\sum_{n=1}^{N}|\alpha_n|^2 e^{-j\omega_n\tau}\sum_{n=1}^{N}|\alpha_n|^2 e^{j\omega_n\tau}\right] - |R_e(\tau)|^2 \\
&= \left(\frac{N^2-N}{N^2}\right)|R_e(\tau)|^2 + E\left[\sum_{n=1}^{N}|\alpha_n|^4\right] - |R_e(\tau)|^2 \\
&= E\left[\sum_{n=1}^{N}|\alpha_n|^4\right] - \frac{|R_e(\tau)|^2}{N} \\
&= Nb^4\Gamma\left[\frac{4+c}{c}\right] - \frac{|R_e(\tau)|^2}{N} \\
\mathcal{L}(N,\sigma,b,\omega_{max},\tau) &= \frac{1}{N}\left[\frac{\Gamma[4/c+1]}{\Gamma[2/c+1]^2} - |R_e(\tau)|^2\right]. \qquad (5.24)
\end{aligned}
$$

For the widely considered Jakes scenario (uniform AOA and equal power $|\alpha_n|^2 = 1/N$), the MSE can be shown to be given by

$$\mathcal{L}(N,\omega_{max},\tau) = \frac{1}{N}\left[1 - J_0^2(\omega_{max}\tau)\right]. \qquad (5.25)$$

From (5.24) it can be seen that the MSE is inversely proportional to the number of paths, which makes the convergence process relatively slower. In Fig. 5.3

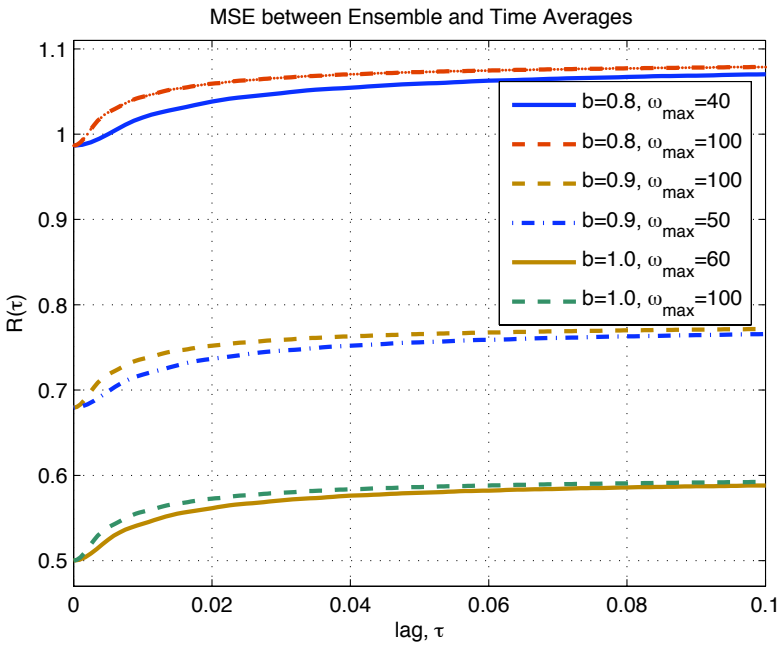


Figure 5.4 Effect of Weibull's $b$ and $\omega_{max}$ on MSE: number of paths $N = 10$, and $\sigma = 30$.

we plot the MSE between the ensemble and time averages. The standard deviation of AOA, $\sigma = 30$, the maximum Doppler frequency, $\omega_{max} = 100Hz$ and the Weibull parameter $b = 0.8$ are assumed in the plot. As the number of paths increase the MSE decreases. For comparison we also plotted the MSE curves for the widely popular Jakes scenario (5.25). It is clear that ergodicity doesn't hold for Jakes scenario also. However, compared to the realistic channel scenario (5.24), Jakes scenario has very low MSE, as seen in Fig. 5.3, the MSE of 20 paths in realistic channel scenario is close to the MSE of a 2 paths Jakes scenario. Which means the MSE convergence of the realistic scenario (Laplacian AOA and Weibull amplitude) is much slower than the Jakes scenario (uniform AOA and $|\alpha_n|^2 = 1/N$). Another interesting observation is that for very small lag, $\tau$, Jakes scenario's MSE is almost zero, while the MSE of realistic channel is a near constant non-zero value for any amount of lag.

In Fig. 5.4 we look at the effect of tail of amplitude on the convergence.

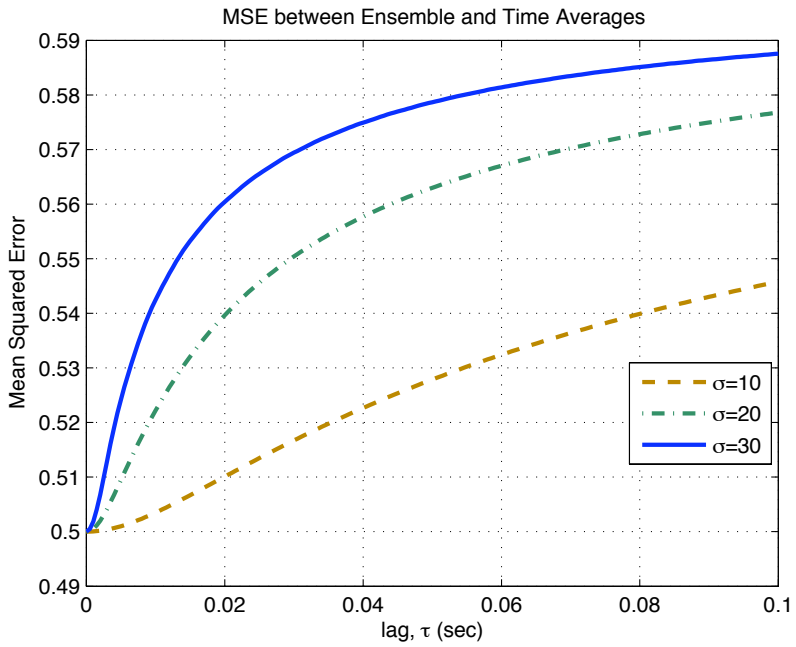


Figure 5.5 Effect of Laplacian's $\sigma$ on MSE: number of paths, $N = 10$, maximum Doppler frequency $\omega_{max} = 100Hz$ and $b = 1.0$.

The MSE increases as $b$ increases. As indicated earlier a higher $b$ indicates a stronger tail, so a higher tail translates into a slower convergence between ensemble and time averages. We also looked at the effect of $\omega_{max}$ on MSE and a smaller $\omega_{max}$ has a lower MSE but its contribution to MSE is seen to be not significant. Number of paths, $N = 10$, and $\sigma = 30$ are assumed in Fig. 5.4. In Fig. 5.5 we look at the effect of the standard deviation of AOA on MSE. A smaller angular spread translates into a smaller MSE. Number of paths, $N = 10$, maximum Doppler frequency $\omega_{max} = 100Hz$ and $b = 1.0$ are assumed in In Fig. 5.5. In all the plots the channel is generated by (5.18).

In summary, though the dominant role in the convergence is played by the number of paths, $N$, other system parameters like standard deviation of angle of arrival, $\sigma$, and the Weibull parameter, $b$, also have a significant effect on the rate of convergence.

## 5.5 Linear Prediction

Assuming that the sinusoidal model is valid for a given scenario and if the resolubility of doppler frequencies is not a problem, then, through prediction the impact of delay can be significantly ameliorated in feedback based communication systems. However, the real-world channel may not remain stationary for long and so the prediction approach can only work within the time-span of stationarity. In the following discussion, except for the fact that the channel is generated by sum of sinusoids (not by Jakes or other models which generate the channel with ergodic properties), no other assumptions are made about the behavior of the channel.

### 5.5.1 Forward-Only Prediction

For a SISO channel, let $\widehat{\mathbf{h}}_{n-1} = [\widehat{h}(n-1), \widehat{h}(n-2), \cdots, \widehat{h}(n-m)]^T$ be the '$m$' previous channel samples ('$m$' is the filter order). The next channel sample, $\widehat{h}(n)$, is given by,

$$\widehat{h}(n) = \sum_{l=1}^{m} (-k_i)\widehat{h}[n-l] + e(n), \tag{5.26}$$

where $-k_i$ are the filter coefficients and $e(n)$ is the Forward prediction error. Obviously the prediction error is going to depend on the selection of the filter coefficients. The two possible non-adaptive methods for estimating the filter co-efficients are LMMSE and Least Squares. The ensemble correlation characteristics are assumed to be known completely in the derivation of LMMSE, so the ergodicity assumption becomes critical. As we pointed out in the previous section, a typical real-world channel is not ergodic and hence predicting the wireless channel by using an LMMSE filter may not be the right choice. Filter co-efficients calculated from Least Squares are data driven, data being the past channel observations. Though some of the previous channel prediction work applied to real world data mentioned that they use the data driven approach instead of statistical approach, the lack of ergodicity is not pointed out as the main reason for using actual data instead of statistics. We now look at obtaining filter coefficients by LS method. Assuming

that we have $M$ total previous channel estimates available, equation (5.26) can be written as

$$\mathbf{Hw} + \mathbf{e} = \mathbf{h}, \tag{5.27}$$

By using the orthogonality principle [111] and [112], we can obtain the LS coefficient vector $\mathbf{w}$ as

$$\mathbf{w} = \left(\mathbf{H}^H\mathbf{H}\right)^{-1}\mathbf{H}^H\mathbf{h} \tag{5.28}$$

In contrast, if the linear LMMSE method is used, the co-efficient vector $\mathbf{w}$ is given by [4]

$$\mathbf{w}_m = \mathbf{R}^{-1}\mathbf{r}, \tag{5.29}$$

where $\mathbf{R}$ is the correlation matrix and $\mathbf{r}$ is the cross-correlation matrix. The elements of $\mathbf{R}$ and $\mathbf{r}$ are given by (5.20) with appropriate lag and maximum doppler frequency. The linear minimum mean squared prediction error is given by

$$\mathcal{J}_{min} = \sigma_h^2 - \mathbf{r}^H\mathbf{R}^{-1}\mathbf{r}, \tag{5.30}$$

where $\sigma_h^2$ is the power of the actual channel. The above equation indicates that, even with perfect past channel estimates, LMMSE method will have a non-zero error, while with an appropriate choice of filter order we can achieve zero-error with Least Squares method.

### 5.5.2 Forward-Backward Prediction

The prediction error can be further reduced by a more effective utilization of available data such as the Forward-Backward method [113]. This method reduces the variance of the estimate (filter co-efficients) as well as the condition number of the data matrix. Co-efficient vector $\mathbf{w}$ is given by

$$\mathbf{w} = \left(\tilde{\mathbf{H}}^H\tilde{\mathbf{H}}\right)^{-1}\tilde{\mathbf{H}}^H\tilde{\mathbf{h}}, \tag{5.31}$$

$\tilde{\mathbf{H}}$ is the Forward-Backward data matrix [113].

### 5.5.3 Rank Reduction

The performance of Forward-Backward algorithm depends on the condition number of the data matrix $\tilde{\mathbf{H}}$. The rank of FB data matrix is equal to the number of sinusoids present in the data [113]. The rank can be even less if some sinusoids are close enough in frequency (as Doppler frequencies are selected randomly), or if they have negligible amplitude. It should be noted that due to the noisy estimates the rank of the channel can be full but the condition number will be high, and this plays a very important role in the quality of the prediction.

To reduce the condition number, there are two possible choices, we can have the model order equal to the number of multipath or we can have a reduced rank approximation of a higher order filter. Fig. 5.8 shows that it is better to use a higher order filter than number of multipath with a low-rank approximation [112] of the FB matrix, this is due to the fact that with higher filter order we have more data available. However, having higher filter order also implies a longer training sequence. Another source of higher condition number is the sampling rate. With a higher sampling rate, the condition number will be high, so in the construction of channel matrix the spacing between channel samples can be increased such that the condition number is smaller. The over sampling of channel can also be utilized to estimate filter coefficients with lower variance, thus reducing the prediction error. Finally, we note that there are other sophisticated data driven approaches that could potentially result in better prediction like Total LS, Structural LS and various sub-space methods. However, they are computationally intensive and so have not been considered in this work.

### 5.5.4 Simulation Results

Fig. 5.6 shows that the LS prediction with Forward-only method outperforms the LMMSE. Simulation parameters for Fig. 5.6: Channel is generated by (5.18) with uniform distribution for AOA and equal amplitude for all the multipath, $|\alpha_n|^2 = 1/N$. 100 iterations, number of paths $N = 6$, filter order $m = 10$,

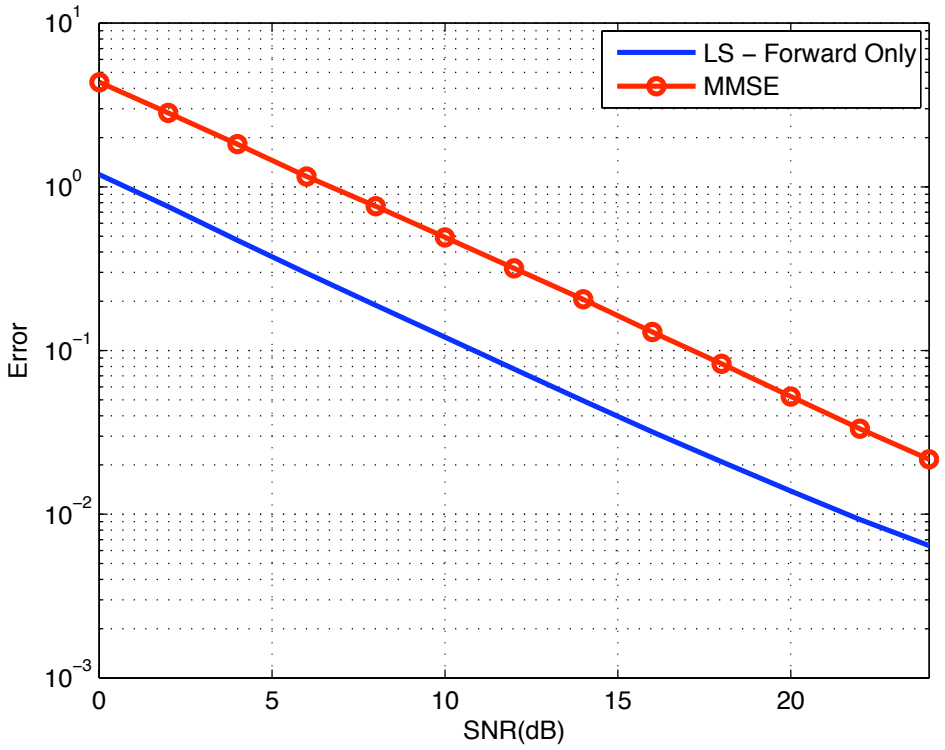


Figure 5.6 LS based forward prediction vs LMMSE prediction: 100 iterations, number of paths $N = 6$, filter order $m = 10$, maximum Doppler frequency $\omega_{max} = 100Hz$, sampling frequency= 300 Hz, training length $M = 40$, number of predicted samples, $P = 180$.

maximum Doppler frequency $\omega_{max} = 100Hz$, sampling frequency=300 Hz, training length $M = 40$, number of predicted samples, $P = 180$. Prediction error for all figures is defined as

$$\mathcal{P}_{error} = \frac{\sum_{l=1}^{P} \left|\widehat{h}(l) - \widehat{h}_p(l)\right|^2}{P}, \tag{5.32}$$

where $\widehat{h}_p(n)$ is the predicted channel and $\widehat{h}(n)$ is the actual channel. In Fig. 5.7, as expected the prediction error using the Forward-Backward method is seen to be less compared to the error in Forward-only approach. Simulation parameters for Fig. 5.7: iterations=100, $N = 10$, $m = 10$, $\omega_{max} = 100Hz$, sampling frequency=300 Hz, $M = 25$, and $P = 160$. Fig. 5.8 shows that it is better to use a filter of order higher than number of multipath and then taking low rank approximation to the

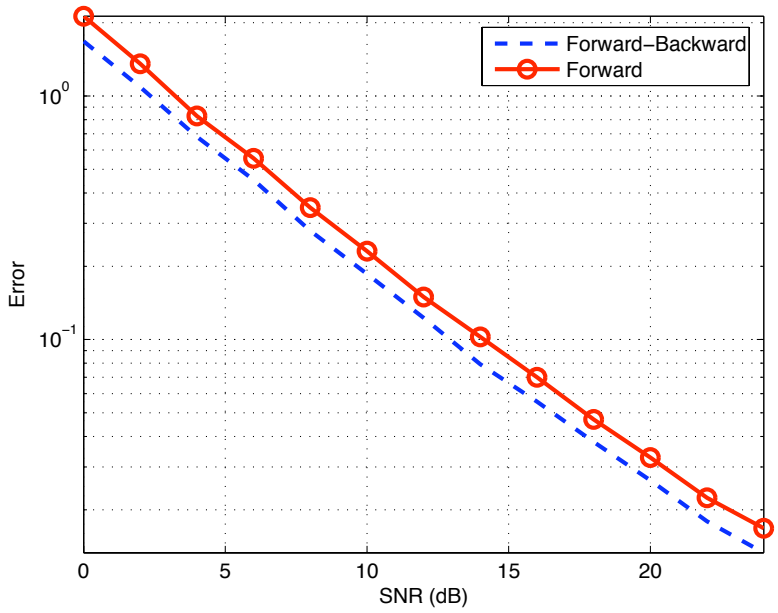


Figure 5.7 Forward-Backward vs forward only prediction, 100 iterations, $N = 10$, $m = 10$, $\omega_{max} = 100Hz$, sampling frequency= 300 Hz, $M = 25$, and $P = 160$.

data matrix of FB. Simulation parameters for Fig. 5.8: Iterations=100, $N = 4$, $m = 10$, $\omega_{max} = 100Hz$, Sampling frequency=300 Hz, $M = 25$, and $P = 160$ and $\rho = 25$ dB.

## 5.6 Conclusion

In this chapter we are first concerned with an accurate and simple way to simulate the wireless channel. However, the non-linear and complex channel model is not amenable to analytical studies. Under certain conditions one can reduce the complicated non-linear model to a simple linear sum-of-sinusoids model. We then take a close look at the crucial link between the prediction of channel based on data driven approaches and statistics driven approach. Given that there will be usually only a few dominant multipath present in a typical wireless channel, the ergodic assumption is shown to be invalid for the sinusoidal channel model. As a consequence of non-ergodicity, Least Squares based approach is proposed to reduce the prediction error instead of the LMMSE approach. Forward-Backward

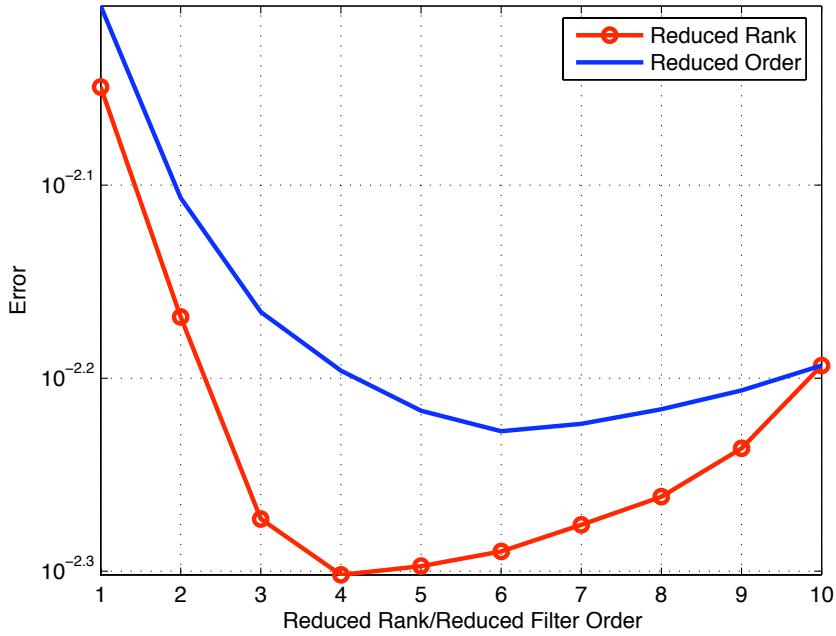


Figure 5.8 Rank reduction and order reduction, 100 iterations, $N = 4$, $m = 10$, $\omega_{max} = 100Hz$, sampling frequency=300 Hz, $M = 25$, and $P = 160$ and $\rho = 25$ dB.

approach reduces the prediction error compared to the Forward-only approach. Rank-reduction along with the correct choice of filter order for a given number of multipath is also shown be an important factor in reducing the prediction error.

**Acknowledgement**

The text of this chapter, in part, has *appeared* in:

- Y. Isukapalli and B. D. Rao, "Ergodicity of wireless channels and temporal prediction," *IEEE Asilomar Conf. on Sig. Syst. and Comp.*, CA, pp. 473-477, Oct. 2006.

The text of this chapter, in part, is manuscript *in preparation*:

- Y. Isukapalli and B. D. Rao, "Multi-antenna wireless channel modeling: statistical properties and prediction," in preparation, *IEEE Transactions on Signal Processing.*

# 6 Conclusion

In this Chapter we summarize the important contributions of the thesis and also discuss about future work. In this thesis we comprehensively studied the modeling of imperfect feedback and analytical evaluation of performance with imperfect feedback. The three main sources of feedback imperfection considered are channel estimation errors, feedback delay, and channel quantization.

## Contributions of the Thesis

1. A general framework, capturing the three forms of feedback imperfection, is developed for spatially independent channels and spatially correlated channels. An extended framework for the packet fading context is also presented.

2. Feedback delay related error term is modeled in two ways. Depending on the system model, the delay related error term can be known or unknown at the receiver. However, estimation related error term is always unknown at the receiver.

3. With channel estimation errors and feedback delay, optimum codebook design algorithm, specific to the modulation format being used, is proposed for minimizing the average symbol error probability loss. Optimum codebook design that minimizes ergodic capacity loss is also proposed.

4. Performance analysis: Closed form analytical expressions are derived for the following scenarios.

(a) Spatially independent channel, delay error term *unknown* at the receiver: Average symbol and bit error probability expressions for both $M$-PSK and rectangular $M$-QAM constellations with Gray code mapping.

(b) Spatially independent channel, delay error term *unknown* at the receiver: Ergodic capacity loss.

(c) Spatially independent channel, delay error term *known* at the receiver: Average symbol error probability (SEP) of $M_1 \times M_2$-QAM constellation.

(d) Spatially independent channel, delay error term *known* at the receiver: Average packet error probability of BPSK constellation.

(e) Spatially correlated channel, no channel estimation errors and no delay: Loss in average SEP of $M_1 \times M_2$-QAM due to finite rate quantization alone.

5. Channel modeling and prediction: For simulation purposes an accurate channel model is developed. the role of ergodicity in wireless channel prediction is studied. Following the sinusoidal channel model, conditions under which the ergodic assumption is valid are presented.

## Future Work

Most of the wireless communication system performance related theoretical studies assume ideal channel estimation and feedback based communication systems generally ignore the effect of delay and channel quantization. The accurate modeling of channel estimation errors in the packet fading context, an important contribution of this thesis, combined with delay along with channel quantization can be useful to study the performance of a number of popular communication systems under realistic assumptions.

We note that though the imperfect feedback modeling presented here is limited to transmit beamforming based MISO systems, it is relatively easy to

adapt the model to other popular MIMO scenarios as well as for multiuser communication setting. Some areas of application include: OFDM, adaptive modulation, opportunistic communication, and an extension of these systems to a multiuser context.

On the analytical front, in the thesis we went through a lot of complicated derivations and some of the ideas used in the derivations can make the analysis of standard wireless communication performance metrics relatively easy. Developing robust feedback schemes can be an interesting future research topic. In this thesis we are beamforming with the available direction. Sometimes space-time codes might perform better if the mismatch between the actual channel and the beamforming vector is significantly higher. So based on the better channel model, and with proper prediction, if the receiver can decide when to use beamforming and when to use space time coding, it can help in significantly improving the performance of the system.

In this thesis we assumed that the index of the codepoint is conveyed to the transmitter without any error, in reality there is a chance that the index itself can be decoded wrongly. Including this form of error along with estimation errors, delay and channel quantization, can make the study of imperfect feedback relatively complete.

# Bibliography


[1] D. Tse and P. Vishwanath, *Fundamentals of wireless communications*, Cambridge University Press, 2005.

[2] W. C. Jakes, *Microwave mobile communications,* John Wiley & Sons, 1974.

[3] H. J-Kuang and J .H Winters, "Sinusoidal modeling and prediction of fast fading processes," *IEEE Global Telecommun. Conf.*, vol. 2, no. 3, pp. 892-897, Nov. 1998.

[4] S. Hu A. D-Hallen and H. Hallen, "Long-range prediction of fading signals," *IEEE Signal Processing Magazine*, vol. 17, no. 3, pp. 62-75, May 2000.

[5] A. Saleh and R. Valenzuela, "A statistical model for indoor multipath propagation," *IEEE Journal on Selected Areas in Commun.*, vol. 5, no. 2, pp. 128-137, Feb. 1987.

[6] T. Svantesson and A. L. Swindlehurst, "A performance bound for prediction of mimo channels," *IEEE Trans. Signal Processing*, vol. 54, no. 2, pp. 520-529, Feb. 2006.

[7] I. E. Telatar, "Capacity of multi-antenna Gaussian channels," *European Trans. Telecommun.,* vol. 10, pp. 585-595, Nov./Dec. 1999.

[8] G. J. Foschini and M. J. Gans, "On limits of wireless communications in a fading environment when using multiple antennas," *Wireless Personal. Commun.,* vol. 6, pp. 311-335, Nov. 1998.

[9] T. K. Y. Lo, "Maximum ratio transmission," *IEEE Trans. Commun.,* vol. 47, no. 10, pp. 1458-1461, Oct. 1999.

[10] S. M. Alamouti, "A simple transmit diversity technique for wireless communications," *IEEE Journal on Selected Areas in Commun.*, vol. 16, no. 8, pp. 1451-1458, Oct. 1998.

[11] V. Tarokh, N. Seshadri, and A. R. Calderbank, "Space-time codes for high data rate wireless communications: Performance criterion and code construction," *IEEE Trans. Info. Theory,* vol. 44, pp. 744-764, 1998.

[12] M. K Simon and M.-S. Alouini, *Digital communications over fading channels: A unified approach to performance analysis,* Wiley Series, Jul. 2000.

[13] A. Narula, M. J. Lopez, M. D. Trott, and G. W. Wornell, "Efficient use of side information in multiple-antenna data transmission over fading channels," *IEEE Journal on Selected Areas in Commun.,* vol. 16, no. 8, Oct. 1998, pp. 1423-1436.

[14] E. Visotsky and U. Madhow, "Space-time transmit precoding with imperfect feedback," *IEEE Trans. Inform. Theory,* vol. 47, no. 6, pp. 2632-2639, Sep. 2001.

[15] S. Srinivasa and S. A. Jafar, "The optimality of transmit beamforming: a unified view," *IEEE Trans. Inform. Theory,* vol. 53, no. 4, pp. 1558-1564, Apr. 2007.

[16] E. N. Onggosanusi, A. Gatherer, A. G. Dabak, and S. Hosur, "Performance analysis of closed-loop transmit diversity in the presence of feedback delay," *IEEE Trans. Commun.,* vol. 49, no. 11, pp. 1618-1630, Sep. 2001.

[17] Y. Chen, and C. Tellambura, "Performance analysis of maximum ratio transmission with imperfect channel estimation," *IEEE Comm. Letters,* vol. 9, no. 4, pp. 322-324, Apr. 2005.

[18] N.-S. Kim and Y. H. Lee, "Effect of channel estimation errors and feedback delay on the performance of closed-loop transmit diversity system," in *Proc. IEEE Signal Proces. Advan. in Wireless Commun.*, pp. 542-545, 2003.

[19] J. Hamalainen and R. Wichman, "The effect of feedback delay to the closed-loop transmit diversity in FDD WCDMA," in *IEEE Symp. on Pers. Indoor and Mobile Radio Commun.*, pp. 27-31, Sep. 2001.

[20] J. Hamalainen and R. Wichman, "Performance analysis of closed-loop transmit diversity in the presence of feedback errors," in *IEEE Symp. on Pers. Indoor and Mobile Radio Commun.*, vol.5, pp. 2297-2301, Sep. 2002.

[21] M. Edlund, M. Skoglund, and B. D. Rao, "On the performance of closed-loop transmit diversity with non-ideal feedback," in *IEEE intern. Conf. Commun.*, Anchorage, Alaska, pp. 3190-3194, May 2003.

[22] K. K. Mukkavilli, A. Sabharwal, E. Erkip, and B. Aazhang, "On beamforming with finite rate feedback in multiple antenna systems," *IEEE Trans. Info. Theory,* vol. 49, no. 10, pp. 2562-2579, Oct. 2003.

[23] D. J. Love, R. W. Heath Jr, and T. Strohmer, "Grassmannian beamforming for multiple-input multiple-output wireless systems," *IEEE Trans. Info. Theory,* vol. 49, no. 10, pp. 2735-2747, Oct. 2003.

[24] W. Santipach and M. L. Honig, "Signature optimization for CDMA with limited feedback," *IEEE Trans. Inform. Theory,* vol. 51, no. 10, pp. 3475-3492, Oct. 2005.

[25] S. Zhou, Z. Wang, and G. Giannakis, "Quantifying the power loss when transmit beamforming relies on finite-rate feedback," *IEEE Trans. Wireless Commun.,* vol. 4, no. 4, pp. 1948-1957, Jul. 2005.

[26] J. C. Roh and B. D. Rao, "Transmit beamforming in multiple-antenna systems with finite rate feedback: A vq-vased approach," *IEEE Trans. Info. Theory,* vol. 52, no. 3, pp. 1101-1112, Mar. 2006.

[27] D. J. Love, R. W. Heath, V. K. N. Lau, D. Gesbert, B. D. Rao, and M. Andrews, An overview of limited feedback in wireless communication system, *IEEE Journal on Sele. Areas on Commun.*, vol. 26, no. 8, pp. 1341-1365, Oct 2008,

[28] R. Annavajjala, P. C. Cosman, and L. B. Milstein, "Performance analysis of linear modulation schemes with generalized diversity combining on Rayleigh fading channels with noisy channel estimates," *IEEE Trans. on Info. Theory*, vol. 53, pp. 4701-4727, Dec. 2007.

[29] J. K. Cavers, "An analysis of pilot symbol assisted modulation for Rayleigh fading channels," *IEEE Trans. Vehic. Technol.,* vol. 40, pp. 686-693, Nov. 1991.

[30] C. R. Rao, *Linear statistical inference and its applications,* John Wiley & Sons, 1973.

[31] E. Chiu, P. Ho, and J. H. Kim, "Performance of analog feedback in closed-loop transmit diversity systems," in *IEEE Wireless Comm. and Network. Conf.*, vol. 3, pp. 1227-1232, Apr. 2006.

[32] R. Annavajjala, "Comments on "Exact error-rate analysis of diversity 16-QAM with channel estimation error," in *IEEE Trans. Commun.,*, vol. 54, no. 3, pp. 393- 396, Mar. 2006.

[33] J. G. Proakis, *Digital Communications,* Fourth Edition, McGraw-Hill, 2001.

[34] M. K. Simon and R. Annavajjala, "On the optimality of bit detection of certain digital modulations," *IEEE Trans. Commun.*, vol. 53, no. 2, pp. 299-307, Feb. 2005.

[35] I. S. Gradshteyn and I. M. Ryzhik, *Table of integrals, series, and products,* Corrected and enlarged edition, Academic Press, Inc., 1980.

[36] R. F. Pawula, S. O. Rice and J. H. Roberts, "Distribution of the phase angle between two vectors perturbed by Gaussian noise," *IEEE Trans. Commun.,* vol. 30, no. 8, pp. 1828-1841, Aug. 1982.

[37] J. Lassing, E. Strom, E. Agrell and T. Ottosson, "Computation of the exact bit error rate of coherent M-ary PSK with Gray code bit mapping," *IEEE Trans. Commun.,* vol. 51, no. 10, pp. 1758-1760, Nov. 2003

[38] E. R. Eaves and A. H. Levesque, "Probability of block error for very slow Rayleigh fading in Gaussian noise," *IEEE Trans. Commun.*, vol. 25, no. 3, pp. 368-374, Mar. 1977.

[39] C. E. Sundberg, "Block error probability for noncoherent FSK with diversity for very slow Rayleigh fading in Gaussian noise," *IEEE Trans. Commun.*, vol. 29, pp. 57-60, Jan. 1981.

[40] F. Adachi and K. Ottno, "Block error probability for noncoherent FSK with diversity reception in mobile radio," *IEEE Elec. Letters*, vol. 24, no. 24, pp. 1523-1525, Nov. 1988.

[41] H. Bischl and E. Lutz, "Packet error rate in the noninterleaved Rayleigh channel," *IEEE Trans. Commun.*, vol. 43, no. 2/3/4, pp. 1375-1382, Feb./Mar./Apr. 1995.

[42] A. Seyoum and N. C. Beaulieu, "Semianalytical simulation for evaluation of block-error rates on fading channels," *IEEE Trans. Commun.*, vol. 46, no. 7, pp. 916-920, Jul. 1998.

[43] J-S. Roh, C-H. Oh, H-J. Kang, and S.-J. Cho, "Packet error probability of multi-carrier CDMA system in fast/slow correlated fading plus interference channel," *Springer Link- Chap. in Inform. and Commun. Tech.*, vol. 2510, pp. 366-376, Jan. 2002.

[44] H. Holma and A Toskala, "WCDMA for UMTS : HSPA evolution and LTE," *Wiley*, $4^{th}$ edition, 2007.

[45] J.R-Jerez, L. G. Alonso, and R. Agusti, "Average block error probability in the reverse link of a packetDS/CDMA system under Rayleigh fading channel conditions," *IEEE Commun. Letters,* vol. 4, no. 4, pp. 116-118, Apr. 2000.

[46] M. R-Garcia, J. M. R-Jerez, C. T-Labao, and A. D-Estrella, "Average block error probability of multicell CDMA packet networks with fast power control under multipath fading," *IEEE Commun. Letters,* vol. 6, no. 12, pp. 538-540, Dec. 2002.

[47] K. A. Hamdi, "Packet-error probability analysis for FH-CDMA unslotted packet networks," *IEEE Trans. Commun.,* vol. 51, no. 2, pp. 151-154, Feb. 2003.

[48] F. F. Digham and M.-S. Alouini, "Average probability of packet error with MRC diversity reception over arbitrarily correlated fading channels," *IEEE Glob. Telecom. Conf.*, vol. 2, pp. 1425-1429, Nov. 2002.

[49] Y. D. Yao, T. Le-Ngoc, and U. H. Sheik, "Block error probabilities in a Nakagami fading channel," *IEEE Vehic. Technol. Conf.*, pp. 130-133, May. 1993.

[50] H. M. Hafez, A. U. H. Sheikh, and B. McPhail. "Experimental evaluation of packet error rates for the 850 MHz mobile channel" *IEE Proc. Comm., Radar and Sig. Proc.*, vol. 132, no.5, pp. 366-374, Aug. 1985.

[51] V. Subotic and S. Primak, "Block-error rate model for DPSK in Rayleigh- and sub-Rayleigh-fading channels" *IEEE Journal on Selected Areas in Commun.*, vol. 23, no. 9, pp. 1875- 1883, Sep. 2005.

[52] J. A. Roberts, "Packet error rates for DPSK and differentially encoded coherent BPSK," *IEEE Trans. Commun.*, vol. 42, no. 2/3/4, pp. 1441-1444, Feb./Mar./Apr. 1994.

[53] J. Lai and N. B. Mandayam, "Packet error rate for burst-error-correcting codes in Rayleighfading channels," *IEEE Vehic. Technol. Conf.*, pp. 1568-1572, May. 1998.

[54] A. Vlavianos, L. K. Law, I. Broustis, S. V. Krishnamurthy, and M. Faloutsos, "Assessing link quality in IEEE 802.11 wireless networks: Which is the right metric?" *IEEE Pers. Indoor and Mobile Radio Comm.*, pp. 1-6, Sep. 2008.

[55] S. S. Tan, M. J. Rim, P. C. Cosman, and L. B. Milstein, "Adaptive modulation for OFDM-based multiple description progressive image transmission?" *IEEE Glob. Telecomm. Conf.*, pp. 1-5, Dec. 2008.

[56] B. Han and S. Lee "Efficient packet error rate estimation in wireless networks" *IEEE Trident Commun.*, pp. 1-9, May. 2007.

[57] Rohde and Schwarz,"802.11 packet error rate testing - hardware implementation," Online: *http://www2.rohde-schwarz.com/file_1344/1GP56_2E.pdf.*

[58] R. Khalili and K. Salamatian, "Evaluation of packet error rate in wireless networks," *Proceedings of Intern. Conf. on Modeling, Analysis and Simulation of Wireless and Mobile Syst.,* 2004.

[59] G. Jakllari, S. V. Krishnamurthy, M. Faloutsos, and S. V. Krishnamurthy, "On broadcasting with cooperative diversity in multi-hop wireless networks," *IEEE Journal on Selected Areas in Commun.*, vol. 25, no. 2, pp. 484-496, Feb. 2007.

[60] T. Yoo, E. Yoon, and A. J. Goldsmith "MIMO capacity with channel uncertainty: Does feedback help?," *IEEE Glob. Telecom. Conf.*, vol. 1, pp. 96-100, Dec. 2004.

[61] Y. Isukapalli and B. D. Rao, "Performance analysis of finite rate feedback MISO systems in the presence of estimation errors and delay" *Proc. IEEE Asilomar Conference on Signal and Systems*, pp. 1931-1935, Oct. 2007.

[62] Y. Isukapalli, R. Annavajjala, and B. D. Rao, "Performance analysis of transmit beamforming for MISO systems with imperfect feedback," *IEEE Trans. Commun.*, vol. 57, no. 1, pp. 222-231, Jan. 2009.

[63] Y. Isukapalli and B. D. Rao, "Analyzing the effect of channel estimation errors on the average block error probability of a MISO transmit beamforming system," *Proc. IEEE Glob. Telecommun. Conf.,* New Orleans, LA, pp.1-6, Dec. 2008

[64] D. V. Duong, G. E. Oien, and K. J. Hole, "Adaptive coded modulation with receive antenna diversity and imperfect channel knowledge at receiver and transmitter," *IEEE Trans. Vehic. Commun.,* vol. 55, no. 2, pp. 458-465, Mar. 2006.

[65] X. Cai and G. B. Giannakis, "Adaptive PSAM accounting for channel estimation and prediction errors," *IEEE Trans. Wireless Commun.,* vol. 4, no. 1, pp. 246-256, Jan. 2005.

[66] E. Chiu, P. Ho,and J. H. Kim, "Transmit beamforming with analog channel state information feedback," *IEEE Trans. Wireless Commun.,* vol. 7, no. 3, pp. 878-887, Mar. 2008.

[67] D. V. Duong and G. E. Oien, "Optimal pilot spacing and power in rate-adaptive MIMO diversity systems with imperfect CSI," *IEEE Trans. Wireless Commun.,* vol. 6, no. 3, pp. 845-851, Mar. 2007.

[68] A. E. Ekpenyong and Y-F. Huang, "On the feedback transfer effort for rate-adaptive multiuser systems," *Proc. IEEE Vehic. Tech. Conf.*, pp. 122-126, May 2006.

[69] K. C. Hwang and K. B. Lee, "Efficient weight vector representation for closed-loop transmit diversity," *IEEE Trans. Commun.,* vol. 52, no. 1, pp. 9-16, Jan. 2004.

[70] N.-S. Kim and Y. H. Lee, "Performance of closed-loop transmit antenna diversity system with channel estimation errors and fading correlation," *Proc. IEEE Sign. Proc. Advances in Wireless Commun.*, pp. 464- 468, Jul. 2004.

[71] Y. Ma, A.Leith, and R. Schober, "Predictive feedback for transmit beamforming with delayed feedback and channel estimation errors," in *Proc. IEEE Intern. Conf. Commun.*, pp. 4678-4682, May. 2008.

[72] Q. Ma and C. Tepedelenlioglu "Comparison of multiuser diversity using STBC and transmit beamforming with outdated feedback," *IEEE IEEE Intern. Conf. on Acous. Speech and Sig. Proce.,* vol. 3, pp. 125-128, Mar. 2005.

[73] K. Choi, "Performance analysis for transmit antenna diversity with/without channel information," *IEEE Trans. Vehic. Commun.,* vol. 51, no. 1, pp. 101-113, Jan. 2002.

[74] S. Zhou and G. B. Giannakis, "How accurate channel prediction needs to be for transmit-beamforming with adaptive modulation over Rayleigh MIMO channels?," *IEEE Trans. Wireless Commun.,* vol. 3, no. 4, pp. 1285-1294, Jul. 2004.

[75] S. Ye and R. S. Blum, and L. J. Cimini, "Adaptive OFDM systems with imperfect channel state information," in *IEEE Trans. Wireless Commun.*, vol. 5, no. 11, pp. 3255-3265, Nov. 2006.

[76] T. J. Willink, "Improving power allocation to MIMO eigenbeams under imperfect channel estimation," *IEEE Commun. Letters,* vol. 9, no. 7, pp. 622-624, Jul. 2005.

[77] A. Olfat and M. Shikh-Bahaei, "Optimum power and rate adaptation for MQAM in Rayleigh flat fading with imperfect channel estimation., *IEEE Trans. Vehic. Tech.,* vol. 57, no. 4, pp. 2622-2627, Jul. 2008.

[78] G. Hu, F. Jiang, Y. Wang, Y. Xu, and P. Zhang, "On the performance of a multi-user multi-antenna system with transmit zero-forcing beamforming and feedback delay," *IEEE Wireless Commun. and Net. Conf.,* pp. 1821-1825, Apr. 2008.

[79] L. H. Ozarow, S. Shamai, and A. D.Wyner, Information theoretic considerations for cellular mobile radio, *IEEE Trans. Veh. Technol.*, vol. 43, no. 2, pp. 359378, May 1994.

[80] E. Biglieri, J. Proakis, and S. Shamai (Shitz), Fading channels: Information-theoretic and communications aspects, *IEEE Trans. Inf. Theory*, vol. 44, no. 6, pp. 26192692, Oct. 1998.

[81] R. Knopp and P. Humblet, On coding for block fading channels, IEEE *Trans. Inf. Theory*, vol. 46, no. 5, pp. 16431646, Jul. 1999.

[82] E. Malkamaki and H. Leib, Evaluating the performance of convolutional codes over block fading channels, IEEE Trans. Inf. Theory, vol. 45, no. 5, pp. 16431646, Jul. 1999.

[83] M. Chiani, A. Conti, andV. Tralli, Further results on convolutional code search for block-fading channels, IEEE Trans. Inf. Theory, vol. 50, no. 6, pp. 13121318, Jun. 2004.

[84] Y. Isukapalli and B. D. Rao, "An analytically tractable approximation for the Gaussian Q-function," *IEEE Communications Letters*, vol.12, no.9, pp. 669-671, Sep. 2008.

[85] M. K Simon, *Probability distributions involving Gaussian random variables: A handbook for engineers and scientists,* Kluwer, 2002.

[86] P. O. Borjesson and C. E. Sundberg, " Simple approximations of the error function Q(x) for communications applications," *IEEE Trans. Commun.,* vol. 27, pp. 639-643, Mar. 1979.

[87] N. C. Beaulieu, " A simple series for personal computer computation of the error function Q()," *IEEE Trans. Commun.,* vol. 37, pp. 989-991, Sep. 1989.

[88] C. Tellambura and A. Annamalai, " Efficient computation of erfc(x) for large arguments," *IEEE Trans. Commun.,* vol. 48, pp. 529-532, Apr. 2000.

[89] M. Chiani, D. Dardari, and M. K. Simon, " New exponential bounds and approximations for the computation of error probability in fading channels," *IEEE Trans. Wireless Commun.,* vol. 2, pp. 840-845, Jul. 2003.

[90] G. K. Karagiannidis and A. S. Lioumpas, "An improved approximation for the Gaussian Q-function," *IEEE Commun. Letters,* vol. 11, no. 8, pp. 644-646, Aug. 2007.

[91] J. S. Dyer and S. A. Dyer, "Corrections to, and Comments on, 'An improved approximation for the Gaussian Q-function'," *IEEE Commun. Letters,* vol. 12, no. 4, pp. 231, Apr. 2008.

[92] S. Zhou and B. Li, "BER criterion and codebook construction for finite-rate precoded spatial multiplexing with linear receivers," *IEEE Trans. Signal Processing,* vol. 54, no. 5, pp. 1653-1665, May 2006.

[93] J. Zheng, E. R. Duni, and B. D. Rao, "Analysis of multiple-antenna systems with finite-rate feedback using high-resolution quantization theory," *IEEE Transactions on Signal Processing,* vol. 55, no. 4, pp. 1461-1476, Apr. 2007.

[94] D. J. Love and R. W. Heath, Jr., "Limited feedback diversity techniques for correlated channels," *IEEE Trans. on Veh. Tech.,* vol. 55, no. 2, pp. 718-722, Mar. 2006.

[95] G. Jöngren and M. Skoglund, "Quantized feedback information in orthogonal space-time block coding," *IEEE Trans. Info. Theory,* vol. 50, no.10, pp. 2473-2482, Oct. 2004.

[96] W. Santipach and M. L. Honig "Capacity of Beamforming with limited training and feedback," *Proc. IEEE Int. Symp. on Inform. Theory*, Seattle, Washington, pp. 376-380, Jul. 2006.

[97] V. Lau, Y. Liu, and T.-A. Chen, " On the design of MIMO block-fading channels with feedback-link capacity constraint," *IEEE Trans. Commun.,* vol. 52, no. 1, pp. 62-70, Jan. 2004.

[98] W. R. Gardner and B. D. Rao., "Theoretical analysis of the high-rate vector quantization of LPC parameters," *IEEE Trans. Speech Audio Process.,* vol. 3, pp. 367-381, Sep. 1995.

[99] J. Zheng, and B. D. Rao, "Analysis of multiple antenna systems with finite-rate channel information feedback over spatially correlated fading channels," *IEEE Transactions on Signal Processing,* vol. 55, no. 9, pp. 4612-4626, Sep. 2007.

[100] Y. Isukapalli and B. D. Rao, "Finite rate feedback for spatially and temporally correlated MISO channels in the presence of estimation errors and feedback delay," *IEEE Global Telecomm. Conf.,* Washington D.C., pp. 2791 2795, Nov. 2007.

[101] Y. Isukapalli, J. Zheng and B. D. Rao, "Average SEP loss analysis of transmit beamforming for finite rate feedback MISO systems with QAM constellation," *IEEE International Conf. on Acous., Speech, and Signal Proces.*, Hawaii, vol. 3, pp. 425-428, Apr. 2007.

[102] R. J. Muirhead, *Aspects of multivariate statistical theory*, Wiley, New York, 1982

[103] M. Abramowitz and I. A. Stegun, *Handbook of mathematical Functions with Formulas, Graphs, and Mathematical Tables.* New York, NY: Dover Publications, ninth ed., 1970.

[104] J. Salz and J. H. Winters, "Effect of fading correlation on adaptive arrays in digital mobile radio", *IEEE Trans. Vehic. Technology,*, vol. 43, no. 4, pp. 1049-1057 , Nov. 1994.

[105] T. Feng and T. R. Field, "Statistical analysis of mobile radio reception: an extension of clarke's model," *IEEE Trans. Commun.*, vol. 56, no. 12, pp. 2007-2012, Dec. 2008.

[106] J. Grolleau, E. Grivel, and M. Najim, "Two Ways to Simulate a Rayleigh Fading Channel Based on a Stochastic Sinusoidal Model," *IEEE Signal Proc. Letters*, vol. 15, no. 1, pp. 107-110, Jan. 2008.

[107] K. Pahlavan, A. H. Levesque, " Wireless information networks," *Wiley*, New York, 1995.

[108] Y. R. Zheng and C. Xiao, Improved models for the generation of multiple uncorrelated Rayleigh fading waveforms, *IEEE Commun. Lett.,* vol. 6, no. 6, pp. 256-258, Jun. 2002.

[109] Y. R. Zheng and C. Xiao, Simulation models with correct statistical properties for Rayleigh fading channels, *IEEE Trans. Commun.,* vol. 51, no. 6, pp. 920-928, Jun. 2003.

[110] I.M. Ryshik and I.S. Gradstein *Tables of series, products and integrals*. Veb Deutscher Verlag Der Wissenschaffen, Berlin, 1963.

[111] S. Haykin, *Adaptive filter theory*, Prentice Hall, 2002.

[112] D. G. Manolakis, V. K. Ingle and S. M. Kogon, *Statistical and adaptive signal processing,*, McGraw-Hill, 2000.

[113] B. D. Rao and K. S. Arun, "Model based processing of signals: a state space approach," *Proceedings of the IEEE*, vol. 80, no. 2, pp. 283-309, Feb. 1992.

[114] A. Saleh and R. Valenzuela, "Evaluation of an ultra-wide-band propagation channel," *IEEE Journal on Selected Areas in Commun.*, vol. 5, no. 2, pp. 128-137, Feb. 1987.